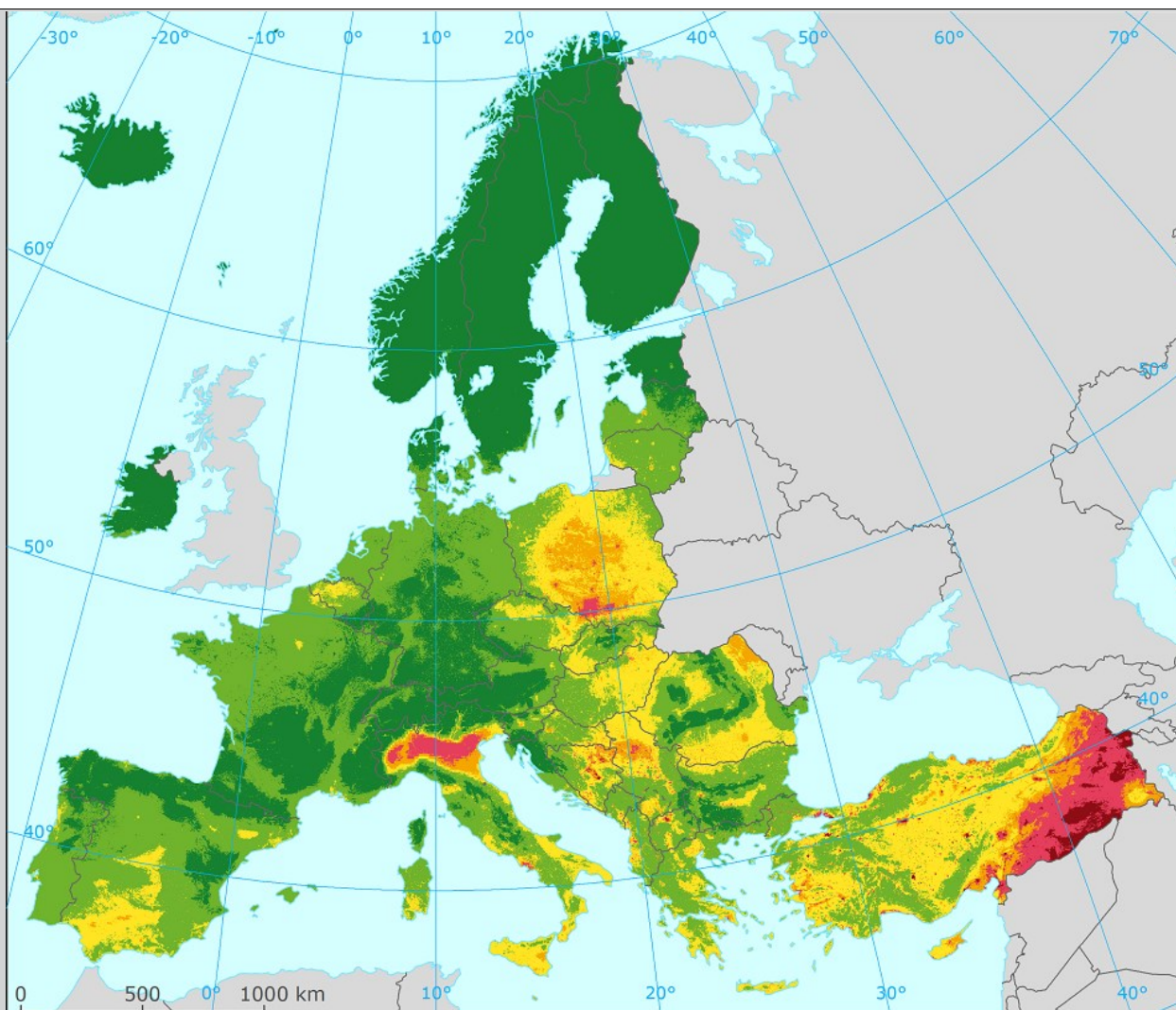


Air quality maps of EEA member and cooperating countries for 2021

PM₁₀, PM_{2.5}, O₃, NO₂, NO_x and BaP spatial estimates and their uncertainties



Authors:

Jan Horálek (CHMI), Leona Vlasáková (CHMI), Markéta Schreiberová (CHMI),
Nina Benešová (CHMI), Philipp Schneider (NILU), Pavel Kurfürst (CHMI),
Frédéric Tognet (INERIS), Jana Schovánková (CHMI), Ondřej Vlček (CHMI),
Marta Garcia Vivanco (CIEMAT), Mark Theobald (CIEMAT), Victoria Gil (CIEMAT)



Cover design: EEA

Cover picture: Concentration map of PM₁₀ indicator 90.4 percentile of daily means for 2021. Units: µg/m³. (Map 2.3 of this report.)

Layout: EEA and ETC HE

Publication Date: January 2024

ISBN 978-82-93970-21-7

Legal notice

Preparation of this report has been co-funded by the European Environment Agency as part of a grant with the European Topic Centre on Human Health and the Environment (ETC HE) and expresses the views of the authors. The contents of this publication does not necessarily reflect the position or opinion of the European Commission or other institutions of the European Union.

Neither the European Environment Agency nor the European Topic Centre on Human Health and the Environment is liable for any consequences stemming from the reuse of the information contained in this publication.

Horálek, J., Vlasáková, L., Schreiberová, M., Benešová, N., Schneider, P., Kurfürst, P., Tognet, F., Schováňková, J., Vlček, O., Vivanco, M. G., Theobald, M., Gil, V. (2023). *Air quality maps of EEA member and cooperating countries for 2021. PM₁₀, PM_{2.5}, O₃, NO₂, NO_x and BaP spatial estimates and their uncertainties* (Eionet Report – ETC HE 2023/3). European Topic Centre on Human Health and the Environment.

The report is available from <https://www.eionet.europa.eu/etcs/all-etc-reports> and <https://zenodo.org/communities/eea-etc/?page=1&size=20>.

EEA activity no. 3 Human Health and the Environment

ETC HE coordinator: Stiftelsen NILU (The climate and environmental research institute NILU)

ETC HE consortium partners: Federal Environment Agency/Umweltbundesamt (UBA), Aether Limited, Czech Hydrometeorological Institute (CHMI), Institut National de l'Environnement Industriel et des Risques (INERIS), Swiss Tropical and Public Health Institute (Swiss TPH), Universitat Autònoma de Barcelona (UAB), Vlaamse Instelling voor Technologisch Onderzoek (VITO), 4sfera Innova S.L.U., klarFAKTe.U

Copyright notice

© European Topic Centre on Human Health and the Environment, 2023

Reproduction is authorized provided the source is acknowledged. [Creative Commons Attribution 4.0 (International)]

More information on the European Union is available on the Internet (<http://europa.eu>).

European Topic Centre on
Human Health and the Environment (ETC HE)
<https://www.eionet.europa.eu/etcs/etc-he>

Contents

- Contents 3
- Acknowledgements 5
- Summary 6
- 1 Introduction 10
- 2 Particulate matter 12
 - 2.1 PM₁₀ annual average 13
 - Concentration map 13
 - Population exposure 14
 - 2.2 PM₁₀ – 90.4 percentile of daily means 18
 - Concentration map 18
 - Population exposure 20
 - 2.3 PM_{2.5} annual average 23
 - Concentration map 23
 - Population exposure 24
- 3 Ozone 28
 - 3.1 Ozone – 93.2 percentile of maximum daily 8-hour means 28
 - Concentration map 28
 - Population exposure 30
 - 3.2 Ozone – SOMO35 and SOMO10 33
 - Concentration maps 33
 - Population exposure 35
 - 3.3 Ozone – AOT40 vegetation and AOT40 forests 41
 - Concentration maps 41
 - Vegetation exposure 44
 - 3.4 Ozone – Phytotoxic Ozone Dose (POD) for crops and trees 47
 - Phytotoxic Ozone Dose maps 49
- 4 NO₂ and NO_x 53
 - 4.1 NO₂ – Annual mean 53
 - Concentration map 53
 - Population exposure 55
 - 4.2 NO_x – Annual mean 58
 - Concentration map 58
- 5 Benzo(a)pyrene 61
 - 5.1 Benzo(a)pyrene – Annual mean 61
 - Concentration map 61
 - Population exposure 62
- 6 Accumulated risks 64
- 7 Exposure trend estimates 65
 - 7.1 Human health PM₁₀ indicators 66
 - 7.2 Human health PM_{2.5} indicator 67
 - 7.3 Human health ozone indicators 68
 - 7.4 Vegetation related ozone indicators 69
 - 7.5 Human health NO₂ indicator 69
- List of abbreviations 71

References.....	73
Annex 1 Methodology	79
A1.1 Mapping methodology.....	79
A1.2 Calculation of population and vegetation exposure.....	81
A1.3 Phytotoxic Ozone Dose above a threshold flux Y (POD _y) calculation	83
A1.4 Methods for uncertainty analysis	91
Annex 2 Input data	93
A2.1 Air quality monitoring data	93
A2.2 Chemical transport modelling outputs	95
A2.3 Other supplementary data	96
Annex 3 Technical details and mapping uncertainties.....	100
A3.1 PM ₁₀	100
A3.2 PM _{2.5}	104
A3.3 Ozone	107
A3.4 NO ₂ and NO _x	114
A3.5 BaP.....	116
Annex 4 Concentration maps including stations.....	118

Acknowledgements

The EEA task manager was Alberto González Ortiz. The external task ETC HE reviewer was Joana Soares (NILU, Norway).

The air quality monitoring data for 2021 were extracted from the AQ e-reporting database by Anna Ripoll and Jaume Targa (4sfera, Spain). The Obukhov length and the air density data for 2021 were calculated by Florian Couvidat (INERIS, France).

Summary

Air quality concentrations maps of the member and cooperating countries of the European Environmental Agency (EEA)⁽¹⁾ have been prepared for the year 2021. The maps are based primarily on air quality data as reported under the Ambient air quality directives (EC, 2004, 2008). The mapping method ('Regression – Interpolation – Merging Mapping') follows the methodology developed earlier (Horálek et al., 2023, and references cited therein); it combines the monitoring data with the results from a chemical transport model and other supplementary data (such as land cover and satellite data).

Population exposure

Concentrations of PM₁₀ (i.e. particulate matter with a diameter of 10 µm or less) continued to be above the European Union (EU) and World Health Organisation (WHO) standards in large parts of Europe. Almost 6 % of the considered European population is exposed to concentrations above the EU PM₁₀ limit value of 40 µg/m³ and 72 % of population is exposed to concentrations above the WHO air quality guidance (AQG) level of 15 µg/m³ (WHO, 2021a). Moreover, 19 % of the population are estimated to live in areas where the 90.4 percentile of the PM₁₀ daily means was above the EU limit value of 50 µg/m³. Approximately 1 % and 6 % of the considered European population (excluding Türkiye in this case of PM_{2.5}) is exposed to concentrations above the EU PM_{2.5} limit value of 25 µg/m³ and to concentrations above the EU PM_{2.5} indicative limit value of 20 µg/m³, respectively. 98 % of the population is exposed to concentrations above the WHO AQG level of 5 µg/m³. Figure S.1 (top) shows that the countries with the highest values of annual averages PM_{2.5} are located in the south-eastern parts of Europe.

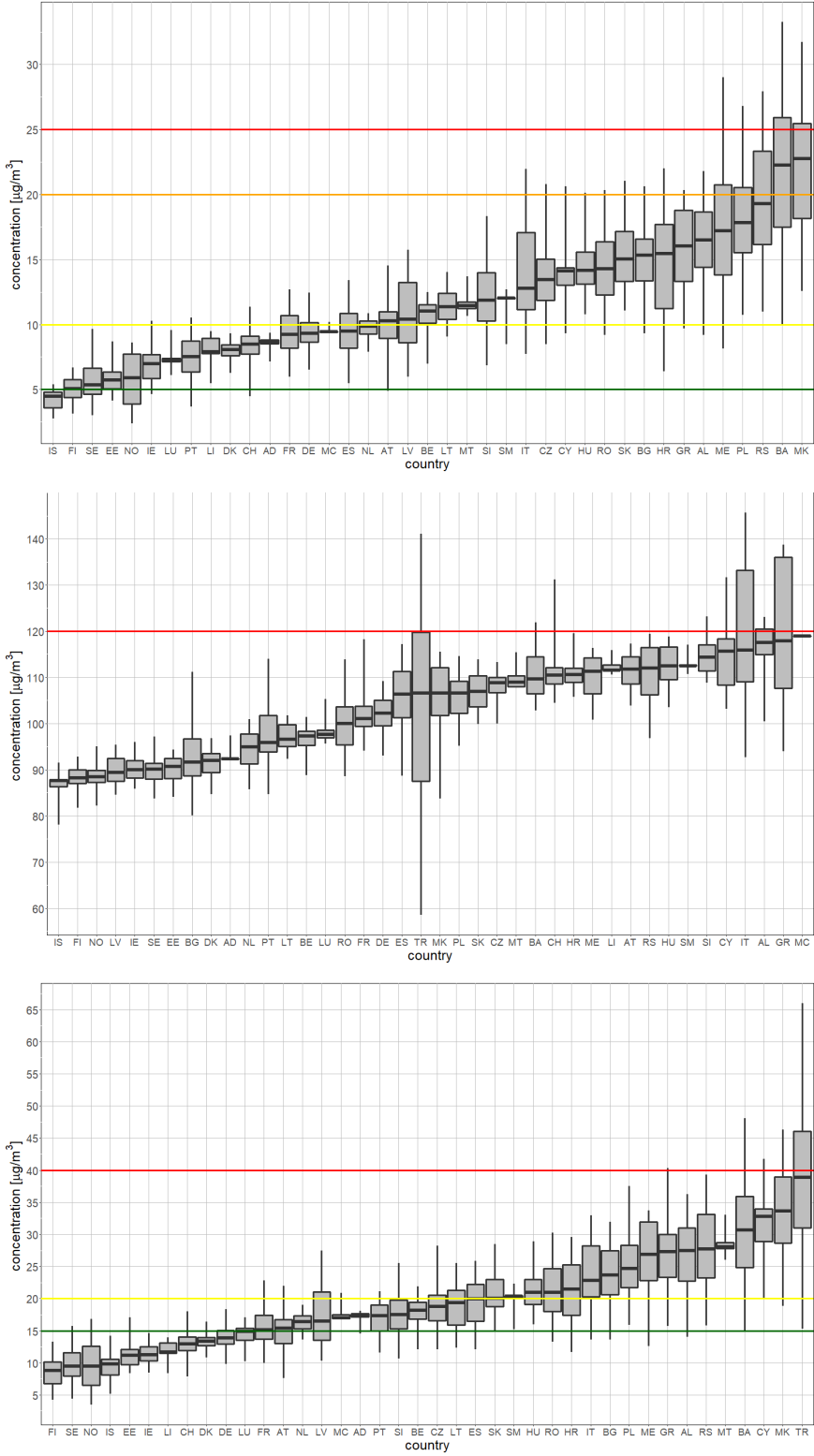
Exposure to ozone concentrations above the EU target value (TV) threshold (a maximum daily 8-hour average value of 120 µg/m³ not to be exceeded more than 25 days per year) in 2021 is particularly evident in large areas of Türkiye and Italy. More than 9 % of the considered European population live in areas where concentrations are above the ozone TV threshold. Figure S.1 (middle) shows that the countries with the highest values of the ozone indicator 93.2 percentile of maximum daily 8-hour means are located in the southern and central parts of Europe.

Approximately 3 % of the considered European population has been exposed to NO₂ concentrations above the EU annual limit value of 40 µg/m³ in 2021. Furthermore, about 74 % of the considered European population has been exposed to annual average concentrations above the WHO AQG level of 10 µg/m³. Figure S.1 (bottom) shows that in all countries apart from Türkiye, the majority of population lived well below the limit value in 2021.

Based on the experimental map of benzo(a)pyrene (BaP), it is estimated that 18 % of the considered European population live in areas where BaP concentrations are above the EU target value. The highest BaP concentrations are shown in Poland, north-eastern Czechia and some populated locations in the central and south-eastern Europe, in the eastern Po Valley in northern Italy, and in Finland.

⁽¹⁾ The EEA member countries are 27 countries of the European Union (EU-27), Iceland, Lichtenstein, Norway, Switzerland, and Türkiye. The EEA cooperating countries are Albania, Bosnia and Herzegovina, Montenegro, North Macedonia, and Serbia including Kosovo under the UN Security Council Resolution 1244/99. In addition, three microstates (Andorra, Monaco and San Marino) are also presented in this report.

Figure S.1: Concentrations of PM_{2.5} annual average (top), O₃ indicator 93.2 percentile of maximum daily 8-hour means (middle) and NO₂ annual average (bottom) to which the population per country was exposed in 2021. The EU limit value (for PM_{2.5} and NO₂) or TV threshold (for O₃) is marked by the red line, the EU indicative limit value by the orange line, the 2005 WHO AQG level by the yellow line and the 2021 WHO AQG by the green line



Note: For each country, the box plot shows the concentration to which a percentage of the population was exposed: 50 % in the case of the black marker, 25 % and 75 % in the cases of the box's edges, 2 % and 98 % in the cases of the whiskers' edges.

Accumulated risks

Out of the total population of 566 million in the mapped area, almost 8 % (42.7 million) live in areas where two or three of these air quality standards are exceeded; 0.23 % (1.2 million people) live in areas where all three standards are exceeded. In 2021, the worst situation has been observed in Greece, Türkiye, Italy (in particular the Po valley) and Cyprus.

Vegetation exposure

In a limited number of cases, concentrations of NO_x are above the EU critical level, although since most of those cases happen in urban areas, this is relevant only if there is vegetation in those areas. Ozone concentrations (AOT40 for vegetation) are above the EU target value threshold for the protection of vegetation in about 18 % of the agricultural areas and above the EU long-term objective in 81 % of the agricultural areas. Ozone concentrations (AOT40 for forests) are above the critical level for the protection of forests in about 63 % of the forested areas.

Critical levels (CL) of Phytotoxic Ozone Dose (POD₆) for wheat has been exceeded in parts of southern and south-eastern Europe. The exceedance of the CL for POD₆ for potato in 2021 is most pronounced in central south-eastern Europe and Türkiye. On the other hand, only in a few parts of the coastal areas POD₆ values above CL for tomato have occurred, similarly as in the previous years.

The CL of POD₁ for beech has been exceeded almost throughout the whole European area mapped, with the exception of limited areas in southern and south-eastern Europe. The CL of POD₁ for spruce has been exceeded almost throughout the whole European area mapped, with the exception of large areas in northern Europe.

Changes over time

Since 2005, maps for most of the pollutants have been prepared in an overall consistent way (although the mapping methodology has been subject to continuous improvement). This enables an analysis of changes in exposure over time. Apart from minor methodological changes, a major change was introduced for PM₁₀ and PM_{2.5} since 2017 maps, taking into account air quality in urban traffic areas.

For some pollutants, maps of several years are not available.

The evolution of the population-weighted concentrations, as a measure of population exposure, is shown in Figure S.2, while the evolution of the agricultural-weighted concentration is presented in Figure S.3. For comparability reasons, the results based on both the old and the new PM mapping methodology have been included in Figure S.2.

The PM population-weighted concentrations show a steady decrease of about 0.6 µg/m³ per year for PM₁₀ annual average and 0.5 µg/m³ per year for PM_{2.5} annual average. It is estimated that the considered European inhabitants have been exposed on average to an annual mean PM₁₀ concentration of 18 µg/m³ and to an annual mean PM_{2.5} concentration of 11 µg/m³ in 2021, being both the lowest values in the seventeen-year time series (together with the year 2020).

For the ozone population-weighted concentration (expressed as SOMO35) no trend is observed for the period 2005-2021, due to the year-to-year variability. Also, no trend is observed for the agricultural-weighted concentration, in terms of AOT40 for vegetation.

The NO₂ population-weighted concentration (in terms of annual average) shows a decrease of about 0.6 µg/m³ per year over the period 2005-2021 and an on-going decrease interrupted in 2021, when a slight increase in relation to 2020 is observed. This is due to the activity recovery after the lockdown due to the COVID-19 pandemics.

Figure S.2: Population-weighted concentration of PM₁₀ (annual mean), PM_{2.5} (annual mean), ozone (SOMO35), and NO₂ (annual mean) in 2005-2021. For PM₁₀ and PM_{2.5}, results based on both the old (blue dots) and the updated (red dots) mapping methodology are presented, where available

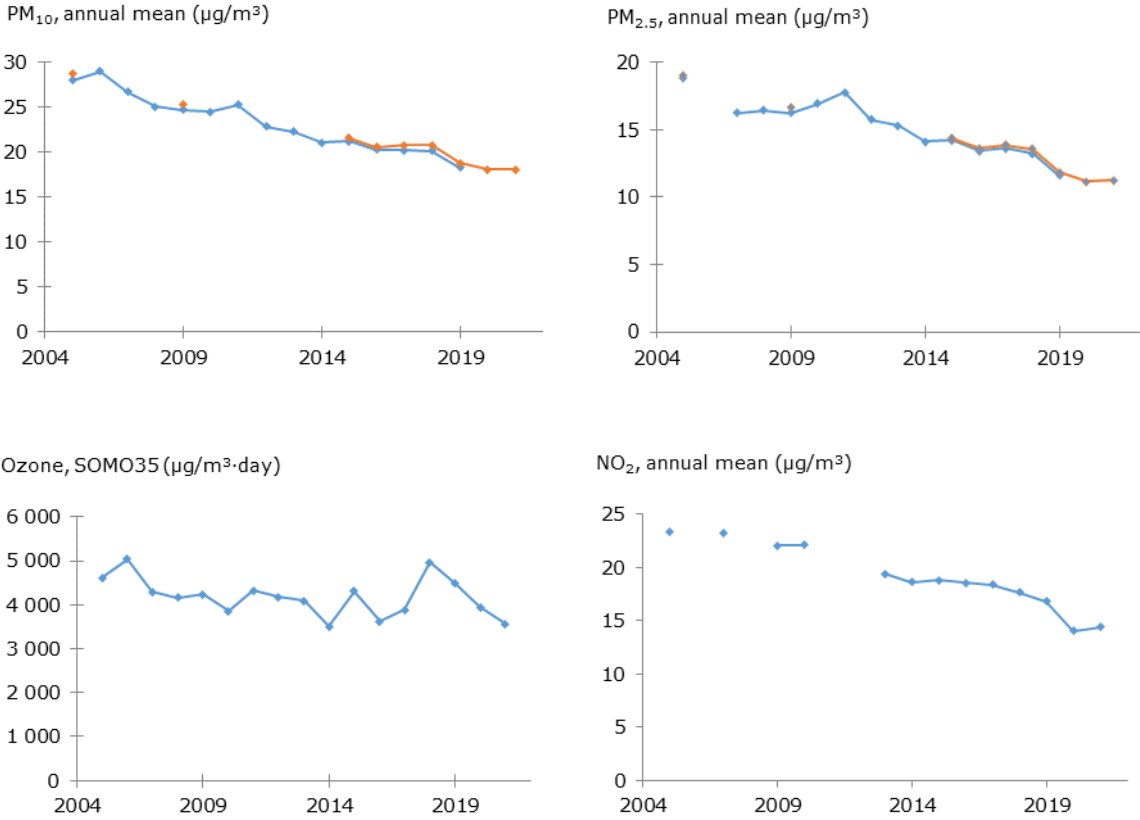
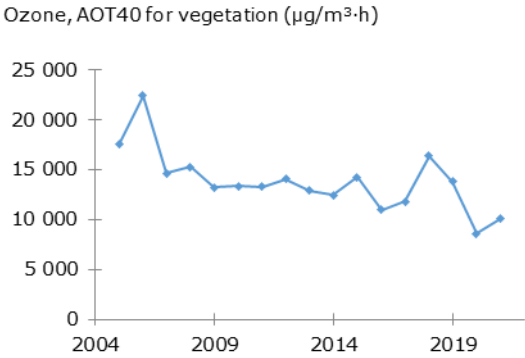


Figure S.3: Agricultural-weighted concentration of ozone indicator AOT40 for vegetation in 2005-2021



1 Introduction

This report provides air quality concentration maps, population exposure and vegetation exposure estimates for 2021 for the area of the EEA member and cooperating countries. It builds on previous similar reports (Horálek et al., 2023, and references cited therein). The analysis is based on interpolation of annual statistics of validated monitoring data from 2021, reported by the EEA member and cooperating countries (and the voluntary reporting microstate of Andorra) in 2021. Two other microstates (Monaco and San Marino) are also included in the assessment. Türkiye (including both European and Asian areas) is included in the mapping area for all pollutants except PM_{2.5}, due to the lack of PM_{2.5} reported data in 2021 to the AQ e-reporting database from rural stations in Türkiye (EEA, 2023a). Compared to the previous reports (Horálek et al., 2023, and references cited therein), the results for the United Kingdom (UK) are not presented in this report, after the country's exit of the European Union.

In this report 2021 results for particulate matter (PM₁₀ and PM_{2.5})⁽²⁾ ozone (O₃), nitrogen dioxide (NO₂), nitrogen oxides (NO_x) and benzo(a)pyrene (BaP) are presented, being the most relevant pollutants for annual updating due to their potential impacts on health and ecosystems. The analysis method applied is similar to that of previous years. Benzo(a)pyrene is presented for the second time in this regular report, based on the method shown in Horálek et al. (2022).

The mapping is primarily based on air quality measurements. It combines monitoring data, chemical transport model results and other supplementary data (such as altitude and meteorology). The method is a linear regression model followed by kriging of the residuals produced from that model ("residual kriging"). It should be noted that this methodology does not allow for formal compliance checking with the legal standards as set by the Ambient air quality directives (EC, 2004, 2008).

The maps of health-related indicators of PM₁₀, PM_{2.5}, and NO₂ are constructed by the improved mapping methodology developed in Horálek et al. (2017b, 2018, 2019): together with the rural and urban background map layers, the urban traffic map layer is constructed and incorporated into the final merged map using the road data. All individual map layers are created at 1 km resolution and land cover and road data are included in the mapping process as supplementary data. The maps of health-related indicators of ozone are created for the rural and urban (including suburban) background areas separately on a grid of 10 km resolution. Subsequently, the rural and urban background maps are merged into one final combined air quality indicator map using a 1 km population density grid, following a weighting criterion applied per grid cell. This fine resolution takes into account the smaller settlements in Europe that are not resolved at the 10 km grid resolution. The maps of ozone and NO_x vegetation-related indicators are constructed at a grid resolution of 2 km and applicable for rural areas only. They are based on rural background measurements; in the case of ozone, they serve as input to the EEA's indicator AIR004 (EEA, 2023b). The map of BaP is constructed using the rural and urban map layers that are created at the 1 km resolution and subsequently merged. The map of BaP is labelled as experimental (as recommended in Horálek et al., 2022) to indicate that it does not yet meet the same accuracy standards as the regularly produced maps of other pollutants.

Among the ozone vegetation-related indicators, maps of Phytotoxic Ozone Dose (POD₆) indicators are also presented, following the conclusions of Colette et al. (2018). POD is the ozone flux through the stomata of leaves above a specific threshold accumulated during a specified time; it is calculated based on methodology described in CLRTAP (2017a) according to Emberson et al. (2000) and Jarvis (1976).

Maps of the POD for representative species of crops in Europe i.e. wheat, potato and tomato have been presented in the regular mapping reports since maps for 2018. Maps of the POD for representative selected trees i.e. beech and spruce are presented in this report for the first time, in agreement with conclusions of Vlasáková et al. (2023). The POD indicator takes into account the plant

⁽²⁾ PM₁₀ and PM_{2.5} are particulate matter with a diameter of 10 µm and 2.5 µm or less, respectively.

physiology, not only the ozone concentrations in the ambient air (as in the AOT40 indicators), and reflects the ozone actually absorbed by the vegetation. It is widely acknowledged that the impact of ozone on vegetation is more closely related to the ozone flux absorbed through the stomata than to the exposure to ozone in the atmosphere (Musselman and Massman, 1998; Nussbaum et al., 2003). The POD annual maps are calculated based on hourly ozone rural maps (created similarly to the annual ozone maps), hourly meteorological data and the soil hydraulic properties data.

Next to the annual indicator maps, tables showing the population exposure to PM₁₀, PM_{2.5}, O₃ and NO₂, and the exposure of vegetation to ozone in terms of AOT40 indicators are presented. The tables of population exposure are prepared using the concentration and population density maps in 1 km² grid resolution. For PM₁₀, PM_{2.5} and NO₂, the population exposure in each grid cell is calculated separately for urban areas directly influenced by traffic and for the background (both rural and urban) areas, in order to better reflect the population exposed to traffic emissions. The tables of the vegetation exposure are prepared using the concentration maps in 2 km grid resolution and the Corine Land Cover 2018 dataset in 100 m resolution (EU, 2020).

All tables present exposure results for individual countries, for the EU-27, for the whole mapped area and for five large European regions. For the country grouping into the regions, see Annex 1 Map A1.1 and below: Northern Europe (N): Denmark (including Faroes), Estonia, Finland, Iceland, Latvia, Lithuania, Norway, Sweden; 2) Western Europe (without UK) (W): Belgium, France north of 45°, Ireland, Luxembourg, Netherlands; Central Europe (C): Austria, Czechia, Germany, Hungary, Liechtenstein, Poland, Slovakia, Slovenia, Switzerland; Southern Europe (S): Andorra, Cyprus, France south of 45°, Greece, Italy, Malta, Monaco, Portugal, San Marino, Spain; South-eastern Europe (SE): Albania, Bosnia and Herzegovina, Bulgaria, Croatia, Kosovo under the UN Security Council Resolution 1244/99, Montenegro, North Macedonia, Romania, Serbia (considered both including and excluding Kosovo)⁽³⁾, Türkiye.

Chapters 2, 3, 4 and 5 present the concentration maps and exposure estimates for particulate matter, ozone, NO₂ and NO_x, and benzo(a)pyrene, respectively. Chapter 4 presents only the concentration map for NO_x; concentrations above the critical level for the protection of vegetation occur in very limited areas and, as such, it is considered not to provide relevant information from the European scale perspective. Chapter 6 provides information of accumulated risks, showing in which areas population is exposed to concentrations above the legal standards for more than one pollutant. Finally, Chapter 7 summarizes the trends in exposure estimates in the period 2005-2021.

Annex 1 describes briefly the different methodological aspects. Annex 2 documents the input data applied in the 2021 mapping and exposure analysis. Annex 3 presents the technical details of the maps and their uncertainty analysis including the cross-validation results. Annex 4 presents the concentration maps including concentration values measured at the stations, in order to provide more complete information of the air quality in 2021 across Europe.

⁽³⁾ In the report, the status-neutral point of view on Kosovo under the UN Security Council Resolution 1244/99 is held.

2 Particulate matter

The Ambient Air Quality Directive (EC, 2008) sets limit values for long-term and for short-term PM₁₀ concentrations and for long-term PM_{2.5} concentrations. The EU long-term annual PM₁₀ limit value is set at 40 µg/m³. The Air Quality Guideline level recommended by the World Health Organization (WHO) in 2005 (WHO, 2005) for the PM₁₀ annual average was 20 µg/m³. In September 2021, WHO introduced its new Air Quality Guidelines (WHO, 2021a). The current Air Quality Guideline level for the PM₁₀ annual average is set to 15 µg/m³. The EU short-term limit value indicates that the daily average PM₁₀ concentration should not exceed 50 µg/m³ during more than 35 days per year. It corresponds to the 90.4 percentile of daily PM₁₀ concentrations in one year. This daily limit value is the most frequently exceeded air quality PM limit value in Europe. The Air Quality Guideline levels recommended by the World Health Organization in 2005 (WHO, 2005) and in 2021 (WHO, 2021a) for short-term PM₁₀ concentrations indicates that the 99 percentile of the daily average PM₁₀ concentrations should not exceed 50 µg/m³ and 45 µg/m³, respectively (99th percentile means 3-4 exceedance days per year).

The EU annual limit value for the annual average PM_{2.5} concentrations (ALV) is set at 25 µg/m³. In EC (2008), there is also an indicative limit value (ILV) of 20 µg/m³ defined as Stage 2, in place since 2020. The Air Quality Guideline level recommended by the World Health Organization in 2005 (WHO, 2005) for the PM_{2.5} annual average was 10 µg·m⁻³. The current Air Quality Guideline level as introduced by the WHO in September 2021 (WHO, 2021a) for the PM_{2.5} annual average is set to 5 µg/m³.

This chapter presents the 2021 situation in relation to of two EU PM₁₀ limit values, i.e. the annual average and the 90.4 percentile of the daily averages, and the PM_{2.5} annual average. The 90.4 percentile of the daily averages is a more relevant PM₁₀ indicator in the context of the Ambient Air Quality Directive (EC, 2008) than the 36th highest daily mean, which was used up to 2013 maps (Horálek et al., 2017a).

The maps of PM₁₀ and PM_{2.5} are based on the improved mapping methodology developed and tested in Horálek et al. (2019). The map layers are created for the rural, urban background and urban traffic areas separately on a grid at 1 km resolution. Subsequently, the urban background and urban traffic map layers are merged together using the gridded GRIP road data (Meijer et al., 2018) into one urban map layer. This urban map layer is further combined with the rural map layer into the final PM₁₀ or PM_{2.5} map using a population density grid at 1 km resolution. For details, see Annex 1, Section A1.1. The supplementary data used are chemical transport model (CTM) output, altitude, wind speed and land cover for rural areas, CTM output for urban background areas and CTM output and wind speed for urban traffic areas (Annex 3, Sections A3.1 and A3.2). For all PM₁₀ and PM_{2.5} indicators, the final combined map is presented in the 1 km grid resolution. Be it noted that this final map is representative for rural and urban background areas, but not for urban traffic areas (which are smoothed in this 1 km spatial resolution).

The current number of PM_{2.5} measurement stations is still somewhat limited and its spatial distribution is irregular over Europe. Therefore, in this paper the mapping of the health-related indicator PM_{2.5} annual average is based on a mapping methodology developed in Denby et al. (2011). This methodology derives additional pseudo PM_{2.5} annual mean concentrations from PM₁₀ annual mean measurement concentrations. As such, it increases the number and spatial coverage of PM_{2.5} 'data points' and these data are used to derive a European wide map of annual mean PM_{2.5}. Pseudo PM_{2.5} stations data are estimated using PM₁₀ measurement data, surface solar radiation, latitude and longitude.

The population exposure tables are calculated based on the concentration maps, according to the methodology described in Horálek et al. (2019), i.e. they are calculated separately for urban areas directly influenced by traffic and for the background (both rural and urban) areas, in order to better reflect the population exposed to traffic. For details, see Annex 1, Equation A1.6.

Annex 3, Sections A3.1 and A3.2 provide details on the regression and kriging parameters applied for deriving the PM₁₀ and PM_{2.5} maps, as well as the uncertainty analysis of these maps.

2.1 PM₁₀ annual average

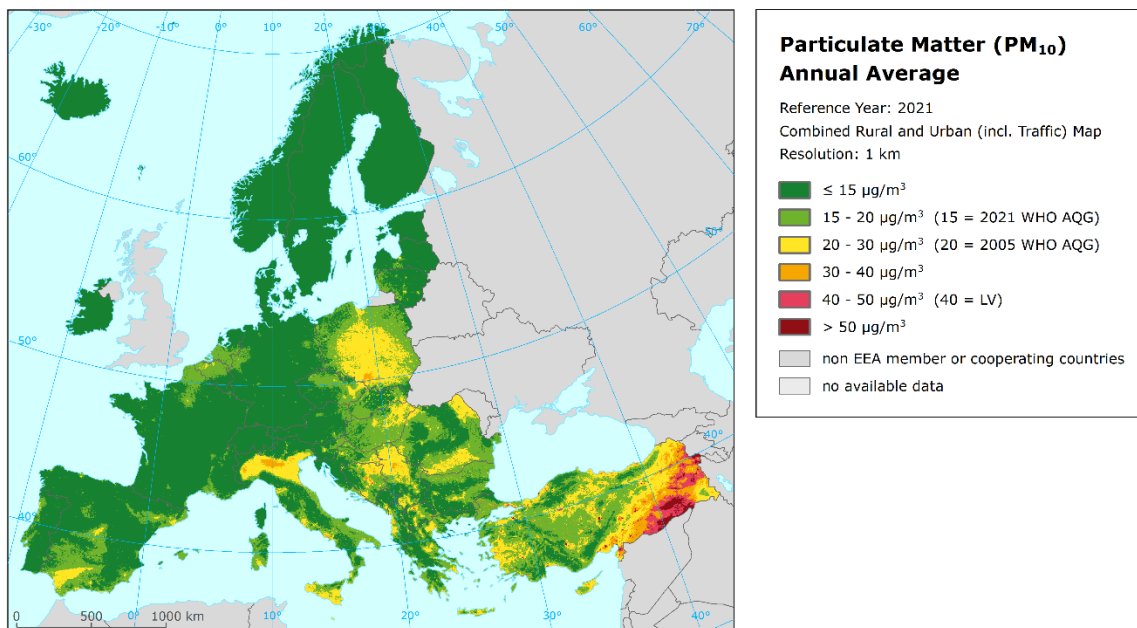
Concentration map

Map 2.1 presents the final combined concentration map for the 2021 PM₁₀ annual average. Red and purple areas indicate concentrations above the limit value (LV) of 40 µg/m³.

The stations are not presented in the map, in order to better visualise the urban areas. However, concentration values from the station measurements used in the kriging interpolation methodology (Annex 3, Section A3.1) are considered to provide relevant information to the concentration map. In Map A4.1 of Annex 44 these point values are presented on top of Map 2.1. This illustrates the smoothing effect that the interpolation method can have on the gridded concentration fields.

Map 2.1 shows annual mean concentrations above the LV in urban areas of south-eastern Europe states (Bosnia and Herzegovina, North Macedonia, Serbia,). A larger, more continuous area with concentrations above LV occurs in the south-eastern and eastern parts of Türkiye. In general, the south-eastern, the south and the central parts of Europe appear with higher concentrations and population-weighted concentrations than the western and the northern parts.

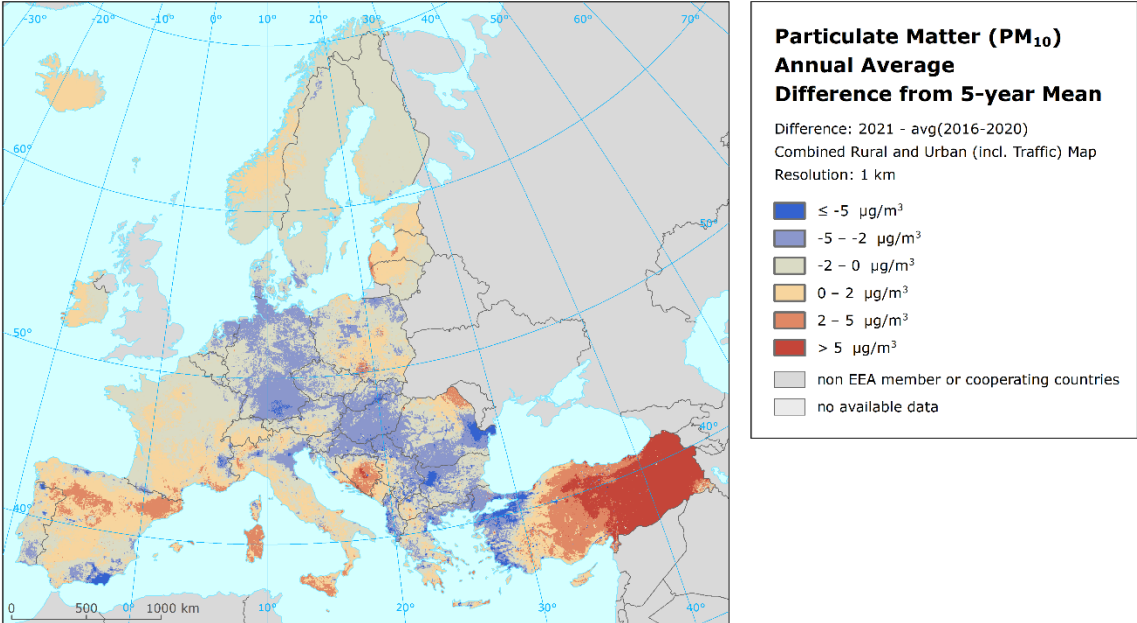
Map 2.1: Concentration map of PM₁₀ annual average, 2021



Map 2.2 presents the difference between 2021 and the five-year mean 2016-2020 for annual average for PM₁₀. Orange to red areas show an increase of PM₁₀ concentration in 2021, while blue areas show a decrease.

At the annual average PM₁₀ difference map the highest increases are observed in Türkiye, parts of southern and south-eastern Europe with the highest increases in Bosnia and Herzegovina and north-eastern Romania, parts of Italy (Sicily and Sardinia), parts of Spain, Portugal and France and parts of central and northern Europe (south of Poland and coastal areas of Lithuania and Latvia. On the other hand, there are decreases in the remaining countries, mainly central Europe, parts of some countries in south-eastern Europe and parts of Spain and Portugal.

Map 2.2: Difference concentrations between 2021 and the five-year mean 2016-2020 for PM₁₀ annual average



Be it noted that besides the actual changes in the concentrations, the variability of the linear regression model and variogram parameters, changes in the measurement network and changes in the dispersion model may cause minor differences in the concentration levels estimated.

The uncertainty of the concentration map can be expressed in relative terms of the absolute Root Mean Square Error (RMSE) uncertainty related to the mean air pollution indicator value for all stations (see Annex 1, Section A1.4). This relative mean uncertainty (RRMSE) of the final combined map of PM₁₀ annual average is 25 % for rural areas and 29 % for urban background areas including Turkish stations (i.e. quite similar to the last years), and respectively 21 % for rural areas and 19 % for urban background areas without Turkish stations (Annex 3, Section A3.1). This means quite good mapping uncertainty, compared to the data quality objective for models of PM₁₀ annual average (i.e. 50 %) as set in the Air Quality Directive (EC, 2008). The main reason for presenting the results also without Turkish stations is to enable the comparison with previous years.

Population exposure

Figure 2.1 give the population frequency distribution for a limited number of exposure classes to PM₁₀ concentrations. More detailed Table 2.1 also presents the 2021 population-weighted concentration and the difference in the population-weighted concentrations between 2021 and the five-year mean 2016-2020 for individual countries, for five European regions, for EU-27, and for the total mapped area according to Equation A1.7.

It is estimated that 71.5 % and 43.5 % of the considered European population⁽⁴⁾, including Türkiye⁽⁵⁾, has been exposed to annual average concentrations above the current 2021 and the 2005 WHO Air Quality Guideline levels of 15 µg/m³ (WHO, 2021a) and 20 µg/m³ (WHO, 2005), respectively. The same is true for 68 % and 35 % of the EU-27 population.

Approximately 6 % of population of the considered mapped area has been exposed to concentrations above the EU annual limit value (ALV) of 40 µg/m³; the same is the case for around 0.1 % of the EU-27 population.

No population has been exposed to concentrations above the ALV in 33 countries. A limited fraction of the population (up to 16 %) has been exposed to concentrations above the ALV in Poland, Serbia, Greece, Cyprus and Bosnia and Herzegovina (in ascending order). More than 24 % of the population has been exposed to concentrations above the ALV in North Macedonia. And, finally, almost 45 % of the population has been exposed to concentrations above the ALV in Türkiye. However, as the current mapping methodology tends to underestimate high values (see Annex 3, Section A3.1), the percentage of population exposed to concentrations above the ALV will most likely be underestimated. Additional population exposure above the ALV could therefore be expected in countries like Poland, Cyprus, North Macedonia, Montenegro, Serbia, Bosnia and Herzegovina, Albania, Türkiye and Greece and where a relatively large fraction (ca. 20-60 %) of the population lives in areas with concentration levels 30-40 µg/m³.

The population-weighted concentration of the annual average for 2021 for the considered European population is estimated to be about 22 µg/m³ including Türkiye and about 19 µg/m³ for the EU-27 only. The value for considered European population including Türkiye and EU-27 decreased by about 1.5 µg/m³ and 1.6 µg/m³ compared to the previous five-year mean 2016-2020. When assessing the absolute change in individual countries, the steepest decrease was found in Bulgaria (6.4 µg/m³), the highest increase was estimated in Türkiye (4.7 µg/m³).

⁽⁴⁾ We consider Europe apart from the United Kingdom, Belarus, Moldova, Ukraine and the European parts of Russia and Kazakhstan.

⁽⁵⁾ The whole Turkish population, both European and Asian.

Table 2.1: Population exposure and population-weighted concentration, PM₁₀ annual average, 2021

Country	ISO	Population (inhbs·1000)	PM ₁₀ – annual average, exposed population (%)						Population-weighted concentration		
			< 15	15-20	20-30	30-40	40-50	> 50	2021	5-year mean	Diff.
Albania	AL	2 830	3.8	11.8	52.0	32.4			26.8	30.4	-3.7
Andorra	AD	79	2.4	97.6					17.2	21.1	-3.9
Austria	AT	8 933	45.5	50.3	4.3				14.8	16.8	-2.0
Belgium	BE	11 555	8.4	73.3	18.3				18.0	19.1	-1.1
Bosnia and Herzegovina	BA	3 271	2.0	9.0	33.9	39.2	15.4	0.5	30.8	32.8	-2.0
Bulgaria	BG	6 917	3.8	17.0	71.9	7.3			23.8	30.1	-6.4
Croatia	HR	4 036	10.1	27.9	60.7	1.3			21.3	23.7	-2.4
Cyprus	CY	9 343		1.9	29.7	60.9	7.4		31.5	33.3	-1.9
Czechia	CZ	10 782	14.7	54.9	29.9	0.6			18.8	21.3	-2.5
Denmark (incl. Faroe Islands)	DK	5 840	95.4	4.6					13.3	15.5	-2.2
Estonia	EE	1 330	94.6	5.4					11.2	11.3	-0.2
Finland	FI	5 534	99.2	0.8					8.6	9.4	-0.8
France (metropolitan)	FR	65 447	47.4	48.6	4.1				15.5	16.5	-1.0
Germany	DE	83 155	74.5	24.9	0.6				14.0	16.3	-2.3
Greece	GR	10 679	1.4	9.0	64.5	22.7	2.4		27.1	28.9	-1.8
Hungary	HU	9 731	0.4	34.4	64.8	0.4			21.2	24.3	-3.1
Iceland	IS	369	100.0						9.4	9.7	-0.3
Ireland	IE	5 006	99.3	0.7					11.4	11.9	-0.5
Italy	IT	59 236	3.7	19.4	62.2	14.8			23.6	24.5	-0.8
Latvia	LV	1 893	37.4	28.3	33.3	1.0			17.3	17.1	0.2
Liechtenstein	LI	39	100.0						12.0	12.7	-0.6
Lithuania	LT	2 796	17.5	38.8	43.8				18.9	18.6	0.4
Luxembourg	LU	635	54.9	45.1					14.4	16.0	-1.6
Malta	MT	516			89.8	10.2			28.5	27.8	0.7
Monaco	MC	37		79.0	21.0				17.8	21.0	-3.2
Montenegro	ME	621	8.3	10.3	41.1	40.3			26.1	26.5	-0.4
Netherlands	NL	17 475	19.4	80.5	0.1				16.3	18.0	-1.7
North Macedonia	MK	2 069	0.5	2.2	29.2	43.8	24.3		33.9	39.5	-5.5
Norway	NO	5 391	97.1	2.9					9.6	10.1	-0.5
Poland	PL	37 840	0.8	14.1	65.8	19.3	0.0		25.3	26.9	-1.6
Portugal (excl. Azores, Madeira)	PT	9 802	25.3	65.5	9.2				17.0	18.1	-1.1
Romania	RO	19 202	6.0	34.8	56.8	2.4			21.4	24.1	-2.7
San Marino	SM	34	1.8	18.6	79.6				20.0	21.3	-1.3
Serbia (incl. Kosovo)	RS	8 534	1.4	6.1	51.3	40.0	1.2		28.1	33.9	-5.8
Slovakia	SK	5 460	2.2	47.5	50.3				20.8	22.9	-2.1
Slovenia	SI	2 109	22.8	54.3	22.8				17.8	20.8	-3.1
Spain (excl. Canarias)	ES	45 154	12.9	38.0	49.1				19.4	20.0	-0.5
Sweden	SE	10 379	97.0	3.0					9.8	11.1	-1.4
Switzerland	CH	8 670	88.1	11.0	0.9				12.9	14.1	-1.2
Türkiye	TR	83 614	1.7	8.3	13.0	32.3	25.2	19.5	39.1	34.4	4.7
Total		566 342	28.5	28.0	27.8	9.4	3.7	2.6	21.5	23.0	-1.5
			56.5				6.3				
EU-27		450 785	32.1	32.7	30.4	4.7	0.1		18.5	20.1	-1.6
			64.8				0.1				
Northern Europe		32 080	85.7	8.0	6.3	0.1			11.6		
Western Europe (without UK)		81 150	39.6	56.0	4.5				15.8		
Central Europe		162 777	44.8	26.6	24.0	4.6	0.0		17.7		
Southern Europe		140 620	12.3	30.5	48.6	8.4	0.2		21.3		
South-Eastern Europe		121 885	2.9	13.7	30.2	25.7	15.9	11.5	33.1		
Kosovo	KS	1 662	0.9	11.4	87.3	0.4			23.4	33.4	-10.0
Serbia (excl. Kosovo)	RS-	6 872	1.5	4.8	42.5	49.7	1.5		29.3	34.0	-4.7

Note: The percentage value "0.0" indicates that an exposed population exists, but it is small and estimated to be less than 0.05 %. Empty cells mean no population in exposure. 5-year mean, i.e. five-year mean 2016-2020. Diff., i.e. difference concentrations between 2021 and five-year mean 2016-2020.

Figure 2.1: Percentage of the population (%) exposed to different PM₁₀ annual averages (µg/m³) at country level, 2021

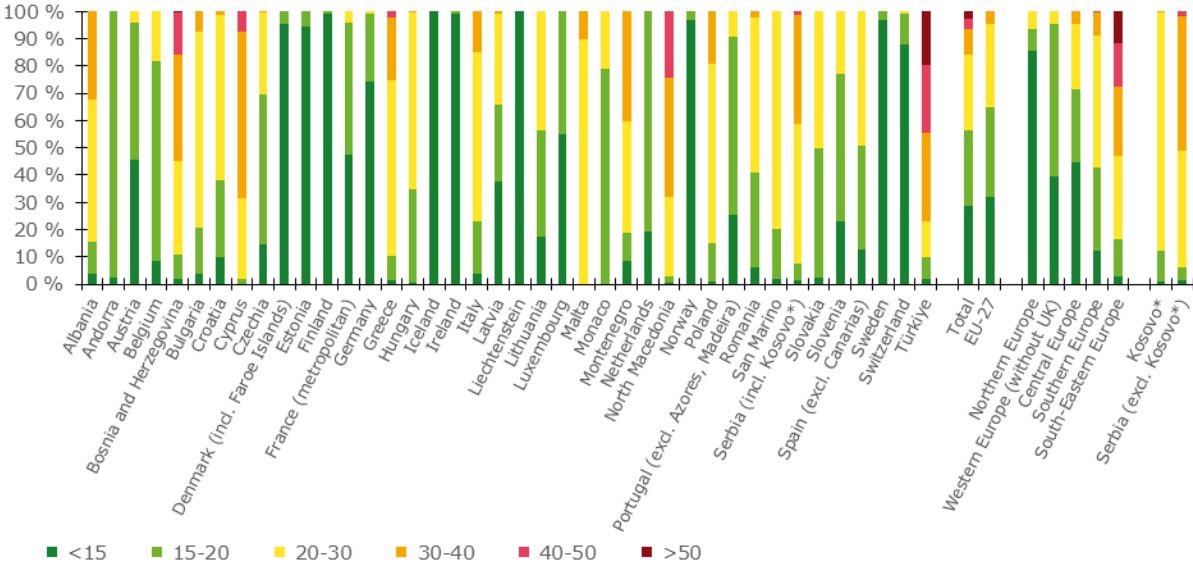
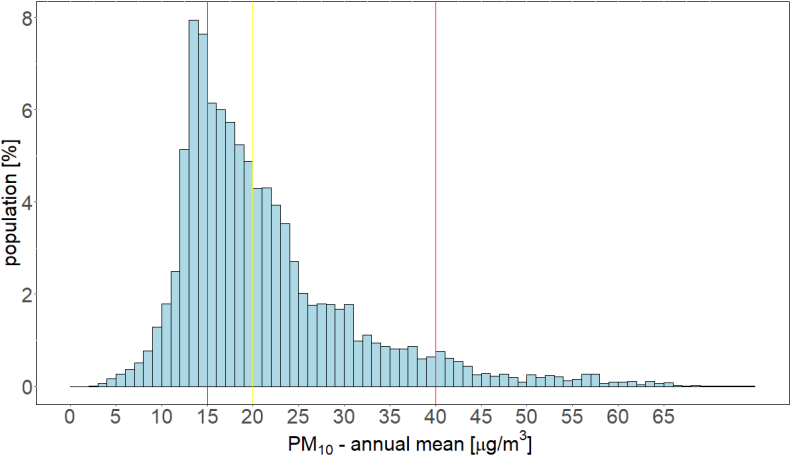


Figure 2.2 shows, for the whole mapped area, the population frequency distribution for exposure classes of 1 µg/m³. The highest population frequency can be seen for classes between 13 and 20 µg/m³. One can see a quite continuous strong decline of population frequency for classes between 20 and 30 µg/m³ and a mild decline for classes beyond 40 µg/m³.

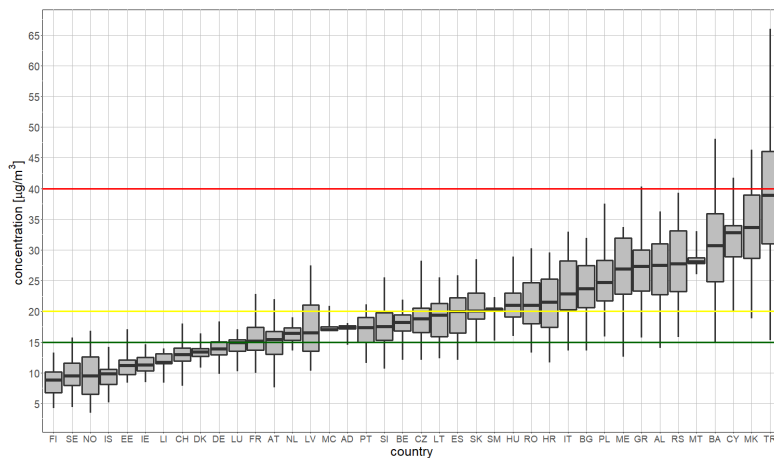
Figure 2.2: Population frequency distribution, PM₁₀ annual average, 2021. The 2021 WHO AQG level (15 µg/m³) is marked by the green line, the 2005 WHO AQG level (20 µg/m³) is marked by the yellow line, the EU annual limit value (40 µg/m³) is marked by the red line



Note: Apart from the population distribution shown in the graph, it was estimated that 0.19 % of population lived in areas with PM₁₀ annual average concentrations between 75 and 246 µg/m³.

Figure 2.3 shows for individual countries the PM₁₀ annual average concentrations to which the population per country was exposed in 2021. It can be seen that the countries with the highest values of PM₁₀ annual average are located in the central and south-eastern parts of Europe.

Figure 2.3: PM₁₀ annual average concentrations to which the population per country was exposed in 2021. The 2021 WHO AQG level (15 µg/m³) is marked by the green line, the 2005 WHO AQG level (20 µg/m³) is marked by the yellow line, the EU annual limit value (40 µg/m³) is marked by the red line



Note: For each country, the box plot shows the concentration to which a percentage of the population was exposed: 50 % in the case of the black marker, 25 % and 75 % in the cases of the box's edges, 2 % and 98 % in the cases of the whiskers' edges.

2.2 PM₁₀ – 90.4 percentile of daily means

The Ambient Air Quality Directive (EC, 2008) describes the PM₁₀ daily limit value (DLV) as “a daily average of 50 µg/m³ not to be exceeded more than 35 times a calendar year”. This requirement can be evaluated by the indicator 36th highest daily mean, which is in principle equivalent to the indicator 90.4 percentile of daily mean. However, for measurement data these two indicators are equivalent only if no data is missing, which is in general not the case. As shown in de Leeuw (2012), the additional uncertainty related to incomplete time series is substantially smaller when using percentile values instead of the x-th highest value. Furthermore, the Air Quality Directive requires the use of the 90.4 percentile when random measurements are used to assess the requirements of the PM₁₀ DLV. As in the previous reports since the maps for 2014 (Horálek et al., 2017a), the PM₁₀ daily means are expressed as the 90.4 percentile instead of the formerly used 36th highest daily mean.

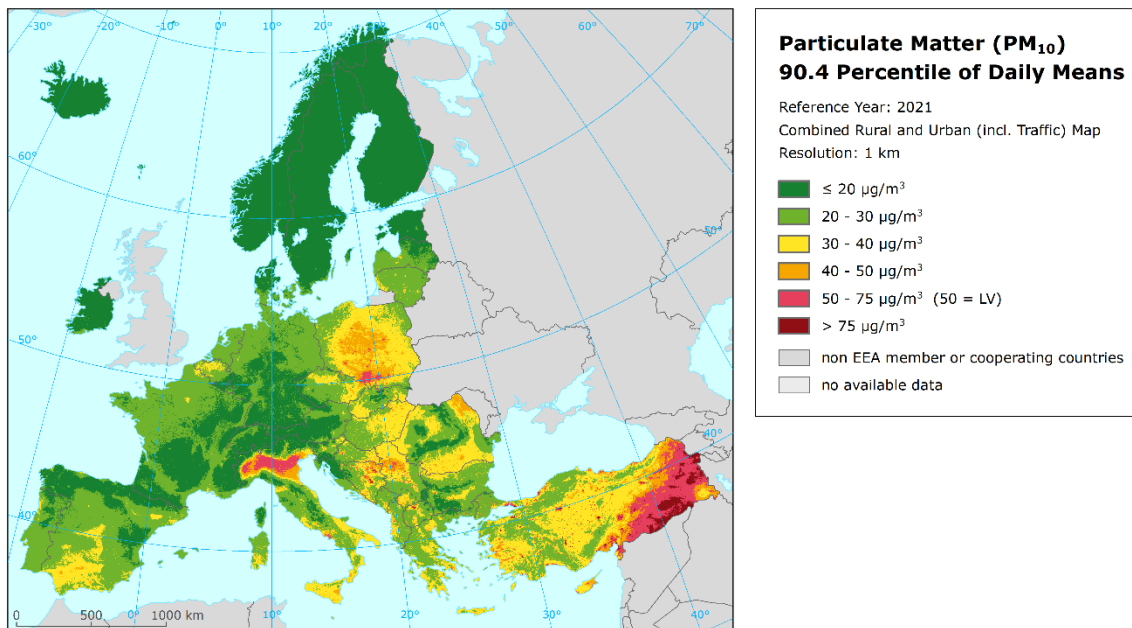
Concentration map

Map 2.3 presents the final combined map, where red and purple marked areas indicate values of the 90.4 percentile of daily means above 50 µg/m³ (i.e. values of this indicator above the DLV of 50 µg/m³ on more than 35 measurement days). The similar mapping procedure as in the case of the annual average is used. The mapping details and the uncertainty analysis are presented in Annex 3. Large areas with concentrations above the DLV are observed in northern Italy (i.e. the Po Valley), in the industrial region Ostrava (Czechia) – Katowice (Poland) – Krakow (Poland) and in south-eastern and eastern parts of Türkiye. Urban and surrounding areas with concentrations above the DLV are observed in Albania, Bosnia and Herzegovina, Bulgaria, Croatia, Cyprus, Greece, Hungary, Italy, Montenegro, North Macedonia, Poland, Romania, Serbia and Türkiye, as in previous years.

In general, the south-eastern, the south and the central parts of Europe appear with higher concentrations and population-weighted concentrations than the western and the northern parts.

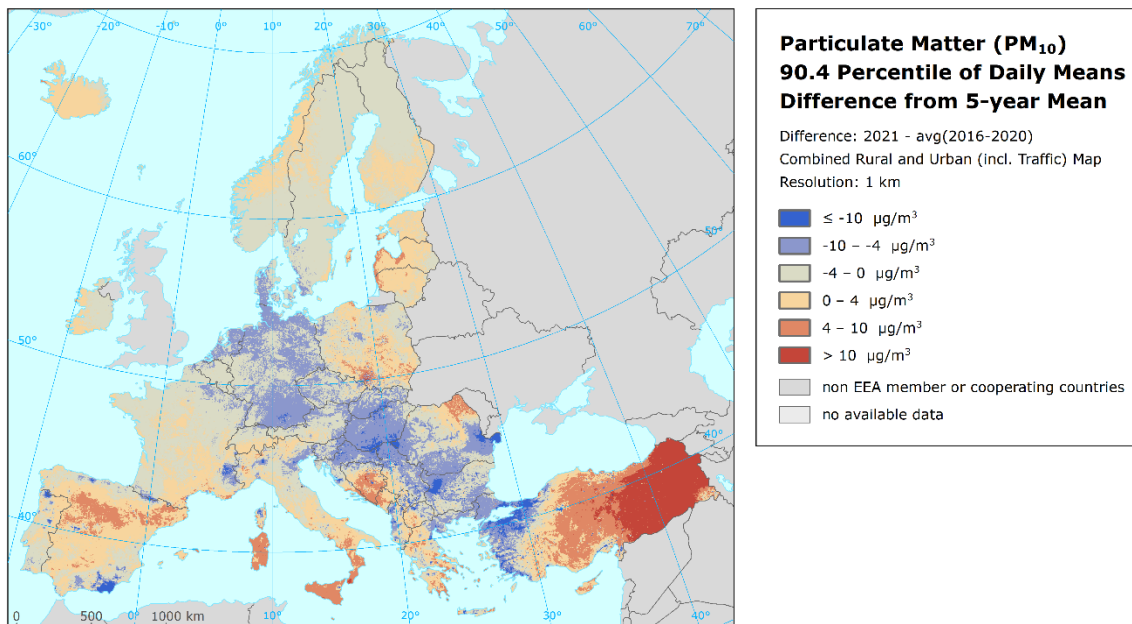
The relative mean uncertainty (relative RMSE) of the final combined map of the 90.4 percentile of PM₁₀ daily means is 28 % for rural areas and 37 % for urban background areas including Turkish stations. The mean uncertainty for the map without Türkiye is 23 % for both rural and urban background areas (Annex 3, Section A3.1). Thus, the mapping uncertainty of this is at the similar level as in the case of the PM₁₀ annual average.

Map 2.3: Concentration map of PM₁₀ indicator 90.4 percentile of daily means, 2021



Map 2.4 presents the difference between 2021 and the five-year mean 2016-2020 for the 90.4 percentile of daily means for PM₁₀. Orange to red areas show an increase of PM₁₀ concentration in 2021, while blue areas show a decrease.

Map 2.4: Difference concentrations between 2021 and the five-year mean 2016-2020 for PM₁₀ 90.4 percentile



The situation is similar to that of the annual average value of PM₁₀. The highest increases are observed in large parts of Türkiye, in parts of southern and south-eastern Europe with the highest increases in Bosnia and Herzegovina and north-eastern Romania, parts of Italy (southern Italy, Sicily and Sardinia),

parts of Spain and France and parts of central and northern Europe (south of Poland and coastal areas of Lithuania and Latvia). On the other hand, there are decreases in the remaining countries, mainly central Europe (Germany, Hungary), parts of some countries in south-eastern Europe (Croatia, Romania and Bulgaria) and parts of Spain and France.

Population exposure

Figure 2.4 give the population frequency distribution for a limited number of exposure classes to PM₁₀ indicator 90.4 percentile of daily means. More detailed Table 2.2 also presents the 2021 population-weighted concentration and the difference in the population-weighted concentrations between 2021 and the five-year mean 2016-2020 for individual countries, for five European regions, for EU-27, and for the total mapped area according to Equation A1.7.

In 2021 about 19 % of the considered European population including Türkiye and 8 % of the EU-27 population are estimated to live in areas with PM₁₀ concentrations above the EU limit value of 50 µg/m³.

No population has been exposed to concentrations above the DLV in 22 countries. A limited fraction of the population (>1-16 %) has been exposed to concentrations above the DLV in Latvia, Czechia, Romania, Hungary, Kosovo, Slovakia, Croatia, Malta and Bulgaria (in ascending order). More than 20 % but less than 50 % of the population has been exposed to concentrations above the DLV in Greece, Poland, Italy and Serbia. More than half of the population has been estimated to be exposed to concentrations above the DLV in Albania (53 %), Cyprus, Bosnia and Herzegovina, Montenegro, Türkiye and North Macedonia (87 %).

The European-wide population-weighted concentration of the 90.4 percentile of PM₁₀ daily means is estimated for 2021 at about 37 µg/m³ for the total mapped area and 32 µg/m³ for the EU-27. The population-weighted concentration of this PM₁₀ indicator decreased by about 3 µg/m³ for the considered European population and for EU-27 and compared to the previous five-year mean 2016-2020. When assessing the absolute change in individual countries, the steepest decrease was found in North Macedonia (17 µg/m³), the highest increase was estimated in Malta (4.4 µg/m³).

Figure 2.4: Percentage of the population (%) exposed to different values of PM₁₀ indicator 90.4 percentile of daily means, 2021

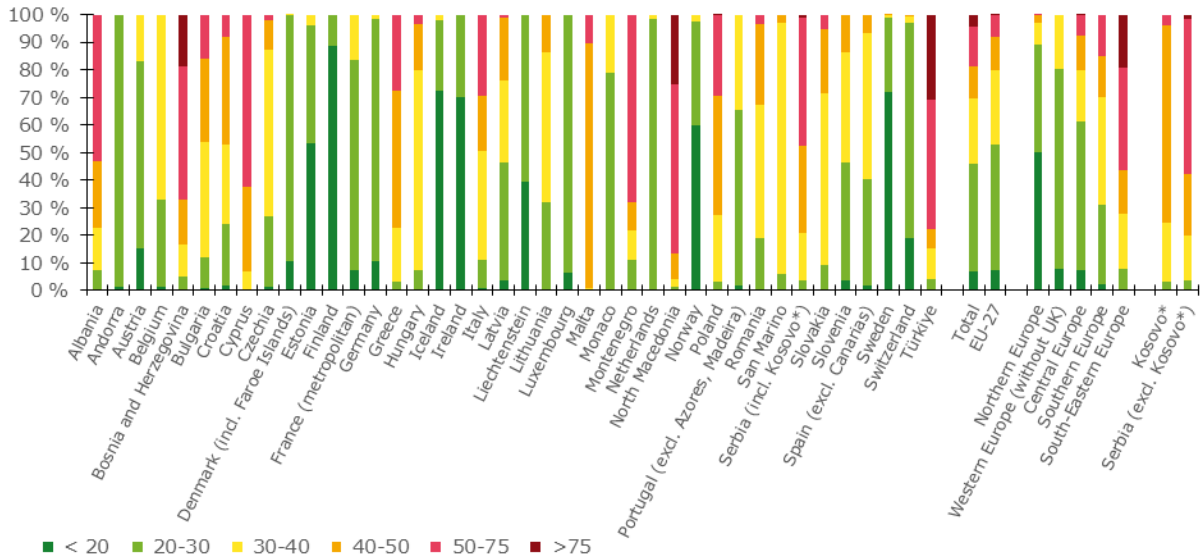


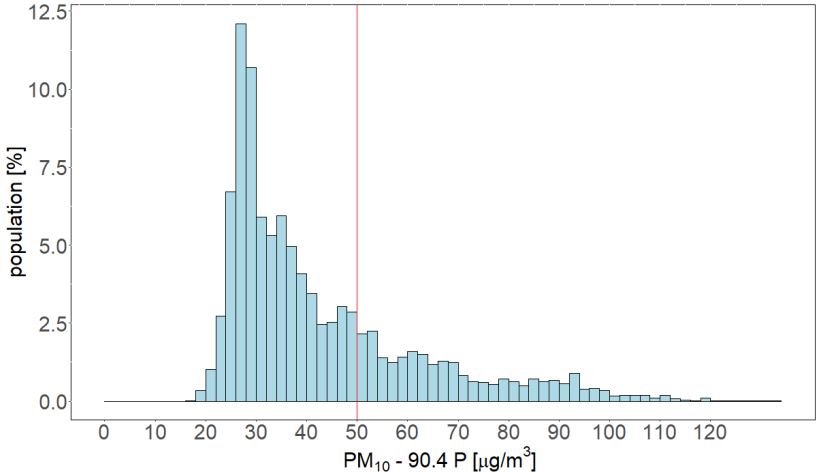
Table 2.2: Population exposure and population-weighted concentrations, PM₁₀ indicator 90.4 percentile of daily means, 2021

Country	ISO	Population (inhbs-1000)	PM ₁₀ - perc90.4, exposed population (%)					Population-weighted concentration			
			< 20	20-30	30-40	40-50	50-75	> 75	2021	5-year mean	Diff.
Albania	AL	2 830	0.0	7.2	15.4	24.3	53.0		47.3	56.0	-8.7
Andorra	AD	79	1.1	98.9					28.8	38.8	-9.9
Austria	AT	8 933	15.1	68.2	16.7				25.7	29.7	-4.1
Belgium	BE	11 555	1.3	31.4	67.3				30.5	33.6	-3.0
Bosnia and Herzegovina	BA	3 271	0.0	4.8	12.0	15.8	48.3	19.0	58.9	68.0	-9.1
Bulgaria	BG	6 917	0.6	11.2	42.1	30.1	15.9	0.0	40.4	54.7	-14.3
Croatia	HR	4 036	1.8	22.0	29.1	38.7	8.3		38.3	46.1	-7.8
Cyprus	CY	9 343			6.7	30.9	62.4		52.3	52.5	-0.2
Czechia	CZ	10 782	1.3	25.5	60.4	10.6	2.2		33.5	38.4	-4.9
Denmark (incl. Faroe Islands)	DK	5 840	10.4	89.4	0.3				22.4	26.3	-4.0
Estonia	EE	1 330	53.3	42.8	4.0				20.1	20.1	0.0
Finland	FI	5 534	88.5	11.5					16.5	16.9	-0.3
France (metropolitan)	FR	65 447	7.2	76.5	16.3	0.0			25.8	27.8	-2.0
Germany	DE	83 155	10.7	87.8	1.5				23.2	27.7	-4.5
Greece	GR	10 679	0.0	3.1	19.5	49.8	27.6		45.9	48.7	-2.8
Hungary	HU	9 731		7.5	72.1	17.0	3.4		36.9	44.1	-7.2
Iceland	IS	369	72.2	25.6	2.2				18.2	17.4	0.8
Ireland	IE	5 006	70.1	29.9	0.0				19.0	21.0	-2.0
Italy	IT	59 236	0.6	10.2	39.6	20.1	29.5		42.4	43.4	-1.0
Latvia	LV	1 893	3.7	42.6	29.8	22.9	1.1		32.2	29.4	2.8
Liechtenstein	LI	39	39.2	60.8		0.7	89.1	10.2	46.6	42.2	4.4
Monaco	MC	37		79.0	21.0				27.4	32.7	-5.3
Montenegro	ME	621	0.0	10.8	10.8	10.5	67.9		51.1	51.9	-0.9
Netherlands	NL	17 475	0.0	98.4	1.6				26.0	30.0	-3.9
North Macedonia	MK	2 069	0.0	1.3	2.6	9.2	61.5	25.4	64.2	81.2	-17.0
Norway	NO	5 391	59.7	37.8	2.5				17.6	18.9	-1.3
Poland	PL	37 840	0.0	3.1	24.3	43.2	29.2	0.1	46.2	48.6	-2.4
Portugal (excl. Azores, Madeira)	PT	9 802	1.7	63.5	34.8				28.3	30.0	-1.7
Romania	RO	19 202	0.3	18.7	48.1	29.6	3.3		36.6	41.5	-4.8
San Marino	SM	34		5.9	91.1	3.0			34.8	38.9	-4.1
Serbia (incl. Kosovo)	RS	8 534	0.1	3.3	17.2	32.0	46.1	1.3	50.6	65.1	-14.6
Slovakia	SK	5 460	0.1	8.9	62.4	23.5	5.2		36.6	42.1	-5.5
Slovenia	SI	2 109	3.7	42.6	40.0	13.8			31.0	38.3	-7.3
Spain (excl. Canarias)	ES	45 154	1.8	38.4	53.0	6.8			31.7	32.5	-0.9
Sweden	SE	10 379	72.1	26.8	1.1	0.0			17.6	20.0	-2.4
Switzerland	CH	8 670	19.0	78.1	2.3	0.6			22.5	25.2	-2.7
Türkiye	TR	83 614	0.0	4.1	10.9	6.9	47.3	30.7	66.9	70.8	-3.9
Total		566 342	6.9	38.9	23.7	11.5	14.6	4.4	37.0	40.4	-3.4
			45.8				19.0				
EU-27		450 785	7.5	45.4	26.8	12.1	8.1	0.0	31.9	34.9	-3.0
			52.9				8.2				
Northern Europe		32 080	50.2	39.0	8.0	2.8	0.1		20.8		
Western Europe (without UK)		81 150	7.6	72.7	19.6				26.1		
Central Europe		162 777	7.1	54.2	18.3	12.9	7.4	0.0	30.8		
Southern Europe		140 620	2.2	28.9	39.0	14.9	15.0		36.6		
South-Eastern Europe		121 885	0.2	7.6	20.0	15.8	37.2	19.2	57.3		
Kosovo	KS	1 662		2.9	21.5	71.5	4.0		42.8	68.2	-25.4
Serbia (excl. Kosovo)	RS-	6 872	0.1	3.4	16.1	22.3	56.4	1.7	52.5	64.4	-11.9

Note: The percentage value "0.0" indicates that an exposed population exists, but it is small and estimated to be less than 0.05 %. Empty cells mean no population in exposure. 5-year mean, i.e. five-year mean 2016-2020. Diff., i.e. difference concentrations between 2021 and five-year mean 2016-2020.

Figure 2.5 shows, for the whole mapped area, the population frequency distribution for exposure classes of $2 \mu\text{g}/\text{m}^3$. One can see the highest population frequency for classes between 26 and 40 $\mu\text{g}/\text{m}^3$ and continuous mild decline of population frequency for classes between 60 and 120 $\mu\text{g}/\text{m}^3$.

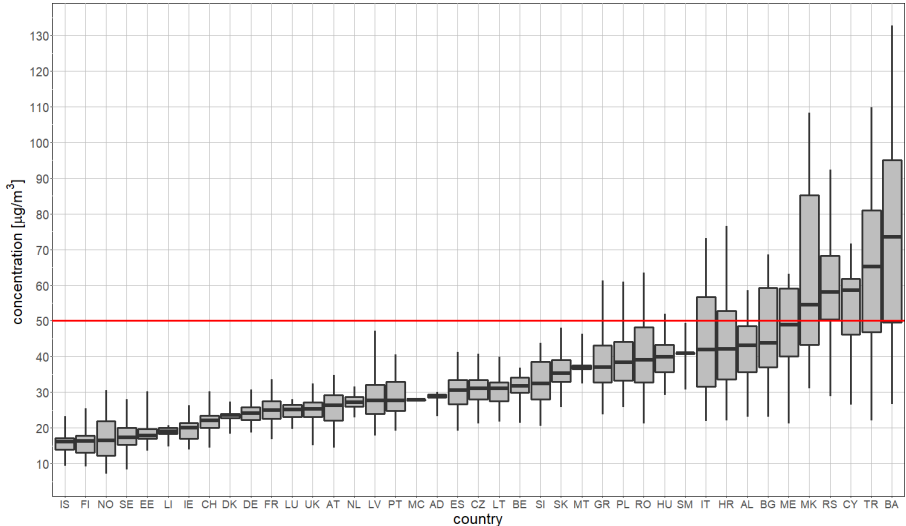
Figure 2.5: Population frequency distribution, PM₁₀ indicator 90.4 percentile of daily means, 2021. The EU daily limit value (50 $\mu\text{g}/\text{m}^3$) is marked by the red line



Note: Apart from the population distribution shown in the graph, it was estimated that 0.25 % of population lived in areas with values of PM₁₀ indicator 90.4 percentile of daily means between 135 and 345 $\mu\text{g}/\text{m}^3$.

Figure 2.6 shows for individual countries the P90.4 of the PM₁₀ daily concentrations to which the population was exposed in 2021. It can be seen that the countries with the highest values of PM₁₀ indicator 90.4 percentile of daily means are located in the central and south-eastern parts of Europe.

Figure 2.6: PM₁₀ expressed as indicator 90.4 percentile of daily means to which the population was exposed in 2021, per country. The EU daily limit value (50 $\mu\text{g}/\text{m}^3$) is marked by the red line



Note: For each country, the box plot shows the concentration to which a percentage of the population was exposed: 50 % in the case of the black marker, 25 % and 75 % in the cases of the box's edges, 2 % and 98 % in the cases of the whiskers' edges.

As in previous years, the daily limit value was more widely exceeded than the annual limit value in 2021.

2.3 PM_{2.5} annual average

Concentration map

Map 2.5 presents the final combined map for the 2021 PM_{2.5} annual average. The dark red areas show concentrations above the ALV of 25 µg/m³. Red areas show concentrations above the indicative LV of 20 µg/m³ defined as Stage 2 (ILV).

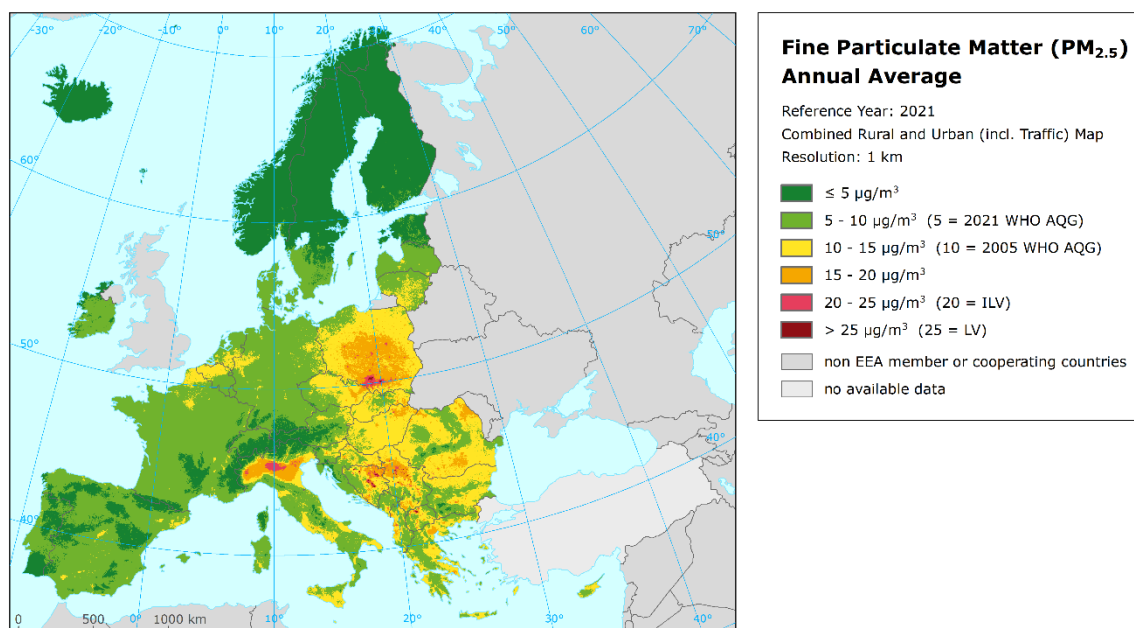
Due to the lack of rural PM_{2.5} stations in Türkiye, no proper interpolation results could be estimated for this country in a rural map. Therefore, the estimated PM_{2.5} values for Türkiye are not presented in the final map.

According to Map 2.3, the areas with the highest PM_{2.5} concentrations appear to be the Po Valley in northern Italy and areas of Bosnia and Herzegovina and Serbia. Concentrations above the ALV appear also around the Balkan city of Skopje, in the Krakow – Katowice (Poland) – Ostrava (Czechia) industrial region and in the area around Warsaw. Different other cities in Romania, Albania, Montenegro, Bulgaria, North Macedonia and Greece also show elevated PM_{2.5} annual average concentrations. Like in the case of PM₁₀, the central and the south and south-eastern parts of Europe show higher concentrations than the western and the northern parts.

Similarly to the PM₁₀, the final map in 1 km resolution is representative for the rural and the urban background areas, but not for the urban traffic areas (which are smoothed in the 1 km resolution).

In order to provide more complete information of the air quality across Europe, the final combined map including the measurement data at stations is presented in Map A4.3 of Annex 4.

Map 2.5: Concentration map of PM_{2.5} annual average, 2021

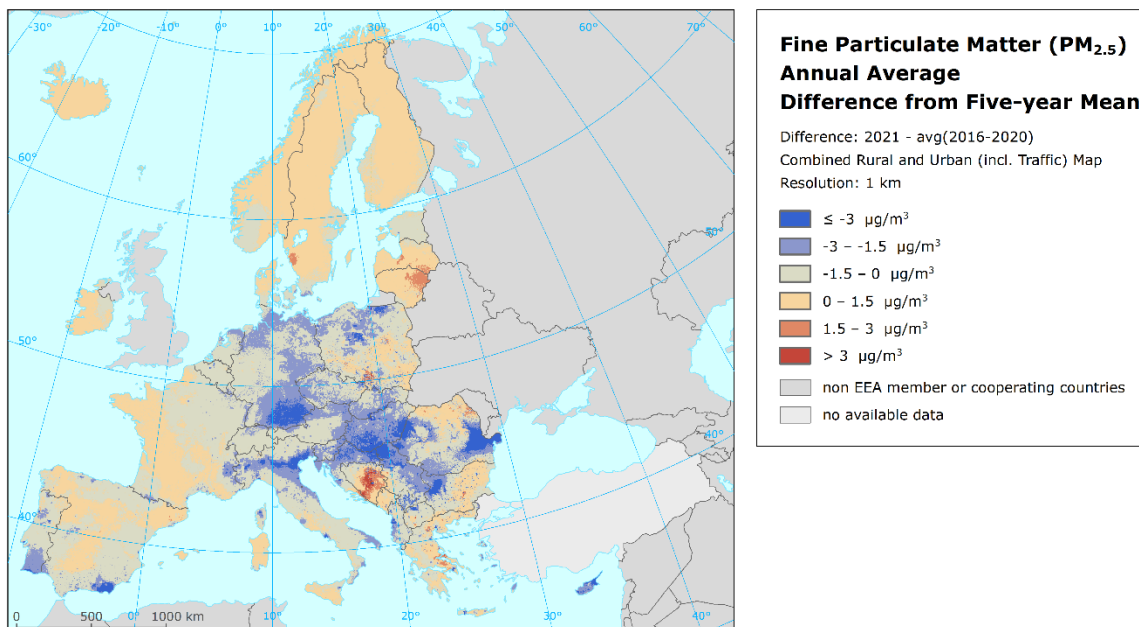


The relative mean uncertainty of the 2021 map of PM_{2.5} annual average is 20 % for rural and 21 % for urban background areas and it is determined exclusively on the actual PM_{2.5} measurement data points, i.e. not on the pseudo stations (Annex 3, Section A3.2). Similarly as in the case of PM₁₀, this uncertainty is satisfactory, compared to the data quality objective for models of PM_{2.5} annual average (i.e. 50 %) as set in the Air Quality Directive (EC, 2008).

Map 2.6 presents the difference between 2021 and the five-year mean 2016-2020 for annual average for PM_{2.5}. Orange to red areas show an increase of PM_{2.5} concentration in 2021, while blue areas show a decrease.

At the annual average PM_{2.5} difference map the highest increases are in parts of southern and south-eastern Europe with the highest increases in Bosnia and Herzegovina and north-eastern Romania, and parts of central and northern Europe (south of Poland, eastern areas of Lithuania and Latvia and area around Gothenburg in Sweden). On the other hand, there are decreases in most of the remaining countries, mainly central Europe (especially in Germany, Hungary, Slovakia), parts of some countries in south-eastern Europe (Croatia, Serbia including Kosovo, Romania) and parts in southern Europe (mainly in the south of Spain and Portugal and the Po Valley in northern Italy).

Map 2.6: Difference concentrations between 2021 and the five-year mean 2016-2020 for PM_{2.5} annual average



Population exposure

Table 2.3 and Figure 2.7 give the population frequency distribution for a limited number of exposure classes to PM_{2.5} concentrations calculated on a grid of 1 km resolution. Table 2.2 also presents the population-weighted concentration for individual countries, large regions, EU-27 and for the total mapping area.

About 98 % and 56 % of the considered European population (excluding Türkiye), has been exposed to annual average concentrations above the current 2021 and the 2005 WHO Air Quality Guideline levels of 5 µg/m³ (WHO, 2021a) and 10 µg/m³ (WHO, 2005), respectively. The same is true for 98 % and 58 % of the EU-27 population.

The total considered and EU-27 population exposed to concentrations above the EU annual limit value (ALV) of 25 µg/m³ has been 1 % and 0.5 %, respectively.

Table 2.3: Population exposure and population-weighted concentration, PM_{2.5} annual average 2021

Country	ISO	Population (inhbs-1000)	PM _{2.5} – annual average, exposed population (%)						Population-weighted concentration		
			< 5	5-10	10-15	15-20	20-25	> 25	2021	5-year mean	Diff.
Albania	AL	2 830		3.8	26.5	47.7	22.0		16.4	20.2	-3.8
Andorra	AD	79	1.1	98.9					8.6	10.5	-1.8
Austria	AT	8 933	2.2	39.6	58.1	0.1			9.9	11.8	-1.9
Belgium	BE	11 555		23.7	76.3				10.7	11.6	-1.0
Bosnia and Herzegovina	BA	3 271	0.0	2.2	11.3	23.2	29.9	33.4	21.9	24.7	-2.8
Bulgaria	BG	6 917	0.0	3.3	43.7	47.3	5.7	0.0	15.1	20.3	-5.2
Croatia	HR	4 036	0.0	18.0	29.6	47.5	4.8	0.0	14.5	17.0	-2.5
Cyprus	CY	9 343		4.0	76.3	13.9	5.8		14.0	14.9	-0.9
Czechia	CZ	10 782	0.0	9.0	65.8	22.7	2.6		13.5	15.7	-2.1
Denmark (incl. Faroe Islands)	DK	5 840	0.8	99.0	0.2				8.0	9.1	-1.1
Estonia	EE	1 330	23.5	76.0	0.5				5.8	5.9	-0.1
Finland	FI	5 534	47.0	53.0					5.0	5.0	0.0
France (metropolitan)	FR	65 447	0.6	64.3	35.1				9.4	10.1	-0.7
Germany	DE	83 155	0.4	70.8	28.8				9.4	11.0	-1.6
Greece	GR	10 679		2.6	42.0	49.9	5.5		15.8	19.6	-3.9
Hungary	HU	9 731		0.3	66.8	30.7	2.2		14.3	16.8	-2.4
Iceland	IS	369	78.4	21.6					4.3	4.6	-0.2
Ireland	IE	5 006	3.8	92.9	3.3				6.9	7.1	-0.2
Italy	IT	59 236	0.2	13.2	54.2	24.2	8.2		13.9	15.7	-1.8
Latvia	LV	1 893	0.1	45.0	52.8	2.1			10.7	10.4	0.3
Liechtenstein	LI	39	0.9	99.1					8.1	8.9	-0.7
Lithuania	LT	2 796		15.5	84.5				11.4	11.5	-0.1
Luxembourg	LU	635		100.0					7.4	9.3	-1.9
Malta	MT	516		0.7	99.3				11.6	11.6	0.0
Monaco	MC	37		79.0	21.0				9.6	12.6	-3.0
Montenegro	ME	621		7.8	31.9	17.0	36.5	6.8	17.2	19.1	-1.8
Netherlands	NL	17 475		60.6	39.4				9.7	10.9	-1.2
North Macedonia	MK	2 069		0.5	5.2	30.7	35.0	28.5	22.3	28.9	-6.6
Norway	NO	5 391	38.8	61.2					5.8	5.5	0.3
Poland	PL	37 840		0.9	19.4	50.8	23.4	5.5	18.1	19.5	-1.4
Portugal (excl. Azores, Madeira)	PT	9 802	10.0	85.8	4.2				7.4	8.5	-1.1
Romania	RO	19 202	0.0	4.8	55.7	37.0	2.5	0.0	14.3	16.6	-2.3
San Marino	SM	34		7.7	92.3				11.7	13.5	-1.7
Serbia (incl. Kosovo)	RS	8 534		1.1	14.6	36.6	35.7	11.9	19.7	24.7	-5.0
Slovakia	SK	5 460	0.0	0.6	49.3	45.5	4.7		15.4	16.7	-1.3
Slovenia	SI	2 109	0.0	20.9	64.0	15.1			12.2	14.7	-2.6
Spain (excl. Canarias)	ES	45 154	1.0	57.9	40.8	0.4			9.5	10.7	-1.2
Sweden	SE	10 379	35.5	63.7	0.8				5.6	5.5	0.2
Switzerland	CH	8 670	3.0	91.7	4.8	0.5			8.3	9.3	-1.0
Total (without Türkiye)		566 342	2.4	41.1	36.2	14.4	4.8	1.1	11.7	13.2	-1.6
			43.5				5.9				
EU-27		450 785	2.0	40.4	39.4	14.0	3.8	0.5	11.5	13.0	-1.5
			42.4				4.3				
Northern Europe		32 080	26.2	62.0	11.7	0.1			6.8		
Western Europe (without UK)		81 150	0.4	56.3	43.3				9.6		
Central Europe		162 777	0.5	42.5	32.7	17.1	6.0	1.3	12.2		
Southern Europe		140 620	1.3	39.1	41.5	14.2	3.9		11.6		
South-Eastern Europe without Türkiye		49 965	0.0	4.6	37.0	38.4	14.0	5.9	16.5		
Kosovo	KS	1 662		0.9	24.3	71.3	3.6	0.0	16.4	25.0	-8.6
Serbia (excl. Kosovo)	RS-	6 872		1.2	12.2	28.2	43.6	14.8	20.4	24.6	-4.1

Note: The percentage value "0.0" indicates that an exposed population exists, but it is small and estimated to be less than 0.05 %. Empty cells mean no population in exposure. 5-year mean, i.e. five-year mean 2016-2020. Diff., i.e. difference concentrations between 2021 and five-year mean 2016-2020.

No population has been exposed to concentrations above the ALV in 32 countries. In Romania, Croatia, Bulgaria and Kosovo (in ascending order) less than 0.004 of population has been exposed to concentrations above the limit value. In Poland, Montenegro, Serbia, North Macedonia and Bosnia and Herzegovina, between > 5 % and 33 % of the population have been exposed above this limit value.

Concentrations above the indicative limit value (ILV) of 20 µg/m³ were found in areas with 6 % of the considered European population and with 4 % of the EU-27 population. No population has been exposed to concentrations above the ILV in 24 countries. In Hungary, Romania, Czechia, Kosovo, Slovakia, Croatia, Greece, Bulgaria, Cyprus and Italy (in ascending order) between 2 and 8 % of the population is exposed to concentrations above the ILV. In Albania, Poland, and Montenegro, 22-43 % of the population suffers from exposures above this ILV; in Serbia, Bosnia and Herzegovina and North Macedonia, more than 58 % of the population have been exposed above this ILV.

Since PM_{2.5} is one of the most relevant pollutants linked to health problems and premature mortality (EEA, 2019) it should be mentioned that at least some part of the population was exposed to PM_{2.5} annual mean concentrations above the 2021 WHO AQG in each country (minimum of 22 % in Iceland). More than 90 % of the population has been exposed to concentrations above the 2021 WHO AQG level in 34 countries. The same is true for 16 countries in case of the 2005 WHO AQG level. The only countries, where the PM_{2.5} annual mean concentrations did not exceed the 2005 WHO AQG level, were Andorra, Finland, Iceland, Liechtenstein, Luxembourg and Norway.

As the current mapping methodology tends to underestimate high values (Annex 3, Section A3.2), the percentages and/or the number of countries with population exposed to concentrations above both the current ALV and the indicative ILV will most likely be higher.

The population-weighted concentration of the PM_{2.5} annual means has been estimated for 2021 at about 12 µg/m³ for both European population (excluding Türkiye) and for the EU-27, which means a decrease about 2 µg/m³ compared to five-year mean for both characteristics. When assessing the absolute change in individual countries, the steepest decrease was found in North Macedonia (6.6 µg/m³), the highest increase was estimated in Latvia and Norway (0.3 µg/m³).

Figure 2.7: Percentage of the population (%) exposed to different values of PM_{2.5} annual average (µg/m³), 2021

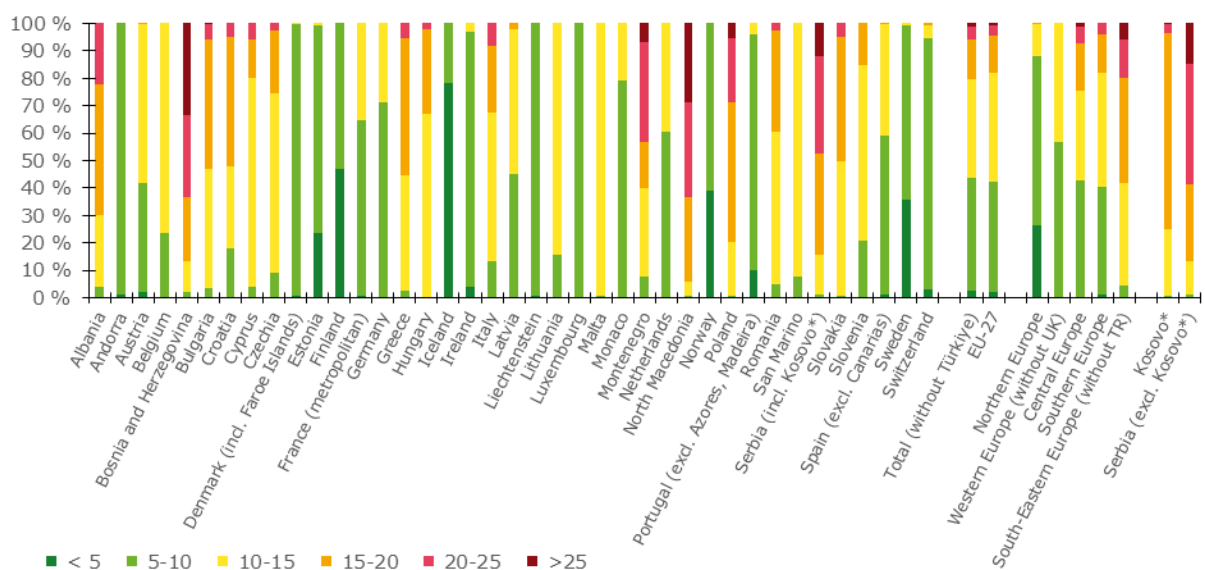
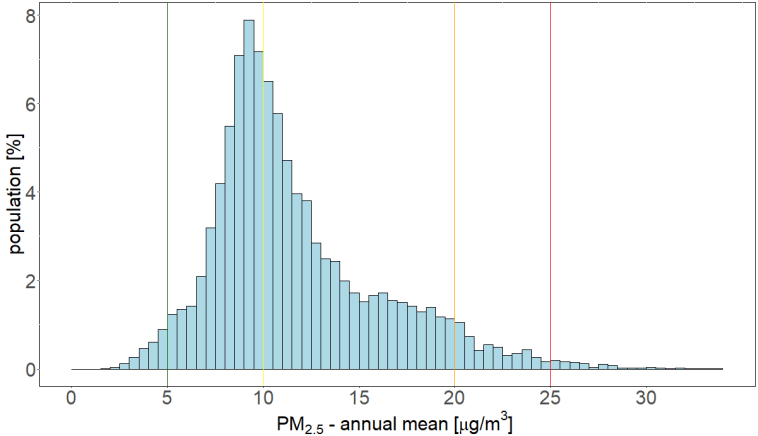


Figure 2.8 shows, for the whole mapped area, the population frequency distribution for exposure classes of 0.5 $\mu\text{g}/\text{m}^3$. The highest population frequency is found for classes between 7 and 14 $\mu\text{g}/\text{m}^3$.

Figure 2.8: Population frequency distribution, PM_{2.5} annual average, 2021. The 2021 WHO AQG level (5 $\mu\text{g}/\text{m}^3$) is marked by the green line, the 2005 WHO AQG level (10 $\mu\text{g}/\text{m}^3$) is marked by the yellow line, the EU annual indicative limit value (20 $\mu\text{g}/\text{m}^3$) is marked by the orange line and the EU annual limit value (25 $\mu\text{g}/\text{m}^3$) is marked by the red line



Note: Apart from the population distribution shown in the graph, it was estimated that 0.01 % of population lived in areas with PM_{2.5} annual average concentrations between 34 and 39 $\mu\text{g}/\text{m}^3$.

The boxplot showing for individual countries the PM_{2.5} annual average concentrations to which the population per country was exposed in 2021 is presented in Summary, Figure S.1.

3 Ozone

For ozone, three health-related indicators, i.e. 93.2 percentile of maximum daily 8-hour means (see below), SOMO35 and SOMO10, and seven vegetation-related indicators, i.e. AOT40 for vegetation, AOT40 for forests, POD_6 for crops (wheat, potato and tomato) and POD_1 for trees (beech and spruce) are considered. For the definition of the SOMO35, SOMO10 and AOT40 and POD indicators, see following sections and Annexes 1 and 2.

The separate rural and urban background health-related indicator map layers are calculated at a resolution of 10 km. Subsequently, the final health-related indicator maps are created by combining rural and urban areas based on the 1 km resolution population density map, following the procedure as described in Annex 1, Section A1.1. The supplementary data used are chemical transport model (CTM) output, altitude and surface solar radiation for rural areas and CTM output, wind speed and surface solar radiation for urban areas (Annex 3). The final concentration maps are presented on the 1 km grid resolution. The population exposure tables are calculated on the basis of these health-related indicator maps.

The vegetation-related indicator maps are created for rural areas only, as urban areas are considered not to represent areas covered by vegetation (although the vegetation located in the outskirts of agglomerations might be omitted by this approach). These maps are calculated from observations at rural background stations and are representative for rural areas only. The supplementary data used are CTM output, altitude and surface solar radiation. These supplementary data sources are the same as those used for the human health related ozone indicators in the rural areas. The maps have a resolution of 2 km. This resolution serves the needs of the EEA's AIR004 indicator on ecosystem exposure to ozone (EEA, 2023b), earlier known as the Core Set Indicator 005.

Annex 3, Section A3.3 provides details on the regression and kriging parameters applied for deriving the maps of the ozone indicators, as well as the uncertainty analysis of the maps.

3.1 Ozone – 93.2 percentile of maximum daily 8-hour means

The Ambient Air Quality Directive (EC, 2008) describes the ozone target value (TV) for the protection of human health as “a maximum daily 8-hour mean of $120 \mu\text{g}/\text{m}^3$ not to be exceeded on more than 25 times a calendar year, averaged over three years”. On an annual basis, what we call the target value threshold⁶, can be evaluated by the indicator 26th highest maximum daily 8-hour mean, which is in principle equivalent to the indicator 93.2 percentile of maximum daily 8-hour means. However, for measurement data these two indicators are equivalent only if no data is missing, which is in general not the case. As shown in de Leeuw (2012), the additional uncertainty related to incomplete time series is substantially smaller when using percentile values instead of the x-th highest value. As in the previous reports since 2014 maps, this ozone indicator is expressed as the 93.2 percentile of maximum daily 8-hour means instead of the formerly used 26th highest maximum daily 8-hour mean. Only 2021 data are considered, and not the three-years average.

Concentration map

Map 3.1 presents the final combined map for 93.2 percentile of maximum daily 8-hour means. In the map, the red and dark red areas show values of the 93.2 percentile of maximum daily 8-hour means above $120 \mu\text{g}/\text{m}^3$ in 2021, i.e. above the TV threshold of $120 \mu\text{g}/\text{m}^3$ on more than 25 days in 2021. Note that in the Ambient Air Quality Directive (EC, 2008) the TV is actually defined as $120 \mu\text{g}/\text{m}^3$ not to be exceeded on more than 25 days per calendar year averaged over three years. Here only 2021 data are presented, and no three-year average has been calculated.

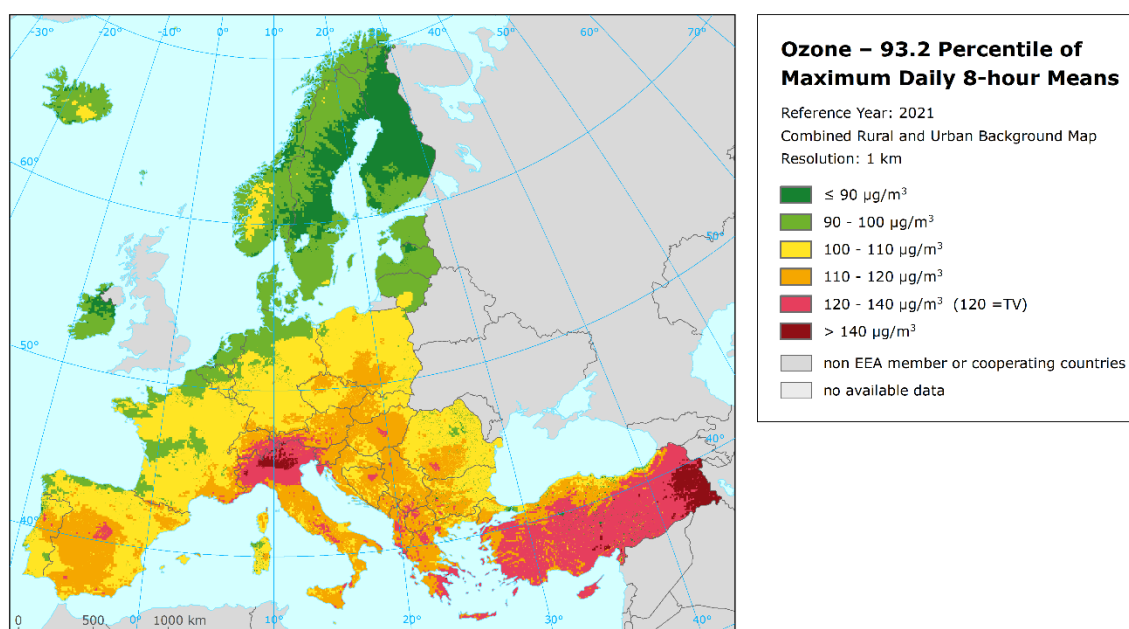
⁶ A maximum daily 8-hour mean of $120 \mu\text{g}/\text{m}^3$ not to be exceeded on more than 25 times a calendar year.

The map shows that percentile values above $120 \mu\text{g}/\text{m}^3$ occur in several areas of Europe in 2021. Those values are particularly evident in large areas of Türkiye and Italy. To a lesser extent, values above $120 \mu\text{g}/\text{m}^3$ occurred in Portugal, Spain, France, Switzerland, Austria, Hungary and all the Balkan countries. In general, the southern, the south-eastern and central parts of Europe show higher ozone concentrations than the northern parts, which is caused mainly by higher solar radiation and temperature in these areas. Nevertheless, concentrations above the TV threshold can occur even in northern Europe during warm year as it was presented for 2018 (Horálek et al., 2021).

In order to provide more complete information of the air quality across Europe, the final combined map including the measurement data at stations is presented in Map A4.4 of Annex 4.

The relative mean uncertainty of the 2021 map of the 93.2 percentile of maximum daily 8-h ozone means is about 7 % for rural and 10 % for urban areas (Annex 3, Section A3.2). The low uncertainty values are influenced by the character of this ozone indicator. Note that the Air Quality Directive (EC, 2008) sets no modelling uncertainty for ozone annual indicators.

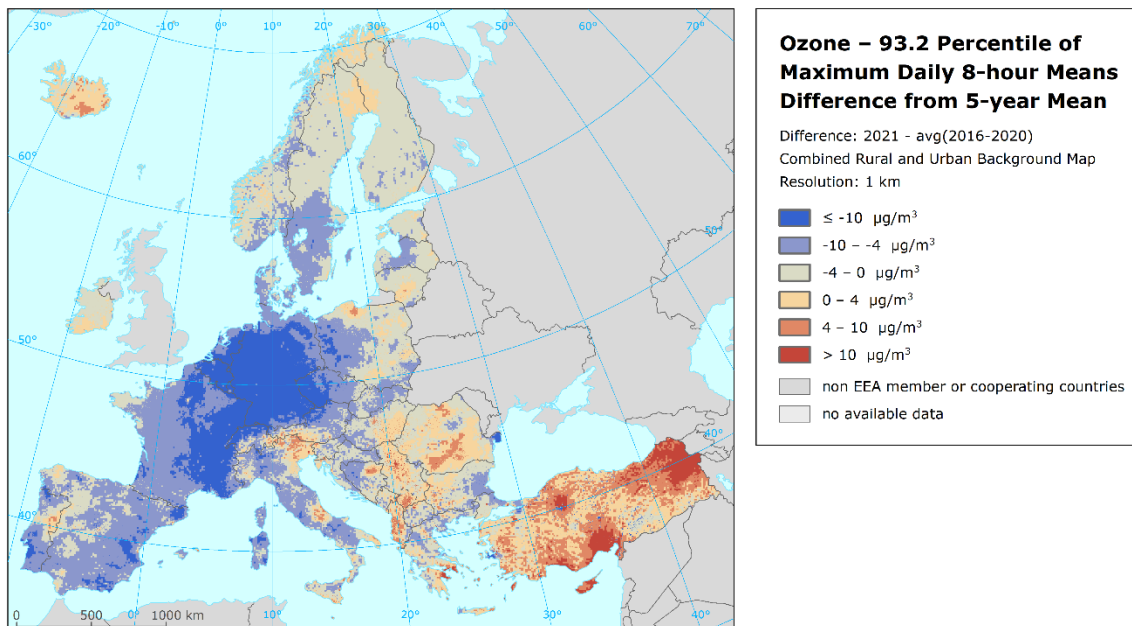
Map 3.1: Concentration map of ozone indicator 93.2 percentile of maximum daily 8-hour means, 2021



Map 3.2. presents the difference between 2021 and the five-year mean 2016-2020 for 93.2 percentile of daily 8-hour maxima for O_3 . Orange to red areas show an increase of O_3 concentration in 2021, while blue areas show a decrease.

The largest increases of 93.2 percentile of daily 8-hour maxima for O_3 (even more than $10 \mu\text{g}/\text{m}^3$) were recorded in several large areas of Türkiye; furthermore, increases in concentrations were also found in a more continuous area of several Balkan countries. Increases in concentrations in smaller areas were also observed in Portugal, Italy and in the northern area of Poland and Scandinavia, Ireland and Iceland. The rest of the total mapped area shows a decrease in 93.2 percentile of daily 8-hour maxima for O_3 , with the deepest decrease observed in the whole of Germany, western Czechia and eastern to central France.

Map 3.2: Difference concentrations between 2021 and the five-year average 2016-2020 for ozone indicators 93.2 percentile of daily 8-hour maxima



Population exposure

Table 3.1 and Figure 3.1 give, for the 93.2 percentile of maximum daily 8-hour means, the population frequency distribution for a limited number of exposure classes. Table 3.1 also presents the population-weighted concentration for individual countries, large regions, EU-27 and for the total mapped area.

It has been estimated that in 2021 9 % of the considered European population (including Türkiye) and around 7 % of the EU-27 population lived in areas where the ozone concentration was above the health-related target value threshold of $120 \mu\text{g}/\text{m}^3$.

No population has been exposed to concentrations above the TV threshold in 17 countries. In Bulgaria, Germany, Poland, Liechtenstein, France (metropolitan), Spain (excl. Canarias), Romania, Portugal (excl. Azores, Madeira), Montenegro, Serbia, Hungary, Malta, Austria, North Macedonia, Croatia, Kosovo, Switzerland, Slovenia, Bosnia and Herzegovina and Cyprus (in ascending order) up to 17 % of population has been exposed to concentrations above the TV threshold. In Türkiye, Albania, Italy and Greece, this was the case for between 24 % and 47 % of the population.

As the current mapping methodology tends to underestimate high values due to interpolation smoothing (Annex 3, Section A3.3), the percentage of population exposed to values above the TV threshold is most likely somewhat underestimated; additional population exposure above the TV threshold might be expected in some other countries: Switzerland, Serbia, Croatia, Albania, Austria, Montenegro, Hungary, Slovenia, Liechtenstein, Monaco and San Marino. The reason is that in these countries the estimated percentage population exposed to the concentrations between $110 \mu\text{g}/\text{m}^3$ and $120 \mu\text{g}/\text{m}^3$ is considerable (more than 50 %).

Table 3.1: Population exposure and population-weighted concentrations, ozone indicator 93.2 percentile of maximum daily 8-hour means, 2021

Country	ISO	Population (inhbs-1000)	Ozone — perc93.2, exposed population (%)						Population-weighted concentration		
			< 90	90-100	100-110	110-120	120-140	> 140	2021	5-year mean	Diff.
Albania	AL	2 830		0.6	9.8	59.6	29.9		116.8	109.7	7.1
Andorra	AD	79		98.1	1.3	0.7			92.7	108.9	-16.2
Austria	AT	8 933			35.7	63.6	0.7	0.0	111.5	116.8	-5.4
Belgium	BE	11 555	3.1	87.3	9.6				96.7	109.5	-12.8
Bosnia and Herzegovina	BA	3 271		0.2	51.9	39.4	8.6		110.8	112.7	-1.9
Bulgaria	BG	6 917	40.6	43.6	12.6	3.1	0.0		93.2	99.2	-6.0
Croatia	HR	4 036			39.9	58.4	1.7		110.7	114.6	-3.9
Cyprus	CY	9 343			37.8	45.1	17.1		114.4	107.7	6.7
Czechia	CZ	10 782		2.1	72.6	25.3			108.0	116.5	-8.5
Denmark (incl. Faroe Islands)	DK	5 840	27.7	72.3	0.1				91.5	97.6	-6.1
Estonia	EE	1 330	44.1	55.9	0.0				90.4	92.9	-2.4
Finland	FI	5 534	75.4	24.6					88.3	90.3	-2.0
France (metropolitan)	FR	65 447	0.4	34.6	54.5	10.3	0.2		102.4	110.8	-8.4
Germany	DE	83 155	0.4	29.3	69.3	1.0	0.0		102.1	114.7	-12.6
Greece	GR	10 679	0.1	7.9	20.5	25.6	45.7	0.2	119.8	111.4	8.4
Hungary	HU	9 731		0.2	28.8	70.7	0.3		112.7	110.3	2.3
Iceland	IS	369	89.1	10.9					87.2	85.2	2.0
Ireland	IE	5 006	51.9	48.0	0.1				90.1	89.6	0.5
Italy	IT	59 236	1.2	3.2	24.5	30.9	25.5	14.6	119.8	123.3	-3.5
Latvia	LV	1 893	52.7	47.2	0.1				90.0	94.8	-4.7
Liechtenstein	LI	39				99.9	0.1		112.0	121.4	-9.4
Lithuania	LT	2 796		75.7	24.3				97.1	96.7	0.4
Luxembourg	LU	635		81.6	18.4				98.4	110.3	-11.9
Malta	MT	516			74.4	25.1	0.6		109.4	105.0	4.3
Monaco	MC	37				100.0			119.0	121.3	-2.3
Montenegro	ME	621			35.8	64.0	0.2		110.3	109.3	1.1
Netherlands	NL	17 475	17.7	77.3	5.1				94.5	105.5	-11.0
North Macedonia	MK	2 069	14.3	7.6	45.9	31.4	0.8		104.1	100.2	3.9
Norway	NO	5 391	75.9	24.0	0.1				88.4	92.4	-4.0
Poland	PL	37 840	0.0	12.0	67.4	20.6	0.0		105.9	108.9	-3.0
Portugal (excl. Azores, Madeira)	PT	9 802	13.5	55.2	25.9	5.3	0.2		97.4	104.2	-6.7
Romania	RO	19 202	5.6	44.4	44.6	5.1	0.2		99.9	98.0	1.9
San Marino	SM	34				100.0			113.0	121.0	-8.0
Serbia (incl. Kosovo)	RS	8 534	0.1	6.4	34.6	58.2	0.7		110.9	101.0	9.8
Slovakia	SK	5 460		3.0	66.8	30.2			107.1	111.4	-4.3
Slovenia	SI	2 109			7.3	87.2	5.5		114.4	116.7	-2.2
Spain (excl. Canarias)	ES	45 154	4.8	14.0	52.7	28.2	0.2		105.5	110.6	-5.1
Sweden	SE	10 379	46.0	53.9	0.1				89.9	95.1	-5.2
Switzerland	CH	8 670			43.8	51.4	4.2	0.5	111.0	121.9	-10.9
Türkiye	TR	83 614	31.9	10.9	12.9	19.9	21.8	2.6	103.1	104.2	-1.2
Total		566 342	9.9	23.5	39.0	18.6	7.0	2.0	104.8	109.8	-5.1
			33.4				9.0				
EU-27		450 785	6.0	26.8	43.9	16.6	4.8	2.0	104.9	111.0	-6.1
			32.8				6.8				
Northern Europe		32 080	48.7	48.9	2.4				90.4		
Western Europe (without UK)		81 150	7.3	56.2	36.0	0.6	0.0		98.2		
Central Europe		162 777	0.2	17.5	62.8	19.2	0.3	0.0	105.3		
Southern Europe		140 620	3.0	11.2	36.0	29.1	14.5	6.2	112.4		
South-Eastern Europe		121 885	22.4	17.0	22.5	22.5	14.0	1.5	103.4		
Kosovo	KS	1 662		1.3	56.2	39.8	2.6		108.9	100.0	8.9
Serbia (excl. Kosovo)	RS-	6 872	0.1	7.7	29.3	62.8	0.2		111.3	101.3	10.1

Note: The percentage value "0.0" indicates that an exposed population exists, but it is small and estimated to be less than 0.05 %. Empty cells mean no population in exposure. 5-year mean, i.e. five-year mean 2016-2020. Diff., i.e. difference concentrations between 2021 and five-year mean 2016-2020.

The overall population-weighted ozone concentrations in terms of the 93.2 percentile of maximum daily 8-hour means has been estimated to be 105 $\mu\text{g}/\text{m}^3$ in 2021 for both the considered European area (including Türkiye) and for the EU-27, i.e. of about 5 $\mu\text{g}/\text{m}^3$ and 6 $\mu\text{g}/\text{m}^3$ less than the five-year 2016-2020 mean concentration, respectively. When assessing the change in individual countries, the steepest absolute decrease was found in Andorra (16.2 $\mu\text{g}/\text{m}^3$), the highest increase was estimated in Serbia, excl. Kosovo (10.1 $\mu\text{g}/\text{m}^3$).

Figure 3.1: Percentage of the population (%) exposed to different values of the ozone indicator 93.2 percentile of maximum daily 8-hour means ($\mu\text{g}/\text{m}^3$), 2021

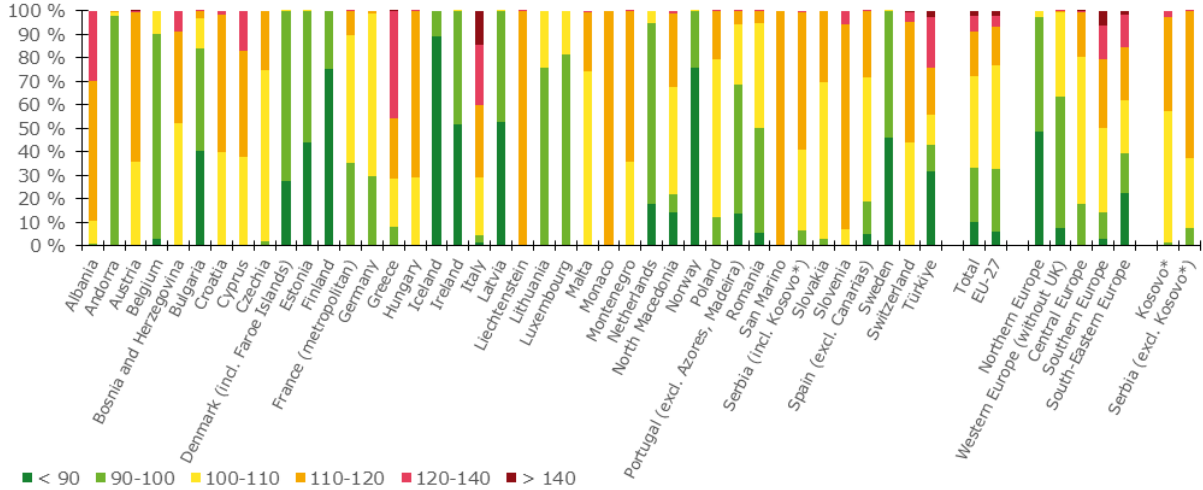
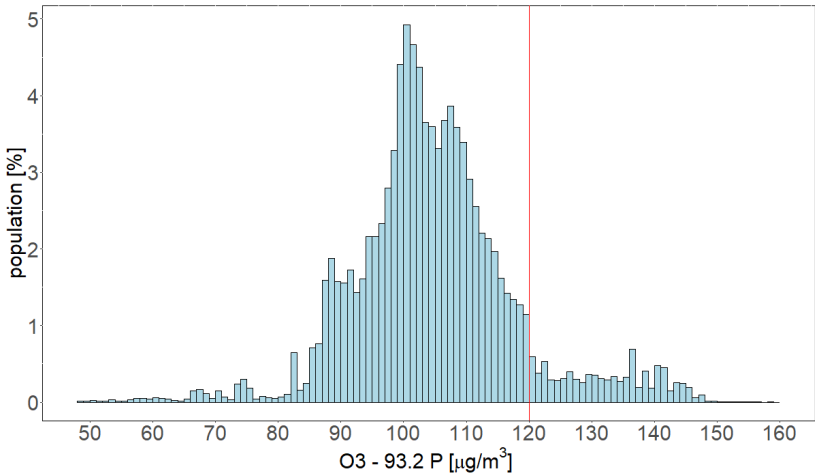


Figure 3.2 shows, for the whole mapped area, the population frequency distribution for exposure classes of 2 $\mu\text{g}/\text{m}^3$. The highest population frequency is found for classes between 98 and 112 $\mu\text{g}/\text{m}^3$. For classes above 112 $\mu\text{g}/\text{m}^3$, a sharp decline of population frequency can be seen.

Figure 3.2: Population frequency distribution, O₃ indicator 93.2 percentile of maximum daily 8-hour means, 2021. The EU target value threshold (120 $\mu\text{g}/\text{m}^3$) is marked by the red line



The boxplot showing for individual countries the ozone concentrations expressed as the indicator 93.2 percentile of maximum daily 8-hour means to which the population per country was exposed in 2021 is presented in Summary, Figure S.1.

3.2 Ozone – SOMO35 and SOMO10

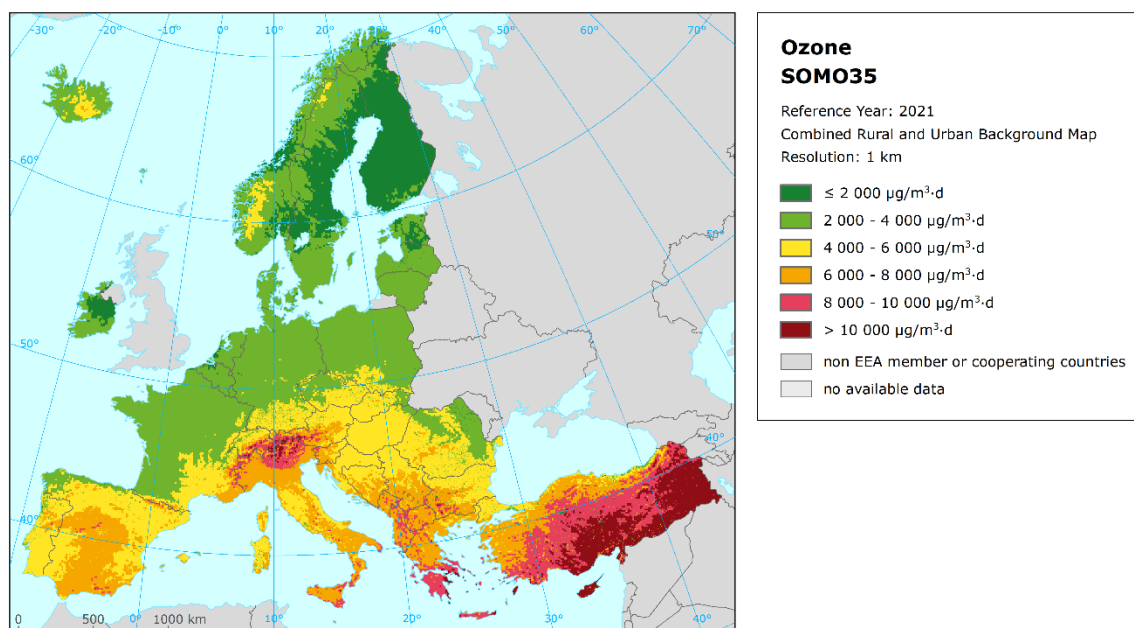
SOMO35 is the annually accumulated ozone maximum daily 8-hourly means in excess of 35 ppb (i.e. $70 \mu\text{g}/\text{m}^3$). It is not regulated in any of the EU air quality directives and there are no limit or target values defined. Nevertheless, it is considered by the WHO as a good indicator of human exposure to ozone (WHO, 2013). Comparing the 93.2 percentile of maximum daily 8-hour means versus the SOMO35 for all background stations shows no simple relationship between the two indicators. However, it seems that the TV threshold of the 93.2 percentile of maximum daily 8-hour means (being $120 \mu\text{g}/\text{m}^3$) is related approximately with a SOMO35 value in the range of $6\,000$ - $8\,000 \mu\text{g}/\text{m}^3\cdot\text{d}$. This comparison motivates a somewhat arbitrarily chosen threshold of $6\,000 \mu\text{g}/\text{m}^3\cdot\text{d}$, in order to facilitate the discussion of the observed distributions of SOMO35 levels in their spatial and temporal context. This threshold is used in this and previous papers (Horálek et al., 2023, and the references cited therein) when dealing with the population exposure estimates.

SOMO10 is the annually accumulated ozone maximum daily 8-hourly means in excess of 10 ppb (i.e. $20 \mu\text{g}/\text{m}^3$). This indicator was introduced due to its link to the health impact assessment, since the WHO recommended using the SOMO10 as an alternative to the SOMO35 when estimating the health impact of ozone (WHO, 2013).

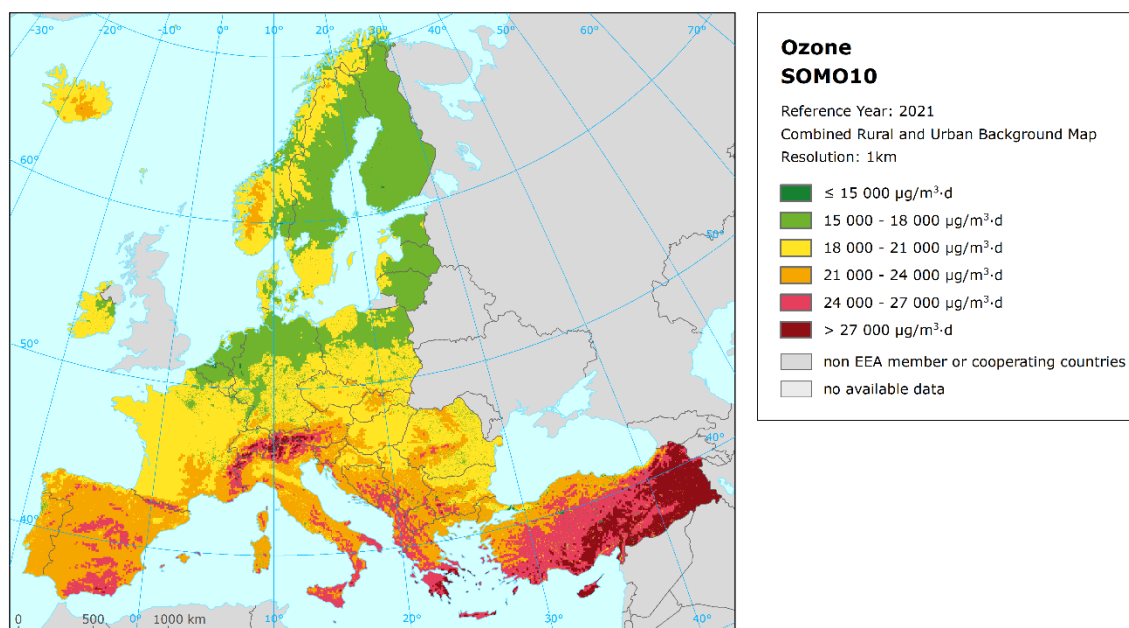
Concentration maps

Maps 3.3 and 3.4 presents the final combined map for SOMO35 and SOMO10. In the final combined map of SOMO35, the red and dark red areas show values above $8\,000 \mu\text{g}/\text{m}^3\cdot\text{d}$, while the orange areas show values above $6\,000 \mu\text{g}/\text{m}^3\cdot\text{d}$. In the case of SOMO10, the boundaries of concentration classes have been chosen quite arbitrary, in order to reflect the concentration distribution of this indicator. In the final combined map of SOMO10, the red and dark red areas show values above $24\,000 \mu\text{g}/\text{m}^3\cdot\text{d}$.

Map 3.3: Concentration map of ozone indicator SOMO35, 2021



Map 3.4: Concentration map of ozone indicator SOMO10, 2021



Like in the case of the 93.2 percentile of the maximum daily 8-hour means, generally the southern and south-eastern parts of Europe show higher ozone SOMO35 and SOMO10 concentrations than the northern parts. Higher levels of ozone also occur more frequently in mountainous areas south of 50 degrees latitude than in lowlands. In 2021, SOMO35 levels > 6 000 µg/m³.d were estimated in almost all of Türkiye, in much of the Balkan countries and Italy and in a large area of Spain.

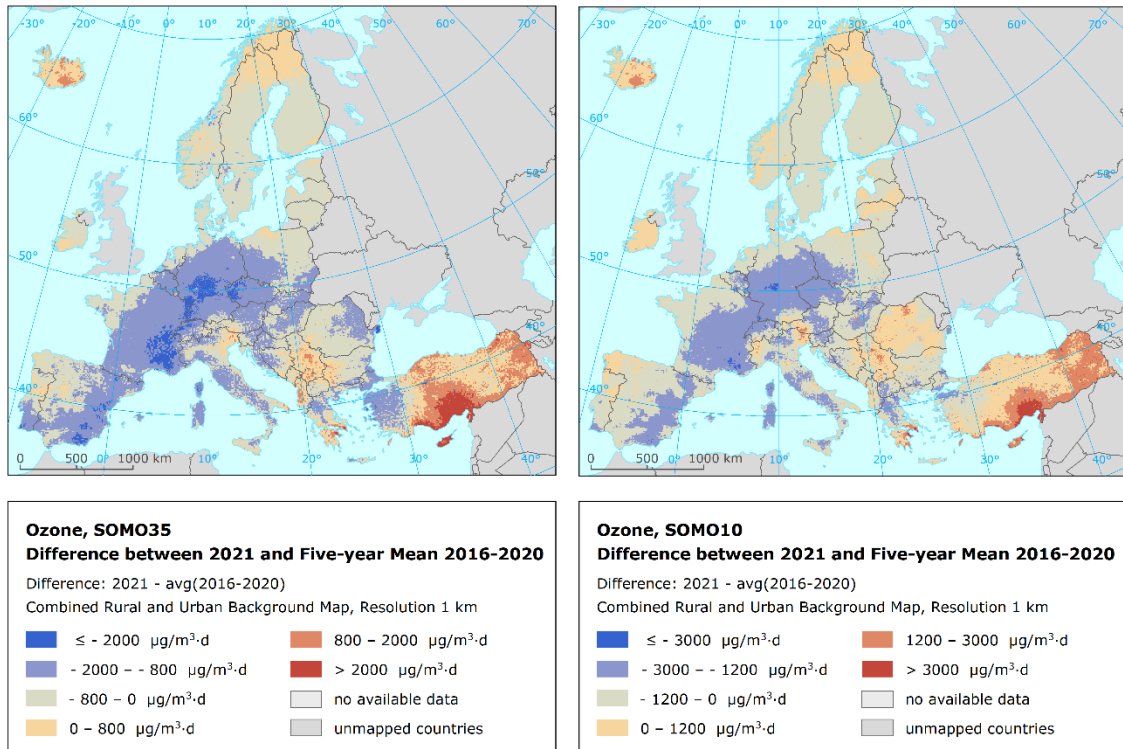
The relative mean uncertainty of the 2021 maps of the SOMO35 and SOMO10 is about 32 % and 11 %, respectively, for rural areas and 37 % and 15 %, respectively, for urban areas (see Annex 3).

Map 3.5 presents the difference between 2021 and the five-year mean 2016-2020 for the O₃ indicators SOMO35 and SOMO10. Orange to red areas show an increase of those O₃ indicators in 2021, while blue areas show a decrease.

The largest increases of SOMO35 levels were recorded in several large areas of Türkiye; furthermore, increases in concentrations were also found in a few areas of several Balkan countries. Increases in concentrations in smaller areas were also observed in Portugal, Spain, Italy and in the northern area of Poland, the Baltic states, Scandinavia, Ireland, and Iceland. The rest of the total mapped area shows a decrease in SOMO35 levels, with the deepest decrease observed in some areas of Germany, Czechia, and France.

In terms of SOMO10, when compared to the five-year average 2016-2020, highest increase has been observed in 2021 in the southern part of Türkiye, in some areas in Italy, the Balkan countries and Iceland. Contrary to that, one can see a decline in most of the rest of Europe.

Map 3.5: Difference concentrations between 2021 and the five-year average 2016-2020 for SOMO35 and SOMO10



Population exposure

SOMO35

Table 3.2 and Figure 3.3 give for SOMO35 the population frequency distribution for a limited number of exposure classes. Table 3.2 also presents the population-weighted concentration for individual countries, large regions, EU-27 and for the total mapped area.

It has been estimated that in 2021 about 15 % of the considered European population (including Türkiye), and about 12 % of the EU-27 population, lived in areas with SOMO35 values above 6 000 µg/m³·d (see above on the motivation of this criterion).

In 2021, like in the previous several years, the northern and western European countries have had almost no inhabitants exposed to SOMO35 concentrations above 6 000 µg/m³·d. No population has been exposed to concentrations SOMO35 concentrations above 6 000 µg/m³·d in 13 countries. In Hungary, Poland, Germany, Slovakia, Romania, Serbia, Andorra, San Marino, Portugal, Liechtenstein, Bulgaria, Switzerland, North Macedonia, France, Bosnia and Herzegovina, Austria, Croatia, Spain and Slovenia (in ascending order) between > 0.1 and 16 % of population has been exposed to SOMO35 concentrations above 6 000 µg/m³·d. In Kosovo, Montenegro, Türkiye, Italy and Greece, between 19 and 76 % of population has been exposed to SOMO35 concentrations above 6 000 µg/m³·d. The largest proportion of the population (between 88 % and 100 %) was exposed to SOMO35 concentrations above 6 000 µg/m³·d in Albania, Cyprus, Malta and Monaco.

Table 3.2: Population exposure and population-weighted concentrations, ozone indicator SOMO35, 2021

Country	ISO	Population (inths-1000)	Ozone — SOMO10, exposed population, 2021 (%)						Population-weighted concentration		
			< 2 000	2 000- 4 000	4 000- 6 000	6 000- 8 000	8 000- 10 000	> 10 000	2021	5-year mean	Diff.
Albania	AL	2 830			11.3	85.2	3.5		6 636	5 876	760
Andorra	AD	79		98.1	1.2	0.8			2 497	5 309	-2 813
Austria	AT	8 933		22.9	71.8	4.8	0.4	0.0	4 599	5 390	-791
Belgium	BE	11 555	11.8	88.2					2 227	3 238	-1 011
Bosnia and Herzegovina	BA	3 271		0.2	94.8	5.0	0.0		5 152	5 540	-389
Bulgaria	BG	6 917	32.8	52.1	11.7	3.3	0.1	0.0	2 668	3 506	-838
Croatia	HR	4 036			89.1	10.9	0.0		5 254	5 883	-629
Cyprus	CY	9 343			0.2	71.3	13.0	15.5	8 189	6 088	2 101
Czechia	CZ	10 782		78.8	21.2				3 651	5 052	-1 401
Denmark (incl. Faroe Islands)	DK	5 840	33.6	66.4	0.0				2 104	2 726	-622
Estonia	EE	1 330	75.8	24.2					1 850	2 082	-232
Finland	FI	5 534	96.6	3.4					1 594	1 735	-140
France (metropolitan)	FR	65 447	0.6	84.2	10.4	4.8	0.0	0.0	3 307	4 314	-1 007
Germany	DE	83 155	1.6	95.4	2.9	0.0	0.0		2 949	4 206	-1 257
Greece	GR	10 679	0.0	5.9	18.7	20.9	44.0	10.6	7 669	6 433	1 236
Hungary	HU	9 731		6.7	93.3	0.0			4 665	4 674	-10
Iceland	IS	369	75.1	24.9					1 922	1 305	617
Ireland	IE	5 006	64.3	35.7	0.1				1 868	1 867	2
Italy	IT	59 236	0.6	7.7	37.6	45.7	8.3	0.0	6 140	6 534	-394
Latvia	LV	1 893	62.4	37.6	0.0				1 855	2 263	-408
Liechtenstein	LI	39			98.5	1.4	0.1		4 351	5 545	-1 194
Lithuania	LT	2 796	0.0	100.0	0.0				2 405	2 447	-42
Luxembourg	LU	635		100.0					2 379	3 579	-1 200
Malta	MT	516				97.1	2.7	0.2	6 646	6 024	623
Monaco	MC	37				100.0			6 917	7 294	-377
Montenegro	ME	621		9.9	54.5	34.4	1.2		5 678	5 613	65
Netherlands	NL	17 475	23.0	77.0	0.0				2 312	3 017	-705
North Macedonia	MK	2 069	1.8	25.0	68.6	4.4	0.2	0.0	4 249	4 120	130
Norway	NO	5 391	83.4	16.5	0.1				1 683	2 166	-483
Poland	PL	37 840	0.2	94.3	5.5	0.0			3 308	3 902	-594
Portugal (excl. Azores, Madeira)	PT	9 802	2.4	72.4	23.8	1.4	0.0		3 472	3 915	-443
Romania	RO	19 202	11.8	74.1	14.1	0.0			3 001	3 246	-245
San Marino	SM	34			98.6	1.4			5 304	6 180	-877
Serbia (incl. Kosovo)	RS	8 534	0.0	21.8	70.0	7.9	0.2		4 741	3 831	909
Slovakia	SK	5 460		49.0	51.0	0.0			3 970	4 773	-804
Slovenia	SI	2 109			83.7	16.2	0.1		5 453	5 861	-408
Spain (excl. Canarias)	ES	45 154	1.1	22.5	62.0	14.3	0.0		4 689	5 399	-710
Sweden	SE	10 379	56.7	43.3	0.0				1 977	2 451	-475
Switzerland	CH	8 670		50.2	45.3	4.0	0.5	0.0	4 155	5 715	-1 560
Türkiye	TR	83 614	14.0	31.5	18.1	16.1	11.9	8.5	5 102	5 016	86
Total		566 342	8.3	53.3	22.9	10.6	3.4	1.4	4 008	4 573	-565
			61.7				15.4				
EU-27			7.0	59.1	21.8	9.5	2.3	0.3	3 807	4 507	-700
		450 785	66.1				12.1				
Northern Europe		32 080	59.4	40.6	0.0				1 917		
Western Europe (without UK)		81 150	10.4	88.3	1.2	0.0	0.0	0.0	2 627		
Central Europe		162 777	0.8	80.0	18.5	0.7	0.0	0.0	3 392		
Southern Europe		140 620	0.8	20.1	42.7	28.5	7.0	0.9	5 472		
South-Eastern Europe		121 885	12.2	36.0	26.6	13.0	7.1	5.0	4 612		
Kosovo	KS	1 662		25.5	55.2	18.6	0.7		4 931	4 380	552
Serbia (excl. Kosovo)	RS-	6 872	0.1	20.9	73.7	5.3	0.1		4 694	3 697	997

Note: The percentage value "0.0" indicates that an exposed population exists, but it is small and estimated to be less than 0.05 %. Empty cells mean no population in exposure. 5-year mean, i.e. five-year mean 2016-2020. Diff., i.e. difference concentrations between 2021 and the five-year mean 2016-2020.

In 2021, the population-weighted ozone concentration in terms of SOMO35 for the total mapped area was estimated to be slightly above 4 000 $\mu\text{g}/\text{m}^3\cdot\text{d}$ i.e. of about 565 $\mu\text{g}/\text{m}^3\cdot\text{d}$ less than the five-year 2016-2020 mean SOMO35 concentration. For the EU-27, it was slightly above 3 800 $\mu\text{g}/\text{m}^3\cdot\text{d}$, i.e. 700 $\mu\text{g}/\text{m}^3\cdot\text{d}$ less than the five-year 2016-2020 mean SOMO35 concentration. When assessing the change in individual countries, the steepest absolute decrease was found in Andorra (2 813 $\mu\text{g}/\text{m}^3\cdot\text{d}$), the highest increase was estimated in Cyprus (2 101 $\mu\text{g}/\text{m}^3\cdot\text{d}$).

Figure 3.3: Percentage of the population (%) exposed to different values of the ozone indicator SOMO35 ($\mu\text{g}/\text{m}^3\cdot\text{d}$), 2021

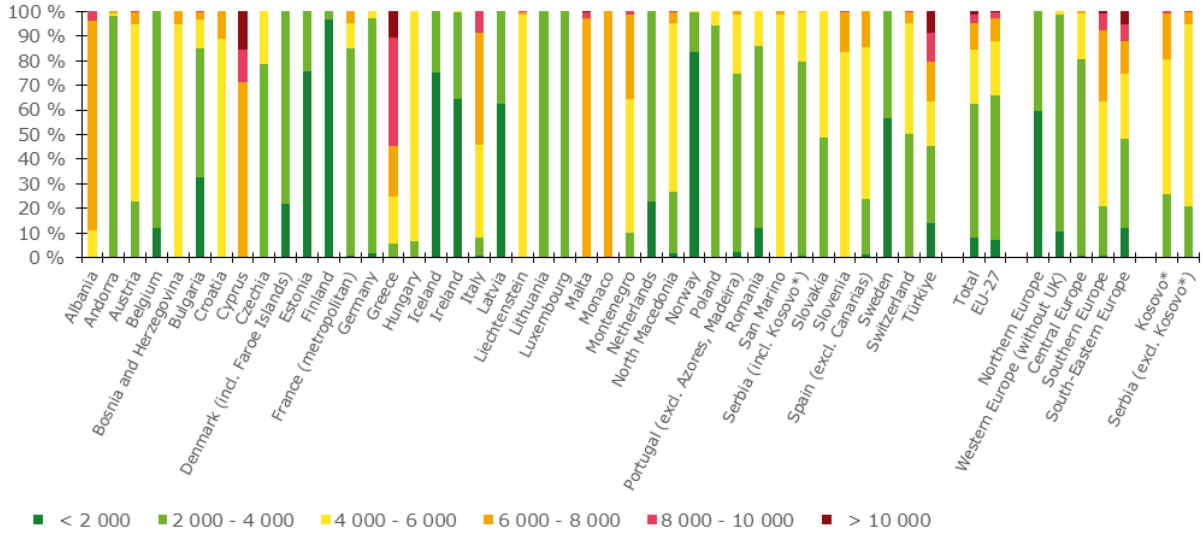


Figure 3.4 shows, for the whole mapped area, the frequency distribution of SOMO35 for population exposure classes of 250 $\mu\text{g}/\text{m}^3\cdot\text{d}$. The highest frequencies are found for classes between 2 000 and 5 000 $\mu\text{g}/\text{m}^3\cdot\text{d}$. One can see a steep decline of population frequency for exposure classes between 5 000 and 8 000 $\mu\text{g}/\text{m}^3\cdot\text{d}$ and a continuous mild decline of population frequency for classes above 8 000 $\mu\text{g}/\text{m}^3\cdot\text{d}$.

Figure 3.4: Population frequency distribution, ozone indicator SOMO35, 2021

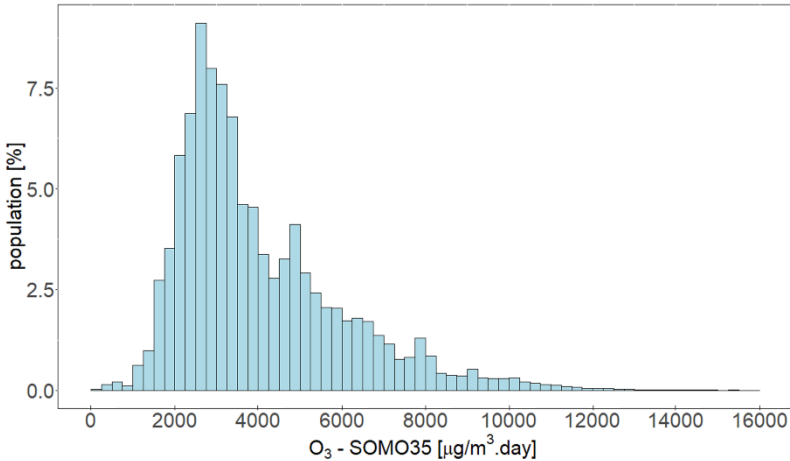
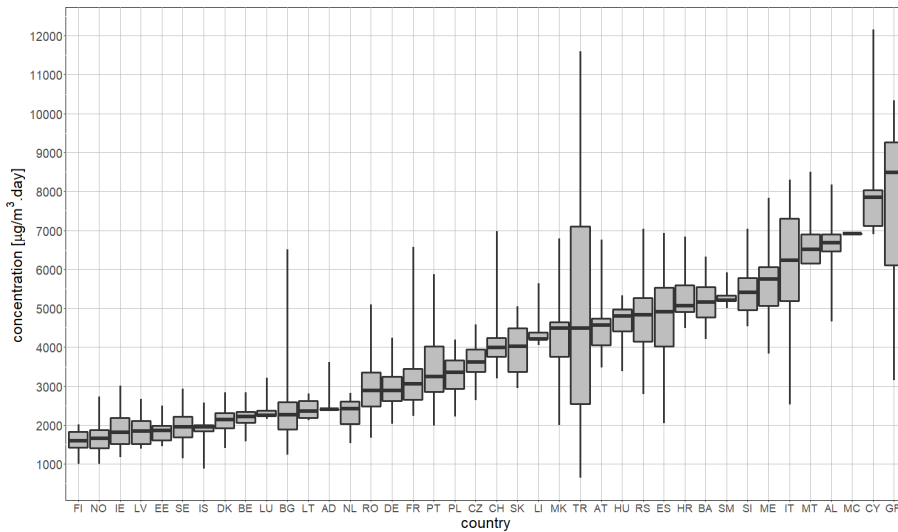


Figure 3.5 shows for individual countries the ozone indicator SOMO35 to which the population was exposed in 2021. It can be seen that the countries with the highest ozone concentrations are located in the southern and south-eastern parts of Europe.

Figure 3.5: Ozone concentrations expressed as indicator SOMO35 to which the population per country was exposed in 2021



Note: For each country, the box plot shows the concentration to which a percentage of the population was exposed: 50 % in the case of the black marker, 25 % and 75 % in the cases of the box's edges, 2 % and 98 % in the cases of the whiskers' edges.

SOMO10

Figure 3.6 and Table 3.3 give for SOMO10 the population frequency distribution for a limited number of exposure classes. Table 3.3 also presents the population-weighted concentration for individual countries, large regions, EU-27 and for the total mapped area.

Figure 3.6: Percentage of the population (%) exposed to different values of the ozone indicator SOMO10 ($\mu\text{g}/\text{m}^3\cdot\text{d}$), 2021

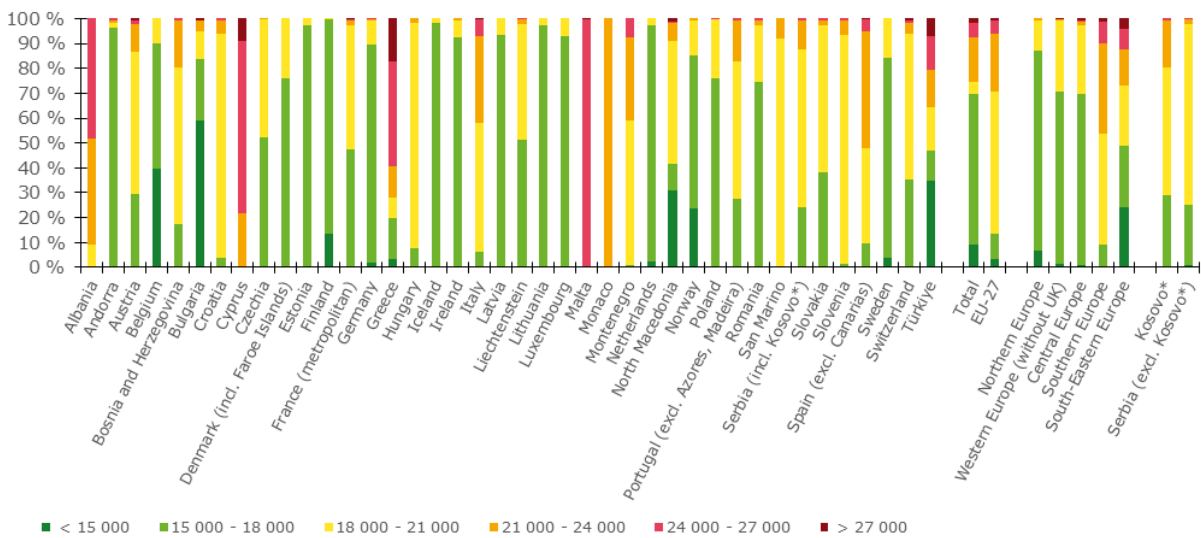


Table 3.3: Population exposure and population-weighted concentrations, ozone indicator SOMO10, 2021

Country	ISO	Population (inhbs-1000)	Ozone — SOMO10, exposed population, 2021 (%)					Population-weighted concentration			
			< 15 000	15 000-18 000	18 000-21 000	21 000-24 000	24 000-27 000	> 27 000	2021	5-year mean	Diff.
Albania	AL	2 830			10.7	80.2	9.0		22 090	21 477	614
Andorra	AD	79		96.6	1.5	1.2	0.8		17 088	20 121	-3 034
Austria	AT	8 933		29.7	57.7	11.3	1.2	0.1	19 153	19 860	-706
Belgium	BE	11 555	7.6	90.6	1.9				15 933	16 701	-768
Bosnia and Herzegovina	BA	3 271		17.2	63.8	18.1	0.9		19 508	20 157	-649
Bulgaria	BG	6 917	59.4	25.0	11.2	4.3	0.2	0.0	15 417	16 920	-1 504
Croatia	HR	4 036		2.8	65.6	31.0	0.6		20 170	20 875	-705
Cyprus	CY	9 343				21.6	69.6	8.8	24 689	20 292	4 396
Czechia	CZ	10 782		52.3	47.2	0.5			18 068	19 834	-1 766
Denmark (incl. Faroe Islands)	DK	5 840		76.1	23.9				17 692	18 130	-437
Estonia	EE	1 330		97.5	2.5				16 639	16 692	-53
Finland	FI	5 534	13.1	86.4	0.5				15 811	16 120	-309
France (metropolitan)	FR	65 447		43.7	45.9	10.1	0.3	0.0	18 449	19 373	-924
Germany	DE	83 155	1.9	88.1	9.8	0.3	0.0		16 876	18 376	-1 501
Greece	GR	10 679	3.3	16.4	8.2	12.5	42.4	17.2	23 339	21 577	1 762
Hungary	HU	9 731		7.8	91.1	1.1			19 092	18 609	484
Iceland	IS	369		89.6	10.4				17 307	15 927	1 380
Ireland	IE	5 006		59.4	40.5	0.0			17 620	16 834	786
Italy	IT	59 236	0.0	6.0	52.2	35.0	6.8	0.0	20 919	21 427	-508
Latvia	LV	1 893		93.6	6.4				16 325	16 672	-346
Liechtenstein	LI	39		51.1	46.9	1.9	0.1		18 174	19 578	-1 404
Lithuania	LT	2 796		97.5	2.5				16 903	16 556	347
Luxembourg	LU	635		93.2	6.8				16 302	17 550	-1 247
Malta	MT	516					99.8	0.2	25 053	23 767	1 287
Monaco	MC	37				100.0			23 464	23 409	56
Montenegro	ME	621		0.1	58.5	33.7	7.7		21 030	20 677	353
Netherlands	NL	17 475	2.2	95.0	2.8				16 619	17 119	-500
North Macedonia	MK	2 069	17.2	50.8	27.5	4.2	0.3	0.0	17 162	17 785	-623
Norway	NO	5 391	23.7	61.7	14.5	0.1			16 414	16 864	-450
Poland	PL	37 840		76.0	23.9	0.1	0.0		17 471	17 881	-411
Portugal (excl. Azores, Madeira)	PT	9 802		27.8	55.4	16.8	0.1		19 101	19 269	-167
Romania	RO	19 202	0.5	74.7	22.9	2.0	0.0		17 033	16 482	551
San Marino	SM	34			92.2	7.8			20 086	21 237	-1 152
Serbia (incl. Kosovo)	RS	8 534	0.1	23.6	64.1	11.7	0.5		19 012	17 107	1 905
Slovakia	SK	5 460		38.7	59.6	1.7	0.0		18 456	19 209	-753
Slovenia	SI	2 109		0.8	67.5	31.0	0.7		20 150	20 687	-537
Spain (excl. Canarias)	ES	45 154		9.4	38.6	47.2	4.7	0.0	20 953	21 328	-376
Sweden	SE	10 379	3.1	81.3	15.6				16 903	17 531	-628
Switzerland	CH	8 670		35.6	59.1	4.6	0.7	0.1	18 524	20 034	-1 509
Türkiye	TR	83 614	34.8	12.5	17.0	15.0	13.5	7.2	18 327	18 033	294
Total without UK		566 342	6.5	44.2	30.6	13.2	4.1	1.3	18 492	18 953	-461
			50.7				5.5				
EU-27			2.0	50.3	31.7	12.8	2.8	0.4	18 503	19 124	-621
		450 785		52.3			3.2				
Northern Europe		32 080	6.7	81.3	12.0	0.0			16 740		
Western Europe (without UK)		81 150	1.5	69.3	28.7	0.5	0.0	0.0	17 274		
Central Europe		162 777	0.9	69.7	27.7	1.5	0.1	0.0	17 519		
Southern Europe		140 620	0.3	8.8	44.7	36.4	8.5	1.4	21 002		
South-Eastern Europe		121 885	24.5	24.5	24.5	14.0	8.3	4.2	18 170		
Kosovo	KS	1 662		29.1	51.4	18.7	0.8		19 319	18 098	1 221
Serbia (excl. Kosovo)	RS-	6 872	0.1	22.2	67.2	10.0	0.4		18 937	16 865	2 073

Note: The percentage value "0.0" indicates that an exposed population exists, but it is small and estimated to be less than 0.05 %. Empty cells mean no population in exposure. 5-year mean, i.e. five-year mean 2016-2020. Diff., i.e. difference concentrations between 2021 and five-year mean 2016-2020.

The population-weighted ozone concentrations, in terms of SOMO10, were estimated to be 18 492 $\mu\text{g}/\text{m}^3\cdot\text{d}$ for the total mapped area. i.e. of about 461 $\mu\text{g}/\text{m}^3\cdot\text{d}$ less than the five-year 2016-2020 mean SOMO10 concentration. For the EU-27, it was 18 503 $\mu\text{g}/\text{m}^3\cdot\text{d}$, i.e. 621 $\mu\text{g}/\text{m}^3\cdot\text{d}$ less than the five-year 2016-2020 mean SOMO10 concentration. When assessing the change in individual countries, the steepest absolute decrease was found in Andorra (3 034 $\mu\text{g}/\text{m}^3\cdot\text{d}$), the highest absolute increase was estimated in Cyprus (4 396 $\mu\text{g}/\text{m}^3\cdot\text{d}$).

Figure 3.7 shows the population frequency distribution of SOMO10 for population exposure classes of 500 $\mu\text{g}/\text{m}^3\cdot\text{d}$. The graph shows the highest frequencies for classes between 16 500 and 22 000 $\mu\text{g}/\text{m}^3\cdot\text{d}$.

Figure 3.7: Population frequency distribution, ozone indicator SOMO10, 2021

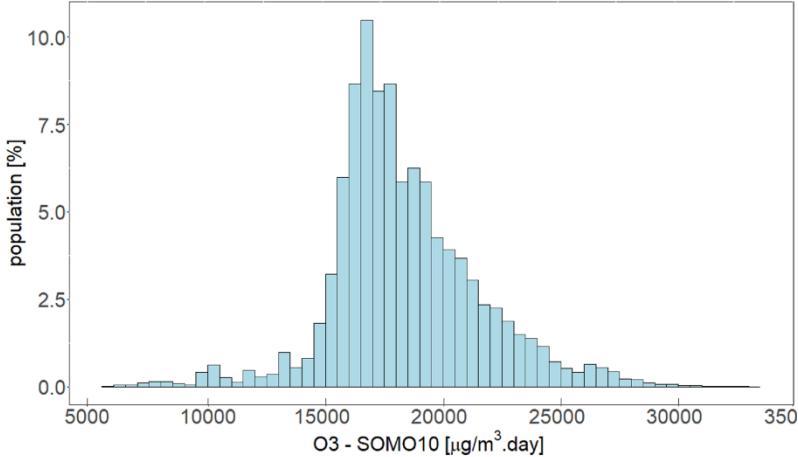
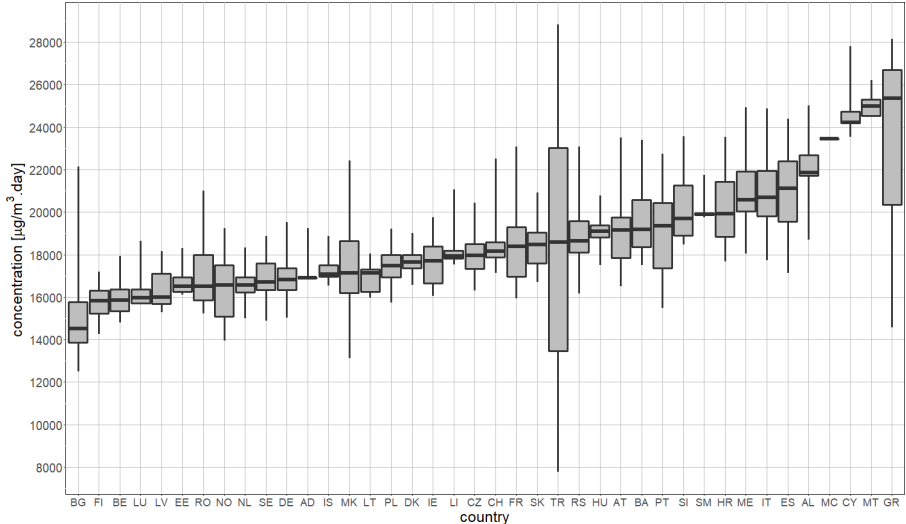


Figure 3.8 shows for individual countries the ozone indicator SOMO10 to which the population was exposed in 2021. It can be seen that the countries with the highest ozone concentrations are located in the southern and south-eastern parts of Europe.

Figure 3.8: Ozone concentrations expressed as indicator SOMO10 to which the population per country was exposed in 2021



Note: For each country, the box plot shows the concentration to which a percentage of the population was exposed: 50 % in the case of the black marker, 25 % and 75 % in the cases of the box's edges, 2 % and 98 % in the cases of the whiskers' edges.

3.3 Ozone – AOT40 vegetation and AOT40 forests

In the Ambient Air Quality Directive (EC, 2008) a target value (TV) and a long-term objective (LTO) for the protection of vegetation from high ozone concentrations accumulated during the growing season have been defined. TV and LTO are specified using “accumulated ozone exposure over a threshold of 40 parts per billion” (AOT40). This is calculated as a sum of the difference between hourly concentrations greater than 40 ppb (i.e. 80 $\mu\text{g}/\text{m}^3$) and 40 ppb, using only observations between 08:00 and 20:00 Central European Time (CET) each day, calculated over three months from 1 May to 31 July. The TV is 18 000 $\mu\text{g}/\text{m}^3\cdot\text{h}$ (averaged over five years) and the LTO is 6 000 $\mu\text{g}/\text{m}^3\cdot\text{h}$.

Note that the term “vegetation” as used in the Ambient Air Quality Directive (EC, 2008) is not further defined. Nevertheless, the TV used in the directive is quite similar as the critical level used in the Mapping Manual (CLRTAP, 2017a) for “agricultural crops” (although the definitions of AOT40 by the EU and the CLRTAP are slightly different), so the term vegetation in the Air Quality Directive has been interpreted as primarily agricultural crops. Therefore, the exposure of agricultural crops has been evaluated here based on the AOT40 for vegetation as defined in the Air Quality Directive and the agricultural areas, defined as the CORINE Land Cover level-1 class 2 Agricultural areas (encompassing the level-2 classes 2.1 Arable land, 2.2 Permanent crops, 2.3 Pastures and 2.4 Heterogeneous agricultural areas), see Section 3.3.2. Note that in addition to these agricultural areas there are several other CLC classes that could be considered “vegetation”, namely level-2 classes 1.4 Artificial, non-agricultural vegetated areas (encompassing the level-3 classes 1.4.1 Green urban areas and 1.4.2 Sport and leisure facilities), 3.1 Forests (see below) and 3.2 Scrub and/or herbaceous vegetation associations.

Next to the AOT40 for vegetation protection, the Ambient Air Quality Directive (EC, 2008) defines also the AOT40 for forest protection, which is calculated similarly as the AOT40 for vegetation, but is summed over six months from 1 April to 30 September. For AOT40 for forests there is no TV defined in the Air Quality Directive. However, there is a critical level (CL) established by the CLRTAP, see CLRTAP (2017a). This critical level is set at 10 000 $\mu\text{g}/\text{m}^3\cdot\text{h}$. Although CLRTAP (2017a) calculates the AOT40 indicators somewhat differently (e.g. it uses the ozone concentration corrected at canopy height), we further use this CL level for the AOT40 for forests calculated according to the EC (2008).

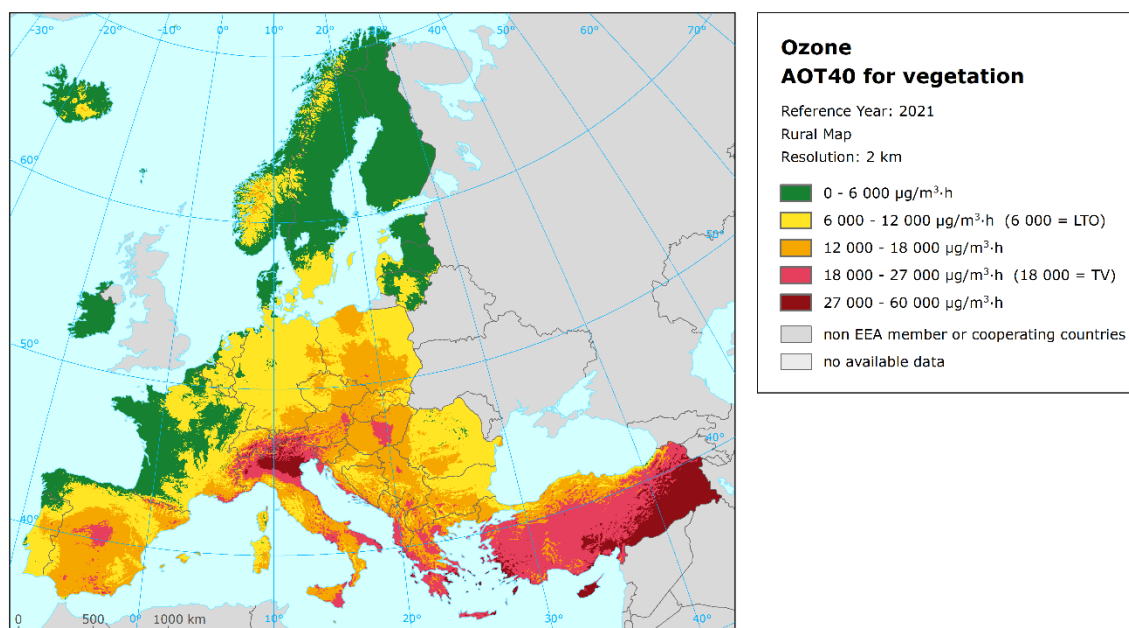
For the exposure of forests evaluation, the CLC level-2 class 3.1 Forests has been used.

The ecosystem based accumulative ozone indicators described in this section are specifically prepared for calculation of the EEA indicator on ecosystem exposure to ozone (EEA, 2023b). For the estimation of the vegetation and forested area exposure to accumulated ozone, the maps in this section are created on a grid of 2 km resolution. The exposure frequency distribution outcomes are based on the overlay with the 100 m grid resolution of the CLC2018 land cover classes.

Concentration maps

The interpolated maps of AOT40 for vegetation and AOT40 for forests are applicable for rural areas only. Map 3.6 presents the final map of AOT40 for vegetation in 2021. Note that in the Ambient Air Quality Directive (EC, 2008) the TV is actually defined as 18 000 $\mu\text{g}/\text{m}^3\cdot\text{h}$ averaged over five years. Here only 2021 data are presented, and no five-year average has been calculated. Therefore, we evaluate the concentrations against what we call the target value threshold, an AOT40 of 18 000 $\mu\text{g}/\text{m}^3\cdot\text{h}$ in 2021.

Map 3.6: Concentration map of ozone indicator AOT40 for vegetation, rural map, 2021

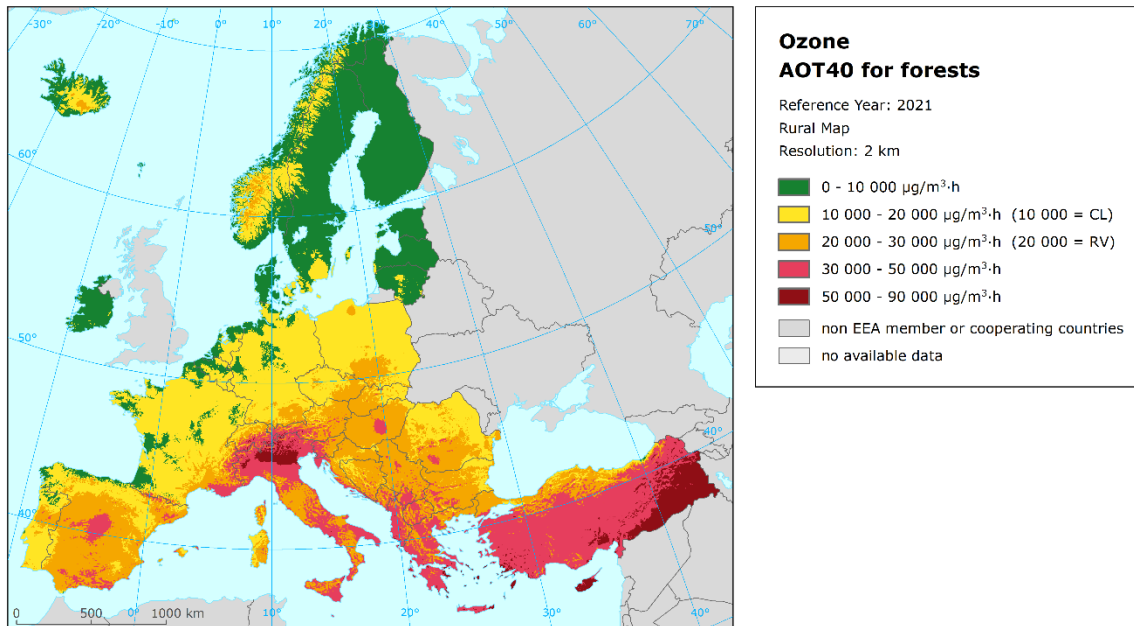


The areas in the map with concentrations above the TV threshold of 18 000 $\mu\text{g}/\text{m}^3\cdot\text{h}$ are marked in red and dark red. The areas below the long-term objective (LTO) are marked in green. AOT40 levels above the TV threshold for vegetation occur specifically in southern of Europe (Italy, relatively smaller parts of Spain, France, Slovenia and the Balkan countries with the largest concentrations above the TV threshold in Greece and Albania) and almost in whole Türkiye. The highest levels (dark red) were estimated in the north of Italy, in south-west of Türkiye and in Cyprus. Furthermore, areas above the TV threshold can also be found partly in central Europe, i.e. in Switzerland, Austria and Hungary. The relative mean uncertainty of the 2021 map of the AOT40 for vegetation is about 40 % (Annex 3, Section A3.3).

Map 3.7 presents the final map of AOT40 for forests in 2021. The areas in the map with concentrations above the critical level (CL) defined by CLRTAP (2017a) are marked in yellow, orange, red and dark red. One can see large, forested areas exceeding this level in most of Europe, with the exception of parts of some northern countries. The highest values of the AOT40 for forests are found mainly in southern Europe and Türkiye although, as it is the case for the AOT40 for vegetation indicator, high levels are also found partly in central Europe, i.e. in Switzerland, Austria, and Hungary. The relative mean uncertainty of the 2021 map of the AOT40 for forests is about 39 % (Annex 3, Section A3.3).

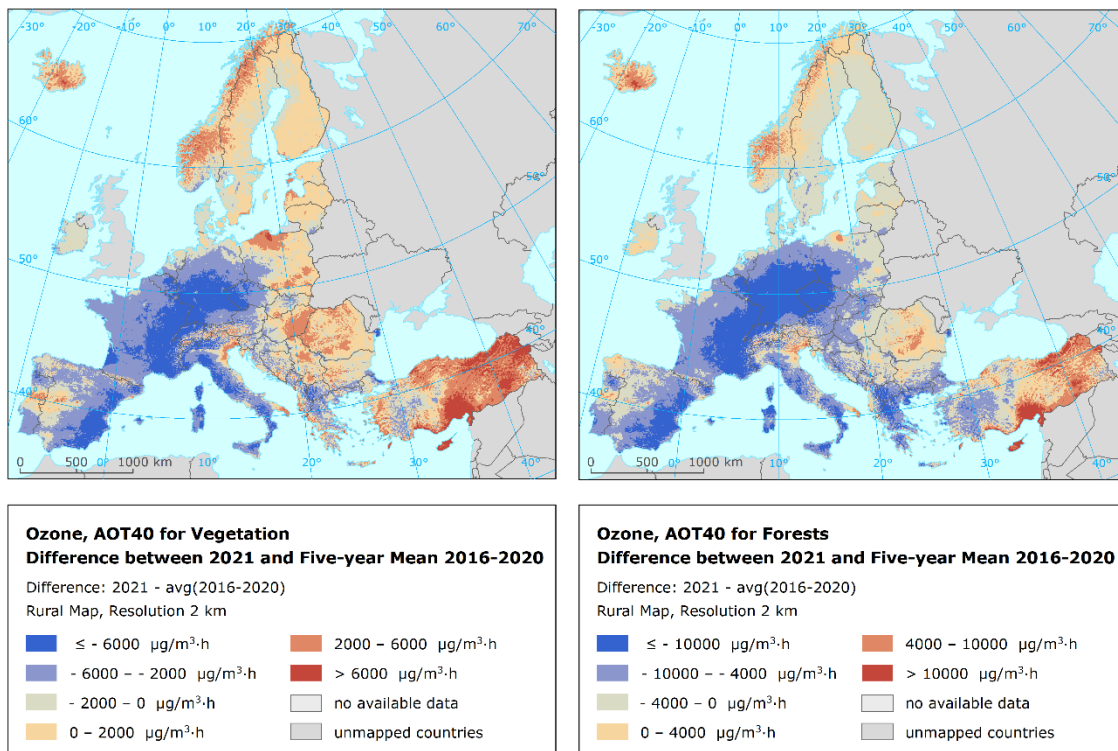
In order to provide more complete information of the air quality across Europe, the AOT40 maps including the AOT40 values based on the actual rural background measurement data at stations are presented in Maps A4.7 and A4.8 of Annex 4.

Map 3.7: Concentration map of ozone indicator AOT40 for forests, rural map, 2021



Map 3.8. presents the difference between 2021 and the five-year mean 2016-2020 for AOT40 for vegetation and for AOT40 for forests. Orange to red areas show an increase of AOT40 in 2021, while blue areas show a decrease.

Map 3.8: Difference concentrations between 2021 and the five-year average 2016-2020 for ozone indicators, AOT40 for vegetation (left) and AOT40 for forests (right)



The largest increases of AOT40 for vegetation were recorded in large area of Türkiye. Increases were also found in the Eastern part of the estimated area and in Iceland and some small parts of Portugal, Spain, and Italy. Otherwise, a decrease in AOT40 is observed in southern, western, and central Europe with the deepest decrease in large parts of Germany, France and the Mediterranean coast of Spain. As far as AOT40 for forests is concerned, the situation is very similar compared to AOT40 for vegetation. However, for AOT40 for forests, no increase has been observed in the Balkan countries and smaller and less extensive increases are observed in central and northern Europe.

Vegetation exposure

Agricultural crops

The rural map with the ozone indicator AOT40 for vegetation has been combined with the land cover CLC2018 map. Following a similar procedure as described in Horálek et al. (2007), the exposure of agricultural areas (as defined above) has been calculated at the country-level.

Table 3.4 gives the absolute and relative agricultural area for each country and for five European regions where ozone concentrations are above the target value (TV) threshold and the long-term objective (LTO) for protection of vegetation as defined in the Ambient Air Quality Directive (EC, 2008). The frequency distribution of the agricultural area over some exposure classes per country is presented as well.

Table 3.4 illustrates that in 2021, almost 18 % of all European agricultural land including Türkiye has been exposed to ozone concentrations above the TV threshold of 18 000 $\mu\text{g}/\text{m}^3\cdot\text{h}$. For the area for the EU-27, it has been about 7 %. None of the agricultural area presents ozone levels in excess of the TV in 13 countries. Agricultural areas with ozone concentrations above TV threshold covered less than 18 % in Czechia, Germany, Portugal, Bulgaria, Poland, France, Slovakia, Bosnia and Herzegovina, Serbia, Montenegro, Liechtenstein, Switzerland, Spain, North Macedonia, Austria, Slovenia, Croatia, and Hungary (in ascending order). In Kosovo, San Marino, Italy, Albania, Malta, and Greece, between 22 % and 59 % of agricultural area has been exposed to ozone concentrations above the TV threshold. The largest proportion of the agricultural area exposed to ozone concentrations above the TV threshold is in Türkiye (78 %) and Cyprus (100 %).

Considering the LTO of 6 000 $\mu\text{g}/\text{m}^3\cdot\text{h}$, the total European area including Türkiye in excess has been about 81 %. For the area for the EU-27, it has been 78 %. In 2021, values of the AOT40 for vegetation above the LTO have occurred in all countries with the exception of Iceland and Ireland. Fewer than 10% of the areas with values above the LTO have occurred in Finland, Norway, and Estonia. Only in a few of the remaining countries (Latvia, Denmark, Sweden, France, and Lithuania), the agricultural area exposed above the LTO in 2021 has been lower than 50 %, since in most of them between 78 % and 100 % of the agricultural area has been exposed to ozone levels in excess of the LTO.

Forests

The rural map with ozone indicator AOT40 for forests was combined with the land cover CLC2018 map. Following a similar procedure as described in Horálek et al. (2007), the exposure of forest areas (as defined above) has been calculated for each country, for the same five European regions as for crops and for Europe as a whole. Table 3.5 gives the absolute and relative forest area where the critical level (CL) set at 10 000 $\mu\text{g}/\text{m}^3\cdot\text{h}$, the same level as defined in CLRTAP (2017a), and the value 20 000 $\mu\text{g}/\text{m}^3\cdot\text{h}$ (which is equal to the earlier used reporting value, RV, as was defined in the repealed ozone directive 2002/3/EC) are exceeded. Next to the forest area in exceedance, the table presents the frequency distribution of the forest area over some exposure classes.

Table 3.4: Agricultural area exposure and agricultural-weighted concentrations, ozone indicator AOT40 for vegetation, 2021

Country	Agricultural area, 2021						Percentage of agricultural area (%)				Agricultural-weighted concentr.			
	Total area (km ²)	> ITO (6 000 µg/m ³ ·h)		> TV (18 000 µg/m ³ ·h)		< 6 000 (%)	6 000- 12 000	12 000- 18 000	18 000- 27 000	> 27 000 (µg/m ³ ·h)	2021	5-year mean	Diff.	
		(km ²)	(%)	(km ²)	(%)		(µg/m ³ ·h)	(µg/m ³ ·h)	(µg/m ³ ·h)					
Albania	8 017	8 017	100.0	4 322	53.9		9.8	36.3	53.9	0.0	17 749	18 694	-945	
Andorra	13	13	100.0	3	24.1		29.2	46.7	24.1		14 836			
Austria	26 827	26 827	100.0	2 305	8.6		6.5	84.9	8.6	0.0	15 235	17 919	-2 684	
Belgium	17 473	14 049	80.4			19.6	80.4				6 499	11 666	-5 168	
Bosnia-Herzegovina	17 023	17 004	99.9	79	0.5	0.1	49.5	50.0	0.5		11 883	13 089	-1 206	
Bulgaria	57 390	57 390	100.0	19	0.0		72.8	27.2	0.0		10 587	10 824	-237	
Croatia	22 168	22 168	100.0	2 790	12.6		25.7	61.7	12.5	0.1	13 800	14 998	-1 198	
Cyprus	4 291	4 291	100.0	4 291	100.0				14.3	85.7	30 213	20 577	9 635	
Czechia	44 784	44 784	100.0	0	0.0		50.3	49.7	0.0		12 365	17 019	-4 654	
Denmark (incl. Faroes)	31 235	9 897	31.7			68.3	31.6	0.0			5 651	6 340	-689	
Estonia	14 252	1 235	8.7			91.3	8.7				4 672	3 662	1 010	
Finland	27 504	632	2.3			97.7	2.3				3 720	2 983	737	
France	323 377	119 947	37.1	592	0.2	62.9	34.5	2.4	0.2		5 915	11 367	-5 452	
Germany	204 463	199 121	97.4	1	0.0	2.6	88.5	8.9	0.0		9 045	13 573	-4 528	
Greece	50 052	50 052	100.0	29 577	59.1		3.1	37.8	52.1	7.0	19 281	20 755	-1 474	
Hungary	60 390	60 390	100.0	10 529	17.4		3.2	79.4	17.4		15 816	14 276	1 540	
Iceland	2 518					100.0					413	985	-572	
Ireland	46 756	0	0.0			100.0	0.0				1 874	3 028	-1 154	
Italy	155 718	155 617	99.9	70 508	45.3	0.1	15.1	39.5	32.7	12.6	18 651	22 171	-3 521	
Latvia	25 532	5 093	19.9			80.1	19.9				5 181	4 188	993	
Liechtenstein	37	37	100.0	1	3.7		89.1	7.2	3.7		11 060	19 388	-8 328	
Lithuania	38 155	16 758	43.9			56.1	43.9				5 957	5 472	485	
Luxembourg	1 351	1 351	100.0				100.0				7 635	13 424	-5 789	
Malta	125	125	100.0	70	56.0			44.0	56.0		19 603	20 157	-554	
Monaco														
Montenegro	2 242	2 242	100.0	81	3.6		35.1	61.3	3.6		13 129	15 218	-2 089	
Netherlands	23 644	18 518	78.3			21.7	78.3				6 815	8 837	-2 022	
North Macedonia	9 146	9 146	100.0	507	5.5		17.5	76.9	5.5		14 411	17 742	-3 331	
Norway	15 637	709	4.5			95.5	4.5				2 929	3 372	-443	
Poland	183 268	183 268	100.0	156	0.1	0.0	53.5	46.4	0.1		11 946	11 322	624	
Portugal	42 566	37 749	88.7	1	0.0	11.3	78.6	10.1	0.0		8 215	10 237	-2 022	
Romania	135 279	133 569	98.7			1.3	80.2	18.5			9 624	8 627	998	
San Marino	42	42	100.0	16	38.7		61.3	38.7			17 751	20 641	-2 889	
Serbia (incl. Kosovo)	46 768	46 768	100.0	1 671	3.6		14.9	81.5	3.6		14 195	13 498	697	
Slovakia	23 100	23 100	100.0	43	0.2		34.3	65.6	0.2		13 845	14 149	-303	
Slovenia	6 986	6 986	100.0	814	11.7		3.9	84.4	11.7	0.0	15 680	17 373	-1 693	
Spain	241 014	226 283	93.9	11 798	4.9	6.1	30.3	58.7	4.9	0.0	12 710	16 294	-3 584	
Sweden	39 035	13 541	34.7			65.3	34.7				5 339	5 315	24	
Switzerland	11 359	11 305	99.5	473	4.2	0.5	68.1	27.3	4.1	0.1	11 402	18 701	-7 298	
Türkiye	339 984	339 432	99.8	266 973	78.5	0.2	5.3	16.0	56.5	22.1	22 361			
Total	2 299 525	1 867 457	81.2	407 621	17.7	18.8	36.5	27.0	13.3	4.4	12 246			
Total without Türkiye	1 959 541	1 528 024	78.0	140 648	7.2	22.0	41.9	28.9	5.8	1.4	10 493	12 773	-2 280	
EU-27	1 846 681	1 432 741	77.6	133 494	7.2	22.4	43.0	27.4	5.8	1.5	10 405	12 756	-2 351	
Northern Europe	193 869	47 864	24.7			75.3	24.7	0.0			4 953			
Western Europe (no UK)	346 009	116 842	33.8	2	0.0	66.2	33.7	0.1	0.0		5 180			
Central Europe	561 215	555 819	99.0	14 323	2.6	1.0	57.2	39.3	2.5	0.0	11 610			
Southern Europe	560 414	511 195	91.2	116 854	20.9	8.8	28.6	41.7	16.1	4.8	14 095			
South-Eastern Europe	638 018	635 737	99.6	276 442	43.3	0.4	30.2	26.1	31.6	11.8	17 221			
Kosovo	4 167	4 167	100.0	897	21.5		6.3	72.2	21.5		15 380	685	685	
Serbia (without Kosovo)	42 601	42 601	100.0	774	1.8		15.8	82.4	1.8		13 312	700	700	

Note: The percentage value "0.0" indicates that an exposed population exists, but it is small and estimated to be less than 0.05 %. Empty cells mean no population in exposure. 5-year mean, i.e. five-year mean 2016-2020. Diff., i.e. difference concentrations between 2021 and the five-year mean 2016-2020.

The CL was exceeded in 2021 at 63 % of all European forested area including Türkiye. For the area of the EU-27 it was exceeded at about 60 %. As in previous years, most countries continue to have in 2021 the whole or considerable forest areas in excess of the CL. In 2021, there were no countries without CL exceedance. Fewer than 10% of the areas with values above the CL have occurred in Finland, Iceland, Estonia, Ireland, Latvia, Sweden and Lithuania. In Denmark and Norway, the areas with the values above CL has been 24 % and 26 %, respectively. In the remaining countries, the CL for AOT40 was exceeded in 81% to 100% of the area of the respective country.

Table 3.5: Forested area exposure and forest-weighted concentrations, ozone indicator AOT40 for forests, 2021

Country	Forested area						Percentage of forested area [%]				Forest-weighted conc. ($\mu\text{g}/\text{m}^3\cdot\text{h}$)		
	Total area (km^2)	> CL ($10\,000\ \mu\text{g}/\text{m}^3\cdot\text{h}$)		> RV ($20\,000\ \mu\text{g}/\text{m}^3\cdot\text{h}$)		< 10 000 (%)	10 000- 20 000	20 000- 30 000	30 000- 50 000	> 50 000	2021	5-year mean	Diff.
		(km^2)	(km^2)	(%)	(km^2)		(%)	($\mu\text{g}/\text{m}^3\cdot\text{h}$)	($\mu\text{g}/\text{m}^3\cdot\text{h}$)	($\mu\text{g}/\text{m}^3\cdot\text{h}$)	($\mu\text{g}/\text{m}^3\cdot\text{h}$)		
Albania	7 104	7 104	100.0	7 084	99.7		0.3	23.0	76.0	0.7	34 377	39 443	-5 066
Andorra	128	128	100.0	18	13.7		86.3	13.7			23 697		
Austria	36 667	36 667	100.0	32 492	88.6		11.4	71.5	17.1	0.0	25 691	32 037	-6 346
Belgium	6 089	5 376	88.3			11.7	88.3				11 897	22 198	-10 302
Bosnia-Herzegovina	23 911	23 911	100.0	19 836	83.0		17.0	78.7	4.2		23 819	27 407	-3 587
Bulgaria	34 675	34 675	100.0	30 369	87.6		12.4	69.7	17.9		25 487	28 372	-2 885
Croatia	19 734	19 734	100.0	18 098	91.7		8.3	67.7	24.0	0.0	26 333	29 997	-3 664
Cyprus	1 458	1 458	100.0	1 458	100.0				9.0	91.0	54 920	43 480	11 440
Czechia	25 867	25 867	100.0	9 551	36.9		63.1	36.9	0.0		19 181	31 457	-12 276
Denmark (incl. Faroes)	3 747	913	24.4			75.6	24.4				8 783	11 831	-3 048
Estonia	21 080	222	1.1			98.9	1.1				5 831	7 265	-1 434
Finland	211 668	0	0.0			100.0	0.0				4 391	5 361	-970
France	143 376	131 936	92.0	28 276	19.7	8.0	72.3	14.9	4.9	0.0	15 521	25 807	-10 286
Germany	108 031	103 037	95.4	9 233	8.5	4.6	86.8	8.4	0.1		14 814	27 375	-12 562
Greece	26 122	26 122	100.0	25 847	98.9		1.1	32.9	63.5	2.6	33 603	41 444	-7 841
Hungary	17 407	17 407	100.0	16 178	92.9		7.1	85.7	7.2		24 340	29 198	-4 858
Iceland	537	2	0.4			99.6	0.4				3 752	3 614	138
Ireland	4 510	59	1.3			98.7	1.3				5 897	5 796	102
Italy	79 052	79 052	100.0	77 582	98.1	0.0	1.9	33.0	56.7	8.4	34 847	40 610	-5 763
Latvia	24 261	1 049	4.3			95.7	4.3				7 597	8 284	-687
Liechtenstein	79	79	100.0	64	80.7		19.3	34.6	46.2		27 626	36 586	-8 959
Lithuania	19 455	1 900	9.8			90.2	9.8				9 104	11 018	-1 914
Luxembourg	937	937	100.0				100.0				14 117	23 940	-9 822
Malta	2	2	100.0	2	100.0				100.0		41 908	43 135	-1 226
Monaco	1	1	100.0	1	100.0				91.3	8.8	44 136	36 497	7 640
Montenegro	5 777	5 777	100.0	5 610	97.1		2.9	55.9	41.2		29 066	33 124	-4 058
Netherlands	3 118	2 533	81.2			18.8	81.2				10 806	16 709	-5 903
North Macedonia	8 144	8 144	100.0	8 116	99.7		0.3	46.0	53.7		30 542	39 485	-8 944
Norway	103 494	26 573	25.7	28	0.0	74.3	25.6	0.0			7 822	7 772	51
Poland	96 966	96 947	100.0	14 909	15.4	0.0	84.6	15.4	0.0		16 721	21 647	-4 927
Portugal	16 512	15 879	96.2	5 022	30.4	3.8	65.8	30.1	0.4		17 736	21 540	-3 804
Romania	71 273	71 272	100.0	37 442	52.5	0.0	47.5	49.7	2.8		20 939	19 791	1 148
San Marino	6	6	100.0	6	100.0			31.2	68.8		30 901	37 797	-6 896
Serbia (incl. Kosovo)	27 211	27 211	100.0	26 786	98.4		1.6	73.5	24.9	0.0	27 565	29 655	-2 090
Slovakia	20 484	20 484	100.0	12 232	59.7		40.3	59.3	0.4		21 066	27 098	-6 032
Slovenia	11 441	11 441	100.0	11 346	99.2		0.8	52.4	46.8	0.0	29 860	33 279	-3 419
Spain	107 927	100 260	92.9	67 141	62.2	7.1	30.7	53.1	9.1	0.0	21 365	27 593	-6 229
Sweden	261 757	23 125	8.8			91.2	8.8				6 516	7 825	-1 309
Switzerland	11 850	11 849	100.0	8 904	75.1	0.0	24.9	48.6	25.8	0.7	25 919	35 221	-9 302
Türkiye	114 886	114 719	99.9	106 641	92.8	0.1	7.0	29.2	57.5	6.1	33 973		
Total	1 676 742	1 053 861	62.9	580 270	34.6	37.1	28.2	22.1	11.5	0.9	16 461		
Total without Türkiye	1 561 857	939 141	60.1	473 629	30.3	39.9	29.8	21.6	8.2	0.6	15 174	19 494	-4 320
EU-27	1 373 615	828 356	60.3	397 178	28.9	39.7	31.4	20.7	7.6	0.6	14 994	19 624	-4 631
Northern	645 997	53 784	8.3	28	0.0	91.7	8.3	0.0			6 136		
Western (without UK)	104 660	91 654	87.6	5 794	5.5	12.4	82.0	5.1	0.4		12 801		
Central	328 793	323 779	98.5	114 909	34.9	1.5	63.5	30.0	4.9	0.0	18 753		
Southern	284 577	272 096	95.6	199 558	70.1	4.4	25.5	39.7	27.4	3.1	25 781		
South-Eastern	312 715	312 548	99.9	259 981	83.1	0.1	16.8	49.2	31.6	2.2	28 074		
Kosovo	4 316	4 316	100.0	4 316	100.0			24.6	75.4	0.0	32 743	34 395	-1 652
Serbia (without Kosovo)	22 894	22 894	100.0	22 470	98.1		1.9	82.7	15.4		26 589	28 760	-2 171

Note: The percentage value "0.0" indicates that an exposed population exists, but it is small and estimated to be less than 0.05 %. Empty cells mean no population in exposure. 5-year mean, i.e. five-year mean 2016-2020. Diff., i.e. difference concentrations between 2021 and the five-year mean 2016-2020.

In 2021, the agricultural-weighted ozone concentration of vegetation-related AOT40 for the EU-27 area was estimated to be $10\,405\ \mu\text{g}/\text{m}^3\cdot\text{h}$, i.e. $2\,351\ \mu\text{g}/\text{m}^3\cdot\text{h}$ less than the five-year 2016-2020 mean. When assessing the change in individual countries, the steepest absolute decrease was found in Liechtenstein ($8\,328\ \mu\text{g}/\text{m}^3\cdot\text{h}$), the highest increase was estimated in Cyprus ($9\,635\ \mu\text{g}/\text{m}^3\cdot\text{h}$). The forest-weighted ozone concentration of forest-related AOT40 for the EU-27 area was estimated to be $14\,994\ \mu\text{g}/\text{m}^3\cdot\text{h}$, i.e. $4\,631\ \mu\text{g}/\text{m}^3\cdot\text{h}$ less than the five-year 2016-2020 mean. When assessing the change in individual countries, the steepest absolute decrease was found in Germany ($12\,562\ \mu\text{g}/\text{m}^3\cdot\text{h}$), the highest increase was estimated in Cyprus ($11\,440\ \mu\text{g}/\text{m}^3\cdot\text{h}$).

In this context, it should be mentioned that the AOT40 indicator is not the best proxy for vegetation damage assessment. AOT40 does not take into account plant physiological control of ozone absorbed doses, which is taken into account in the POD (i.e. Phytotoxic Ozone Dose) indicators, as discussed in

Section 3.4. POD indicators are known to be more related with ozone effects on plant growth than ambient air ozone concentrations alone. The AOT40 does not take into account the influence of meteorological conditions on growing season timing. Growing season's start and end dates can change across Europe, and between years for a given site, depending on factors such as air temperature, solar radiation, photoperiod or rainfall. High temperature and dry weather favouring ozone pollution cause a reduction of ozone absorbed doses by plants due to plant physiological response to drought (i.e. the vegetation closes its stomata protecting itself from the exposure to ozone). However, plants may still be sensitive to ozone in such weather conditions, as illustrated by foliar injury records in Aleppo pine stands growing in southern France (CLRTAP, 2016) or controlled experimental results (e.g. Alonso et al., 2014).

3.4 Ozone – Phytotoxic Ozone Dose (POD) for crops and trees

Ozone is generally recognized to be the most relevant pollutant for plants. Visible injury, reduction in growth, changes in biomass partitioning, or a higher susceptibility to pathogen attack can be the effect of ozone influence (Krupa et al., 2000). As mentioned above, scientific evidence suggests that observed effects of ozone on vegetation are more strongly related to the uptake of ozone through the stomatal leaf pores into the leaf interior (stomatal flux) than to the concentration in the atmosphere around the plants (Mills et al., 2011; Reich, 1987; Ashmore et al., 2004).

The cumulative stomatal ozone fluxes (F_{sto}) through the stomata of leaves found at the top of the canopy are calculated over the course of the growing season based on ambient ozone concentration and stomatal conductance (g_{sto}) to ozone. The stomatal conductance has been calculated using a multiplicative stomatal conductance model (Emberson et al., 2000) based on Jarvis (1976) as a function of species-specific maximum g_{sto} (expressed on a single leaf-area basis), phenology, and prevailing environmental conditions (photosynthetic photon flux density, PPF), air temperature, vapour pressure deficit (VPD), and soil moisture.

POD_Y (Phytotoxic Ozone Dose) is the accumulated plant uptake (flux) of ozone above a threshold of Y during a specified time or growth period. The flux-based POD_Y metrics are preferred in risk assessment over the concentration-based AOT40 exposure index. AOT40 accounts for the atmospheric ozone concentration above the leaf surface and is therefore biologically less relevant for ozone impact assessment than POD_Y as it does not take into account how ozone uptake is affected by climate, soil and plant factors.

Several POD_Y indicators are described in CLRTAP (2017a). POD_YSPEC is a species or group of species-specific POD_Y that requires comprehensive input data and is suitable for detailed risk assessment. POD_YIAM is a vegetation-type specific POD_Y that requires less input data and is suitable for large-scale modelling, including integrated assessment modelling. POD_YSPEC is further used in this report.

For crops (wheat, potato and tomato), the Y value is taken equal to 6 nmol/m² PLA s⁻¹ (i.e. per unit projected leaf area) as recommended in CLRTAP (2017a). For the details of POD_Y (and specifically POD₆SPEC as used in this report) calculation, see Annex 1, Section A1.3.

The species-specific flux models and associated response functions and critical levels for ozone-sensitive crops and cultivars can be used to quantify the potential negative impacts of O₃ on the security of food supplies at the local and regional scale. They can be used to estimate yield losses, including economic losses. A flux-threshold Y of 6 (POD₆SPEC) provides the strongest flux-effect relationships for crops (Pleijel et al., 2007). O₃ effects proved to be significant at a 5 % reduction of the effect parameter (Mills et al., 2011), hence critical levels (CL) were determined for this 5 % reduction of the effect parameter (i.e. yield, weight or quality of grain, tuber or fruit), based on the slope of the function. The POD₆SPEC CLs for crops were determined based on this reduction of relevant yield or weight, as shown in Table 3.6.

Wheat, potato and tomato are considered as representative species of crops in Europe (tomato can be regarded as representative horticultural crop for the Mediterranean and Black Sea regions, which

is the case of potato for other regions). Therefore, POD₆SPEC for these crops (labelled further simply as POD₆ for wheat, potato and tomato, respectively) are recommended for regular map construction. This report presents maps of POD₆ for wheat (*Triticum aestivum*), potato (*Solanum tuberosum*) and tomato (*Solanum lycopersicum*).

Table 3.6: POD₆SPEC critical levels for crops as determined by CLRTAP

Crop	Effect parameter	POD ₆ SPEC critical level
Wheat	grain yield	1.3 mmol/m ² PLA
Wheat	1000-grain weight	1.5 mmol/m ² PLA
Wheat	protein yield	2.0 mmol/m ² PLA
Potato	tuber yield	3.8 mmol/m ² PLA
Tomato	fruit yield	2 mmol/m ² PLA
Tomato	fruit quality	3.8 mmol/m ² PLA

Source: CLRTAP, 2017a

Regarding trees, beech (*Fagus sylvatica*) and Norway spruce (*Picea abies*) were selected as the tree species for which the most comprehensive parameterization for POD is available. For them, the Y value is taken equal to 1 nmol/m² PLA s⁻¹ (i.e. per unit projected leaf area). For the details of POD_Y (and specifically POD₁SPEC as used in this report) calculation, see Vlasáková et al. (2023).

A uniform O₃ flux threshold of Y = 1 nmol/m²/s PLA (projected leaf area) was adopted for use in species-specific phytotoxic O₃ doses (POD_YSPEC) for all tree species at the O₃ Critical Levels workshop in Madrid, November 2016 (CLRTAP, 2017a), based on data and analyses presented in Büker et al. (2015). Anav et al. (2022) illustrated that POD₁ is the most reliable simple estimate of O₃ risk and recommended the use of this metric by policy makers as an air quality standard to protect vulnerable forest ecosystems in the future. The POD₁SPEC critical levels for forest trees were set to values for an acceptable biomass loss, as shown in Table 3.7.

Table 3.7: POD₁SPEC critical levels for trees as determined by CLRTAP

Tree	Effect parameter	POD ₁ SPEC critical level
Beech	4 % annual reduction of the whole tree biomass	5.2 mmol/m ² PLA
Spruce	2 % annual reduction of the whole tree biomass	9.2 mmol/m ² PLA

Source: CLRTAP, 2017a

The POD maps have been calculated based on the hourly ozone concentration maps, together with the meteorological and soil hydraulic properties data, based on the methodology described in Annex 1, Section A1.3. The calculation has been executed in 0.1° x 0.1° resolution. The hourly ozone maps are created for rural areas only, based on rural background stations. The POD maps are therefore applicable to rural areas only. Next to this, it should be noted that in the POD calculations for wheat and potato, all growing areas are considered rain-fed (i.e. without irrigation), see Colette et al. (2018). Thus, the maps are directly applicable only for areas without irrigation. If applied for irrigated areas, the POD values for wheat and potato might be somewhat underestimated. On the other hand, no limitation of stomatal conductance due to soil moisture can be assumed for tomato, since it is an irrigated horticultural crop (see Annex 1, Section A1.3).

The hourly ozone maps needed for POD calculation have been calculated at the 2 km resolution, based on rural background measurements. The maps for each hour of the year 2021 have been constructed using the same methodology as the annual maps, i.e. the multiple linear regression followed by the kriging of its residuals (see Annex 1, Section A1.1) based on the measurement data, chemical transport

model (CAM5-Ensemble forecast) output, altitude and the surface solar radiation. For details, see Annex 3, Section A3.3.

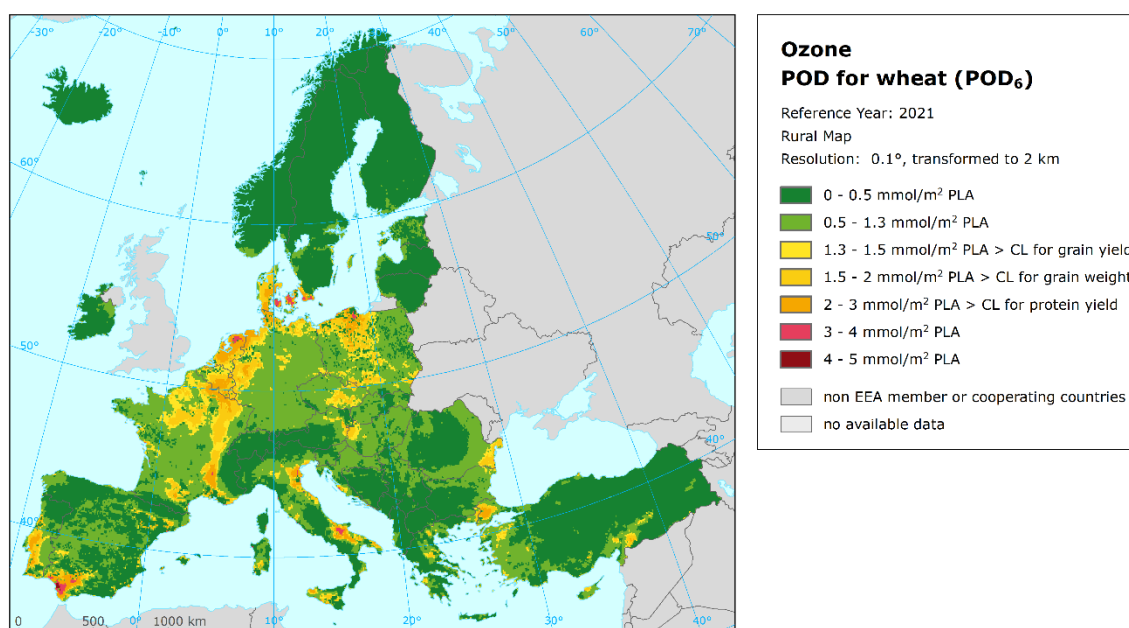
Phytotoxic Ozone Dose maps

Maps 3.9 to 3.11 present the maps of Phytotoxic Ozone Dose (POD₆) for wheat, potato and tomato and maps 3.12 and 3.13 present the maps of POD₁ for beech and spruce in 2021. Generally, high values of the POD can be found in different parts of Europe since the POD is dependent not only on ozone levels but also on the environmental conditions and plant phenology. The lowest levels of the POD usually occur in areas with lower ozone concentrations (e.g. northern European regions) and/or in areas where environmental conditions limit the ozone stomatal conductance (dry and warm areas, including parts of the southern, south-western and south-eastern Europe). On the other hand, higher POD values can occur in areas with lower ozone concentrations, but favourable conditions for the stomatal conductance.

Crops

The areas in the Map 3.9 with POD₆ values below the lowest CL for wheat (i.e. 1.3 mmol/m² PLA for grain yield) are marked in dark green and green. The areas with POD₆ values in between CLs for grain yield and 1 000-grain weight (i.e. between 1.3 mmol/m² PLA and 1.5 mmol/m² PLA) and in between CLs for 1 000-grain weight and protein yield (i.e. between 1.5 mmol/m² PLA and 2 mmol/m² PLA) are marked in yellow and dark yellow, respectively. The areas with POD₆ values above the CL for protein yield of wheat (i.e. 2 mmol/m² PLA) are marked in orange, red and dark red.

Map 3.9: Phytotoxic Ozone Dose (POD₆) for wheat, rural map, 2021

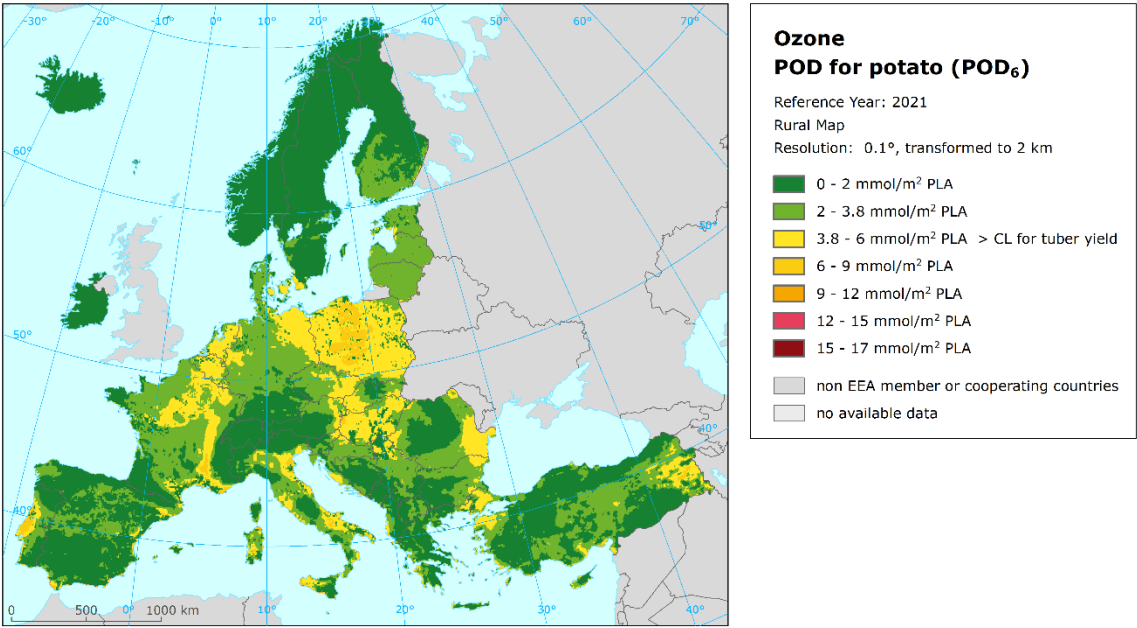


In 2021, POD₆ values for wheat above the highest CL (i.e. for protein yield) are found in northern Europe (parts of Denmark and a small area in the south of Sweden), central Europe (parts of Poland and Germany), western Europe (parts of France and the Benelux countries) and in southern and south-eastern Europe (parts of Portugal, south of Spain, parts of Italy and Türkiye). In addition, the lower CLs for grain yield and 1 000-grain weight were exceeded in parts of central Europe (Germany, Czechia, Poland, Austria, Hungary), western Europe (France and Benelux) and in parts of southern Europe (Portugal, Spain, Italy, Greece, Romania, and Türkiye).

Map 3.10 presents the map of POD_6 for potato in 2021. The areas with POD_6 values above the CL for tuber yield of potato (i.e. 3.8 mmol/m² PLA) are marked in yellow, dark yellow, orange, red and dark red. Areas below this CL are marked in green and dark green.

In 2021, POD_6 values for potatoes higher than CL for tuber yield occurred in central Europe (almost all of Poland and Hungary, parts of Czechia, Slovakia, Austria and Germany), in western Europe (parts of France and the Benelux countries), in parts of southern Europe (Portugal, smaller parts of southern coast of Spain and France, parts of Italy except for its north and parts of some Balkan states like Croatia, Greece, Romania, Albania, Bulgaria, Cyprus and parts of Türkiye). The lowest POD_6 values for potatoes in 2021 are found in northern Europe, but also in parts of central, western and southern Europe and Türkiye.

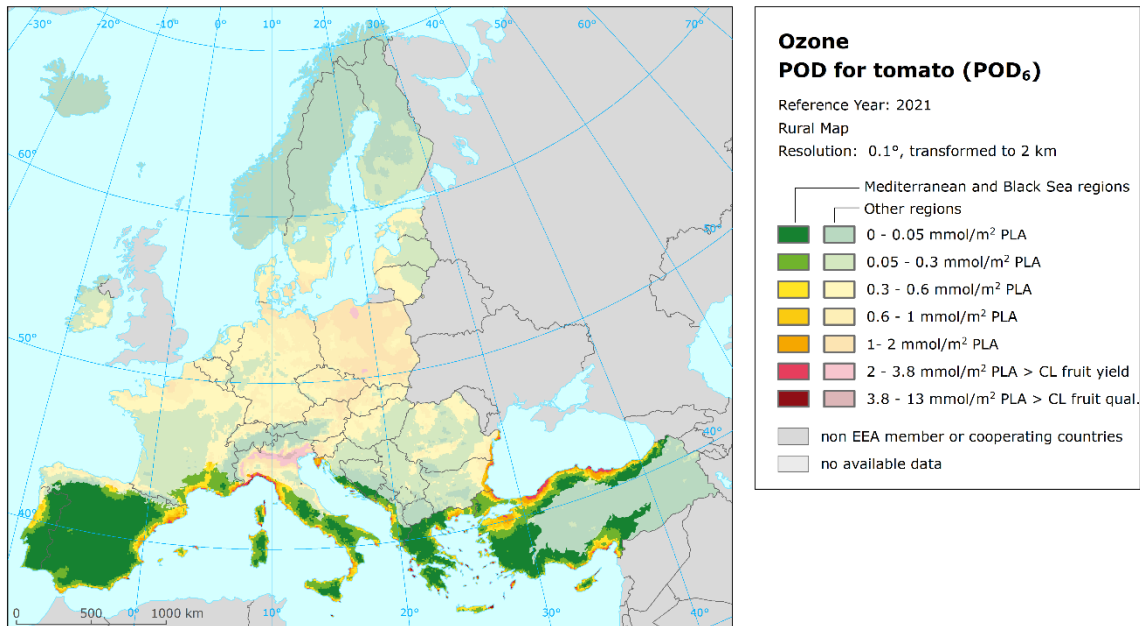
Map 3.10: Phytotoxic Ozone Dose (POD_6) for potato, rural map, 2021



Map 3.11 presents the map of POD_6 for tomato in 2021. The areas with POD_6 values above the CL for fruit yield (i.e. 2 mmol/m² PLA) are marked in red and dark red, the areas with POD_6 values above the CL for fruit quality (i.e. 3.8 mmol/m² PLA) in dark red. The Modelling and Mapping Manual (CLRTAP, 2017a) defines the parameterization for tomato for the Mediterranean area. EU-27 agriculture statistics show that 70 % of tomato in 2020 was produced in Italy, Spain, Portugal, and Greece (EC, 2021). In the colder regions of Europe, tomato would be mostly grown in greenhouses where the methodology used to compute ozone concentrations and uptake is not applicable. For the purpose of completeness, the POD_6 has been modelled even for non-Mediterranean areas using the same parameterization (lighter colours in the Map 3.11).

Most of the Mediterranean areas showed the values of POD_6 for tomato below the CLs for tomato in 2021. POD_6 values above CL occurred mainly in some coastal areas of Spain, France, Italy, Greece, and Türkiye.

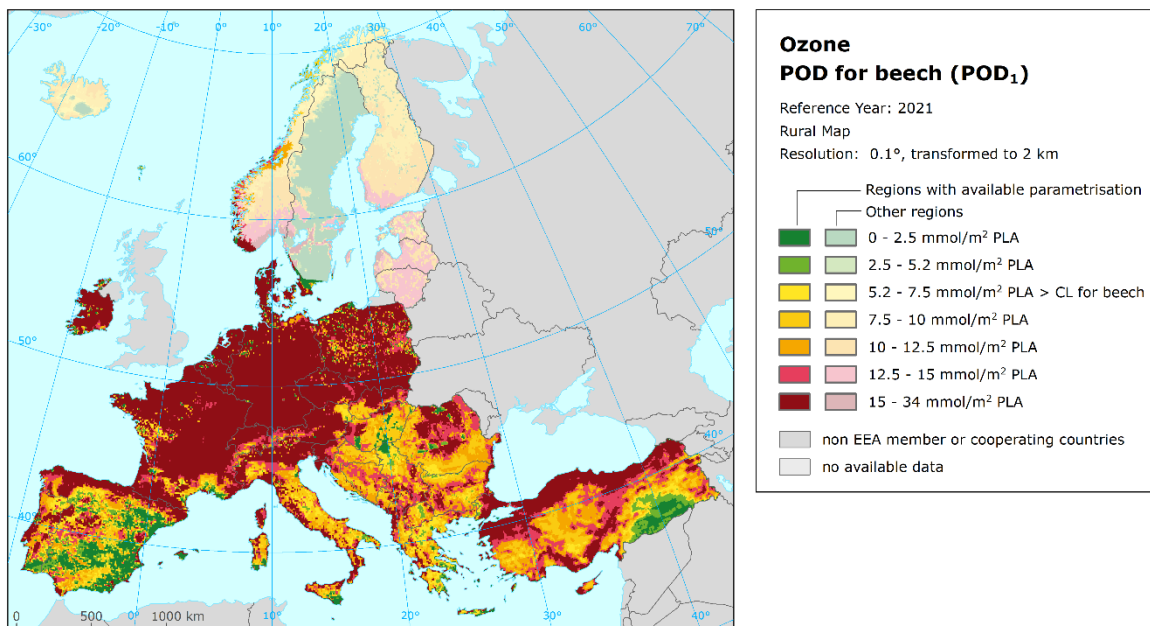
Map 3.11: Phytotoxic Ozone Dose (POD₆) for tomato, rural map, 2021



Trees

Map 3.12 shows the map of POD₁ for beech in 2021. The areas with POD₁ values below the CL for beech (i.e. 5.2 mmol/m² PLA) are marked in dark green and green. The areas with POD₁ values above the CL for beech are marked in yellow, dark yellow, orange, red and dark red. Since no parametrization for beech in the Boreal, Arctic and Alpine > 50° biogeographical regions is available, these areas are marked in lighter colours.

Map 3.12: Phytotoxic Ozone Dose (POD₁) for beech, rural map, 2021



The CL for beech was exceeded in almost the entire European mapped area, with the exception of large areas in Portugal, Spain and Türkiye and many small areas throughout the mapped area (e.g. in southern France, Sardinia and Sicily, Hungary, Serbia, Romania, Northern Macedonia and Greece).

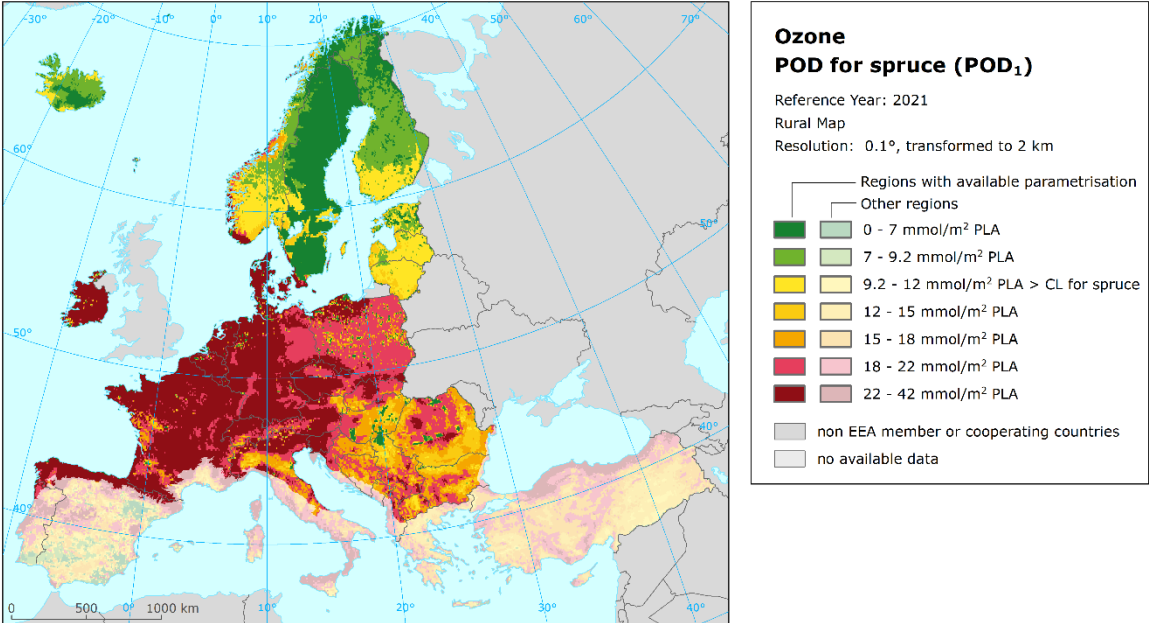
The highest levels of POD₁ for beech in 2021 are found in almost all central and western Europe, in northern Europe (Denmark), parts of southern and south-eastern Europe (the north of Spain, parts of Italy, areas of the Balkan countries and various parts of Türkiye)..

Map 3.13 presents the map of POD₁ for spruce in 2021. The areas with POD₁ values below the CL for spruce (i.e. 9.2 mmol/m² PLA) are marked in dark green and green. The areas with POD₁ values above the CL for spruce are marked in yellow, dark yellow, orange, red and dark red. Since no parametrization for spruce in the Mediterranean, Anatolian and Black Sea biogeographical regions is available, this area is marked in lighter colours.

The CL for spruce has been exceeded almost throughout the whole European area mapped, with the exception of large areas in northern Europe. Nevertheless, according to CLRTAP (2020), the start of the growing season in northern Europe is earlier than the start of the growing season calculated by the current recommended latitude model (boreal region). As a result of this earlier start of the growing season, POD₁ values in northern Europe (boreal region) could be higher than those presented. Unfortunately, a better approach for the start of the growing season for spruce is not currently available in this region.

However, many smaller areas with PODs below CL can be found in almost every country in Europe, especially in Hungary, Romania and Serbia.

Map 3.13: Phytotoxic Ozone Dose (POD₁) for spruce, rural map, 2021



4 NO₂ and NO_x

The methodology for creating the concentration maps follows the same principle as for the rest of pollutants: a linear regression model on the basis of European wide station measurement data, followed by kriging of the residuals produced from that regression model (residual kriging).

The map on NO₂ is based on an improved mapping methodology developed in Horálek et al. (2017b, 2018). The map layers are created for the rural, urban background and urban traffic areas separately on a grid at 1 km resolution. Subsequently, the urban background and urban traffic map layers are merged using the gridded road data into one urban map layer. This urban map layer is further combined with the rural map layer into the final NO₂ map using a population density grid at 1 km resolution. For details, see Annex 1, Section A1.1. Supplementary data used consist of chemical transport model (CTM) output, altitude, Sentinel-5P satellite data, wind speed, population density and land cover indicators for rural areas; for urban background areas these are CTM output and temperature, altitude, Sentinel-5P satellite data, wind speed, population density and land cover indicators; for traffic areas the CTM output, altitude, and Sentinel-5P satellite data are used (Annex 3, Section A3.4). The final concentration map is presented at the 1 km grid resolution. Be it noted that this final map is representative for rural and urban background areas, but not for urban traffic areas (which are smoothed at this 1 km spatial resolution).

The map of the vegetation-related indicator NO_x annual average is created on a grid at 2 km resolution, based on rural background measurements only, as vegetation is considered not to be extensively present at urban and suburban areas. Hence, this map is applicable to rural areas only. The resolution is chosen equally to the one of the vegetation indicator for ozone.

The population exposure to NO₂ has been calculated based on the methodology described in Horálek et al. (2017b), i.e. according to Equation A1.6 of Annex 1. It has been calculated separately for urban areas directly influenced by traffic and for the background (both rural and urban) areas, in order to better reflect the population exposed to traffic. Based on this, the different concentration levels in urban background and traffic areas inside the 1 km x 1 km grid cells are taken into account. Thus – like for PM₁₀ and PM_{2.5} – the population exposure refers not only to the rural and urban background areas, but to the urban traffic locations as well. However, it should be mentioned that only population density data at 1 km resolution has been used. This means that contrary to the concentration levels, the population density is constant within each 1 km grid cell. This shortcoming can increase the uncertainty of the population exposure results.

Annex 3 provides details on the regression and kriging parameters applied for deriving the maps, as well as the uncertainty analysis of the maps.

4.1 NO₂ – Annual mean

The Ambient Air Quality Directive (EC, 2008) sets two limit values (LV) for NO₂ for the human health protection. The first one is an annual LV (ALV) at the level of 40 µg/m³. This is the same concentration level as recommended by the World Health Organization for the NO₂ annual average as the 2005 Air Quality Guideline level (WHO, 2005). Nevertheless, the current WHO Air Quality Guideline level for the NO₂ annual average is set to 10 µg/m³, as introduced in 2021 (WHO, 2021a). The second one is an hourly LV (HLV, 200 µg/m³ not to be exceeded on more than 18 hours per year). Concentrations above the HLV were observed in 0.5 % (16 stations) of all reporting stations only in 2021, mostly at urban traffic stations, see Targa et al. (2023). In view of this low number of exceedances, the short-term LV has not been included in the mapping procedures.

Concentration map

Map 4.1 presents the final combined concentration 1 km resolution map for the 2021 NO₂ annual average. According to Map 4.1, the areas where NO₂ concentrations were above the ALV of 40 µg/m³

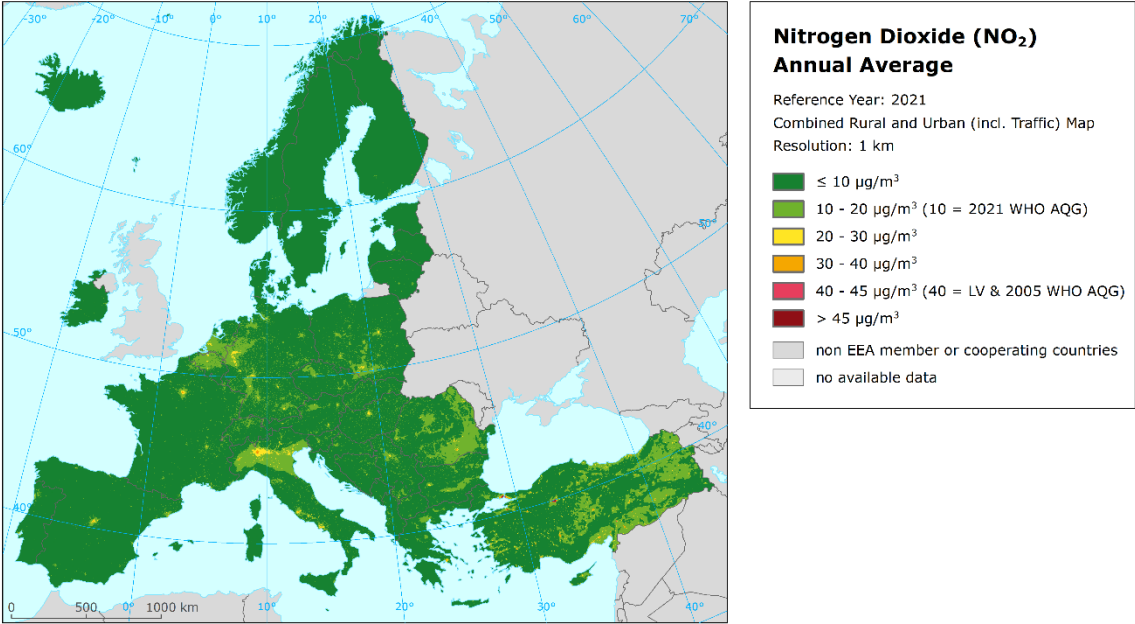
include urbanized parts of some large cities, particularly Milan, Ankara and Istanbul, and some other smaller cities in Türkiye. Some other cities show NO₂ levels above 30 µg/m³, e.g. in France, Greece, Italy, Romania, Spain, and Türkiye. Most of the European area shows NO₂ levels below 20 µg/m³, with most of the rural areas below 10 µg/m³. Some larger areas above 20 µg/m³ can be found in the Po Valley, the Benelux, the German Ruhr region, in the Île de France region and around Rome and Naples and in the Krakow – Katowice (PL) – Ostrava (CZ) industrial region.

It should be noted that the interpolated map is created at 1 km resolution only. Although the urban traffic map layer is used in the map creation, the traffic locations are smoothed in the 1 km resolution. Thus, the maps as such refers to the rural and urban background situations only, while the concentrations above the NO₂ limit values occur mostly at local hotspots such as dense traffic locations and densely urbanised and industrialised areas. Such concentrations are mostly not visible in the 1 km resolution map.

The relative mean uncertainty of the NO₂ annual average map is 34 % for rural and 25 % for urban background areas (Annex 3, Section A3.4). This means slightly worse mapping uncertainty in rural areas compared to the quality objective for models of NO₂ annual average (i.e. 30 %) as set in the Air Quality Directive (EC, 2008).

In order to provide more complete information of the air quality across Europe, the final combined map including the measurement data at stations is presented in Map A4.9 of Annex 4.

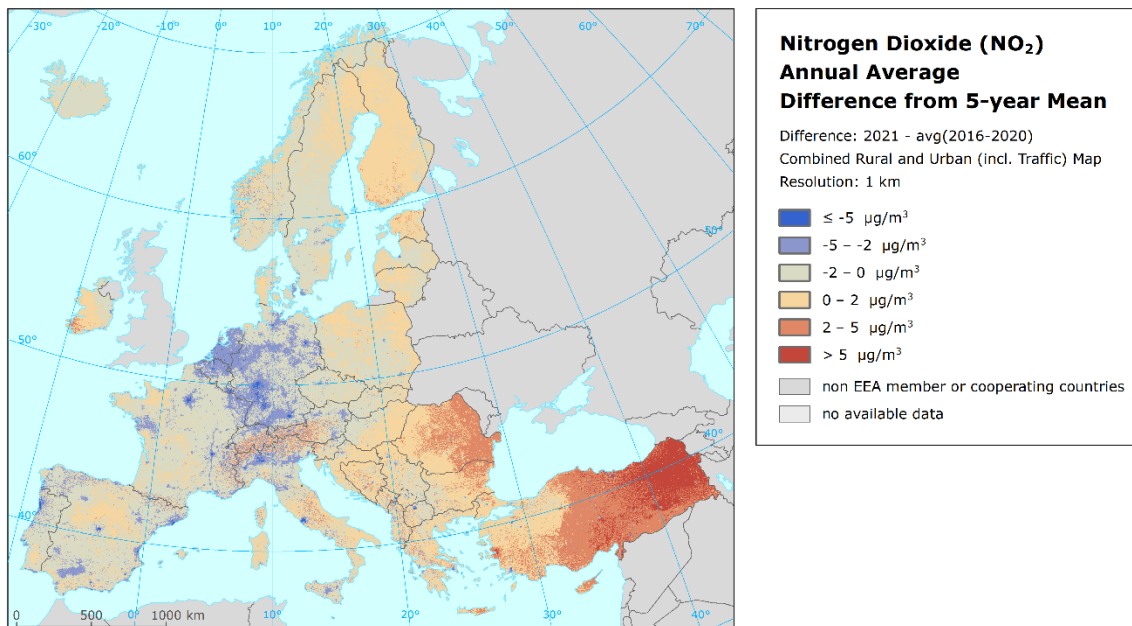
Map 4.1: Concentration map of NO₂ annual average, 2021



Map 4.2 presents the difference between 2021 and the five-year mean 2016-2020 for NO₂ annual average. Orange to red areas show an increase of NO₂ concentration in 2021, while blue areas show a decrease.

At the annual average NO₂ difference map the highest increases are observed in Türkiye, parts of southern and south-eastern Europe with the highest increases in Romania, parts of Italy (central and northern), Austria and Switzerland. An increase is also observed in western and northern Europe, specifically in Ireland and in disconnected areas of Finland and Estonia. On the other hand, there are decreases in some countries, mainly central Europe (in Benelux and Germany).

Map 4.2: Difference concentrations between 2021 and the five-year average 2016-2020 for NO₂ annual average



Population exposure

Table 4.1 and Figure 4.1 give the population frequency distribution for a limited number of exposure classes calculated on a grid of 1x1 km² resolution. Table 4.1 also presents the population-weighted concentration for individual countries, large regions, EU-27 and for the whole mapping area.

It has been estimated that in 2021 almost 3 % of the considered European population including Türkiye and around 0.3 % of the EU-27 population lived in areas with NO₂ annual average concentrations above the EU limit value of 40 µg/m³ (i.e. equivalent to the previous 2005 WHO AQG).

About 74 % of the considered European population including Türkiye and 72 % of the EU-27 population has been exposed to annual average concentrations above the current 2021 WHO AQG level of 10 µg/m³ (WHO, 2021a).

No population has been exposed to concentrations above the ALV in 34 countries. In Poland, France, Italy, Romania, Cyprus and Greece up to 3 % of population has been exposed to concentrations above the limit value. In Türkiye, this is the case for 18 % of the population.

The population-weighted concentration of the NO₂ annual mean has been estimated for 2021 at about 16 µg/m³ for total mapped area and 14 for the EU-27, which means a decrease of about 2 µg/m³ and 3 µg/m³ compared to the five-year mean, respectively. When assessing the change in individual countries, the steepest absolute decrease was found in Monaco (6 µg/m³), and the highest absolute increase was estimated in Cyprus (1 µg/m³).

Table 4.1: Population exposure and population-weighted concentration, NO₂ annual average, 2021

Country	ISO	Population (inhbs·1000)	NO ₂ — annual average, exposed population (%)					Population-weighted concentration			
			< 10	10-20	20-30	30-40	40-45	> 45	2021	5-year mean	Diff.
Albania	AL	2 830	34.5	55.1	10.4				12.6	14.7	-2.1
Andorra	AD	79	1.9	97.6	0.4				17.0	18.9	-1.9
Austria	AT	8 933	26.5	54.1	18.7	0.8			14.4	17.2	-2.9
Belgium	BE	11 555	8.0	75.1	15.6	1.3			15.7	19.2	-3.5
Bosnia and Herzegovina	BA	3 271	31.0	59.4	9.6				12.9	14.3	-1.4
Bulgaria	BG	6 917	10.8	61.6	26.1	1.5			17.5	18.4	-0.9
Croatia	HR	4 036	33.3	59.1	6.6	1.1			12.6	14.4	-1.8
Cyprus	CY	9 343	8.9	12.7	70.0	6.2	2.2		22.9	21.8	1.2
Czechia	CZ	10 782	24.8	69.5	5.7	0.1			13.1	14.5	-1.4
Denmark (incl. Faroe Islands)	DK	5 840	83.8	15.8	0.4				7.3	9.1	-1.8
Estonia	EE	1 330	77.9	22.1					7.1	6.9	0.2
Finland	FI	5 534	79.4	20.6	0.0				7.2	7.7	-0.5
France (metropolitan)	FR	65 447	42.6	42.4	10.1	4.2	0.6	0.1	12.7	15.5	-2.8
Germany	DE	83 155	17.9	67.3	13.2	1.7			14.7	18.3	-3.6
Greece	GR	10 679	21.8	40.9	26.6	8.1	1.1	1.5	17.8	20.0	-2.1
Hungary	HU	9 731	15.5	63.8	18.0	2.7			15.5	16.6	-1.1
Iceland	IS	369	88.1	9.3	2.6				6.6	9.8	-3.1
Ireland	IE	5 006	67.1	30.1	2.8				8.3	9.9	-1.5
Italy	IT	59 236	16.1	49.1	27.9	6.3	0.7	0.0	17.8	20.4	-2.6
Latvia	LV	1 893	50.4	49.3	0.3				9.9	11.0	-1.1
Liechtenstein	LI	39	2.6	96.3	1.1				14.8	16.9	-2.0
Lithuania	LT	2 796	40.0	55.9	4.1				10.8	11.2	-0.3
Luxembourg	LU	635	17.0	73.0	10.0				14.0	18.9	-4.9
Malta	MT	516	56.3	35.5	8.2				10.3	12.8	-2.5
Monaco	MC	37		79.0	21.0				18.3	24.1	-5.8
Montenegro	ME	621	35.8	61.0	3.2				11.0	13.8	-2.8
Netherlands	NL	17 475	8.1	79.3	12.6	0.0			15.5	19.2	-3.7
North Macedonia	MK	2 069	8.8	82.6	6.6	2.1			14.9	17.7	-2.7
Norway	NO	5 391	68.5	29.4	2.0				7.8	10.1	-2.3
Poland	PL	37 840	29.1	57.6	12.4	0.8	0.0		13.7	14.6	-0.9
Portugal (excl. Azores, Madeira)	PT	9 802	49.7	45.4	4.9	0.0			10.7	14.9	-4.1
Romania	RO	19 202	7.9	58.4	25.2	7.7	0.5	0.3	18.6	18.1	0.5
San Marino	SM	34	7.7	87.6	4.6				13.6	14.8	-1.3
Serbia (incl. Kosovo)	RS	8 534	15.9	65.8	17.4	0.9			15.6	17.6	-2.0
Slovakia	SK	5 460	23.5	73.0	3.5				12.4	13.6	-1.2
Slovenia	SI	2 109	33.7	57.6	8.8				12.9	14.6	-1.7
Spain (excl. Canarias)	ES	45 154	29.8	48.3	17.2	4.7			14.8	18.8	-4.1
Sweden	SE	10 379	86.9	12.8	0.3				6.5	8.3	-1.8
Switzerland	CH	8 670	13.8	77.4	8.5	0.3			14.2	17.5	-3.3
Türkiye	TR	83 614	14.6	20.5	28.0	19.1	5.6	12.2	26.3	25.7	0.5
Total			26.0	49.8			0.9	1.7		18.1	-2.1
		566 342	75.8	16.5	5.0	2.6			15.9		
EU-27			27.8	53.8			0.2	0.1		17.0	-2.5
		450 785	81.5	15.1	3.0	0.3			14.4		
Northern Europe		32 080	75.2	23.9	0.9				7.6		
Western Europe (without UK)		81 150	31.9	53.4	11.0	3.2	0.4	0.1	13.6		
Central Europe		162 777	21.5	64.8	12.5	1.3	0.0		14.3		
Southern Europe		140 620	26.2	47.3	21.1	4.9	0.4	0.1	15.7		
South-Eastern Europe		121 885	15.0	37.2	24.4	12.8	3.4	7.3	22.2		
Kosovo	KS	1 662	20.9	67.2	11.9				14.4	15.8	-1.4
Serbia (excl. Kosovo)	RS-	6 872	14.7	65.5	18.7	1.2			15.9	18.0	-2.1

Note: The percentage value "0.0" indicates that an exposed population exists, but it is small and estimated to be less than 0.05 %. Empty cells mean no population in exposure. 5-year mean, i.e. five-year mean 2016-2020. Diff., i.e. difference concentrations between 2021 and the five-year mean 2016-2020.

Figure 4.1: Percentage of the population (%) exposed to different values of NO₂ annual average (µg/m³), 2021

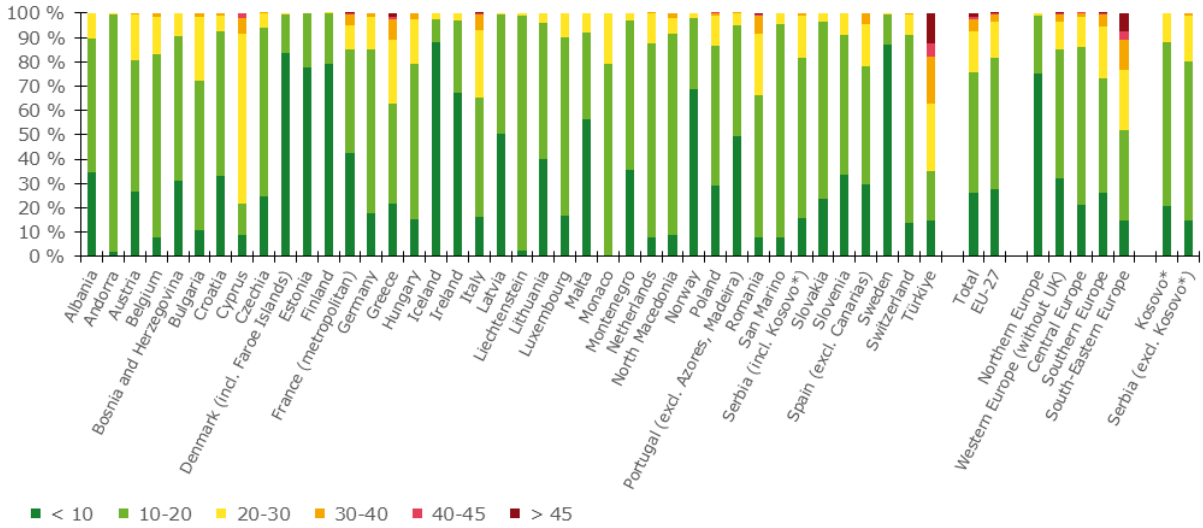
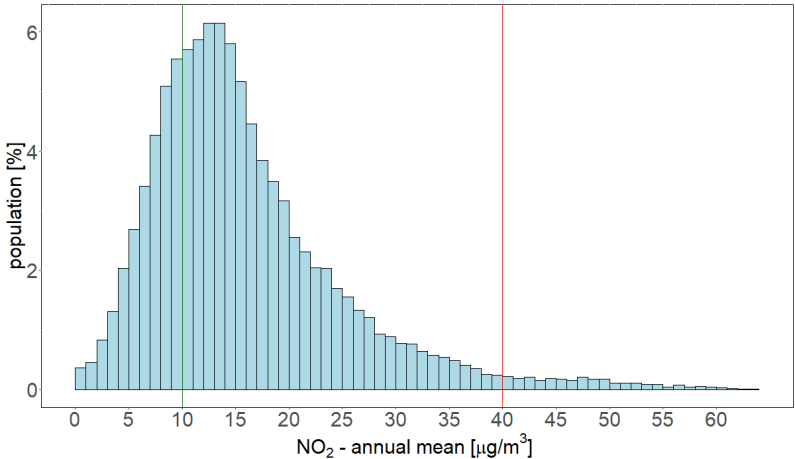


Figure 4.2 shows, for the whole mapped area, the population frequency distribution for exposure classes of 1 µg/m³. One can see the highest population frequency for classes between 7 and 19 µg/m³, continuous decline of population frequency for classes between 20 and 30 µg/m³ and continuous mild decline of population frequency for classes between 31 and 60 µg/m³.

Figure 4.2: Population frequency distribution, NO₂ annual average, 2021. NO₂ annual mean concentrations to which the population per country was exposed in 2021. The 2021 WHO AQG level (10 µg/m³) is marked by the green line, the EU annual limit value and 2005 WHO AQG level (40 µg/m³ in both cases) are marked by the red line



The boxplot showing for individual countries the NO₂ annual average concentrations to which the population per country was exposed in 2021 is presented in Summary, Figure S.1.

4.2 NO_x – Annual mean

Concentration map

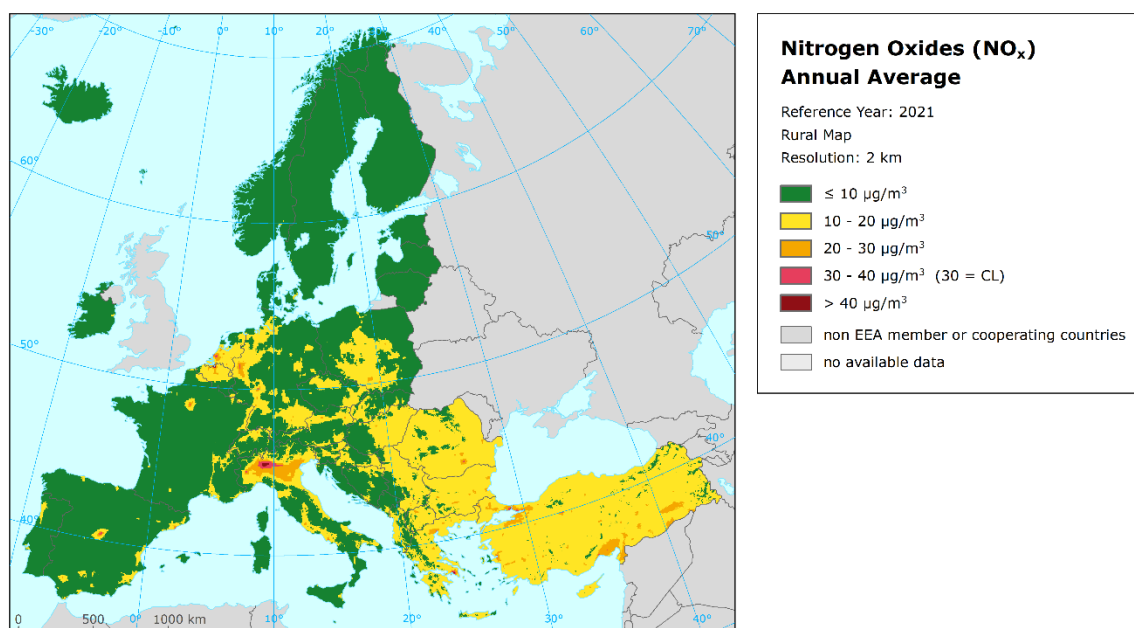
The Ambient Air Quality Directive (EC, 2008) sets a critical level (CL) for the protection of vegetation for the NO_x annual mean at 30 µg·m⁻³. According to this directive, the sampling points targeted at the protection of vegetation and natural ecosystems shall be in general sited more than 20 km away from agglomerations or more than 5 km away from other built-up areas. Thus, only the observations at rural background stations are used for the NO_x mapping and the resulting map is representative for rural areas only.

The number of NO_x measurement stations is limited. The mapping of the NO_x annual average has been therefore performed on the basis of an approach presented in Horálek et al. (2007). This approach derives additional pseudo NO_x annual mean concentrations from NO₂ annual mean measurement concentrations and increases as such the number and spatial coverage of NO_x ‘data points’, and applies these data to the NO_x mapping. Section A1.1 of Annex 1 provides some details.

Map 4.3 presents the concentration map of NO_x annual average. It concerns rural areas only, representing an indicator for vegetation exposure to NO_x.

Most of the European area shows NO_x levels below 20 µg/m³. However, in the Po Valley, part of the Netherlands and Belgium, the German Ruhr region and around some larger European cities (typically being the national capitals or large cities) NO_x concentrations above the CL are observed. Furthermore, around many other larger European cities concentrations just below the CL are observed. These concentrations are expected to be the result of large emissions from transport in and around the cities, as well as energy production and industrial facilities taking place at these areas. These values above the CL would be relevant only for the so-called peri-urban vegetation where patches of agricultural land and of natural or planted vegetation can be found. On the contrary, low concentrations (below 10 µg/m³) are observed in large areas of Portugal, Spain, France, Italy, Croatia, Bosnia and Herzegovina, Montenegro, Hungary, Germany, Poland, Czechia, Slovakia, Scandinavia, Iceland, Ireland and the Baltic States.

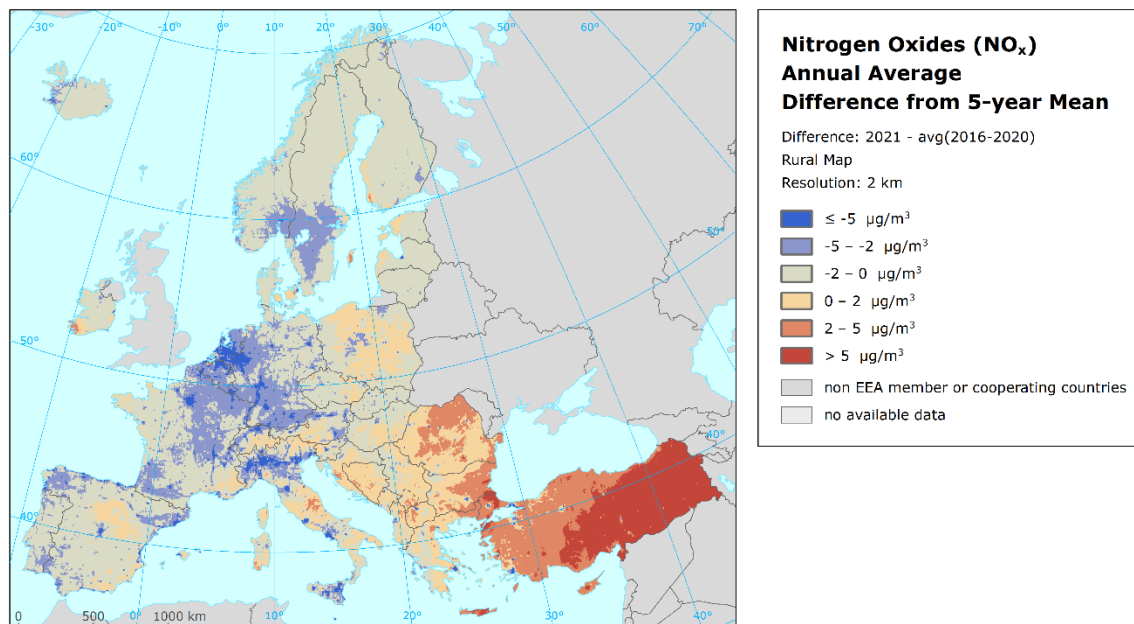
Map 4.3: Concentration map of NO_x annual average, rural map, 2021



The relative mean uncertainty of this rural map is 42 %. This means worse mapping uncertainty compared to the quality objective for models of NO_x annual average (i.e. 30 %) as set in the Air Quality Directive (EC, 2008). This higher relative uncertainty is highly influenced by the low concentration values of NO_x in most of the areas. The NO_x annual average rural map including the data measured at rural background stations is presented in Map A4.10 of Annex 4. The map illustrates the lack of the NO_x rural stations in the Balkan area.

Map 4.4 presents the difference between 2021 and the five-year mean 2016-2020 for annual average for NO_x. Orange to red areas show an increase of NO_x concentration in 2021, while blue areas show a decrease. The highest increases can be seen in Türkiye, Bulgaria and Romania and other countries of south and south-eastern Europe. Notable decreases are seen in western Europe (mainly in France and Benelux) and in Scandinavia. Other discontinuous areas where NO_x concentrations decreased were found in southern European countries (Spain, Portugal, France, Italy).

Map 4.4: Difference of concentrations between 2021 and the five-year average 2016-2020 for NO_x annual average



Vegetation exposure has not been calculated for NO_x, as the CL applies actually to vegetation only, which is by nature mostly allocated in rural areas where there has been limited CL exceedance observed. Therefore, values above the CL for protection of the vegetation would occur in limited vegetation areas only and, as such, is considered not to provide essential information from the European scale perspective. Furthermore, contrary to vegetation exposure to high ozone concentrations in Europe that leads to considerable damage, vegetation exposure to NO_x pollution is of minor importance in terms of actual impacts. On the other hand, NO_x concentrations contribute in part to the total N-deposition, which leads to acidifying and eutrophying effects on vegetation. These effects, especially eutrophication, are still very important in Europe (e.g. EMEP, 2020). However, these effects on vegetation cannot be expressed by an exposure to NO_x as many oxidized and reduced nitrogen compounds contribute to total atmospheric nitrogen deposition.

Concerning the potential exposure estimate of vegetation and natural ecosystems to NO_x there is an additional dilemma: which receptor types should be selected to estimate the exposure and CL exceedance of vegetation and natural ecosystems? An option would be the use of CLC classes (e.g. like

in Horálek et al., 2008); nevertheless, this classification is too general. Another option would be the NATURA 2000 database. However, that data source contains a wide series of receptor types, species and classes. Serious additional efforts would be needed to conclude on the most relevant set of receptors from the NATURA 2000 geographical database.

Currently, the ICP Vegetation Coordination Centre is performing a review of NO_x CLs in relation to vegetation. The existing NO_x CLs were first proposed in 1988 and set at an unchanged annual level (30 µg/m³) since 1993. Therefore, it was deemed timely to review evidence around NO_x CLs (CLRTAP, 2022).

5 Benzo(a)pyrene

An annual average map for benzo(a)pyrene (BaP) has been produced and is presented in the regular mapping report for the second time. In agreement with the conclusions of Horálek et al. (2022), it is labelled as an experimental map to indicate that it does not yet meet the same accuracy standards as the regularly produced maps of other pollutants.

The map of BaP is based on the mapping methodology developed and tested in Horálek et al. (2022). The methodology for creating the concentration maps follows the same principle as for the rest of pollutants: a linear regression model based on European wide station measurement data, followed by kriging of the residuals produced from that regression model (residual kriging). The map layers are created for the rural and urban background areas separately on a grid at 1 km resolution. For details, see Annex 1, Section A1.1. Supplementary data used in the linear regression for rural areas consist of chemical transport model (CTM) output, altitude, temperature, wind speed and land cover; for urban background areas they are CTM output and temperature (Annex 3, Section A3.5). The final concentration map is presented at a 1 km grid resolution.

Due to the poor spatial coverage of the BaP measurement stations, so-called pseudo BaP stations have also been used in addition. Pseudo BaP data in locations with PM_{2.5} measurements (or with pseudo PM_{2.5} data based on PM₁₀ measurements) and with no BaP measurements have been estimated based on the exponential regression of the observed BaP concentrations with the PM_{2.5} data, geographical coordinates and the land cover. Due to quite high uncertainty of the pseudo data, they are only used in areas with a lack of BaP measurements. Due to the serious lack of Turkish data, Türkiye is not included in the mapping area. Annex 3, Section A3.5 provides details on the regression and kriging parameters applied for deriving the BaP map, as well as the uncertainty analysis of this map.

The 2004 Ambient Air Quality Directive (EC, 2004) sets a target value for ambient air concentration of BaP, as a marker for the carcinogenic risk of PAHs in ambient air. The target value (TV) for BaP (measured in PM₁₀) is set to 1 ng/m³ as an annual mean.

A reference level (RL) of 0.12 ng/m³ was estimated assuming an acceptable risk of additional lifetime cancer risk of approximately 1 case in 100 000 (WHO, 2021b).

Both the EU target value (1 ng/m³) and the estimated WHO RL (0.12 ng/m³) are based on the WHO lung cancer unit risk for PAH mixtures (8.7×10^{-5} per ng/m³ BaP) and correspond to an additional lifetime cancer risk of approximately 9 cases and 1 case in 100 000 exposed individuals, respectively (WHO, 2021b).

5.1 Benzo(a)pyrene – Annual mean

Concentration map

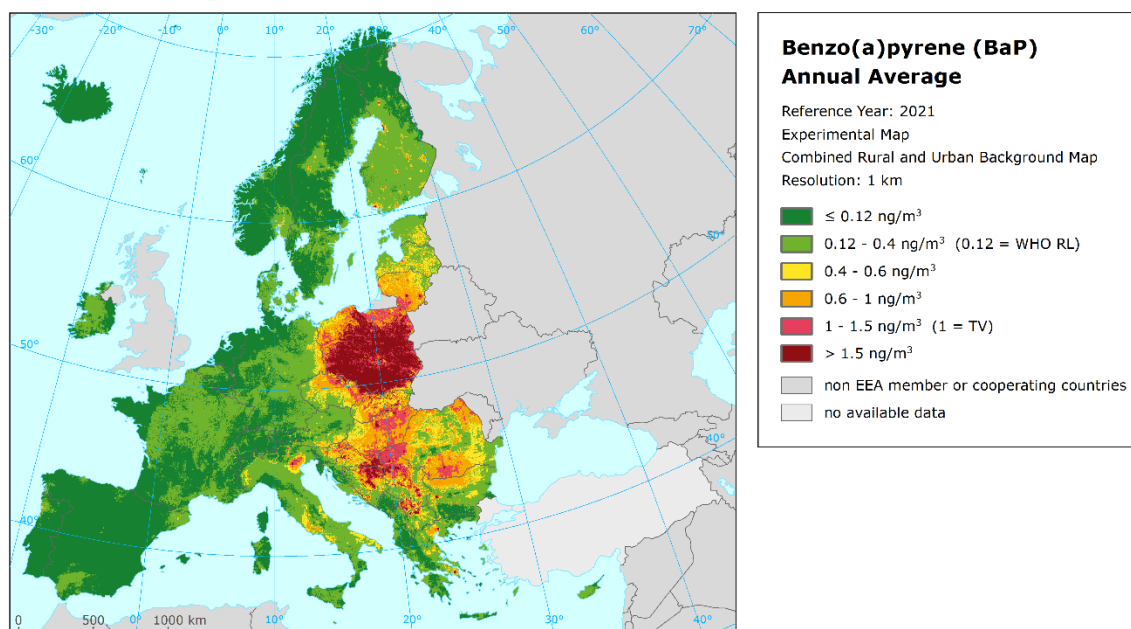
Map 5.1 presents the final combined concentration 1 km resolution map for the 2021 BaP annual average. Red and purple areas indicate concentrations above 1.0 ng/m³.

The highest BaP concentrations are shown in Poland, north-eastern Czechia and some populated locations in central and south-eastern Europe, northern Europe (mainly the Baltic states and towns and cities in Finland) and the eastern Po Valley in northern Italy. By contrast, western and southern Europe (except Greece and Italy) have low BaP values. Generally lower levels of BaP concentrations in natural areas can be seen, compared with the other land cover types.

The relative mean uncertainty of the 2021 map of BaP annual average is 144 % for rural and 87 % for urban areas and determined exclusively on the actual BaP measurement data points, i.e. not the pseudo stations (Annex 3, Section A3.5). This uncertainty is considerably high (especially in the rural areas) with respect to the quality objective for models for BaP annual average (i.e. 60 %) as set in the European directive (EC, 2004).

The high uncertainty in the rural areas is probably highly affected (besides the low density of the rural stations) by the fact that stations classified as “rural background” comprise both regional stations with low BaP values and stations located in villages, which are often highly influenced by local heating leading to high BaP concentrations.

Map 5.1: Concentration map of benzo(a)pyrene annual average, 2021, experimental map



Population exposure

Table 5.1 gives the population frequency distribution for a limited number of exposure classes to BaP concentrations, as well as the population-weighted concentration. Due to the experimental character of the benzo(a)pyrene map and its high uncertainty, the population exposure is presented only for EU-27, for five European regions and for the total mapping area, not for individual countries.

Table 5.1: Population exposure and population-weighted concentration, benzo(a)pyrene annual average, 2021, based on the experimental map

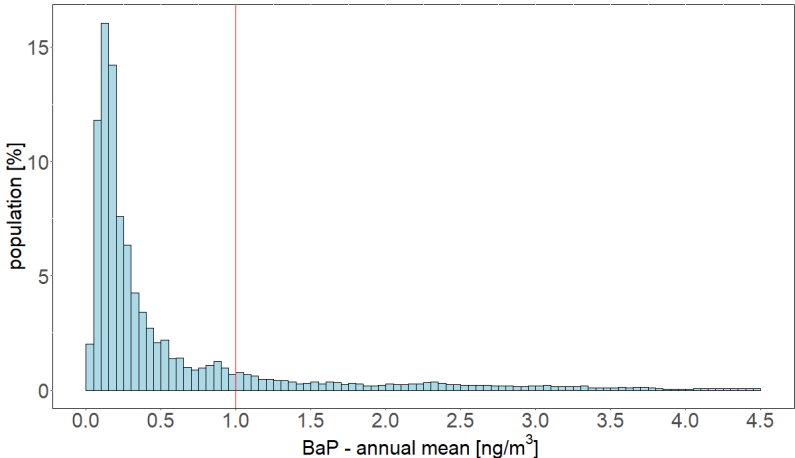
Area	Population [in hbs·1000]	BaP – annual average, exposed population, 2021 [%]						BaP ann. avg. Pop. weighted
		< 0.12	0.12-0.4	0.4-0.6	0.6-1.0	1.0-1.5	> 1.5	
Northern Europe	32 080	6.5	39.7	27.2	15.6	6.5	4.4	0.54
Western Europe (without UK)	144 566	38.1	61.7	0.2	0.0	0.0		0.15
Central Europe	162 777	10.0	45.2	5.5	7.5	6.5	25.3	1.05
Southern Europe	140 620	29.9	51.7	10.7	5.0	1.6	1.1	0.27
South-Eastern Europe without Türkiye	49 965	0.7	11.5	12.5	28.9	15.2	31.2	1.60
Total	530 007	19.6	46.1	8.4	8.3	4.8	12.8	0.68
EU-27	435 073	20.3	47.0	8.4	8.5	4.7	11.1	0.61

Note: The percentage value "0.0" indicates that an exposed population exists, but it is small and estimated to be less than 0.05 %. Empty cells mean no population in exposure.

Based on the experimental map, it is estimated that 18 % of the population living in the considered (i.e. mapped) European area was exposed to concentrations above 1.0 ng/m³ in 2021. Further, it is estimated that about 80 % of the population living in the considered (i.e. mapped) European area was exposed to concentrations above the WHO RL of 0.12 ng/m³. The population-weighted concentration of the BaP annual average for 2021 for the considered European countries is estimated to be about 0.7 ng/m³.

Figure 5.1 shows, for the whole mapped area, the population frequency distribution for exposure classes of 0.05 ng/m³. The highest population frequency is found for classes between 0.05 and 0.30 ng/m³. A quite continuous decline of population frequency is visible for classes above 0.30 ng/m³.

Figure 5.1: Population frequency distribution, benzo(a)pyrene annual average, 2021. The value 1.0 ng/m³ is marked by the red line

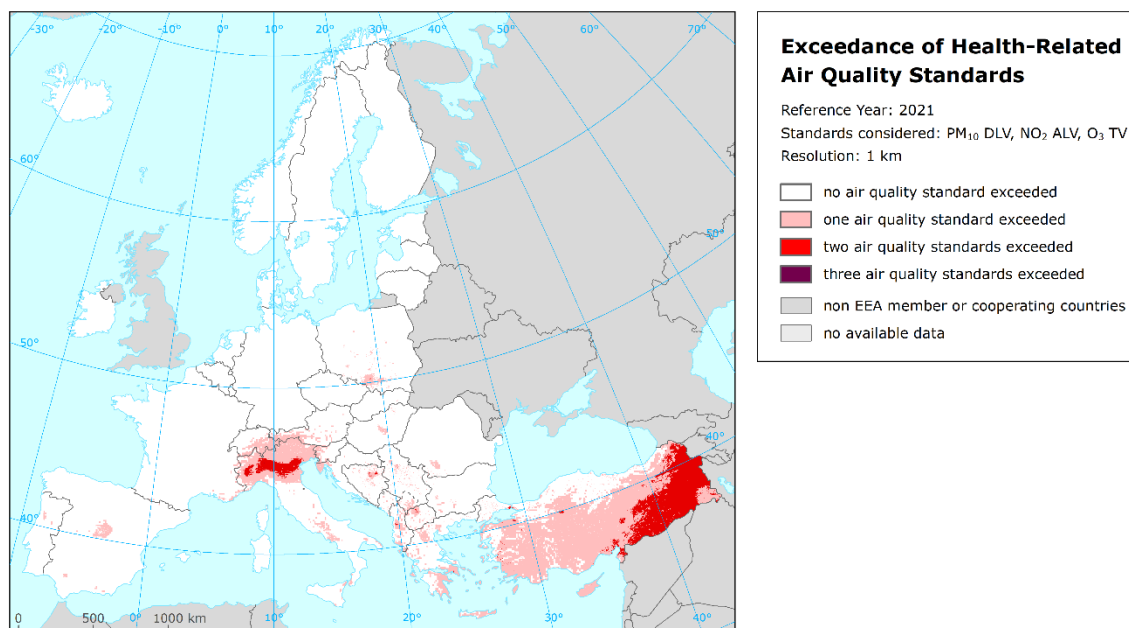


Note: Apart from the population distribution shown in the graph, it was estimated that 2.0 % of population lived in areas with BaP annual average concentrations between 4.5 and 15.6 ng/m³.

6 Accumulated risks

Although the spatial distributions of PM, NO₂ and ozone concentrations differ widely, the possibility of an accumulation of risk resulting from high exposures to all three pollutants cannot be excluded. The maps for the three most frequently exceeded EU standards (PM₁₀ daily limit value, O₃ target value and NO₂ annual limit value) have been combined, see Map 6.1.

Map 6.1: Exceedance of Health-Related Air Quality Standards, 2021



The combined population exposure shows the following results: out of the total population of 566 million in the mapped area, almost 8 % (42.7 million) people live in areas where two or three of these air quality standards are exceeded; 0.23 % (1.2 million) people live in areas where all three standards are exceeded. The worst situation is observed in Greece, Türkiye, Italy (in particular the Po valley) and Cyprus, where 2.6 %, 0.7 %, 0.6 % and 0.001 % lived in areas where all three standards are exceeded, respectively.

7 Exposure trend estimates

This report has presented the 2021 interpolated maps for the PM₁₀, PM_{2.5}, ozone and NO₂ human health related air pollution indicators (annual average and the 90.4 percentile of PM₁₀ daily means, annual average for PM_{2.5}, the 93.2 percentile of maximum daily 8-hour means, SOMO35 and SOMO10 for ozone, and the annual average for NO₂), as well as the BaP annual average experimental map, together with tables showing the frequency distribution of the estimated population exposures and the population-weighted concentration per country (apart from BaP), large European region, EU-27 and the total mapping area.

Furthermore, interpolated maps of ozone and NO_x vegetation related air pollution indicators have been produced. More specifically, these include maps of the ozone indicator AOT40 for vegetation and AOT40 for forests, and tables with the frequency distribution of estimated land area exposures and agricultural- and forest- weighted concentration per country, large region, EU-27 and the total mapping area. In addition, the maps of the Phytotoxic Ozone Dose (POD) for crops (wheat, potato and tomato) and trees (spruce and beech), and the NO_x annual average map have been produced, but without exposure estimates.

A mapping approach similar to previous years (Horálek et al., 2023 and references therein) based primarily on observational data has been used. With the interpolated air pollution maps and exposure estimates for the year 2021 completed, a seventeen-year overview of comparable exposure estimates has been obtained (with full time series coverage for PM₁₀ and ozone, except SOMO10 and POD indicators, with one year missing for PM_{2.5} and with four years missing for NO₂). In this chapter these multi-annual overviews of exposure estimates are provided for each of the indicators of PM₁₀, PM_{2.5} and ozone (except SOMO10 and POD_v), including a brief trend analysis.

For the previous years, mapping results as presented in Horálek et al. (2023) and previous mapping reports have been used. Since 2017 results, PM₁₀ and PM_{2.5} maps have been prepared based on the updated method (Horálek et al., 2019). For comparability reasons, results for 2015-2019 (and partly also for 2005 and 2009) are presented in two variants for these pollutants, i.e. based on the old and the updated methodologies. Ozone maps based on the 1 km merging resolution as tested in Horálek et al. (2010) and routinely applied since 2008 results are used for the whole period, due to consistency.

For the human health indicators, the exposure estimates are expressed, on one hand, as population-weighted concentration and, on the other hand, as percentage of population exposed to concentrations above the limit/target value. For the vegetation related indicators, the exposure estimates are expressed as the agricultural- and forest-weighted concentrations, as well as the agricultural or forest areas exposed to concentrations above defined thresholds.

It should be noted that the percentage of population, agricultural area, or forest area exposed is a less robust indicator compared to the population-weighted, agricultural-weighted, or forest-weighted concentration, as a small concentration increase (or decrease) may lead to a major increase (or decrease) of population, agricultural or forest area exposed. This is not the case when taking the population-weighted or agricultural/forest-weighted concentration as indicator. Therefore, the trend analysis is done based on the population-weighted, agricultural-weighted and forest-weighted concentrations only.

When thinking about a trend, the following should be taken into account: (i) the meteorologically induced variations, (ii) the uncertainties involved in the interpolation (Annex 3), and (iii) the year-to-year variation of the station density and their spatial distribution, which induce a variation in interpolated maps from year to year. In addition, one should be aware of the fact that different trends in various parts of Europe may occur. However, bearing in mind these limitations here a trend analysis is provided for the period 2005-2021 on the population-, agricultural- and forest-weighted concentrations for the total mapping area.

For comparability reasons, in this chapter the results for the total mapped area do not include Türkiye, because 2016 was the first year for which the area of Türkiye was mapped. Next to this, the results for the total mapped area include United Kingdom in this chapter. For the 16-year time series 2005-2020, the overall exposure included the United Kingdom (see Horálek et al., 2023, and the references therein). Therefore, the overall exposure for the total area including the United Kingdom has been calculated also for 2021. This value was easily available, as the mapping domain includes the United Kingdom (see Section A1.1).

7.1 Human health PM₁₀ indicators

Table 7.1 summarises the average concentration to which the considered European population has been exposed to over the seventeen-year period 2005-2021 for both human health PM₁₀ indicators, expressed as the population-weighted concentration, and the percentage of population exposed to PM₁₀ concentrations above limit values (LV), i.e. the annual (ALV) and daily (DLV) limit value, respectively.

For the years 2012 and 2013 both the 36th highest value and the 90.4 percentile of daily mean(s) have been calculated. Their results demonstrate an underestimation of almost 1 µg/m³ at the 36th highest daily mean. One may conclude that this underestimation is caused by the fact that when calculating the 36th highest daily mean value there is no correction for the missing values at incomplete time series. Whereas the 90.4 percentile of daily means adjusts for such missing data.

As the PM₁₀ maps for 2021 (as presented in Chapter 2) have been constructed using the updated methodology as developed and tested in Horálek et al. (2019), the table presents the results for 2015-2019 (and 2005 and 2009, for annual average) both based on the updated and the old methodologies, for comparability reasons.

Table 7.1: Population-weighted concentration and percentage of the considered European population (including United Kingdom, without Türkiye) exposed to concentrations above the PM₁₀ limit values (LV) for the protection of health for 2005 to 2021

PM ₁₀		meth.	2005	2006	2007	2008	2009	2010	2011	2012	2013	2014	2015	2016	2017	2018	2019	2020	2021
Annual Average																			
Popul.-weighted concentration [µg/m ³]	old	28.0	28.9	26.6	25.1	24.6	24.5	25.3	22.9	22.2	21.1	21.2	20.2	20.2	20.1	18.3			
	new	28.6				25.3							21.6	20.5	20.8	20.8	18.7	18.0	18.1
Popul. exposed > ALV (40 µg/m ³) [%]	old	13.3	10.9	7.1	5.9	6.0	5.2	7.2	3.4	2.6	2.0	0.6	1.7	2.9	2.1	0.3			
	new	11.5				6.2							0.7	1.7	3.3	2.4	0.5	0.6	0.3
36th Highest Daily Mean / 90.4 Percentile of Daily Means																			
Popul.-weighted conc. [µg/m ³]	36 th high. old	47.4	48.3	44.7	41.9	41.6	42.0	44.9	40.0	38.6									
	90.4 perc. old								40.8	39.4	37.1	36.9	35.7	36.1	34.5	32.1			
	90.4 perc. new											37.5	36.1	37.0	35.4	32.8	31.5	31.1	
Popul. exposed > DLV (50 µg/m ³) [%]	36 th high. old	35.9	37.2	27.6	20.3	17.0	20.8	24.8	16.9	16.4									
	90.4 perc. old								18.1	17.3	13.3	14.7	14.0	15.8	12.0	7.2			
	90.4 perc. new											16.2	14.6	17.0	13.2	8.1	9.1	8.7	

In 2021 the population exposed to annual mean concentrations of PM₁₀ above the limit value of 40 µg/m³ has been 0.3 % of the total population (calculated using the new methodology), which is the lowest percentage in the seventeen years' time series. Furthermore, it is estimated that the considered European inhabitants have been exposed on average to an annual mean PM₁₀ concentration of 18 µg/m³, being (together with 2020) the lowest value in the seventeen years' time series. The comparison of results for 2015-2018 illustrates well that a clear decrease in the population-weighted concentration does not lead necessarily to a similar decrease in the percentage of population exposed to concentrations above a certain standard.

In the seventeen-year time series, the percentage of people living in areas with concentrations above the annual LV is lower in the latest nine years (2013-2021) than in the first eight years. The overall

picture of the population-weighted annual mean concentration of the whole considered mapping area (i.e. including United Kingdom and without Türkiye) demonstrates a downward trend of about $-0.6 \mu\text{g}/\text{m}^3$ per year for the years 2005-2021, based on the old mapping method results for 2005-2019 and the new methodology for 2020-2021 (for trend estimation methodology, see Annex 1, Section A1.2). This trend is statistically significant (at the strongest level ***, i.e. 0.001) and expresses a mean decrease of $0.6 \mu\text{g}/\text{m}^3$ per year.

In 2021 almost 9 % of the considered European population have lived in areas where concentrations have been above the PM_{10} daily limit value (calculated using the 90.4 percentile and the new methodology), being the second lowest of the seventeen-year period. The overall population-weighted concentration of the 90.4 percentile of the PM_{10} daily means (formerly the 36th highest daily mean) is estimated to be about $31 \mu\text{g}/\text{m}^3$ in 2021 for the whole mapping area, which is the lowest of the seventeen years considered. This is the case even though the 36th highest daily means (i.e. possibly underestimated data if applied instead of the 90.4 percentiles, see above) have been used in the 2005-2011 calculations. The population-weighted concentrations of the whole considered mapping area show a statistically significant (at the strongest level ***, i.e. 0.001) downward trend of about $-1.0 \mu\text{g}/\text{m}^3$ per year for the years 2005-2021, for the daily LV related indicator 90.4 percentile of daily means (formerly the 36th highest daily mean), as calculated based on the old mapping method results for 2005-2019 and the new methodology for 2020-2021.

7.2 Human health $\text{PM}_{2.5}$ indicator

Table 7.2 summarises for human health $\text{PM}_{2.5}$ indicator (annual average) the population-weighted concentration and the percentage of the considered European population exposed to $\text{PM}_{2.5}$ concentrations above the EU LV for the years 2005 to 2021 (without 2006, for which neither a map nor a population exposure was prepared).

As in the case of PM_{10} , the $\text{PM}_{2.5}$ maps for 2021 (as presented in Chapter 3) has been constructed using the updated methodology. The table presents the results for 2005, 2009 and 2015-2019 (all the years for which maps using both methods are available) both based on the updated and the old methodology, for comparability reasons.

Table 7.2: Population-weighted concentration and percentage of the considered European population (including United Kingdom, without Türkiye) exposed to concentrations above the $\text{PM}_{2.5}$ limit value (LV) for the protection of health for 2005 to 2021

$\text{PM}_{2.5}$	method	2005	2006	2007	2008	2009	2010	2011	2012	2013	2014	2015	2016	2017	2018	2019	2020	2021
Annual average																		
Pop.-weighted concentration [$\mu\text{g}\cdot\text{m}^{-3}$]	old	18.8	not mapped	16.2	16.4	16.2	16.9	17.8	15.7	15.3	14.1	14.2	13.4	13.6	13.2	11.6		
	new	19.0				16.6							14.3	13.6	13.8	13.5	11.8	11.1
Popul. exposed > LV (25 $\mu\text{g}\cdot\text{m}^{-3}$) [%]	old		16.8	8.2	7.9	7.6	8.3	13.3	9.1	5.8	4.2	6.3	5.4	7.0	4.1	0.9		
	new					7.6							6.5	5.4	7.2	4.5	1.2	1.1

The percentage of population exposed in 2021 to annual mean concentrations of $\text{PM}_{2.5}$ above the LV of $25 \mu\text{g}/\text{m}^3$ has been 1.0 %, which is the lowest value in the seventeen years' time series. Furthermore, it is estimated that the considered European inhabitants have been exposed on average to an annual mean $\text{PM}_{2.5}$ concentration of $11 \mu\text{g}/\text{m}^3$ in 2021, being (together with 2020) the lowest values in the time series.

The trend analysis of the population-weighted concentrations across the period 2005-2021 for the total mapping area has been executed, based on the old mapping method results for the period 2005-2019 and the new method for 2020-2021. At European scale a statistical significant (at the level ***, i.e. 0.001) downward trend can be observed, estimated to be $-0.5 \mu\text{g}/\text{m}^3$ per year.

7.3 Human health ozone indicators

Table 7.3 summarises the exposure levels of the considered European inhabitants in terms of population-weighted concentrations for two human health ozone indicators. Furthermore, it presents the percentage of considered European population exposed to concentrations above the target value (TV) threshold and above a level of 6 000 µg/m³·d for the SOMO35 for the years 2005 to 2021.

Table 7.3: Population-weighted concentration and percentage of the considered European population (including United Kingdom, without Türkiye) exposed to concentrations above the target value (TV) threshold for the protection of health and a SOMO35 threshold of 6 000 µg/m³·d for 2005 to 2021

Ozone		2005	2006	2007	2008	2009	2010	2011	2012	2013	2014	2015	2016	2017	2018	2019	2020	2021
26th highest daily max. 8-h mean / 93.2 percentile of daily max. 8-h means																		
Pop.-w. conc. [µg.m ⁻³]	26 th high.	111.4	117.6	110.0	109.4	107.7	106.5	108.4	107.3	108.3								
Pop.-w. conc. [µg.m ⁻³]	93.2 perc.								107.9	108.9	102.9	110.4	104.8	105.0	114.4	109.9	107.3	102.9
Pop. exp. > TV (120 µg.m ⁻³)	26 th high.	29.5	49.8	24.9	13.6	14.9	15.8	15.0	19.0	15.0								
Pop. exp. > TV (120 µg.m ⁻³)	93.2 perc.								20.2	15.9	5.6	34.0	8.4	12.9	34.8	20.3	7.4	5.8
SOMO35																		
Pop.-weighted concentr. [µg.m ⁻³ .d]		4622	5045	4291	4164	4233	3850	4318	4174	4089	3500	4312	3619	3890	4962	4478	3945	3563
Pop. exp. > 6000 µg/m ³ ·d	[%]	26.8	27.1	26.3	17.0	23.2	15.9	22.0	23.2	18.8	9.4	22.2	11.7	19.1	31.3	20.0	8.6	10.6

For 2012 and 2013, both the 26th highest value and the 93.2nd percentile of maximum daily 8-hour mean(s) have been calculated. It demonstrates an underestimation of about 0.6 µg/m³ at the 26th maximum daily 8-hour mean, which is caused by the fact that when calculating this indicator there is no correction for the missing values in the incomplete measurement time series.

Using the 93.2 percentile of ozone maximum daily 8-hour means it is estimated that 6 % of the population have lived in 2021 in areas where concentrations were above the ozone target value (TV) threshold of 120 µg/m³, which is the second lowest number of the seventeen-year period. The overall population-weighted ozone concentration in terms of the 93.2 percentile maximum daily 8-hour means in the background areas is estimated at about 103 µg/m³ for the total mapping area, which is (together with 2014) the lowest value of the whole seventeen-year period (it should be noted that for 2005-2011 the 26th highest value of the maximum daily eight-hour mean was considered instead).

Examining the time series for 2005-2021, it can be concluded that 2005, 2006, 2015 and 2018 are exceptional years with high ozone concentrations, leading to increased exposure levels compared to the other thirteen years. The years 2014, 2016, 2020 and 2021 show the lowest exposure levels in the seventeen years' time series for the 93.2 percentile of the maximum daily 8-hour means.

The trend analysis of the population-weighted concentrations for the 93.2 percentile of the maximum daily 8-hour means across the period 2005-2021 for the total considered mapping area does not estimate a statistically significant trend. The reason is the ozone variability, which higher values occurring with warm and dry summers.

A similar tendency is observed for SOMO35. In 2005-2007, a bit more than one-fourth of the population have lived in areas where a level of 6 000 µg/m³·d ⁽⁷⁾ has been exceeded, with the highest level in 2006. In the period of 2008-2019, it fluctuated from about 16 % to 23 % of the population, except 2014 with about 9 %, 2016 with about 12 %, and 2018 with about one-third of the population.

The population-weighted SOMO35 concentrations show the second lowest value in 2021. Trend analysis on the population-weighted concentration for the total mapping area shows no trend for the period 2005-2021. The reason is the same as in the case of the 93.2 percentile of the maximum daily 8-hour means.

⁽⁷⁾ Note that the 6 000 µg/m³·d does not represent a health-related legally binding 'threshold'. In this and previous papers it represents a somewhat arbitrarily chosen threshold to facilitate the discussion of the observed distributions of SOMO35 levels in their spatial and temporal context. For motivation of this choice, see Section 4.2.

7.4 Vegetation related ozone indicators

Exposure indicators describing the agricultural and forest areas exposed to accumulated ozone concentrations above defined thresholds are summarised in Table 7.4. Those thresholds are the target value (TV) threshold of 18 000 $\mu\text{g}/\text{m}^3\cdot\text{h}$ and the long-term objective (LTO) of 6 000 $\mu\text{g}/\text{m}^3\cdot\text{h}$ for the AOT40 for vegetation, and the former reporting value (RV) of 20 000 $\mu\text{g}/\text{m}^3\cdot\text{h}$ and the critical level (CL) of 10 000 $\mu\text{g}/\text{m}^3\cdot\text{h}$ for the AOT40 for forests.

Table 7.4: Percentages of the considered European agricultural and forest area (including United Kingdom, without Türkiye) exposed to ozone concentrations above the target value (TV) threshold and the long-term objective (LTO) for AOT40 for vegetation, and above critical level (CL) and reporting value (RV) for AOT40 for forests and agricultural- and forest-weighted concentrations for 2005 to 2021

Ozone	2005	2006	2007	2008	2009	2010	2011	2012	2013	2014	2015	2016	2017	2018	2019	2020	2021
AOT40 for vegetation																	
Agr. area exp. > TV (18 000 $\mu\text{g}/\text{m}^3$ [%])	48.5	69.1	35.7	37.8	26.0	21.3	19.2	30.0	22.1	17.8	31.4	14.7	23.8	39.7	29.7	3.0	6.7
Agr. area exp. > LTO (6 000 $\mu\text{g}/\text{m}^3$ [%])	88.8	97.6	77.5	95.5	81.0	85.4	87.9	86.4	81.0	85.5	79.7	74.1	73.4	95.1	84.0	71.0	73.2
Agr.-weighted concentr. [$\mu\text{g}/\text{m}^3\cdot\text{h}$]	17481	22344	14597	15214	13157	13310	13255	14041	12838	12427	14223	10942	11750	16311	13735	8544	10041
AOT40 for forests																	
For. area exp. > RV (20 000 $\mu\text{g}/\text{m}^3$ [%])	59.1	69.4	48.4	50.2	49.2	49.3	53.0	47.2	44.1	37.7	52.4	41.9	38.9	56.1	51.4	34.4	29.9
For. area exp. > CL (10 000 $\mu\text{g}/\text{m}^3$ [%])	76.4	99.8	62.1	79.6	67.4	63.4	68.6	65.0	67.2	68.2	59.8	60.0	55.4	86.7	84.0	58.0	59.5
For.-weighted concentration [$\mu\text{g}/\text{m}^3\cdot\text{h}$]	25900	31154	23744	21951	23532	19625	21892	21580	21753	17124	21150	17573	16798	25397	22343	14584	15070

In 2021, some 7 % of all agricultural land (crops) has been exposed to accumulated ozone concentrations (AOT40 for vegetation) above the target value (TV) threshold, which is the second lowest value in the seventeen-year time series. About 73 % of all agricultural land has been exposed to levels in excess of the long-term objective (LTO), which is also the second lowest values in the seventeen-year period. The agricultural-weighted AOT40 concentration shows the second lowest value in 2021.

The trend analysis of the agricultural-weighted concentrations for the AOT40 for vegetation across the period 2005-2021 for the total considered mapping area does not estimate any statistically significant trend. The reason again is the ozone variability correlated with the variability of meteorology.

For the ozone indicator AOT40 for forests, the level of 20 000 $\mu\text{g}/\text{m}^3\cdot\text{h}$ (earlier used reporting value, RV) has been exceeded in about 30 % of the considered European forest area in 2021, which is the lowest value of the whole time series. The forest area exceeding the CL has been in 2021 almost 60 %, which is the third lowest percentage of the seventeen-year period. The temporal pattern of the concentrations above the AOT40 for forests CL shows some similarity with those of the AOT40 for vegetation, despite their different definitions and receptors and their natural difference in area type characteristics and occurrence. Their annual variability is, however, heavily dependent on meteorological variability.

The trend analysis of the forest-weighted concentrations for the AOT40 for forests across the period 2005-2021 for the total considered mapping area shows a slight downward trend of about -438 $\mu\text{g}/\text{m}^3\cdot\text{d}$ per year, for the period 2005-2021, however at the lowest level of statistical significance (+, i.e. 0.1).

7.5 Human health NO_2 indicator

Table 7.5 summarises the development in exposure levels of the considered European population for the human health NO_2 indicator (annual average), in terms of population-weighted concentrations and percentage of population exposed to concentrations above the annual LV (40 $\mu\text{g}/\text{m}^3$), for the years 2005, 2009, 2010 and 2013 to 2021, for which the maps based on the current methodology are available. The population-weighted concentration is presented additionally also for 2007, although

based on different mapping methodology than the other years. This 2007 value is probably slightly underestimated; based on Horálek et al. (2017b), one can suppose the true value would be of about 1 % higher (i.e. it would be about 23.5 $\mu\text{g}/\text{m}^3$).

Table 7.5: Population-weighted concentration and percentage of the considered European population (including United Kingdom, without Türkiye) exposed to concentrations above the NO₂ limit value (LV) of 40 $\mu\text{g}/\text{m}^3$ for the protection of health for 2005 to 2021

NO ₂	2005	2006	2007	2008	2009	2010	2011	2012	2013	2014	2015	2016	2017	2018	2019	2020	2021
Annual average																	
Popul.-weighted conc. [$\mu\text{g}/\text{m}^3$]	23.3	not mapped	23.3	not mapped	22.1	22.1	not mapped		19.4	18.6	18.8	18.6	18.4	17.6	16.8	14.0	14.4
Pop. exp. > LV (40 $\mu\text{g}/\text{m}^3$) [%]	7.9	mapped		mapped	5.6	4.9	not mapped		3.2	2.8	3.2	2.8	3.0	1.8	1.3	0.2	0.2

In 2021 the population exposed to NO₂ annual mean concentrations above the limit value of 40 $\mu\text{g}/\text{m}^3$ has been 0.2 % of the total population, which is (together with 2020) the lowest in the whole series. Furthermore, it is estimated that the considered European inhabitants have been exposed on average to an annual mean NO₂ concentration of 14 $\mu\text{g}/\text{m}^3$, again the lowest in the whole series, together with 2020.

Trend analysis on the population-weighted concentration for the total mapping area shows a downward trend of about -0.6 $\mu\text{g}/\text{m}^3$ per year, for the period 2005-2021, which is statistically significant (at the highest level ***, i.e. 0.001).

List of abbreviations

Abbreviation	Name	Reference
ALV	Annual Limit Value	
AOT40	Accumulated Ozone exposure over a Threshold of 40 ppb (i.e. 80 µg/m ³) in a specific period	http://eur-lex.europa.eu/LexUriServ/LexUriServ.do?uri=OJ:L:2008:152:0001:0044:EN:PDF
AQ	Air Quality	
CL	Critical Level	https://icpvegetation.ceh.ac.uk/chapter-3-mapping-critical-levels-vegetation
CLC	CORINE Land Cover	https://land.copernicus.eu/pan-european/corine-land-cover
CLRTAP	Convention on Long-range Transboundary Air Pollution (Air Convention)	https://unece.org/environment-policy/air
CORINE	Co-ORdinated INformation on the Environment	https://land.copernicus.eu/pan-european/corine-land-cover
CTM	Chemical Transport Model	
CSI	Core Set of Indicators	https://www.eea.europa.eu/ims
Defra	UK Department for Environment Food & Rural Affairs	
DLV	Daily Limit Value	
ECMWF	European Centre for Medium-Range Weather Forecasts	https://www.ecmwf.int/
EBAS	EMEP dataBASE	https://ebas.nilu.no/
EEA	European Environment Agency	www.eea.europa.eu
EMEP	European Monitoring and Evaluation Programme	https://www.emep.int/
ETC/ACM	European Topic Centre on Air pollution and Climate change Mitigation	https://www.eionet.europa.eu/etcs
ETC/ATNI	European Topic Centre on Air pollution, Noise, Transport and Industrial pollution	https://www.eionet.europa.eu/etcs
ETC HE	European Topic Centre on Human Health and the Environment	https://www.eionet.europa.eu/etcs
EU	European Union	https://european-union.europa.eu
GMTED	Global Multi-resolution Terrain Elevation Data	
GRIP	Global Roads Inventory Dataset	
HLV	Hourly Limit Value	
ICP	International scientific Cooperative Programme	https://icpvegetation.ceh.ac.uk/
ILV	Indicative Limit Value	

Abbreviation	Name	Reference
JRC	Joint Research Centre	https://ec.europa.eu/info/departments/joint-research-centre_en
LV	Limit Value	http://eur-lex.europa.eu/LexUriServ/LexUriServ.do?uri=OJ:L:2008:152:0001:0044:EN:PDF
NILU	Norwegian Institute for Air Research	https://www.nilu.no/
NO ₂	Nitrogen dioxide	
NO _x	Nitrogen oxides	
O ₃	Ozone	
ORNL	Oak Ridge National Laboratory	https://www.ornl.gov/
PLA	Projected Leaf Area	https://icpvegetation.ceh.ac.uk/chapter-3-mapping-critical-levels-vegetation
PM ₁₀	Particulate Matter with a diameter of 10 micrometres or less	
PM _{2.5}	Particulate Matter with a diameter of 2.5 micrometres or less	
POD ₆	Phytotoxic Ozone Doze above a threshold of 6 nmol/m ² PLA s ⁻¹	https://icpvegetation.ceh.ac.uk/chapter-3-mapping-critical-levels-vegetation
POD ₁	Phytotoxic Ozone Doze above a threshold of 1 nmol/m ² PLA s ⁻¹	https://icpvegetation.ceh.ac.uk/chapter-3-mapping-critical-levels-vegetation
R ²	Coefficient of determination	
RIMM	Regression – Interpolation – Merging Mapping	
RMSE	Root Mean Square Error	
SOMO10	Sum of Ozone Maximum daily 8-hour means Over 10 ppb (i.e. 20 µg/m ³)	
SOMO35	Sum of Ozone Maximum daily 8-hour means Over 35 ppb (i.e. 70 µg/m ³)	
TV	Target Value	http://eur-lex.europa.eu/LexUriServ/LexUriServ.do?uri=OJ:L:2008:152:0001:0044:EN:PDF
UK	United Kingdom	
UN	United Nations	https://www.un.org
UNECE	United Nations Economic Commission for Europe	https://unece.org/
UTC	Coordinated Universal Time	
WHO	World Health Organization	https://www.who.int/

References

- Alonso, R., et al., 2014, 'Drought stress does not protect *Quercus ilex* L. from ozone effects: results from a comparative study of two subspecies differing in ozone sensitivity', *Plant Biology* 16, pp. 375-384 (<https://onlinelibrary.wiley.com/doi/10.1111/plb.12073>) accessed 21 January 2021.
- Anav, A., et al., 2022, 'Legislative and functional aspects of different metrics used for ozone risk assessment to forests', *Environmental Pollution* 295(118690) (<https://doi.org/10.1016/j.envpol.2021.118690>) accessed 11 July 2022.
- Ashmore, M., et al., H., 2004, 'New directions: a new generation of ozone critical levels for the protection of vegetation in Europe', *Atmospheric Environment* 38, pp. 2213-2214 (<https://doi.org/10.1016/j.atmosenv.2004.02.029>) accessed 20 November 2020.
- Büker, P., et al., 2015, 'New flux based dose-response relationships for ozone for European forest tree species', *Environmental Pollution* 206, pp. 163-174 (<https://doi.org/10.1016/j.envpol.2015.06.033>) accessed 27 April 2022.
- CLRTAP, 2016, *Forest condition in Europe*, 2016 Technical Report of ICP Forests, UNECE Convention on Long-range Transboundary Air Pollution (<https://www.icp-forests.org/pdf/TR2016.pdf>) accessed 19 November 2020.
- CLRTAP, 2017a, *Manual for modelling and mapping critical loads & levels. Chapter III: "Mapping Critical levels for Vegetation"*, UNECE Convention on Long-range Transboundary Air Pollution (<https://icpvegetation.ceh.ac.uk/chapter-3-mapping-critical-levels-vegetation>) accessed 7 May 2021.
- CLRTAP, 2017b, *Scientific Background Document A of Chapter 3 of "Manual on methodologies and criteria for modelling and mapping critical loads and levels of air pollution effects, risks and trends"* (<https://icpvegetation.ceh.ac.uk/sites/default/files/ScientificBackgroundDocumentAOct2018.pdf>) accessed 11 December 2020.
- CLRTAP, 2020, *Scientific Background Document B of Chapter 3 of "Manual on methodologies and criteria for modelling and mapping critical loads and levels of air pollution effects, risks and trends"* (<https://icpvegetation.ceh.ac.uk/sites/default/files/Scientific%20Background%20document%20B%20June%202020.pdf>) accessed 11 December 2020.
- CLRTAP, 2022, *ICP Vegetation: Review of NOx critical levels, full workshop report* (https://icpvegetation.ceh.ac.uk/sites/default/files/NOx_critical_levels_workshop_REPORT.pdf) accessed 22 November 2022.
- Colette, A., et al., 2018, *Long term evolution of the impacts of ozone air pollution on agricultural yields in Europe. A modelling analysis for the 1990-2010 period*, Eionet Report ETC/ACM 2018/15 (https://www.eionet.europa.eu/etcs/etc-atni/products/etc-atni-reports/eionet_rep_etcacm_2018_15_o3impacttrends) accessed 26 August 2020.
- Cressie, N., 1993, *Statistics for spatial data*, Wiley series, New York.
- Danielson, J. J. and Gesch, D. B., 2011, *Global multi-resolution terrain elevation data 2010 (GMTED2010)*, U.S. Geological Survey Open-File Report, pp. 2011-1073 (<https://pubs.er.usgs.gov/publication/ofr20111073>) accessed 19 November 2020.

Defra, 2023, *UK Air information resource*, Data archive, UK Department for Environment Food & Rural Affairs (<https://uk-air.defra.gov.uk/data/>). Data extracted in April 2023.

De Leeuw, F., 2012, *AirBase: a valuable tool in air quality assessments at a European and local level*, ETC/ACM Technical Paper 2012/4 (http://www.eionet.europa.eu/etcs/etc-atni/products/etc-atni-reports/etcacm_tp_2012_4_airbase_aqassessment) accessed 26 August 2020.

Denby, B., et al., 2008, 'Comparison of two data assimilation methods for assessing PM₁₀ exceedances on the European scale', *Atmospheric Environment* 42, pp. 7122-7134 (<https://doi.org/10.1016/j.atmosenv.2008.05.058>) accessed 26 August 2020.

Denby, B., et al., 2011, *Mapping annual mean PM_{2.5} concentrations in Europe: application of pseudo PM_{2.5} station data*, ETC/ACM Technical Paper 2011/5 (http://www.eionet.europa.eu/etcs/etc-atni/products/etc-atni-reports/etcacm_tp_2011_5_spatialpm2-5mapping) accessed 26 August 2020.

De Smet, P., et al., 2011, *European air quality maps of ozone and PM₁₀ for 2008 and their uncertainty analysis*, ETC/ACC Technical Paper 2010/10 (http://www.eionet.europa.eu/etcs/etc-atni/products/etc-atni-reports/etcacc_tp_2010_10_spatagmaps_2008) accessed 26 August 2020.

Deumier, J. M. and Hannon, C., 2010, 'La période d' initiation de la tubérisation: comment la repérer?' (in French), CNIPT (<http://www.cnipt.fr/wp-content/uploads/2013/10/Irrigation-juin-2010.pdf>) accessed 8 February 2021.

EC, 2004, *Directive 2004/107/EC of the European Parliament and of the Council of 15 December 2004 relating to arsenic, cadmium, mercury, nickel and polycyclic aromatic hydrocarbons in ambient air*, OJ L 23, 26.1.2005, 3-16 (<https://eur-lex.europa.eu/legalcontent/EN/TXT/PDF/?uri=CELEX:32004L0107&from=EN>) accessed 10 June 2022.

EC, 2008, *Directive 2008/50/EC of the European Parliament and of the Council of 21 May 2008 on ambient air quality and cleaner air for Europe*, OJ L 152, 11.06.2008, 1-44 (<http://eur-lex.europa.eu/LexUriServ/LexUriServ.do?uri=OJ:L:2008:152:0001:0044:EN:PDF>) accessed 26 May 2021.

EC, 2021. *The tomato market in the EU: Vol. 1: Production statistics* (https://agriculture.ec.europa.eu/data-and-analysis/markets/overviews/market-observatories/fruit-and-vegetables/tomatoes-statistics_en) accessed 6 December 2022.

ECMWF, 2023, *CAMS Regional: European air quality analysis and forecast data documentation* (<https://confluence.ecmwf.int/display/CKB/CAMS+Regional%3A+European+air+quality+analysis+and+forecast+data+documentation>) accessed 2 October 2023.

EEA, 2010, *ORNL Landscan 2008 Global Population Data conversion into EEA ETRS89-LAEA5210 1km grid* (by Hermann Peifer of EEA) (<https://sdi.eea.europa.eu/catalogue/geoss/api/records/1d68d314-d07c-4205-8852-f74b364cd699>) accessed 26 August 2020.

EEA, 2018, *Guide for EEA map layout. EEA operational guidelines*, January 2015, version 5 (https://www.eionet.europa.eu/gis/docs/GISguide_v5_EEA_Layout_for_map_production.pdf) accessed 26 August 2020.

EEA, 2019, *Healthy environment, healthy lives: how the environment influences health and well-being in Europe*, EEA Report 21/2019 (<https://www.eea.europa.eu/publications/healthy-environment-healthy-lives>) accessed 2 June 2021.

EEA, 2023a, *Air Quality e-Reporting. Air quality database* (<https://www.eea.europa.eu/data-and-maps/data/aireporting-8>). Data extracted in March 2023.

EEA, 2023b, *Exposure of Europe's ecosystems to ozone* (<https://www.eea.europa.eu/ims/exposure-of-europes-ecosystems-to-ozone>) accessed 6 September 2023.

Emberson, L. D., et al., 2000, 'Modelling stomatal ozone flux across Europe', *Environmental Pollution* 109, pp. 403-413 ([https://doi.org/10.1016/S0269-7491\(00\)00043-9](https://doi.org/10.1016/S0269-7491(00)00043-9)) accessed 26 May 2021.

EMEP, 2020, *Transboundary particulate matter, photo-oxidants, acidifying and eutrophying components*, EMEP Report 1/2020 (https://emep.int/publ/reports/2020/EMEP_Status_Report_1_2020.pdf) accessed 22 January 2021.

EMEP, 2022, *Data of HMs and POPs for the EMEP region*, Meteorological Synthesizing Centre – East (MCS-E) (<https://www.msceast.org/index.php/pollution-assessment/emep-domain-menu/data-hm-pop-menu>) accessed 30 September 2022.

ESA, 2019, *Land cover classification gridded maps from 1992 to present derived from satellite observations* (<https://cds.climate.copernicus.eu/cdsapp#!/dataset/satellite-land-cover>) accessed 17 February 2021.

EU, 2020, *Corine land cover 2018 (CLC2018) raster data*, 100x100m² gridded version 2020_20 (<https://land.copernicus.eu/pan-european/corine-land-cover/clc2018>) accessed 19 November 2020.

Eurostat, 2014, *GEOSTAT 2011 grid dataset*, Population distribution dataset (<http://ec.europa.eu/eurostat/web/gisco/geodata/reference-data/population-distribution-demography>) accessed 26 August 2020.

Eurostat, 2023, *Population on 1 January by age and sex* (https://ec.europa.eu/eurostat/databrowser/view/DEMO_PJAN/default/table) accessed 20 July 2023.

Gilbert, R. O., 1987, *Statistical Methods for Environmental Pollution Monitoring*, Van Nostrand Reinhold, New York.

Gusev, A., et al., 2005, *Regional Multicompartment Model MSCE-POP*, EMEP/MSC-E Technical Report 5/2005 (http://www.msceast.org/reports/5_2005.pdf) accessed 9 December 2021.

Gusev, A., et al., 2022, *EURODELTA-Carb exercise: Intercomparison of modelled estimates of benzo(a)pyrene (BaP) in Europe*, HARMO 2022 conference proceedings (https://www.harmo.org/Conferences/Proceedings/Aveiro/publishedSections/00488_107_h21-168-alexey-gusev.pdf) accessed 6 September 2023.

Haberle, J. and Svoboda, P., 2015, 'Calculation of available water supply in crop root zone and the water balance of crops', *Contributions to Geophysics and Geodesy* 45, pp. 285-298 (https://www.researchgate.net/publication/293194127_Calculation_of_available_water_supply_in_crop_root_zone_and_the_water_balance_of_crops) accessed 21 January 2021.

Horálek, J., et al., 2007, *Spatial mapping of air quality for European scale assessment*, ETC/ACC Technical paper 2006/6 (http://www.eionet.europa.eu/etcs/etc-atni/products/etc-atni-reports/etcacc_techpaper_2006_6_spat_ag) accessed 26 August 2020.

Horálek, J., et al., 2008, *European air quality maps for 2005 including uncertainty analysis*, ETC/ACC Technical paper 2007/7 (http://www.eionet.europa.eu/etcs/etc-atni/products/etc-atni-reports/etcacc_tp_2007_7_spatagmaps_ann_interpol) accessed 26 August 2020.

Horálek, J., et al., 2010, *Methodological improvements on interpolating European air quality maps*, ETC/ACC Technical Paper 2009/16 (http://www.eionet.europa.eu/etcs/etc-atni/products/etc-atni-reports/etcacc_tp_2009_16_improv_spatagmapping) accessed 26 August 2020.

Horálek, J., et al., 2016, *Application of FAIRMODE Delta tool to evaluate interpolated European air quality maps for 2012*, ETC/ACM Technical Paper 2015/2 (http://www.eionet.europa.eu/etcs/etc-atni/products/etc-atni-reports/etcacm_tp_2015_2_delta_evaluation_aqmaps2012) accessed 26 August 2020.

Horálek, J., et al., 2017a, *European air quality maps for 2014*, ETC/ACM Technical Paper 2016/6 (https://www.eionet.europa.eu/etcs/etc-atni/products/etc-atni-reports/etcacm_tp_2016_6_aqmaps2014) accessed 30 September 2022.

Horálek, J., et al., 2017b, *Inclusion of land cover and traffic data in NO₂ mapping methodology*, ETC/ACM Technical Paper 2016/12 (http://www.eionet.europa.eu/etcs/etc-atni/products/etc-atni-reports/etcacm_tp_2016_12_lc_and_traffic_data_in_no2_mapping) accessed 27 May 2021.

Horálek, J., et al., 2018, *Satellite data inclusion and kernel based potential improvements in NO₂ mapping*, ETC/ACM Technical Paper 2017/14 (http://www.eionet.europa.eu/etcs/etc-atni/products/etc-atni-reports/etcacm_tp_2017_14_improved_aq_no2mapping) accessed 27 May 2021.

Horálek, J., et al., 2019, *Land cover and traffic data inclusion in PM mapping*, Eionet Report ETC/ACM 2018/18 (<http://www.eionet.europa.eu/etcs/etc-atni/products/etc-atni-reports/etc-acm-report-18-2018-land-cover-and-traffic-data-inclusion-in-pm-mapping>) accessed 27 May 2021.

Horálek, J., et al., 2021, *Potential use of CAMS modelling results in air quality mapping under ETC/ATNI*, Eionet Report ETC/ATNI 2019/17 (<https://doi.org/10.5281/zenodo.4627762>) accessed 15 June 2021.

Horálek, J., et al., 2022, *Benzo(a)pyrene (BaP) annual mapping*, Eionet Report ETC/ATNI 2021/18 (<https://doi.org/10.5281/zenodo.5898376>) accessed 26 August 2022.

Horálek, J., et al., 2023, *European air quality maps for 2020*, Eionet Report ETC/ATNI 2022/12 (<https://doi.org/10.5281/zenodo.7657071>) accessed 31 May 2023.

Jarvis, P. G., 1976, 'The interpretation of the variation in leaf water potential and stomatal conductance found in canopies in the field', *Philosophical Transactions of the Royal Society of London*, Series B: Biological Sciences 273, pp. 593-610 (<https://doi.org/10.1098/rstb.1976.0035>) accessed 26 May 2021.

JRC, 2009, *Population density disaggregated with Corine land cover 2000*, 100x100 m² grid resolution, EEA version (<http://www.eea.europa.eu/data-and-maps/data/population-density-disaggregated-with-corine-land-cover-2000-2>) accessed 26 August 2020.

JRC, 2016, *Maps of indicators of soil hydraulic properties for Europe*, dataset/maps downloaded from the European Soil Data Centre (<http://esdac.jrc.ec.europa.eu/content/maps-indicators-soil-hydraulic-properties-europe>) accessed 8 December 2020.

Krupa, S., et al., 2000, 'Ambient ozone and plant health', *Plant Disease* 85, pp. 4-12 (<https://apsjournals.apsnet.org/doi/pdf/10.1094/pdis.2001.85.1.4>) accessed 8 December 2020.

Kuenen, J., et al., 2021, *Copernicus Atmosphere Monitoring Service regional emissions version 4.2* (CAMS-REG-v4.2) Copernicus Atmosphere Monitoring Service [publisher] ECCAD [distributor], (<https://doi.org/10.24380/0vzb-a387>) accessed 6 August 2022.

MDA, 2015, *World Land Cover at 30m resolution from MDAUS BaseVue 2013* (<https://www.arcgis.com/home/item.html?id=1770449f11df418db482a14df4ac26eb>) accessed 17 February 2021.

Meijer, J. R., et al., 2018, 'Global patterns of current and future road infrastructure', *Environmental Research Letters* 13, 0640 (<https://doi.org/10.1088/1748-9326/aabd42>) accessed 10 June 2019.

METEO FRANCE, et al., 2023, *CAMS European air quality forecasts, ENSEMBLE data. Copernicus Atmosphere Monitoring Service (CAMS) Atmosphere Data Store (ADS)* (<https://ads.atmosphere.copernicus.eu/cdsapp#!/dataset/cams-europe-air-quality-forecasts?tab=overview>) accessed on 2 October 2023.

Mills, G., et al., 2011, 'New stomatal flux-based critical levels for ozone effects on vegetation', *Atmospheric Environment* 45, pp. 5064-5068 (<https://doi.org/10.1016/j.atmosenv.2011.06.009>) accessed 19 November 2020.

Musselman, R. C. and Massman, W. J., 1998, 'Ozone flux to vegetation and its relationship to plant response and ambient air quality standards', *Atmospheric Environment* 33, pp. 65-73 ([https://doi.org/10.1016/S1352-2310\(98\)00127-7](https://doi.org/10.1016/S1352-2310(98)00127-7)) accessed 26 May 2021.

NILU, 2023, *EBAS, database of atmospheric chemical composition and physical properties* (<http://ebas.nilu.no>). Data extracted in April 2023.

Nussbaum, S., et al., 2003, 'High-resolution spatial analysis of stomatal ozone uptake in arable crops and pastures', *Environmental International* 129, pp. 385-392 (<https://www.ncbi.nlm.nih.gov/pubmed/12676231>) accessed 26 May 2021.

Pedersen, S. M., et al., 2005, *Potato production in Europe - a gross margin analysis*, University of Copenhagen, FOI WorkingPaper Vol. 2005 No. 5, pp. 1-39 (<https://curis.ku.dk/ws/files/135440168/5.pdf>) accessed 26 May 2021.

Pleijel, H., et al., 2007, 'Ozone risk assessment for agricultural crops in Europe: Further development of stomatal flux and flux-response relationships for European wheat and potato', *Atmospheric Environment* 41, pp.3022-3040 (<https://doi.org/10.1016/j.atmosenv.2006.12.002>) accessed 8 December 2020.

Reich, P. B., 1987, 'Quantifying plant response to ozone: a unifying theory', *Tree Physiology* 3, pp. 63-91 (<https://doi.org/10.1093/treephys/3.1.63>) accessed 19 November 2020.

Simpson, D., et al., 2012, 'The EMEP MSC-W chemical transport model – technical description', *Atmospheric Chemistry and Physics* 12, pp. 7825-7865 (<https://doi.org/10.5194/acp-12-7825-2012>) accessed 26 August 2020.

Targa, J., et al., 2023, *Status report of air quality in Europe for year 2021, using validated data*, Eionet Report ETC HE 2023/1 (<https://www.eionet.europa.eu/etcs/etc-he/products/etc-he-products/etc-he-reports/etc-he-report-2023-1-status-report-of-air-quality-in-europe-for-year-2021-using-validated-data>) accessed 5 September 2023.

UN, 2023, *World Population Prospects 2022*, United Nations, Department of Economic and Social Affairs, Population Division (<https://population.un.org/wpp/Download/Standard/Population/>) accessed 20 July 2023.

van Geffen, J., et., 2019, 'TROPOMI ATBD of the total and tropospheric NO₂ data products', KNMI (<https://sentinel.esa.int/documents/247904/2476257/Sentinel-5P-TROPOMI-ATBD-NO2-data-products>) accessed 30 August 2021.

van Geffen, J., et al., 2020, 'S5P TROPOMI NO₂ slant column retrieval: Method, stability, uncertainties and comparisons with OMI', *Atmospheric Measurement Techniques* 13, pp. 1315–1335 (<https://doi.org/10.5194/amt-13-1315-2020>) accessed 30 August 2021.

Veefkind, J. P., et al., 2012. 'TROPOMI on the ESA Sentinel-5 Precursor: A GMES mission for global observations of the atmospheric composition for climate, air quality and ozone layer applications', *Remote Sensing of Environment* 120, pp. 70–83 (<https://doi.org/10.1016/j.rse.2011.09.027>) accessed 30 August 2021.

Vivanco, M. G., et al., 2023, *Evaluación de la calidad del aire en España mediante modelización combinada con mediciones. Reevaluación año 2021. Informe Técnico, CIEMAT, Ref. 5/2023.*

Vlasáková, L., et al., 2023. *Evaluation of European-wide map creation of flux-based ozone indicator POD for selected tree species*, Eionet Report ETC HE 2022/23 (<https://www.eionet.europa.eu/etcs/etc-he/products/etc-he-products/etc-he-reports/etc-he-report-2022-23-evaluation-of-european-wide-map-creation-of-flux-based-ozone-indicator-pod-for-selected-tree-species>) accessed 12 June 2023.

WHO, 2005, *WHO Air quality guidelines for particulate matters, ozone, nitrogen dioxide and sulphur dioxide, Global update 2005*, World Health Organization (<https://apps.who.int/iris/handle/10665/107823>) accessed 16 November 2022.

WHO, 2013, *Review of evidence on health aspects of air pollution: REVIHAAP project: technical report*, World Health Organization (<https://apps.who.int/iris/handle/10665/341712>) accessed 16 November 2022.

WHO, 2021a, *WHO global air quality guidelines: particulate matter (PM_{2.5} and PM₁₀), ozone, nitrogen dioxide, sulfur dioxide and carbon monoxide*, World Health Organization (<https://apps.who.int/iris/handle/10665/345329>) accessed 10 December 2021.

WHO, 2021b, *Human health effects of polycyclic aromatic hydrocarbons as ambient air pollutants* (<https://www.who.int/europe/publications/i/item/9789289056533>) accessed 22 September 2022.

Annex 1 Methodology

A1.1 Mapping methodology

Previous mapping reports like Horálek et al. (2007, 2010, 2017b, 2018, 2019, 2022), De Smet et al. (2011), Denby et al. (2011) discuss methodological developments and details on spatial interpolations and their uncertainties of air quality maps. No changes took place in the mapping methodology with respect to the preceding report (Horálek et al., 2023). This annex summarizes the currently applied method for all the considered indicators. The mapping method has been evaluated with the FAIRMODE Delta tool in Horálek et al. (2016). The method is called the *Regression – Interpolation – Merging Mapping* (RIMM).

Pseudo PM_{2.5}, NO_x and BaP station data estimation

To supplement PM_{2.5} measurement data, in the mapping procedure data from so-called pseudo PM_{2.5} stations are also used. These data are the estimates of PM_{2.5} concentrations at the locations of PM₁₀ stations with no PM_{2.5} measurement. These estimates are based on PM₁₀ measurement data and different supplementary data, using linear regression:

$$\hat{Z}_{PM_{2.5}}(s) = c + b \cdot Z_{PM_{10}}(s) + a_1 X_1(s) + a_2 X_2(s) + \dots + a_n X_n(s) \quad (A1.1)$$

where $\hat{Z}_{PM_{2.5}}(s)$ is the estimated value of PM_{2.5} at the station s ,
 $Z_{PM_{10}}(s)$ is the measurement value of PM₁₀ at the station s ,
 c, b, a_1, \dots, a_n are the parameters of the linear regression model calculated based on the data at the points of stations with both PM_{2.5} and PM₁₀ measurements,
 $X_1(s), \dots, X_n(s)$ are the values of other supplementary variables at the station s ,
 n is the number of other supplementary variables used in the linear regression.

When applying this estimation method, all background stations (either classified as rural, urban or suburban) are handled together for estimating PM_{2.5} values at background pseudo stations. For details, see Denby et al. (2011). For estimating PM_{2.5} values at urban traffic pseudo stations, Equation A1.1 is applied for the urban traffic stations. For details, see by Horálek et al. (2019).

To supplement NO_x measurement data, NO_x values are estimated at locations of NO₂ stations with no NO_x data. The estimates are calculated similarly as in Horálek et al. (2007), using regression:

$$\hat{Z}_{NO_x}(s) = a_1 Z_{NO_2}(s)^2 + a_2 Z_{NO_2}(s) + c \quad (A1.2)$$

where $\hat{Z}_{NO_x}(s)$ is the estimated value of NO_x at the station s ,
 $Z_{NO_2}(s)$ is the measurement value of NO₂ at the station s ,
 a_1, a_2, c are the parameters of the regression calculated based on the data at the points of measuring stations with both NO_x and NO₂ measurements.

To supplement BaP measurement data, BaP concentrations are estimated at the locations with PM_{2.5} data with no BaP measurements. These estimates are based on PM_{2.5} measurement data (or PM_{2.5} pseudo stations data) and different supplementary data, using exponential regression:

$$\hat{Z}_{BaP}(s) = \exp(c + b \cdot Z_{PM_{2.5}}(s) + a_1 X_1(s) + a_2 X_2(s) + \dots + a_n X_n(s)) \quad (A1.3)$$

where $\hat{Z}_{BaP}(s)$ is the estimated value of BaP at the station s ,
 $Z_{PM_{2.5}}(s)$ is the measurement (or estimated) value of $PM_{2.5}$ at the station s ,
 c, b, a_1, \dots, a_n are the parameters of the linear regression model calculated based on the data at the locations of stations with both BaP and $PM_{2.5}$ measurements,
 $X_1(s), \dots, X_n(s)$ are the values of other supplementary variables at the station s ,
 n is the number of other supplementary variables used in the linear regression.

When applying this estimation, all background stations (either classified as rural, urban or suburban) are handled together for estimating BaP values at background pseudo stations. The reason for introducing the exponential regression is the exponential relation between BaP and $PM_{2.5}$. In agreement with Horálek et al. (2022), the pseudo BaP data are only calculated in areas with a lack of BaP data (see Annex 3, Section A3.5). The estimates are calculated primarily for the locations with $PM_{2.5}$ measured data with no BaP measurements. In the limited areas with a lack of both BaP and $PM_{2.5}$ measurements, pseudo $PM_{2.5}$ data (see Eq. A1.1) calculated for locations with PM_{10} measurements are used.

Interpolation

The mapping method used is a linear regression model followed by kriging of the residuals produced from that model (residual kriging). Interpolation is therefore carried out according to the relation:

$$\hat{Z}(s_0) = c + a_1 X_1(s_0) + a_2 X_2(s_0) + \dots + a_n X_n(s_0) + \hat{R}(s_i) \quad (A1.4)$$

where $\hat{Z}(s_0)$ is the estimated value of the air pollution indicator at the point s_0 ,
 $X_1(s_0), X_2(s_0), \dots, X_n(s_0)$ are the n individual supplementary variables at the point s_0 ,
 c, a_1, a_2, \dots, a_n are the $n+1$ parameters of the linear regression model calculated based on the data at the measurement points,
 $\hat{R}(s_i)$ is the spatial interpolation of the residuals of the linear regression model at the point s_0 calculated based on the residuals at the measurement points.

For different pollutants and area types (rural, urban background, and in the case of PM and NO_2 , also urban traffic), different supplementary data are used, depending on their improvement to the fit of the regression. Ordinary kriging is used to interpolate the residuals:

$$\hat{R}(s_i) = \sum_{i=1}^N \lambda_i R(s_i), \sum_{i=1}^N \lambda_i = 1 \quad (A1.4a)$$

where $R(s_i)$ are the residuals in the points of the measuring stations s_i ,
 $\lambda_1, \dots, \lambda_N$ are the weights estimated based on the variogram,
 N is the number of the stations used in the interpolation.

The variogram (as a measure of a spatial correlation) is estimated using a spherical function (with parameters nugget, sill, range). For details, see Horálek et al. (2007), Section 2.3.5 and Cressie (1993).

For $PM_{2.5}$, NO_x and BaP, both measurement data and the estimated data from the pseudo stations are used. For the PM_{10} and $PM_{2.5}$ indicators, prior to linear regression and interpolation, a logarithmic transformation is applied to measurement and modelling concentrations. After interpolation, a back-transformation is applied. For details, see De Smet et al. (2011) and Denby et al. (2008).

For the vegetation-related indicators (AOT40 for vegetation and forests, POD, and NO_x) only rural maps are constructed based on rural background stations, based on the assumption that no vegetation is located in urban areas. For the health-related indicators, the rural and urban background map layers (and for PM and NO_2 also urban traffic map layer) are constructed separately and then merged.

Merging of rural and urban background (and urban traffic) map layers

Health related indicator map layers are created for rural and urban background areas on a grid at resolution of 1 km (for PM, NO₂ and BaP) and 10 km (for ozone), and for urban traffic areas at 1 km (for PM and NO₂). The rural background map layer is based on rural background stations, the urban background map layer on urban and suburban background stations and the potential urban traffic map layer is based on urban and suburban traffic stations. The separate treatment of the map layers is based on the assumption that the estimated rural values are lower (PM₁₀, PM_{2.5}, NO₂ and BaP) or higher (ozone) than the estimated urban background map values. In the limited areas where this criterion does not hold, a joint urban/rural map layer (created using all background stations regardless of their type) is used, as long as its value lies in between the rural and urban background map value. Thus, the adjusted rural and urban background map layers are calculated and further used. For details, see De Smet et al. (2011).

Subsequently, the separate map layers are merged into one combined final map at 1 km resolution, according to

$$\begin{aligned}\hat{Z}_F(s_0) &= (1 - w_U(s_0)) \cdot \hat{Z}_R(s_0) + w_U(s_0)(1 - w_T(s_0)) \cdot \hat{Z}_{UB}(s_0) + w_T(s_0) \cdot \hat{Z}_{UT}(s_0) \\ &\quad \text{for PM}_{10}, \text{PM}_{2.5}, \text{ and NO}_2 \\ &= (1 - w_U(s_0)) \cdot \hat{Z}_R(s_0) + w_U(s_0) \cdot \hat{Z}_{UB}(s_0) \text{ for ozone and BaP} \quad (\text{A1.5})\end{aligned}$$

where $\hat{Z}_F(s_0)$ is the resulting estimated concentration value in a grid cell s_0 for the final map,
 $\hat{Z}_R(s_0)$ is the estimated value in a grid cell s_0 for the rural background map layer,
 $\hat{Z}_{UB}(s_0)$ is the estimated value in a grid cell s_0 for the urban background map layer,
 $\hat{Z}_{UT}(s_0)$ is the estimated value in a grid cell s_0 for the urban traffic map layer,
 $w_U(s_0)$ is the weight representing the ratio of the urban character of the a grid cell s_0 ,
 $w_T(s_0)$ is the weight representing the ratio of areas exposed to traffic air quality in a grid cell s_0 .

The weight $w_U(s_0)$ is based on the population density grid, while $w_T(s_0)$ is based on the buffers around the roads. For further details, see Horálek et al. (2017b).

In all calculations and map presentations the EEA standard projection ETRS89-LAEA5210 (also known as ETRS89 / LAEA Europe, see www.epsg-registry.org) is used. The interpolation and mapping domain consists of the areas of all EEA member and cooperating countries, and other microstates, as far as they fall within the EEA map extent Map_2c (EEA, 2018). Due to the interpolation methodology, the interpolation and mapping domain also includes the area of the United Kingdom. However, although they have been calculated, the results for the United Kingdom are not presented in this report, after this country left the EU.

A1.2 Calculation of population and vegetation exposure

Population and vegetation exposure estimates are based on the interpolated concentration maps, population density data and land cover data.

Population exposure

Population exposure is calculated for individual countries (apart from BaP), for large regions, for EU-27 and for the whole mapping area. For ozone and BaP, it is calculated from the air quality maps and population density data, both at 1 km resolution. For each concentration class, the total population per country as well as the European-wide total is determined. For PM and NO₂, the population exposure is calculated separately for areas where the air quality is considered to be directly influenced by traffic and for the background (both rural and urban) areas. For each concentration class 'j', the percentage population per country as well as the European-wide total is determined according to:

$$P_j = \frac{\sum_{i=1}^N I_{Bij} (1 - w_U(i)w_T(i))p_i + \sum_{i=1}^N I_{Tij}w_U(i)w_T(i)p_i}{\sum_{i=1}^N p_i} \cdot 100 \quad (\text{A1.6})$$

where P_j is the percentage population living in areas of the j -th concentration class in either the country or in Europe as a whole,
 p_i is the population in the i -th grid cell,
 I_{Bij} is the Boolean 0-1 indicator showing whether the background air quality concentration (estimated by the combined rural/urban background map layer) in the i -th grid cell is within the j -th concentration class ($I_{Bij} = 1$), or not ($I_{Bij} = 0$),
 I_{Tij} is the Boolean 0-1 indicator showing whether the traffic air quality concentration in the i -th grid cell is within the j -th concentration class ($I_{Tij} = 1$), or not ($I_{Tij} = 0$),
 $w_U(s_0)$ is the weight representing ratio of the urban character of the a grid cell s_0 ,
 $w_T(s_0)$ is the weight representing the ratio of the urban character of the a grid cell s_0 ,
 $w_T(s_0)$ is the weight representing ratio of areas exposed to traffic air quality in a grid cell s_0 .
 N is the number of grid cells in the country, in the region or in the whole mapped area.

In addition, the exposure for individual countries, large regions, EU-27 and the whole area is expressed also as the population-weighted concentration, i.e. the average concentration weighted according to the population in a 1 km x 1 km grid cell:

$$\hat{c} = \frac{\sum_{i=1}^N c_i p_i}{\sum_{i=1}^N p_i} \quad (\text{A1.7})$$

where \hat{c} is the population-weighted average concentration in the country, large region, EU-27 or in the whole mapping area,
 p_i is the population in the i^{th} grid cell,
 c_i is the concentration in the i^{th} grid cell (based on the final merged map),
 N is the number of grid cells in the country or in Europe as a whole.

Vegetation exposure

Vegetation exposure for individual countries, large regions, EU-27 and for the total mapping area is calculated based on the air quality maps and land cover data, both in the 2 km resolution grid. For each concentration class, the total agricultural and forest area per country as well as European-wide is determined.

Next to this, per-country and European-wide exposure are expressed as the agricultural- and forest-weighted concentration, i.e. the average concentration weighted according to the agricultural and forest area in a 1 km x 1 km grid cell, similarly like in Eq. A1.7.

Estimation of trends

For detecting and estimating the trends in time series of annual values of population exposure, the non-parametric Mann-Kendall's test for testing the presence of the monotonic increasing or decreasing trend is used. Next to that, the non-parametric Sen's method for estimating the slope of a linear trend is executed. For details, see Gilbert (1987). The significance of the Mann-Kendal test is shown by the usual way, i.e. + for 0.1, * for 0.05, ** for 0.01, and *** for 0.001.

Geographical distribution of countries to large regions for use in the assessment

The population and vegetation exposure and population-, agricultural- and forest-weighted concentration is presented, apart from the individual countries, the EU-27 and the whole mapped area, also in five large European regions. For this purpose, the countries have been grouped into five large European regions as follows. See also Map A1.1.

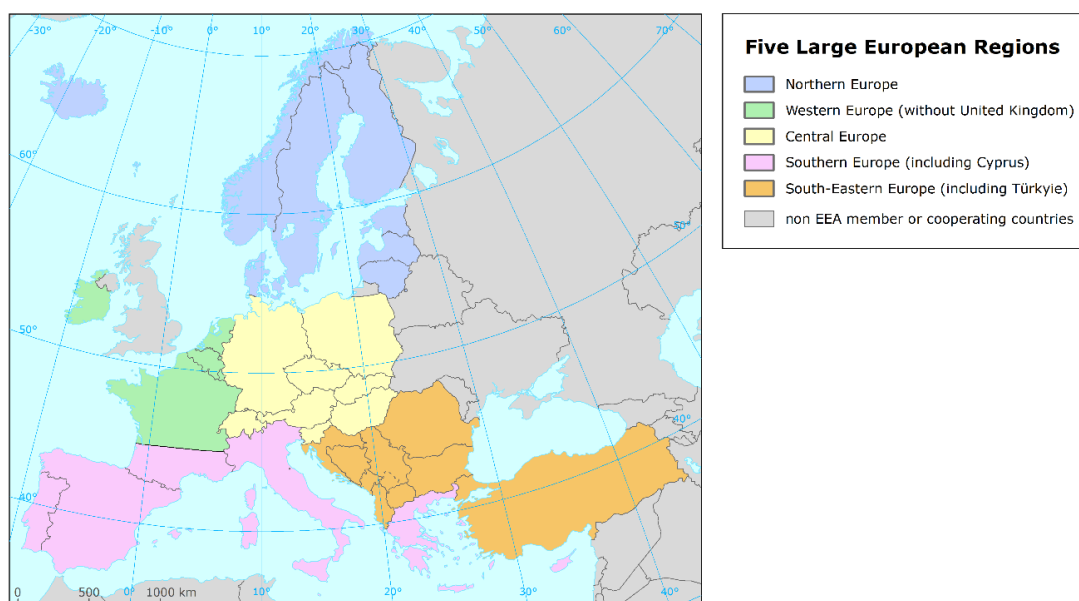
- 1) Northern Europe (N): Denmark (including Faroes), Estonia, Finland, Iceland, Latvia, Lithuania, Norway, Sweden;
- 2) Western Europe (without United Kingdom) (W): Belgium, France north of 45°, Ireland, Luxembourg, Netherlands;

3) Central Europe (C): Austria, Czechia, Germany, Hungary, Liechtenstein, Poland, Slovakia, Slovenia, Switzerland;

4) Southern Europe (S): Andorra, Cyprus, France south of 45°, Greece, Italy, Malta, Monaco, Portugal, San Marino, Spain;

5) South-eastern Europe (SE): Albania, Bosnia and Herzegovina, Bulgaria, Croatia, Montenegro, North Macedonia, Romania, Serbia including Kosovo under the UN Security Council Resolution 1244/99, Türkiye.

Map A1.1: Five large European regions



A1.3 Phytotoxic Ozone Dose above a threshold flux Y (POD_Y) calculation

The calculation of the phytotoxic ozone dose above a threshold Y (POD_Y) as described below follows the methodology described in the Manual for modelling and mapping critical loads & levels of the Long-Range Transboundary Air Pollution Convention (CLRTAP) in its most recent available revision (CLRTAP, 2017a), including some specifications presented in the Scientific background documents of this manual (CLRTAP, 2017b, 2020), as prepared by the International scientific Cooperative Programme on effects of air pollution on natural vegetation and crops of the Working Group on Effects of the CLRTAP (ICP Vegetation). The steps to be taken are presented in Table A1.1.

Table A1.1: Steps to calculate POD_Y of flux-based critical levels

1	Decide on the species and biogeographical region(s) to be included.
2	Obtain the ozone concentrations at the top of the canopy for the species or vegetation-specific accumulation period.
3	Calculate the hourly stomatal conductance of ozone (g_{sto}).
4	Model the hourly stomatal flux of ozone (F_{sto}).
5	Calculation of POD_Y from F_{sto} .

Source: CLRTAP, 2017a.

The cumulative stomatal ozone fluxes (F_{sto}) are calculated over the course of the growing season based on ambient ozone concentration and stomatal conductance (g_{sto}) to ozone. g_{sto} is calculated using a multiplicative stomatal conductance model proposed by Jarvis (1976) and modified by Emberson et al.

(2000) as a function of species-specific maximum g_{sto} (expressed on a single leaf-area basis), phenology, and prevailing environmental conditions (photosynthetic photon flux density (PPFD)), air temperature, vapour pressure deficit (VPD), and soil moisture.

Hourly averaged stomatal ozone fluxes (F_{sto}) in excess of a threshold Y (expressed in $\text{mmol/m}^2 \text{ PLA s}^{-1}$) are accumulated over a species or vegetation-specific accumulation period during daylight hours, in order to get the phytotoxic ozone dose above the threshold Y (POD_Y).

Crops

For the wheat as for other crop species, the Y value is taken equal to $6 \text{ nmol/m}^2 \text{ PLA s}^{-1}$. Although several POD indicators are proposed in CLRTAP (2017a), POD_6 is recommended for wheat, as the hourly averaged stomatal ozone fluxes above a value of 6 are more relevant for that crop. For potato and tomato, POD_6 is also recommended. Two POD_6 versions are available in CLRTAP (2017a): POD_6IAM (which is a simplified version recommended for Integrated Assessment Modelling) and POD_6SPEC (which is specific to a given specie). Here, POD_6SPEC was preferred and used, in agreement with Colette et al. (2018).

Obtaining the ozone concentrations at the top of the canopy for the species or vegetation-specific accumulation period

The ozone concentration at the top of the canopy (nmol/m^3) in the given hour H is calculated according to

$$c(z_1) = c(z_{m, O_3}) * \left[1 - \frac{R_a(z_{tgt}, z_{m, O_3})}{R_a(d+z_0, z_{m, O_3}) + R_b + R_{surf}} \right] \quad (\text{A1.8})$$

where $c(z_1)$ is ozone concentration at the top of the canopy,
 $c(z_{m, O_3})$ is the ozone concentration measured at the height z_m ,
 $R_a(x, y)$ is the aerodynamic resistance between the height of y and the height of x ,
 R_b is the resistance to ozone diffusion in the laminar sub-layer,
 R_{surf} is the overall resistance to ozone deposition to the underlying surfaces,

$$\text{while } R_a(z_{tgt}, z_{m, O_3}) = \frac{1}{k \cdot u^*} \left[\ln \left(\frac{z_{m, O_3} - d}{z_{tgt} - d} \right) - \Psi_H \left(\frac{z_{m, O_3} - d}{L} \right) + \Psi_H \left(\frac{z_{tgt} - d}{L} \right) \right] \quad (\text{A1.8a})$$

$$R_a(d + z_0, z_{m, O_3}) = \frac{1}{k \cdot u^*} \left[\ln \left(\frac{z_{m, O_3} - d}{z_0} \right) - \Psi_H \left(\frac{z_{m, O_3} - d}{L} \right) + \Psi_H \left(\frac{z_0}{L} \right) \right] \quad (\text{A1.8b})$$

$$R_b = \frac{2}{k \cdot u^*} \left(\frac{Sc}{Pr} \right)^{2/3} \quad (\text{A1.8c})$$

$$R_{surf} = \frac{1}{\frac{LAI}{R_{sto}} + \frac{SAI}{R_{ext}} + \frac{1}{R_{inc} + R_{soil}}} \quad (\text{A1.8d})$$

where k is the von Kármán constant (equal to 0.41),
 z_{tgt} is the top canopy height (the target height),
 z_{m, O_3} is the height of the available ozone measurement above the canopy,
 z_0 is the roughness length, usually assumed as 1/10 of the canopy height,
 L is the Obukhov length,
 d is the displacement height, usually assumed as 2/3 of the canopy height,
 u^* is the friction velocity,
 Sc is the Schmidt number for ozone (equal to 0.41),
 Pr is the Prandtl number of air (equal to 0.71),
 LAI is the projected leaf area in [m^2/m^2],
 SAI is the surface area of the canopy in [m^2/m^2],

⁽⁸⁾ PLA, or the projected leaf area, is the total area of the sides of the leaves that are projected towards the sun. PLA is different to the total leaf area, which accounts for both sides of the leaves.

$\psi_H(\dots) = \psi_H(\zeta)$ is the similarity function for heat with ζ as the argument ⁽⁹⁾,

according to

$$\begin{aligned} (\zeta) &= 2 && \text{when } \zeta < 0 \\ &= -5\zeta && \text{when } \zeta \geq 0 \end{aligned} \quad (\text{A1.8e})$$

with $x = (1 - 16 * \zeta)^{1/4}$ (A1.8f)

and R_{ext} is the resistance to cuticular deposition of ozone (equal to 2 500 s/m);
 R_{soil} is the soil resistance (equal to 200 s/m¹),

while $R_{sto} = 1/g_{sto}$ (A1.8g)

$R_{inc} = b.SAI.h / u^*$ (A1.8h)

where g_{sto} is the actual stomatal conductance,
 b is the empirical constant (equal to 14 m⁻¹),
 h is the height of the canopy.

Calculation of the hourly stomatal conductance of ozone (g_{sto})

The basis of the approach used for calculating phytotoxic ozone doses is the calculation of an instantaneous stomatal conductance g_{sto} in the given hour H, according to the equation

$$g_{sto} = g_{max} * [\min(f_{phen}, f_{O3})] * f_{light} * \max[f_{min}, (f_{temp} * f_{VPD} * f_{SW})] \quad (\text{A1.9})$$

where g_{sto} is the actual stomatal conductance in [mmol O₃ /m² PLA per second],
 g_{max} is the species-specific maximum stomatal conductance in [mmol O₃ /m² PLA per second], see Table A1.2,
 f_{phen} is the relative proportion function for the phenology for the different stage of growing,
 f_{O3} is the relative proportion function for the influence of ozone on stomatal flux by promoting premature senescence,
 f_{min} is the species-specific relative minimum stomatal conductance that occurs during daylight hours, see Table A1.2,
 $f_{temp}, f_{VPD}, f_{SW}, f_{light}$ are relative proportion functions for leaf stomata respond to temperature, air humidity, soil moisture and light.

Parameters $f_{phen}, f_{O3}, f_{light}, f_{temp}, f_{VPD}, f_{SW}$ and f_{min} are expressed as relative proportion functions, taking values between 0 and 1 as a proportion of g_{max} . These functions allow taking into account irradiance (f_{light}), temperature (f_{temp}), water vapour deficit at leaves level (f_{vpd}), soil moisture (f_{sw}), phenology for the different stage of growing (f_{phen}) and the influence of ozone on stomatal flux by promoting premature senescence (f_{O3}). f_{min} is the minimum relative value of stomatal conductance during the daylight.

The parameter f_{phen} is calculated based on the accumulation of thermal time over the growing season of the crop being considered (Colette et al., 2018), according to CLRTAP (2017a). For wheat and potato, the accumulation period is defined for each year using the effective temperature sum (ETS) in °C for days in excess of 0 °C, while for tomato for days in excess of 10 °C.

For wheat, the total accumulation period during which wheat is sensitive to ozone exposure is 200 °C days and 300 °C days before mid-anthesis (mid-point in flowering) to 700 °C days to 550 °C days after mid-anthesis for Atlantic, Boreal and Continental regions and Mediterranean region, respectively. The timing of mid-anthesis is estimated by starting at the first date after 1 January (or just 1 January) when the temperature exceeds 0 °C. The mean daily temperature is then accumulated (temperature sum), and mid-anthesis is estimated to be a temperature sum of 1075 °C days for Atlantic, Boreal and

⁽⁹⁾ For more details see CLRTAP (2017b).

Continental regions and 1250 °C days for Mediterranean region, which in general corresponds to bread wheat.

For potato, the accumulation period stands between 330 °C days before the tuber initiation date and 800 °C days after this date. The tuber initiation date is considered to be homogeneous throughout Europe. The reasons for its simplification are a) heterogeneous climatic conditions in the European countries naturally lead to different time of potato planting (Pedersen et al., 2005) followed by different time of the tuber initiation and b) lack of detailed local data availability for modelling and mapping.

As discussed ⁽¹⁰⁾ with the French national Chamber of agriculture (APCA, <http://chambres-agriculture.fr>), the tuber initiation starts 15 days after the transplantation in the field, which occurs in May. Therefore, the fixed date for the tuber initiation was set to June 1st.

For tomato, the accumulation period is from 250 °C days to 1500 °C days after transplantation in the field over a base temperature of 10 °C. The timing of the transplantation is set on the date June 1st.

The parameter f_{phen} is calculated according to following equations:

in the case of wheat:

$$\begin{aligned}
 f_{phen} &= 1 && \text{when } (f_{phen_2_ETS} + f_{phen_1_ETS}) \leq ETS \leq (f_{phen_2_ETS} + f_{phen_3_ETS}) \\
 &= 1 - \left(\frac{f_{phen_a}}{f_{phen_4_ETS} - f_{phen_3_ETS}} \right) * (ETS - f_{phen_3_ETS}) \\
 &&& \text{when } (f_{phen_2_ETS} + f_{phen_3_ETS}) < ETS \leq (f_{phen_2_ETS} + f_{phen_4_ETS}) \\
 &= f_{phen_e} - \left(\frac{f_{phen_e}}{f_{phen_5_ETS} - f_{phen_4_ETS}} \right) * (ETS - f_{phen_4_ETS}) \\
 &&& \text{when } (f_{phen_2_ETS} + f_{phen_4_ETS}) < ETS \leq f_{phen_5_ETS}
 \end{aligned} \tag{A1.9a}$$

in the case of potato (formulated based on CLRTAP, 2017b):

$$\begin{aligned}
 f_{phen} &= 1 - \left(\frac{1 - f_{phen_a}}{f_{phen_1_ETS}} \right) * ETS && \text{when } f_{phen_1_ETS} \leq ETS < 0 \\
 &= 1 - \left(\frac{1 - f_{phen_e}}{f_{phen_2_ETS}} \right) * ETS && \text{when } 0 < ETS \leq f_{phen_2_ETS}
 \end{aligned} \tag{A1.9b}$$

in the case of tomato (formulated based on CLRTAP, 2017b):

$$f_{phen} = \frac{ETS - f_{phen_2_ETS}}{A_{start_ETS} - f_{phen_2_ETS}} \quad \text{when } A_{start_ETS} \leq ETS < A_{end_ETS} \tag{A1.9c}$$

where ETS is the effective temperature sum in °C days using a base temperature of 0 °C for wheat and potato and a base temperature of 10 °C for tomato (see Table A1.2); for wheat, ETS is set to 0 °C days at mid-anthesis day. Then A_{start_ETS} will be at 200 °C days before mid-anthesis, and A_{end_ETS} will be at 700 °C days after mid-anthesis over a base temperature of 0 °C; for potato, ETS is set to 0 °C days at tuber initiation day. Then A_{start_ETS} will be at 330 °C days before tuber initiation and A_{end_ETS} at 800 °C days after tuber initiation over a base temperature of 0 °C; for tomato, ETS is set to 0 °C days at transplantation day in the field. Then A_{start_ETS} will be at 250 °C days after transplantation in the field and A_{end_ETS} at 1500 °C days after transplantation in the field over a base temperature of 10 °C,

⁽¹⁰⁾ There is a lack of information on a date of potato tuber initiation in Europe. It should ideally rely on existing models based on agricultural practices, local climatology, ground properties, and location. INERIS, while developing the POD script, relied on contents of discussions with the French National Chamber of Agriculture (consultation with APCA, March 2018; Deumier and Hannon, 2010). Based on the information given that the tuber initiation starts 15 days after the transplantation in the field, which occurs in May in France, a fixed date of June 1st has been chosen for France and applied also for the rest of Europe. This date should be revised according to the availability of more accurate information on potato plantations in Europe.

f_{phen_a} , f_{phen_e} is the phenology function, which consists of terms describing rate changes of g_{max} expressed as fractions (see Table A1.2),
 $f_{phen_1_ETS}$, $f_{phen_2_ETS}$, $f_{phen_3_ETS}$, $f_{phen_4_ETS}$, $f_{phen_5_ETS}$ are °C days (see Table A1.2; $f_{phen_1_ETS}$ and $f_{phen_5_ETS}$ define period crops to be sensitive to ozone exposure),
 A_{start_ETS} and A_{end_ETS} are the effective temperature sums (counted from the day of the mid-anthesis for wheat, from the day of the tuber initiation for potato and from the day of the transplantation in the field for tomato) above a base temperature of 0 °C for wheat and potato and 10 °C for tomato at the start and end of the O_3 accumulation period respectively; see Table A1.2.

The parameter f_{O_3} in the case of wheat is calculated according to equation

$$f_{O_3} = [(1+(POD_0/14)^8)^{-1}] \quad (A1.9d)$$

while $POD_0 = \sum_{n=A_{start}}^{H-1} F_{sto}(n) \cdot \frac{3600}{10^6}$ (A1.9e)

where POD_0 is the ozone flux already accumulated since the beginning of the vegetation period A_{start} up to the last hour $H-1$,
 $F_{sto}(n)$ is the hourly ozone flux in the hour n , calculated in the previous steps based on Equation A1.10, while $F_{sto}(A_{start})$ is equal to 0.

The parameter (ozone function) f_{O_3} in the case of potato is calculated according to equation

$$f_{O_3} = [(1+(AOT0/40)^5)^{-1}] \quad (A1.9f)$$

where $AOT0$ is accumulated ozone concentration from the start of the vegetation period A_{start} up to the last hour $H-1$.

The parameter (ozone function) f_{O_3} in the case of tomato is not determined.

The parameter f_{light} is calculated according to

$$f_{light} = 1 - \text{EXP}[-light_a * \text{PPFD}] \quad (A1.9g)$$

while $\text{PPFD} = \text{SSRD} * 0.5 * 4.5$ (A1.9h)

where PPFD represents the photosynthetic photon flux density [$\mu\text{mol}/\text{m}^2$ per second],
 $light_a$ is a light parameter (see Table A1.2),
 SSRD represents the surface net solar radiation in [W/m^2].

The parameter f_{temp} is calculated according to:

$$f_{temp} = \begin{cases} f_{min}, & [(T - T_{min}) / (T_{opt} - T_{min})] * [(T_{max} - T) / (T_{max} - T_{opt})]^{bt} \text{ when } T_{min} < T < T_{max} \\ f_{min}, & \text{when } T_{min} > T > T_{max} \end{cases} \quad (A1.9i)$$

while $bt = (T_{max} - T_{opt}) / (T_{opt} - T_{min})$ (A1.9j)

where T_{min} , T_{max} and T_{opt} are minimum, maximum and optimum temperatures determining leaf stomata opening (see Table A1.2)

The parameter f_{VPD} is calculated according to:

$$f_{VPD} = \min\{1, \max\{f_{min}, [(1-f_{min}) * (VPD_{min} - VPD) / (VPD_{min} - VPD_{max})] + f_{min}\}\} \quad (A1.9k)$$

while $VPD = e_s(T_a) * (1-h_r)$ (A1.9l)

$$e_s(T_a) = a \exp[bT_a / (T_a + c)] \quad (A1.9m)$$

where VPD_{min} is the minimum vapour pressure deficit determining leaf stomata opening,
 VPD_{max} is the maximum vapour pressure deficit determining leaf stomata opening,
 T_a is the air temperature [°C],
 h_r is the relative humidity [%]/100,
 $e_s(T_a)$ is the potential (saturation) water vapour pressure,

a, b, c are the empirical constants ($a = 0.611$ kPa, $b = 17.502$, $c = 240.97$ °C).

The ΣVPD (i.e. the function describing stomatal re-opening in the afternoon) is taken into account for maps $POD_{\gamma}SPEC$ for wheat and potato in 2021. ΣVPD (kPa) should be calculated for daylight hours until dawn of the next day. If $\Sigma VPD \geq \Sigma VPD_{crit}$, g_{sto} calculated using Equation A1.9 is valid if smaller or equal to g_{sto} of the preceding hour. If g_{sto} is larger than g_{sto} of the preceding hour, given that ΣVPD is larger than or equal to ΣVPD_{crit} , it is replaced by the g_{sto} of the preceding hour.

Table A1.2: Parametrisation for $POD_{\gamma}SPEC$ for wheat flag leaves and the upper-canopy sunlit leaves of potato and tomato, for different biogeographical regions

Parameter	Units	(Bread) Wheat		Potato	Tomato
		Atlantic, Boreal, Continental (Pannonia, Steppic)	Mediterranean	Atlantic, Boreal, Continental (Mediterranean Pannonia, Steppic)	Mediterranean
g_{max}	mmol O ₃ /m ² PLA per second	500	430	750	330
f_{min}	fraction	0.01	0.01	0.01	0.06
light_a	-	0.0105	0.0105	0.005	0.0125
T_{min}	°C	12	12	13	18
T_{opt}	°C	26	28	28	28
T_{max}	°C	40	39	39	37
VPD_{max}	kPa	1.2	3.2	2.1	1
VPD_{min}	kPa	3.2	4.6	3.5	4
ΣVPD_{crit}	kPa	8	16	10	-
f_{O_3}	POD0 mmol O ₃ /m ² PLA per second	14	-	-	-
f_{O_3}	AOT0, ppmh	-	-	40	-
f_{O_3}	exponent	8	-	5	-
Astart_ETS	°C day	-	-	-	250
Aend_ETS	°C day	-	-	-	1500
Leaf dimension	cm	2	2	4	3
Canopy height	m	1	0.75	1	2
f_{phen_a}	fraction	0.3	0.5	0.4	1
f_{phen_b}	fraction	-	-	-	-
f_{phen_c}	fraction	-	-	-	-
f_{phen_d}	fraction	-	-	-	-
f_{phen_e}	fraction	0.7	0.5	0.2	0.0
$f_{phen_1_ETS}$	°C day	-200	-300	-330	0
$f_{phen_2_ETS}$	°C day	0	0	800	2770
$f_{phen_3_ETS}$	°C day	100	70	-	-
$f_{phen_4_ETS}$	°C day	525	312	-	-
$f_{phen_5_ETS}$	°C day	700	550	-	-
mid-anthesis	°C day	1075	1250	-	-

Source: CLRTAP, 2017a; González-Fernández et al., 2013; González-Fernández (personal communication, May 2021).

The parameter f_{SW} is replaced by f_{SMI} (where SMI represents Soil Moisture Index with maximum at field capacity), taking values between 0 and 1 as a proportion of g_{max} (with 0 for soil moisture at and below wilting point), following the parameterization given in Simpson et al. (2012), similar to the plant available water (PAW) parameterization f_{PAW} as defined for wheat in CLRTAP (2017a). The basic equation used for f_{SW} resp. f_{SMI} is:

$$\begin{aligned}
 f_{SMI} &= 0 && \text{for } SMI \leq 0 \\
 &= \frac{SMI}{PAW_t} && \text{for } 0 < SMI \leq PAW_t \\
 &= 1 && \text{for } SMI > PAW_t
 \end{aligned}
 \tag{A1.9n}$$

while
$$SMI = \frac{SWLL - PWP}{FC - PWP} \quad (A1.9o)$$

where PAW_t is the threshold amount of water in the soil available to the plants, above which stomatal conductance is at a maximum, set to 0.5,
 $SWLL$ is the soil moisture in [m^3/m^3],
 PWP is the permanent wilting point in [cm^3/cm^3],
 FC is the field capacity in [cm^3/cm^3].

The Soil Moisture Index using the EMEP methodology as described in Simpson et al. (2012) and CLRTAP (2020) is used. It is computed using the soil moisture variable available from a meteorological model, which represents the water content in m^3 of water per m^3 of ground [m^3/m^3] in a specific ground level, in dependence on the available dataset. For soil moisture, the ECWMF's ERA5-Land variable Volume of water in soil layer 3 (i.e. 28-100 cm) has been used, see Section 3.3. The level of soil layer was chosen based on recommendation of Haberle and Svoboda (2015). The soil moisture is quite a sensitive parameter in the calculation of the POD. Next to the soil moisture, the soil moisture index also takes into account the permanent wilting point and the field capacity; they are taken from JRC soil database (JRC, 2016), see Annex 2, Section A2.3.

No limitation of stomatal conductance due to soil moisture can be assumed for tomato, since it is an irrigated horticultural crop. Thus, f_{SMI} for this crop could be established to $f_{SMI} = 1$ over the whole range of SMI values to remove limitation due to soil moisture deficit.

Modelling the hourly stomatal flux of ozone (F_{sto})

Once the hourly stomatal conductance of ozone (g_{sto}) and all relevant variables are computed, the stomatal flux of ozone (F_{sto}) can be calculated, based on the assumption that the concentration of ozone at the top of the canopy represents a reasonable estimate of the concentration at the upper surface of the laminar layer for a sunlit upper canopy leaf. F_{sto} is calculated according to the CLRTAP (ICP Vegetation) methodology, thus the fraction of the ozone taken up by the stomata is given using a combination of the stomatal conductance, the external leaf, or cuticular, resistance and the leaf surface resistance. The hourly stomatal flux in the given hour H is calculated according to

$$F_{sto} = c(z_1) * g_{sto} * \frac{r_c}{r_b + r_c} \quad (A1.10)$$

where F_{sto} is the hourly stomatal flux of ozone in [$nmol/m^2$ PLA per second]
 $c(z_1)$ is the concentration of ozone at canopy top in [$nmol/m^3$]
 r_b is the quasi-laminar resistance in [s/m]
 r_c is the leaf surface resistance in [s/m]
 g_{sto} is the actual stomatal conductance in [m/s],

while
$$r_c = 1/(g_{sto} + g_{ext}) \quad (A1.10a)$$

$$r_b = 1.3 * 150 * \sqrt{\frac{L}{u(z_1)}} \quad (A1.10b)$$

where g_{ext} is the external leaf, or cuticular, resistance in [m/s], equal to 1/2500 m/s
 $u(z_1)$ is the wind speed at height z_1 (z_1 is the canopy top)
 L is the cross-wind leaf dimension (2 cm, see Table A1.2)

while
$$u_{(z1)} = \frac{u^*}{k} * \ln\left(\frac{z_1 - d}{z_0}\right) \quad (A1.10c)$$

where k is the von Kármán constant (equal to 0.41)
 d is the displacement height usually assumed as 2/3 of the canopy height,
 z_1 is the top of the canopy
 z_0 is the roughness length usually assumed as 1/10 of the canopy height
 u^* is the friction velocity.

Box A1.1 shows the conversion of stomatal conductance and ozone concentration to units demanded for POD_Y calculation.

Box A1.1: Conversion of stomatal conductance g_{sto} and ozone concentration to units demanded for POD_Y calculation

Stomatal conductance g_{sto} has to be converted from units $mmol/m^2$ per second to units m/s (since all the resistances are expressed in the unit of s/m). At standard temperature ($20\text{ }^\circ\text{C}$) and air pressure ($1.013 \times 10^5\text{ Pa}$), the conversion is made by dividing the conductance in $mmol/m^2$ per second by 41 000 to give conductance in m/s .

To convert the **ozone concentration (C)** at canopy height from $\mu\text{g}/m^3$ resp. ppb to $nmol/m$, the following equation should be used:

$$C [nmol \cdot m^{-3}] = C [ppb] * P/(R \cdot T) = C [\mu\text{g}/m^3] / 2 * P/(R \cdot T) \quad (A1.11)$$

where P is the atmospheric pressure in Pa,
 R is the universal gas constant of $8.31447\text{ J/mol per Kelvin}$
 T is the air temperature in Kelvin.

At standard temperature ($20\text{ }^\circ\text{C}$) and air pressure ($1.013 \times 10^5\text{ Pa}$), the concentration in ppb should be multiplied by 41.56 to calculate the concentration in $nmol/m^3$.

Source: CLRTAP, 2017a

In the routine used in this report (Section 2.3), an alternative conversion of the ozone concentrations from $\mu\text{g}/m^3$ resp. ppb to $nmol/m^3$ is done, using the air density instead of the atmospheric pressure, according to

$$C [nmol \cdot m^{-3}] = C [ppb] * \rho / N_a * 10^6 = C [\mu\text{g}/m^3] / 2 * \rho / N_a * 10^6 \quad (A1.12)$$

where ρ is the air density showing the number of the molecules in cm^{-3} ,
 N_a is the Avogadro constant, which is equal to $6.022 \cdot 10^{23}\text{ mol}^{-1}$.

Calculation of POD_Y from F_{sto}

Hourly averaged stomatal ozone fluxes (F_{sto}) in excess of a Y threshold are accumulated over a species or vegetation-specific accumulation period using the following equation:

$$POD_Y = \sum_n (F_{sto}(n) - Y) \cdot \frac{3600}{10^6} \quad (A1.13)$$

while Y (for wheat, potato or tomato) = $6\text{ nmol}/m^2\text{ PLA per second}$

where POD_Y is the phytotoxic ozone dose related to the threshold Y , in $[mmol/m^2\text{ PLA}]$,
 $F_{sto}(n)$ is the hourly ozone flux in the hour n of the accumulation period.

The value Y (in $[nmol/m^2\text{ PLA s}^{-1}]$) is subtracted from each hourly averaged F_{sto} (in $[nmol/m^2\text{ PLA s}^{-1}]$) value and the F_{sto} (after the subtracting of Y) is accumulated only when $F_{sto} > Y$, during daylight hours (when global radiation is more than $50\text{ W}/m^2$). The value is then converted to hourly fluxes by multiplying by 3 600 and to $mmol$ by dividing by 10^6 to get the stomatal ozone flux in $mmol/m^2\text{ PLA}$.

Trees

The POD maps for selected trees, i.e. beech (*F. sylvatica*) and spruce (*P. abies*), are created with calculated hourly POD values which are based on hourly O_3 concentrations, hourly meteorological parameters such as temperature, vapour pressure deficit, solar radiation and soil hydraulic property data. The hourly O_3 concentrations are calculated by combining the monitoring data from rural background stations, chemical transport modelling data and other supplementary data (Horálek et al., 2023).

The calculation of the phytotoxic O₃ dose above a threshold Y (POD₁) as described in Vlasáková et al. (2023) follows precisely the methodology described in the Manual for modelling and mapping critical loads & levels of the CLRTAP in its most recent available revision (CLRTAP, 2017a), including some specifications presented in the Scientific Background Documents of this manual (CLRTAP, 2017b, 2020), as prepared by the International scientific Cooperative Programme on effects of air pollution on natural vegetation and crops of the Working Group on Effects of the CLRTAP (ICP Vegetation).

A1.4 Methods for uncertainty analysis

The uncertainty estimation of the European map is based on leave-one-out cross-validation. This cross-validation method computes the quality of the spatial interpolation for each point of measurement (i.e. monitoring station) from all available information except from the point in question, i.e. it withholds one data point and then makes a prediction at the spatial location of that point. This procedure is repeated for all measurement points in the available set. The predicted and measurement values at these points are plotted in the form of a scatter plot. With help of statistical indicators (see below), the quality of the predictions is demonstrated objectively. The advantage of the nature of this cross-validation technique is that it enables evaluation of the quality of the predicted values at locations without measurements, as long as they are within the area covered by the measurements.

In addition, a simple comparison is made between the point measurement data and the estimated values of the 1 km x1 km grid cells (for PM and NO₂) or the 10 km x10 km grid cells (for ozone) for the separate rural and urban background (and urban traffic, where relevant) map layers and the 1 km x 1 km grid cells for the final combined maps, for the health-related indicators, and the 2 x 2 km grid cells in the case of AOT40 and NO_x. Note that the grid cell value is the mean estimated value of this grid cell area. The estimated value within a grid cell will only approximate the predicted value(s) at the station(s) lying within that cell. This additional analysis has not been performed for BaP.

Cross-validation

The results of cross-validation are described by the statistical indicators and scatter plots. The main indicator used is root mean squared error (RMSE) and the additional ones are relative RMSE (RRMSE), which is expressed in relative terms (by relating the RMSE to the mean of the air pollution indicator value for all stations), and bias (mean prediction error, MPE):

$$RMSE = \sqrt{\frac{1}{N} \sum_{i=1}^N (\hat{Z}(s_i) - Z(s_i))^2} \quad (A1.14)$$

$$RRMSE = \frac{RMSE}{\bar{Z}} \cdot 100 \quad (A1.15)$$

$$bias(MPE) = \frac{1}{N} \sum_{i=1}^N (\hat{Z}(s_i) - Z(s_i)) \quad (A1.16)$$

where $\hat{Z}(s_i)$ is the air quality indicator value derived from the measured concentration at the i^{th} point, $i = 1, \dots, N$,
 $Z(s_i)$ is the air quality estimated indicator value at the i^{th} point using other information, without the indicator value derived from the measured concentration at the i^{th} point,
 $RRMSE$ is the relative RMSE, expressed in percent,
 \bar{Z} is the arithmetic average of the indicator values $Z(s_1), \dots, Z(s_N)$, as derived from measurement concentrations at the stations $i = 1, \dots, N$,
 N is the number of the measuring points.

Other indicators are R^2 and the regression equation ($y = a.x + c$) parameters slope (a) and intercept (c), following from the scatter plot between the predicted (using cross-validation) and the observed concentrations. RMSE should be as small as possible, bias (MPE) should be as close to zero as possible, R^2 should be as close to 1 as possible, slope a should be as close to 1 as possible, and intercept c should be as close to zero as possible (in the regression equation $y = a.x + c$).

In the cross-validation of PM_{2.5}, NO_x and BaP, only stations with PM_{2.5}, NO_x and BaP measurement data, respectively, are used (not the pseudo PM_{2.5}, NO_x and BaP stations, see Annex 1 Section A1.1).

Comparison of the point measurement and interpolated grid values

The comparison of point measurement and predicted grid values is described by the linear regression equation and its parameters and statistical values. The comparison is executed separately for rural and urban background (and urban traffic, where relevant) map layers and for the final combined map. In the case of PM_{2.5} and NO_x, only the stations with actual PM_{2.5} and NO_x measurement data are used (not the pseudo PM_{2.5} and NO_x stations). This analysis is done for PM, ozone, NO₂ and NO_x, not for BaP.

The point observation – point cross-validation prediction analysis (Annex 3, sections “Uncertainty estimated by cross-validation”) describes interpolation performance at point locations when there is no observation (as it follows the leave-one-out approach). In this case, the smoothing effect of the interpolation is most prevalent.

The point observation – grid prediction approach indicates performance of the value for the grid cell (either in 1 km, 2 km or 10 km resolution) with respect to the observations that are located within that cell. As such, some variability is due to smoothing but it also includes smoothing due to spatial averaging into the grid cells. As such, the point-grid validation approach tells us how well our interpolated and aggregated grid values approximate the measurements at the actual station (point) locations. Whereas the point-point approach tells us how well our interpolated values estimate the indicator at a point where there is no actual measurement at that location, under the constraint that the point lies within the area covered by measurements.

Annex 2

Input data

The types of input data in this paper are similar as in Horálek et al. (2023), apart from the modelling data: instead of the EMEP model results, the CHIMERE model output has been used for BaP mapping, see Section A2.2. The air quality, modelling, satellite and meteorological data as used in Horálek et al. (2023) has been updated for 2021. For readability of this paper, the list of the input data is reproduced here. The key data is the air quality measurements at the monitoring stations extracted from the Air Quality e-Reporting database EEA (2023a), including geographical coordinates (*latitude, longitude*).

The supplementary data cover the whole mapping domain and are converted into the EEA reference projection ETRS89-LAEA5210 on a 1 km grid resolution (for health-related indicators apart from ozone) resp. a 10 km grid resolution (ozone). The data for the maps of vegetation related indicators (particularly AOT40) were converted – like in the previous reports (Horálek et al., 2023, and references cited therein) – into a 2 km resolution to allow accurate land cover exposure estimates to be prepared for use in the EEA indicator on ecosystem exposure to ozone (EEA, 2023b).

A2.1 Air quality monitoring data

Air quality station monitoring data for the relevant year as extracted from the official EEA Air Quality e-Reporting database, EEA (2023a) in March 2023 has been used. This data set has been supplemented with British stations from the Defra (2023) database ⁽¹¹⁾ and with several EMEP rural stations from the EBAS (NILU, 2023) database not reported to the Air Quality e-Reporting database. Specifically, additional 6 stations for PM₁₀, 4 for PM_{2.5}, 6 for NO₂ and 3 NO_x from the EBAS database and additional 77 British stations for PM₁₀, 69 for PM_{2.5}, 62 for ozone, 133 for NO₂, 11 for NO_x and 25 for BaP from the data archive Defra (2023) have been added, for mapping purposes.

The following pollutants and aggregations are considered:

PM ₁₀	– annual average [$\mu\text{g}/\text{m}^3$], year 2021
	– 90.4 percentile of the daily average values [$\mu\text{g}/\text{m}^3$], year 2021
PM _{2.5}	– annual average [$\mu\text{g}/\text{m}^3$], year 2021
Ozone	– 93.2 percentile of the maximum daily 8-hour average values [$\mu\text{g}/\text{m}^3$], year 2021
	– SOMO35 [$\mu\text{g}/\text{m}^3\cdot\text{day}$], year 2021
	– SOMO10 [$\mu\text{g}/\text{m}^3\cdot\text{day}$], year 2021
	– AOT40 for vegetation [$\mu\text{g}/\text{m}^3\cdot\text{hour}$], year 2021
	– AOT40 for forests [$\mu\text{g}/\text{m}^3\cdot\text{hour}$], year 2021
	– hourly values [$\mu\text{g}/\text{m}^3$], all hours of the year 2021 (for the purpose of POD ₆ mapping)
NO ₂	– annual average [$\mu\text{g}/\text{m}^3$], year 2021
NO _x	– annual average [$\mu\text{g}/\text{m}^3$], year 2021
NO	– annual average [$\mu\text{g}/\text{m}^3$], year 2021 (for the purposes of NO _x mapping only)
BaP	– annual average [ng/m^3], year 2021

The exact values of percentiles are actually 90.41 in the case of PM₁₀ daily means and 93.15 in the case of ozone maximum daily 8-hour means.

For a considerable number of stations NO_x is measured, but it is not reported as such but separately as NO and NO₂. For these stations reporting NO and NO₂ separately, the NO_x concentrations were derived according to the equation

⁽¹¹⁾ The United Kingdom exited the European Union in January 2020 and does not report air quality data to the AQ e-reporting database. Nevertheless, in order to enable the interpolation across the whole mapping domain, the publicly available British data from the Defra database have also been used in the analysis.

$$NO_x = NO_2 + \frac{46}{30} \cdot NO \quad (A2.1)$$

In this equation, all components are expressed in $\mu\text{g}/\text{m}^3$, with a molecular mass for NO of 30 g/mol and for NO_2 of 46 g/mol.

SOMO35 is the annual sum of the differences between maximum daily 8-hour concentrations above $70 \mu\text{g}/\text{m}^3$ (i.e. 35 ppb) and $70 \mu\text{g}/\text{m}^3$. SOMO10 is the annual sum of the differences between maximum daily 8-hour means above $20 \mu\text{g}/\text{m}^3$ (i.e. 10 ppb) and $20 \mu\text{g}/\text{m}^3$. AOT40 is the sum of the differences between hourly concentrations greater than $80 \mu\text{g}/\text{m}^3$ (i.e. 40 ppb) and $80 \mu\text{g}/\text{m}^3$, using only observations between 08:00 and 20:00 CET, calculated over the three months from May to July for AOT40 for vegetation and over the six months from April to September for AOT40 for forests.

Only the stations with annual data coverage of at least 75 percent are used. In the case of SOMO35, SOMO10 and AOT40 indicators, a correction for the missing data is applied according to the equation

$$I_{corr} = I \cdot \frac{N_{max}}{N} \quad (A2.2)$$

where I_{corr} is the corrected indicator (SOMO35, SOMO10 or AOT40 for vegetation or for forests),
 I is the value of the given indicator without any correction,
 N is the number of the available daily resp. hourly data in a year for the given station,
 N_{max} is the maximum possible number of the days or hours applicable for the indicator.

For the indicators relevant to human health (i.e. for all PM_{10} and $\text{PM}_{2.5}$ indicators, ozone indicators 93.2 percentile of maximum daily 8-hour means, SOMO35 and SOMO10, and NO_2 and BaP annual averages), data from stations classified as *background* (for all the three types of area, *rural*, *urban* and *suburban*) are considered; for PM_{10} and $\text{PM}_{2.5}$ and NO_2 , also *urban* and *suburban traffic* stations are considered. (Throughout the paper, the urban and suburban stations are handled together). *Industrial* stations are not considered, as they represent local concentration levels that cannot be easily generalized for the whole map. For the indicators relevant to vegetation damage (i.e. for ozone AOT40 and POD_6 parameters and NO_x annual average), only *rural background* stations are considered; the relevant maps are constructed (and applicable) for rural areas only. In the case of existing data (with sufficient annual time coverage) from two or more different measurement devices in the same station location, the average of these data is used.

The stations from French overseas areas (departments), Svalbard, Azores, Madeira and Canary Islands were excluded. These areas outside the EEA map extent Map_2c (EEA, 2018) were excluded from the interpolation and mapping domain, as the interpolation should be performed across a generally compact territory.

Table A2.1 shows the number of the measurement stations (not pseudo stations) selected for the individual pollutants and their respective indicators.

Table A2.1: Number of stations selected for each pollutant indicator and area type, 2021

Station type	PM ₁₀		PM _{2.5}		Ozone			NO ₂	NO _x	BaP
	Ann. avg.	90.4 perc.	Ann. avg.	Health related	AOT40 for veg.	AOT40 for for.	POD _x	Ann. avg.	Ann. avg.	Ann. avg.
Rural background	414	412	253	563	567	571	595	492	417	110
Urban/suburb. backgr.	1591	1585	976	1273	-	-	-	1477	-	481
Urban/suburb. traffic	814	812	464	-	-	-	-	1241	-	-

For the $\text{PM}_{2.5}$ mapping, in addition to the $\text{PM}_{2.5}$ stations, 181 rural background, 614 urban/suburban background and 376 urban/suburban traffic PM_{10} stations (at locations without $\text{PM}_{2.5}$ measurement) have been also used for the purpose of calculating the pseudo $\text{PM}_{2.5}$ station data.

In the case of NO_x, 369 stations with NO_x reported data have been used, while for 48 stations NO_x values are calculated from reported NO₂ and NO data using Eq. A2.1. Next to this, for the NO_x mapping 76 additional rural background NO₂ stations (at locations without NO_x measurement) were also used for the purpose of calculating the pseudo NO_x station data.

For the BaP mapping, in addition to the BaP stations, 63 rural and 63 urban background pseudo BaP station data calculated based on the PM_{2.5} measurements have also been used.

A2.2 Chemical transport modelling outputs

In the previous years (up to the maps for 2019), EMEP MSC-W (formerly called Unified EMEP) model was used, specifically its model results for year Y based on meteorology for year Y and emissions for year Y-1. However, the EMEP model results for 2021 based on the emissions for 2020 (as well as earlier the model results for 2020 based on the emissions for 2019) were not prepared by the EMEP modelling team. The reason was that the emissions for 2020 were supposed not to be a good approximation of the 2021 emissions, as the year 2020 was a special year due to the COVID-19 situation.

Instead of the EMEP model results, the CAMS Ensemble Forecast model output has been used for all pollutants apart from the BaP, in agreement with Horálek et al. (2021), which recommended this modelling product as an alternative to the EMEP model. The CAMS Ensemble Forecast model output, as provided by the Copernicus Atmosphere Monitoring Service (CAMS) at a regional scale over Europe, consists of an ensemble of involved air quality models run operationally. (In 2021, the number of the involved models was nine.) All models use the same CAMS-REG anthropogenic emissions and current meteorology from the operational ECMWF IFS forecast. The models provide (together with other products) a 96-hour forecast made available at 08:00 UTC on the day of the forecast. The forecast data product is available on an hourly time resolution and at a spatial resolution of 0.1° x 0.1°, which corresponds roughly to 5-10 km x 10 km. Each model forecast is combined into the Ensemble Forecast by taking the median of all modelling results. For further details see ECMWF (2023).

In this report, the CAMS Ensemble Forecast data (for the lead hour 0-23) for 2021 have been used (METEO FRANCE et al., 2023). All the models used in ensemble were run using the CAMS-REG-AP_v4.2_REF2.1 emissions representative of 2017 (ECMFW, 2023). For more information on emissions, see Kuenen et al. (2021). All modelling data have been aggregated to the same set of parameters as for the air quality observations:

- PM₁₀ – annual average [$\mu\text{g}/\text{m}^3$], year 2021
 - 90.4 percentile of the daily means [$\mu\text{g}/\text{m}^3$], year 2021 (aggregated from daily means)
- PM_{2.5} – annual average [$\mu\text{g}/\text{m}^3$], year 2021
- Ozone – 93.2 percentile of the highest maximum daily 8-hour average value [$\mu\text{g}/\text{m}^3$], year 2021
 - (aggregated from hourly means)
 - SOMO35 [$\mu\text{g}/\text{m}^3\cdot\text{day}$], year 2021 (aggregated from hourly means)
 - SOMO10 [$\mu\text{g}/\text{m}^3\cdot\text{day}$], year 2021 (aggregated from hourly means)
 - AOT40 for vegetation [$\mu\text{g}/\text{m}^3\cdot\text{hour}$], year 2021 (aggregated from hourly means)
 - AOT40 for forests [$\mu\text{g}/\text{m}^3\cdot\text{hour}$], year 2021 (aggregated from hourly means)
- NO₂ – annual average [$\mu\text{g}/\text{m}^3$], year 2021
- NO_x – annual average [$\mu\text{g}/\text{m}^3$], year 2021

Due to the complete temporal data coverage available at the modelled data, the PM₁₀ indicator 90.4 percentile of daily means is identical with the 36th highest daily mean and the ozone indicator 93.2 percentile of maximum daily 8-hour means is identical with the 26th highest maximum daily 8-hour mean.

The data were re-gridded into the reference EEA 10 km x 10 km grid (for ozone health related indicators), 1 km x 1 km grid (for PM and NO₂) and 2 km x 2 km grid (for vegetation related indicators).

For BaP, the model used is the three-dimensional Eulerian chemistry transport model CHIMERE (version: chimere 2013), as run by CIEMAT (Vivanco et al., 2023). Meteorological data used as input to the model were obtained from simulations of the Integrated Forecasting System (IFS) of the European Centre for Medium-Range Weather Forecasts (ECMWF), which were obtained from the MARS archive at the ECMWF through the access provided for research projects by the Spanish State Meteorological Agency (AEMET). The model was run at a spatial resolution of 0.15° x 0.15° (circa 15 km x 15 km) for a domain covering the whole mapping domain, apart from Iceland. A simulation with a similar treatment for BaP (implemented in a more recent version of CHIMERE) was included in a multi-model comparison, which concluded that CHIMERE and the EMEP MSC-E POP model (used in previous mapping reports) were the two best-performing models (Gusev et al. 2022). The parameter used is

Benzo(a)pyrene – annual average [ng/m³], year 2021.

The CHIMERE model output has been used instead of the previously used EMEP model run by MSC-E, due to the lack of the EMEP modelling data for 2021 (as the MSC-E funding for 2023 was suspended according to the decision of the CLRTAP Executive Body, due to the aggression of Russia against Ukraine). The domain of the CHIMERE model output does not cover Iceland. Thus, an alternative BaP map using the *EMEP MSC-E POP* model output for 2020 (EMEP, 2022) has been constructed and applied for the area of Iceland (see Annex 3 Section A3.5). The EMEP MSC-E POP model is a three-dimensional Eulerian multi-compartment chemistry transport model (Gusev et al., 2005). Its resolution is 0.1°x0.1°, i.e. circa 10 km x 10 km.

A2.3 Other supplementary data

Meteorological parameters

The meteorological data used are the ECWMF data extracted from the CDS (Climate Data Store, <https://cds.climate.copernicus.eu/cdsapp#!/home>). Hourly data for 2021 are used. Most of the data come from the reanalysed data set ERA5-Land at a 0.1°x0.1° resolution (of CDS), namely the indicators:

Surface solar radiation [MWs/m²] – variable “Surface solar radiation downwards”

Temperature [K] – variable “2m temperature”

Wind speed [m/s] – calculated based on variables “10m u-component of wind” and “10m v-component of wind”

Relative humidity [%] – calculated based on variables “2m temperature” and “2m dewpoint temperature”

Soil water – variable “Volumetric soil water layer 3”, i.e. layer of 28-100 cm (used for POD only)

Wind speed (WV) is derived from the “10m u-component of wind” (10U) and “10m v-component of wind” (10V) according to relation

$$WV = \sqrt{(10U)^2 + (10V)^2} \quad (\text{A2.3})$$

Relative humidity (RH) is derived by means of the saturated water vapour pressure (e_t) as a function of “2m temperature” (2T) and “2m dew point temperature” (2D) according to relation

$$RH = \frac{e_{2D}}{e_{2T}} \cdot 100, \text{ with } e_t = 6.1365^{\frac{17.502 \cdot t}{24097+t}} \quad (\text{A2.4})$$

where t is 2T and 2D, respectively.

In the coastal areas (where the data from ERA5-Land are not available), the same parameters from the reanalysed data set ERA5 in 0.25°x0.25° resolution are applied. Next to this, the following data (not available in the ERA5-Land data set) from the ERA5 data set is also used:

Friction velocity [m/s] – variable “Friction velocity”. The friction velocity (also known as the shear-stress velocity) has the dimensions of velocity.

Next to the meteorological data of ERA5-Land and ERA5, the following indicators based on the meteorological ECWFMF's IFS (Integrated Forecasting System) data and coming from the CHIMERE pre-processing are used, being the hourly data for 2021 in 0.1°x0.1° resolution:

Obukhov length [m] – the stability of the atmospheric surface layer expressed in terms of the Obukhov length L ($1/L = 0$ if the atmosphere is neutral, $1/L < 0$ if the atmosphere is unstable, $1/L > 0$ if the atmosphere is stable).

Air density [molec/cm³] – expressed the number of the molecules in cm³.

Most of the meteorological parameters are used for POD_y maps only. For other maps than POD_y, annual aggregations based on hourly data are used, namely for the parameters:

Wind speed – annual average [m/s¹], year 2021
Relative humidity – annual average [%], year 2021
Surface solar radiation – annual average of daily sum [MWs/m²], year 2021

All meteorological data were re-gridded and converted into the reference EEA 1 km resolution grid, 10 km resolution grid and 2 km resolution grid, in the ETRS89-LAEA5210 projection.

Altitude

The altitude data field (in meters) of Global Multi-resolution Terrain Elevation Data 2010 (GMTED2010) is used, with an original grid resolution of 15 arcseconds (some 463 m at 60N). Source: U.S. Geological Survey Earth Resources Observation and Science, see Danielson and Gesch (2011). The field is converted into the ETRS 1989 LAEA projection. (The resolution after projection was 449.2 m). In the following step, the raster dataset was resampled to 100 m resolution and shifted to the extent of EEA reference grid. Finally, the dataset was spatially aggregated into 1 km, 2 km and 10 km resolutions. Next to this, another aggregation has been executed based on the 1 km grid cells, i.e., the floating average of the circle with a radius of 5 km around all relevant grid cells.

Population density and population totals

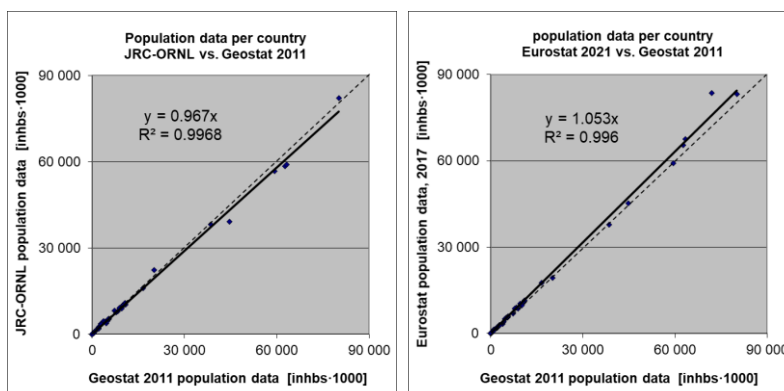
Population density (in inhbs/km², census 2011) is based on Geostat 2011 grid dataset, Eurostat (2014). The dataset is in 1 km resolution, in the EEA reference grid.

For regions not included in the Geostat 2011, alternative sources were used. Primarily, JRC (Joint Research Centre) population data in resolution 100 m were used (JRC, 2009). The JRC 100 m resolution population density data is spatially aggregated into the reference 1 km EEA grid. For regions that are neither included in the Geostat 2011 nor in the JRC database, population density data from ORNL LandScan Global Population Database, <https://landscan.ornl.gov/> was used. This dataset in 30 arcsec x30 arcsec resolution; based on the annual mid-year national population estimates for 2008 (from the Geographic Studies Branch, US Bureau of Census, <http://www.census.gov>) was earlier re-projected and converted from its original WGS1984 30 arcsec x30 arcsec grids into EEA's reference projection ETRS89-LAEA5210 at 1 km resolution by the EEA (EEA, 2010). The areas lacking Geostat 2011 data, and supplemented with JRC or ORNL data were: Faroe Islands and northern Cyprus (ORNL). As such, the Geostat 2011 1 km data and these supplements cover the entire mapping area.

To verify the consistency of merging Geostat 2011 with JRC and ORNL data, the Geostat 2011 data were compared to the JRC supplemented with ORNL data on the basis of the national population totals of the individual countries. Additionally, the national population totals for the Geostat 2011 gridded data were verified with the Eurostat national population data for 2021 (Eurostat, 2023). Figure A2.1 presents both comparisons. From these verifications, one can conclude a high correlation of the national population totals of each data source. Slight underestimation of the supplemented JRC and ORNL data in comparison with the Geostat 2011 data can be seen, which is caused by the fact that the Geostat 2011 data is more up-to-date than both the JRC and the ORNL data source. Geostat 2011 and Eurostat 2021 data correlate even better and leads to a similar conclusion. Based on this, in the further

calculations on national population totals the actual Eurostat data for 2021 (Eurostat, 2023) were used, as described further.

Figure A2.1: Correlation of national population totals for JRC supplemented with ORNL (left) and Eurostat 2021 (right) with Geostat 2011



Population density data can be used to classify the spatial distribution of each type of area (rural, urban or mixed population density) in Europe. This information is used to select and weight the air quality values, grid cell by grid cell and merge them into a final combined map (Annex 1). Furthermore, it is used to estimate population health exposure and percentages above standards per country, large regions, EU-27 and for the total mapping area, including involved uncertainties. These activities take place on the 1 km resolution grid in accordance with the recommendations of Horálek et al. (2010). The supplemented Geostat data (as described above) are used in all the calculations.

National population totals presented in the exposure tables of this paper are based on Eurostat national population data for 2021 (Eurostat, 2023). For France, Portugal and Spain, the population totals of areas outside the mapping area (i.e. French overseas departments Azores, Madeira and Canarias) are subtracted. For Andorra, Bosnia and Herzegovina, Monaco, San Marino, Faroe Islands and Kosovo with no data for 2021 in the Eurostat database, the population totals are based on UN (2023). For Cyprus, population of the northern part of Cyprus (based on <http://www.devplan.org>) is added to the population total based on Eurostat.

Land cover

CORINE Land Cover 2018 (CLC2018) – 100 m resolution, Version 2020_20 is used (EU, 2020). For Andorra that is missing in this database, World Land Cover at 30m resolution from MDAUS BaseVue 2013 (MDA, 2015) resampled to 100m resolution is used. For areas that are neither included in the CLC2018 nor in the World Land Cover database (i.e. Jan Mayen and some border areas), ESA Climate Change Initiative Global Land Cover for 2018 (ESA, 2019) is used, resampled to 100m resolution.

In agreement with Horálek et al. (2017b), the 44 CLC classes have been re-grouped into the 8 more general classes. In this paper four of these general classes are used, see Table A2.2.

Table A2.2: General land cover classes, based on CLC2018 classes, used in mapping

Label	General class description	CLC classes grid codes	CLC classes codes	CLC classes description
HDR	High density residential areas	1	111	Continuous urban fabric
LDR	Low density residential areas	2	112	Discontinuous urban fabric
AGR	Agricultural areas	12-22	211-244	Agricultural areas
NAT	Natural areas	23-34	311-335	Forest and semi natural areas

Two aggregations are used, i.e. into 1 km resolution grid and into the circle with radius of 5 km. For each general CLC class, the high land use resolution is spatially aggregated into the 1 km EEA standard

grid resolution. The aggregated grid square value represents for each general class the total area of this class as percentage of the total 1 km x 1 km area. For details, see Horálek et al. (2017b).

Road type vector data

GRIP (Meijer et al., 2018) vector road type data provided by the Netherlands Environmental Assessment Agency (PBL) are used for the weighting procedure of the urban background and the urban traffic map layers (Annex 1, Section A1.1). The road types are distributed into 5 classes, from highways to local roads and streets. In agreement with Horálek et al. (2017b), road classes No. 1 “Highways”, No. 2 “Primary roads” and No. 3 “Secondary roads” are used.

Percentage of the area influenced by traffic is represented by buffers around the roads: for the individual classes 1-3 and for classes 1-3 together, at all 1 km x 1 km grid cells; a buffer of 75 metres distance at each side from each road vector is taken for the roads of classes 1 and 2, while a buffer of 50 metres is taken for the roads of class 3. For details, see Horálek et al. (2017b).

Satellite data

The annual average NO₂ dataset was constructed based on data from the TROPOspheric Monitoring Instrument (TROPOMI) onboard of the Sentinel-5 Precursor satellite (Veefkind et al., 2012). All available swath-based Level-2 data with an irregular pixel geometry was acquired for the year 2021. The spatial resolution of the product was 5.5 km by 3.5 km. The product used is the S5P_OFFL_L2_NO2 product (van Geffen et al., 2019, 2020) and it provides the tropospheric vertical column density of NO₂, i.e. a vertically integrated value over the entire troposphere. All overpasses for a specific day were then mosaicked using HARP (<https://stcorp.github.io/harp/doc/html/index.html>) and retrievals with a quality assurance values greater than 0.75 (indicating high quality and cloud-free conditions) were gridded to a regular projected grid for all area with a 1 km spatial resolution in a ETRS89 / ETRS-LAEA (EPSG 3035) projection. The daily gridded files were subsequently averaged to an annual mean. I.e. the parameter used is

NO₂ – annual average tropospheric vertical column density (VCD) [number of NO₂ molecules per cm² of earth surface], year 2021 (aggregated from cloud-free high-quality daily data).

Soil hydraulic properties data

JRC data called "Maps of indicators of soil hydraulic properties for Europe" in 1 km resolution are used for POD calculations, JRC (2016). Namely the following indicators are used:

Wilting Point – water content at wilting point [cm³/cm³],
Field Capacity – water content at field capacity [cm³/cm³].

Annex 3

Technical details and mapping uncertainties

This annex contains technical details on the linear regression models and the residual kriging as used in the mapping. Furthermore, uncertainty estimates for the maps of the indicators are given.

A3.1 PM₁₀

Technical details on the mapping and uncertainty estimates for both PM₁₀ indicators maps annual average (Map 2.1) and 90.4 percentile of daily means (Map 2.2) are presented in this section.

Technical details on the mapping

Table A3.1 presents the estimated parameters of the linear regression models (c , a_1 , a_2 , ...) and of the residual kriging (nugget, sill, range) and includes the statistical indicators of both the regression and the kriging, for both PM₁₀ indicators. The linear regression and ordinary kriging of its residuals are applied on the logarithmically transformed data of both measurement and modelled PM₁₀ values. In Table A3.1 the standard error and variogram parameters (nugget, sill and range) refer to these transformed data, whereas RMSE and bias refer to the interpolation after a back-transformation. Since 2017 maps, an updated methodology as developed and tested under Horálek et al. (2019) has been used, i.e. including land cover among the supplementary data and using the traffic urban map layer.

The adjusted R^2 and standard error are indicators for the fit of the regression relationship, where the adjusted R^2 should be as close to 1 as possible and the standard error should be as small as possible. The adjusted R^2 for the rural areas was 0.57 at the annual average and 0.55 at the 90.4 percentile of daily means (P90.4); for the urban background areas 0.33 at the annual average and 0.32 at the P90.4; for the urban traffic areas 0.45 at the annual average and 0.37 at the P90.4.

Table A3.1: Parameters and statistics of linear regression model and ordinary kriging of PM₁₀ indicators annual average and 90.4 percentile of daily means for 2021 in rural, urban background and urban traffic areas for the final combined map

		Annual average			90.4 percentile of daily means		
		Rural areas	Urb. b. ar.	Urb. tr. ar.	Rur. ar.	Urb. b. ar.	Urb. tr. ar.
Linear regression model (LRM, Eq. A1.3)	c (constant)	1.62	0.90	1.63	1.85	1.13	2.18
	a_1 (log. CAMS model)	0.780	0.817	0.59	0.704	0.773	0.49
	a_2 (altitude GMTED)	-0.00013			-0.00011		
	a_3 (wind speed)	<i>non signif.</i>		-0.038	<i>non signif.</i>		-0.058
	a_4 (relative humidity)	-0.012			-0.011		
	a_5 (land cover NAT)	-0.0015			-0.0014		
	Adjusted R^2	0.57	0.33	0.45	0.55	0.32	0.37
	Stand. Error [$\mu\text{g}/\text{m}^3$]	0.28	0.33	0.25	0.28	0.35	0.28
Ordinary kriging (OK) of LRM residuals	Nugget	0.029	0.017	0.019	0.031	0.018	0.016
	Sill	0.104	0.056	0.038	0.107	0.072	0.055
	Range [km]	1000	240	450	1000	280	760
LRM + OK of its residuals	RMSE [$\mu\text{g}/\text{m}^3$]	3.8	6.4	4.1	7.1	14.2	7.6
	Relative RMSE [%]	25.3	28.7	19.2	27.5	36.6	20.9
	Bias (MPE) [$\mu\text{g}/\text{m}^3$]	0.0	0.0	-0.1	0.0	0.1	-0.2

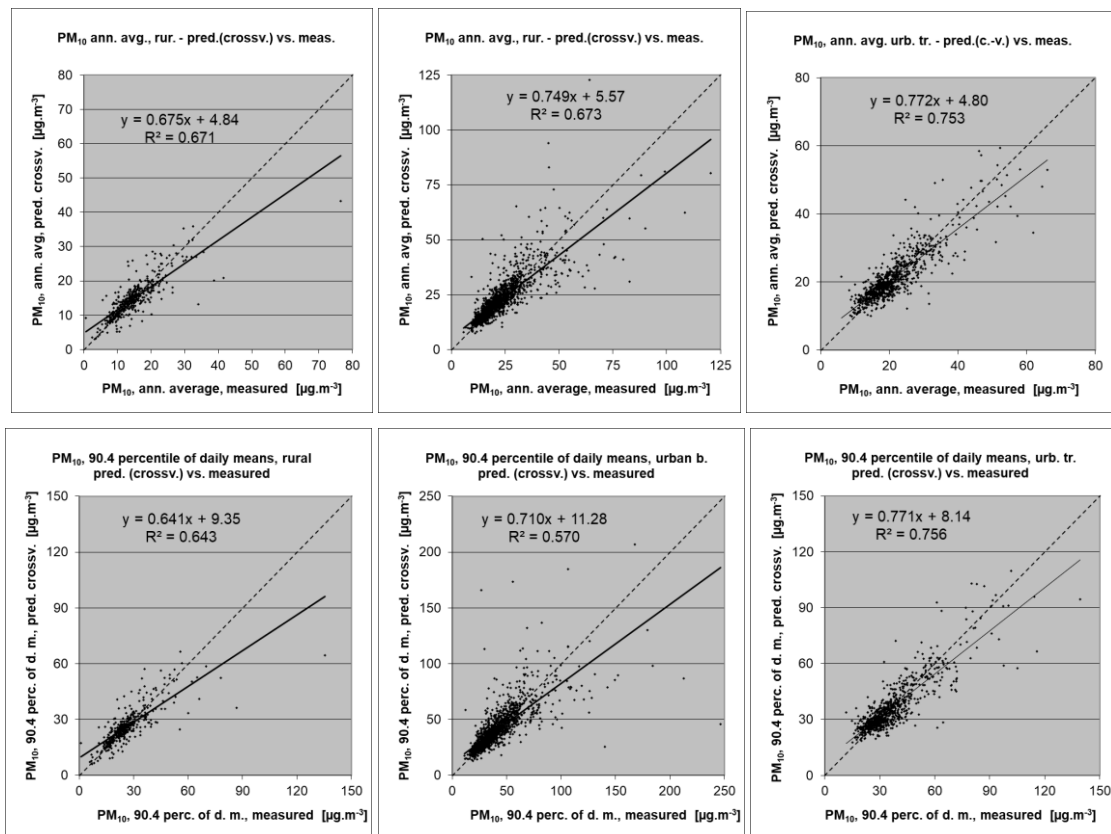
RMSE (the smaller the better) and bias (the closer to zero the better), highlighted by orange, are the cross-validation indicators, showing the quality of the resulting map. The bias indicates to what extent the predictions are under- or overestimated on average. Further in this section, more detailed uncertainty analysis is presented.

Uncertainty estimated by cross-validation

Using RMSE as the most common indicator, the absolute mean uncertainty of the final combined map at areas 'in between' the station measurements (i.e. at locations without measurements, as long as they are within the area covered by the measurements) can be expressed in $\mu\text{g}/\text{m}^3$. Table A3.1 shows that the absolute mean uncertainty of the final combined map of PM_{10} annual average and 90.4 percentile of daily means expressed by RMSE is $3.8 \mu\text{g}/\text{m}^3$ and $7.1 \mu\text{g}/\text{m}^3$ for the rural areas, $6.4 \mu\text{g}/\text{m}^3$ and $14.2 \mu\text{g}/\text{m}^3$ for the urban background areas, and $4.1 \mu\text{g}/\text{m}^3$ and $7.6 \mu\text{g}/\text{m}^3$ for the urban traffic areas, respectively. Alternatively, one can express this uncertainty in relative terms by relating the absolute RMSE uncertainty to the mean air pollution indicator value for all stations. This relative mean uncertainty (Relative RMSE) of the final combined map of PM_{10} annual average and 90.4 percentile of daily means is 25.3 % and 27.5 % for rural areas, 28.7 % and 36.6 % for urban background areas, and 19.2 % and 20.9 % for urban traffic areas, respectively. These quite high numbers in urban background areas compared to previous years up to 2015 are caused by inclusion of Türkiye since 2016 mapping. For the mapping results without Türkiye, the relative mean uncertainty is 21.3 % and 23.1 % for rural areas, 19.4 % and 23.1 % for urban background areas and 17.8 % and 19.4 % for urban traffic areas, respectively. Nevertheless, the relative uncertainty values including Türkiye fulfil the data quality objectives for models as set in Annex I of the Air Quality Directive (EC, 2008).

Figure A3.1 shows the cross-validation scatter plots, obtained according to Annex 1, Section A1.4 for rural, urban background and urban traffic areas, for both PM_{10} indicators. The R^2 indicates that the variability is attributable to the interpolation for about 67 % and 64 % at the rural areas, for 67 % and 57 % at the urban background areas, and for about 75 % and 76 % at the urban traffic areas, for the annual average and the 90.4 percentile of daily means, respectively.

Figure A3.1: Correlation between cross-validated predicted (y-axis) and measurement values for PM_{10} indicators annual average (top) and 90.4 percentile of daily means (bottom) for 2021 for rural (left), urban background (middle) and urban traffic (right) areas



The trend line in the scatter-plots deviates at the lowest values somewhat above, and at higher values below the symmetry axis, indicating that the interpolation methods tend to underestimate the high concentrations and overestimate the low concentrations. For example, in urban background areas for annual average an observed value of 40 µg/m³ is estimated in the interpolations to be about 36 µg/m³, about 11 % lower. This underestimation at high values is common to all spatial interpolation methods. It could be reduced by either using a higher number of stations with an improved spatial distribution, or by introducing an improved regression that uses either other supplementary data or more advanced chemical transport model (resp. model in finer resolution).

Comparison of point measurement values with the predicted grid value

In addition to the above point observation – point prediction cross-validation, a simple comparison has been made between the point observation values and interpolated prediction values spatially averaged at grid cells. This point observation – grid averaged prediction comparison indicates to what extent the predicted value of a grid cell represents the corresponding measurement values at stations located in that cell. The comparison has been made primarily for the separate rural, urban background and urban traffic map layers at 1 km resolution. (One can directly relate this comparison result to the cross-validation results of Figure A3.1). Apart from this, the comparison has been done also for the final combined maps at the same 1 km resolution. Figure A3.2 shows the scatterplots for these comparisons, for PM₁₀ annual average only as an illustration. The results of the point observation – point prediction cross-validation of Figure A3.1 and those of the point observation – grid averaged prediction validation for separate rural, urban background and urban traffic map layers, and for the final combined maps are summarised in Table A3.2 for both PM₁₀ indicators.

Figure A3.2: Correlation between predicted grid values from rural (upper left), urban background (upper middle) and urban traffic (upper right) map layer and final combined map (all bottom) (y-axis) versus measurements from rural (left), urban/suburban background (middle) and urban/suburban traffic stations (right) (x-axis) for PM₁₀ annual average 2021

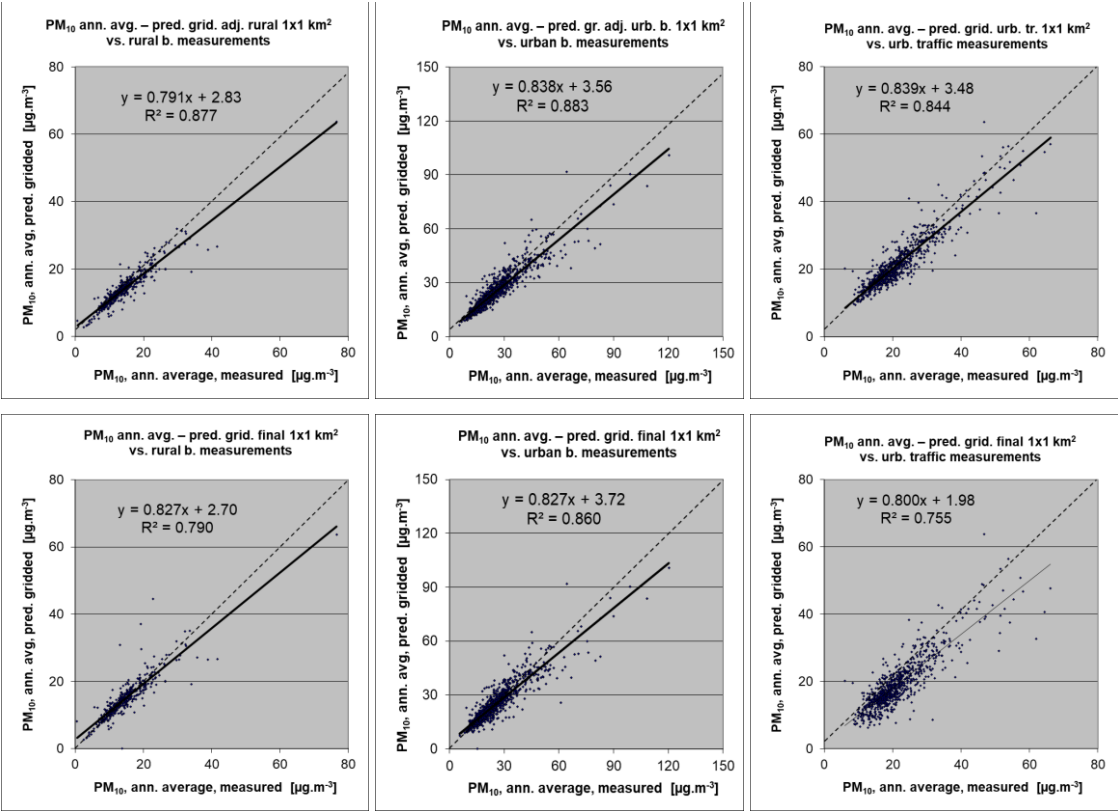


Table A3.2: Statistical indicators from the scatter plots for the predicted grid values from separate (rural, urban background or urban traffic) map layers and final combined map versus the measurement point values for rural (upper left), urban background (upper right) and urban traffic (bottom left) stations for PM₁₀ indicators annual average (top) and 90.4 percentile of daily means (bottom) for 2021

PM ₁₀	rural backgr. stations				urban/suburban backgr. stations			
	RMSE	bias	R ²	lin. r. equation	RMSE	bias	R ²	lin. r. equation
Annual average								
cross-val. prediction, separate (r or ub) map layer	3.8	0.0	0.671	y = 0.675x + 4.84	6.4	0.0	0.673	y = 0.749x + 5.57
grid prediction, 1x1 km ² separ. (r or ub) map layer	2.4	-0.3	0.877	y = 0.791x + 2.83	3.8	0.0	0.883	y = 0.838x + 3.56
grid prediction, 1x1 km ² final combined map	3.0	0.1	0.790	y = 0.827x + 2.70	4.1	-0.1	0.860	y = 0.827x + 3.72
90.4 percentile of daily means								
cross-val. prediction, separate (r or ub) map layer	7.1	0.0	0.643	y = 0.641x + 9.35	14.2	0.1	0.570	y = 0.710x + 11.28
grid prediction, 1x1 km ² separ. (r or ub) map layer	4.7	-0.5	0.861	y = 0.760x + 5.73	6.9	-0.1	0.895	y = 0.834x + 6.30
grid prediction, 1x1 km ² final combined map	5.5	0.1	0.787	y = 0.791x + 5.57	7.6	-0.3	0.871	y = 0.821x + 6.61
PM ₁₀	urban/suburban traffic stations							
	RMSE	bias	R ²	lin. r. equation				
Annual average								
cross-valid. prediction, urban traffic map layer	4.1	-0.1	0.753	y = 0.772x + 4.80				
grid prediction, 1x1 km ² urban traffic map layer	3.3	0.0	0.844	y = 0.839x + 3.48				
grid prediction, 1x1 km ² final combined map	5.8	0.1	0.755	y = 0.800x + 1.98				
90.4 percentile of daily means								
cross-valid. prediction, urban traffic map layer	7.6	-0.2	0.756	y = 0.771x + 8.14				
grid prediction, 1x1 km ² urban traffic map layer	4.7	-2.3	0.857	y = 0.850x + 5.58				
grid prediction, 1x1 km ² final combined map	8.6	-3.7	0.749	y = 0.782x + 4.30				

By comparing the scatterplots and the statistical indicators for the separate rural, urban background and urban traffic map layers with the final combined map, one can evaluate the level of representation of the rural, urban background and urban traffic areas in the final combined map. Both the rural and the urban air quality are fairly well represented in the 1 km final combined map, while the traffic air quality is underestimated in this spatial resolution. One can conclude that the final combined map in 1 km resolution is representative for rural and urban background areas, but not for urban traffic areas.

The Table A3.2 shows a better relation (i.e. lower RMSE, higher R², smaller intercept and slope closer to 1) between station measurements and the interpolated values of the corresponding grid cells at either rural, urban background or urban traffic areas than it does at the point cross-validation predictions. That is because the simple comparison between point measurements and the gridded interpolated values shows the uncertainty at the actual station locations (points), while the point cross-validation prediction simulates the behaviour of the interpolation at point positions assuming no actual measurement would exist at that point. The uncertainty at measurement locations is introduced partly by the smoothing effect of the interpolation and partly by the spatial averaging of the values in the 1 km grid cells. The level of the smoothing effect leading to underestimation at areas with high values is there smaller than in situations where no measurement is represented in such areas. For example, in urban background areas the predicted interpolation gridded annual average value in the separate rural map will be about 37 µg/m³ at the corresponding station with the measurement value of 40 µg/m³. This means an underestimation of about 7 %. It is a slightly less than the prediction underestimation of 11 % at the same point location, when leaving out this one actual measurement point and the interpolation is done without this station (see the previous subsection).

A3.2 PM_{2.5}

Technical details and uncertainty estimates for Map 2.3 with the PM_{2.5} annual average are presented in this section.

Technical details on the mapping

Like for PM₁₀, an updated methodology as developed and tested under Horálek et al. (2019) has been used, i.e. including the land cover among supplementary data and using the traffic urban map layer.

Table A3.3 presents the regression coefficients determined for pseudo PM_{2.5} stations data estimation, based on the 1050 rural and urban/suburban background and 407 urban/suburban traffic stations that have both PM_{2.5} and PM₁₀ measurements available (see Section 2.1.1).

Table A3.3: Parameters and statistics of linear regression model for generating pseudo PM_{2.5} annual average data for 2021 in rural and urban background (left) and urban traffic (right) areas

		Rural and urban background areas	Urban traffic areas
Linear regression model (LRM, Eq. A1.1)	c (constant)	21.5	41.1
	b (PM ₁₀ measurement data)	0.669	0.464
	a1 (surface solar radiation)	-0.003	-0.004
	a2 (latitude)	-0.232	-0.536
	a3 (longitude)	0.081	0.104
	Adjusted R²	0.83	0.72
	Standard Error [µg.m⁻³]	2.1	2.3

Table A3.4 presents the estimated parameters of the linear regression models (c, a₁, a₂,...) and of the residual kriging (nugget, sill, range) and includes the statistical indicators of both the regression and the kriging of its residuals. The same supplementary data as in Horálek et al. (2019) has been used. Like in the case of PM₁₀, the linear regression is applied on the logarithmically transformed data of both measurement and modelled PM_{2.5} values. Thus, the standard error and variogram parameters refer to these transformed data, whereas RMSE and bias refer to the interpolation after the back-transformation.

Table A3.4: Parameters and statistics of linear regression model and ordinary kriging of PM_{2.5} annual average 2021 in rural, urban background and urban traffic areas for final combined map

PM _{2.5}		Annual average		
		Rural areas	Urban b. areas	Urban tr.. areas
Linear regression model (LRM, Eq. A1.3)	c (constant)	0.71	0.70	0.78
	a1 (log. CAMS model)	0.788	0.779	0.733
	a2 (altitude GMTED)	-0.00032		
	a3 (wind speed)	-0.038		
	a4 (land cover NAT1)	-0.0011		
		Adjusted R²	0.58	0.43
	Standard Error [µg.m⁻³]	0.32	0.29	0.24
Ordinary kriging (OK) of LRM residuals	nugget	0.029	0.018	0.005
	sill	0.129	0.063	0.058
	range [km]	1000	250	1000
LRM + OK of its residuals	RMSE [µg.m⁻³]	1.7	2.6	2.3
	Relative RMSE [%]	19.5	20.7	20.5
	Bias (MPE) [µg.m⁻³]	0.1	0.0	-0.1

The adjusted R² and standard error are indicators for the quality of the fit of the regression relation. The adjusted R² is 0.58 for the rural areas, 0.43 for urban background areas and 0.62 for urban traffic

areas. Quite weaker regression relation in the urban background areas causes a higher impact of the interpolation part of the interpolation-regression-merging methodology in these areas.

RMSE and bias – highlighted in orange – are the cross-validation indicators, showing the quality of the resulting map; the bias indicates to what extent the predictions are under- or overestimated on average. Only stations with PM_{2.5} measurement data are used for calculating the RMSE and the bias (i.e. the pseudo PM_{2.5} stations are not used). These statistical indicators are calculated excluding the pseudo stations because they are estimated values only, not actual measurement values. According to Denby et al (2011), the pseudo PM_{2.5} data does not satisfy the quality objectives for fixed monitoring alone. The pseudo stations are used as they improve the mapping estimate, whereas the actual measurements can be used for evaluating the quality of the map. For the future, it will be considered to quit the application of the PM_{2.5} pseudo stations as the current number of the actual PM_{2.5} measurement stations has increased over time such that the use of pseudo PM_{2.5} stations may not contribute enough any longer to improve the mapping estimates.

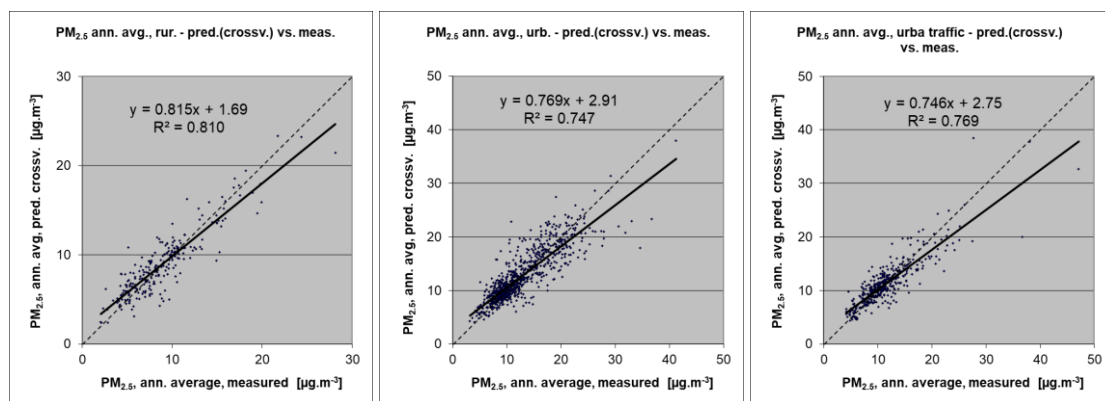
Due to the lack of rural stations in Türkiye for PM_{2.5}, no proper interpolation results could be presented for this country in a rural map, so the estimated PM_{2.5} values for Türkiye are not presented in the final map. Thus, the stations located in Türkiye have not been used in the uncertainty estimates (although used in the mapping process), as they lie outside the mapping area.

Uncertainty estimated by cross-validation

Table A3.4 shows that the absolute mean uncertainty of the final combined map of PM_{2.5} annual average expressed as RMSE is 1.7 µg/m³ for the rural areas, 2.6 µg/m³ for the urban background areas and 2.3 µg/m³ for the urban traffic areas. On the other hand, the relative mean uncertainty (Relative RMSE) of the final combined map of PM_{2.5} annual average is 19.5 % for rural areas, 20.7 % for urban background areas and 20.5 % for urban traffic areas. These relative uncertainty values fulfil the data quality objectives for models as set in Annex I of the Air Quality Directive (EC, 2008).

Figure A3.3 shows the cross-validation scatter plots, obtained according to Section A1.3, for different area types. The R² indicates that about 81 % of the variability is attributable to the interpolation for the rural areas, 75 % for the urban background areas and 77 % for the urban traffic areas.

Figure A3.3: Correlation between cross-validated predicted and measurement values for PM_{2.5} annual average 2021 for rural (left), urban background (middle) and urban traffic (right) areas



The scatter plots indicate that in areas with high concentrations the interpolation methods tend to underestimate the levels. E.g., in urban background areas an observed value of 25 µg/m³ is estimated in the interpolations to be about 22 µg/m³, which is an underestimated prediction of about 11 %. This underestimation at high values is an inherent feature of all spatial interpolations. It could be reduced

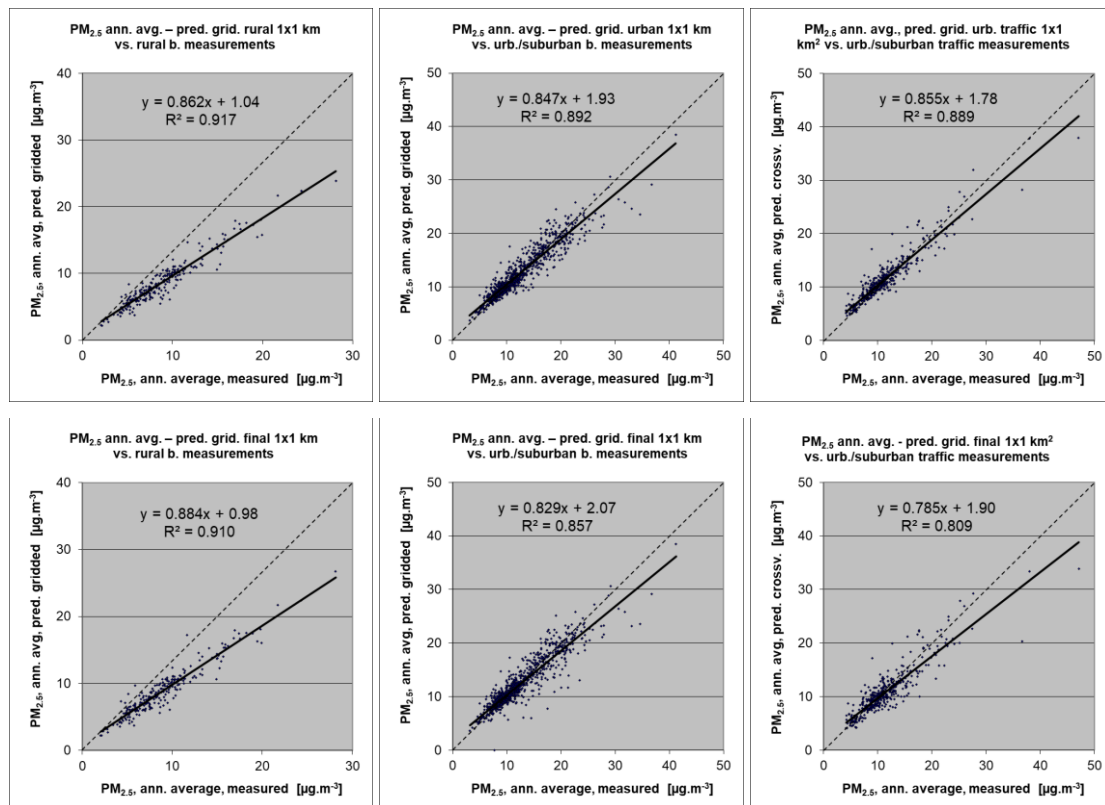
by either using a higher number of the stations at improved spatial distribution, or by introducing a closer regression that uses either other supplementary data or more improved CTM output.

Comparison of point measurement values with the predicted grid value

Like for PM₁₀, a simple comparison has been made between the point observation values and interpolated prediction values spatially averaged in grid cells, in addition to the cross-validation. The comparison has been made primarily for the separate rural, urban background and urban traffic map layers at 1 km resolution. Next to this, the comparison has been done also for the final combined maps at the same 1 km resolution. Figure A3.4 shows the scatterplots for these comparisons.

The results of the point observation – point prediction cross-validation of Figure A3.3 and those of the point observation – grid averaged prediction validation Figure A3.4 for separate map layers and for the final combined map are summarised in Table A3.5.

Figure A3.4: Correlation between predicted grid values from rural (upper left), urban background (upper middle) and urban traffic (upper right) map layer and final combined map (all bottom) (y-axis) versus measurements from rural (left), urban/suburban background (middle) and urban/suburban traffic stations (right) (x-axis) for PM_{2.5} annual average 2021



By comparing the scatterplots and the statistical indicators for separate rural, urban background and urban traffic map layers with the final combined maps, one can evaluate the level of representation of the rural, urban background and urban traffic areas in the final combined map. Similar results as for PM₁₀ can be observed: the final combined map in 1 km resolution is fairly well representative for rural and urban background areas, but not for urban traffic areas.

Like in the case of PM₁₀, Table A3.5 shows a better correlated relation with the station measurements (i.e. lower RMSE, higher R², smaller intercept and slope closer to 1) for the simply interpolated gridded values than for the point cross-validation predictions, at rural, urban background and urban traffic map

areas. That is because the simple comparison shows the uncertainty at the actual station locations, while the cross-validation prediction simulates the behaviour of the interpolation (within the area covered by measurements) at point positions assuming no actual measurements would exist at these points.

The uncertainty at measurement locations is introduced partly by the smoothing effect of the interpolation and partly by the spatial averaging of the values in the 1 km x 1 km grid cells. For example, in urban background areas the predicted interpolation gridded value in the final map will be about 23 µg/m³ at the corresponding station with the measurement value of 25 µg/m³ (calculated based on the linear regression equation), which coincides with an underestimation of about 8 %.

Table A3.5: Statistical indicators from the scatter plots for the predicted grid values from separate (rural, urban background or urban traffic) map layers and final combined map versus the measurement point values for rural (upper left), urban background (upper right) and urban traffic (bottom left) stations for PM_{2.5} annual average 2021

PM _{2.5}	rural backgr. stations				urban/suburban backgr. stations			
	RMSE	bias	R ²	lin. r. equation	RMSE	bias	R ²	lin. r. equation
cross-val. prediction, separate (r or ub) map layer	1.7	0.1	0.810	y = 0.815x + 1.69	2.6	0.0	0.747	y = 0.769x + 2.91
grid prediction, 1x1 km ² separ. (r or ub) map layer	1.2	-0.2	0.917	y = 0.862x + 1.04	1.7	0.0	0.892	y = 0.847x + 1.93
grid prediction, 1x1 km ² final merged map	1.2	0.0	0.910	y = 0.884x + 0.98	1.9	-0.1	0.857	y = 0.829x + 2.07

PM _{2.5}	urban/suburban traffic stations			
	RMSE	bias	R ²	lin. r. equation
cross-val. prediction, urban traffic map layer	2.3	-0.1	0.769	y = 0.746x + 2.75
grid prediction, 1x1 km ² urban traffic map layer	1.6	0.1	0.889	y = 0.855x + 1.78
grid prediction, 1x1 km ² final merged map	2.2	-0.6	0.809	y = 0.785x + 1.90

A3.3 Ozone

In this section, the technical details and the uncertainty estimates are presented for the maps of ozone health-related indicators 93.2 percentile of maximum daily 8-hour means, SOMO35 and SOMO10 (Maps 3.1-3.3), as well as for the maps of ozone vegetation-related indicators AOT40 for vegetation and AOT40 for forests (Maps 3.4 and 3.5). Next to this, the details of POD_v (i.e. POD₆ and POD₁) maps are presented.

Technical details on the mapping

Table A3.6 presents the estimated parameters of the linear regression models and of the residual kriging, including the statistical indicators of both the regression and the kriging.

The adjusted R² and standard error show the quality of the fit of the regression relation. For the rural areas, all indicators show the value of the adjusted R² between 0.54 and 0.63. For the urban areas, the adjusted R² is 0.38 for 93.2 percentile of daily 8-hour maximums, 0.41 for SOMO35 and 0.22 for SOMO10. For the vegetation-related indicators the urban maps are not constructed. RMSE and bias – highlighted by orange – are the cross-validation indicators, showing the quality of the resulting map.

Table A3.6: Parameters and statistics of linear regression model and ordinary kriging for ozone indicators 93.2 percentile of maximum daily 8-hourly means, SOMO35 and SOMO10 in rural and urban areas for the final combined map and for O₃ indicators AOT40 for vegetation and for forests in rural areas for 2021

		93.2 perc. of dmax 8h		SOMO35		SOMO10		AOT40v	AOT40f
		Rur. areas	Urb. ar.	Rur. ar.	Urb.ar.	Rur. ar.	Urb.ar.	Rur. ar.	Rur. ar.
Linear regression model (LRM, Eq. A1.3)	c (constant)	-21.6	13.6	-349	1826	391	2798	-236	-413
	a1 (CAM5 model)	1.25	0.99	0.95	0.73	0.91	0.74	1.07	1.00
	a2 (altitude GMTED)	0.0144		2.90		3.59		7.92	14.44
	a3 (wind speed)		-3.67		-459.7		<i>n. sign.</i>		
	a4 (s. solar radiation)	<i>n. sign.</i>	<i>n. sign.</i>	<i>n. sign.</i>	<i>n. sign.</i>	<i>n. sign.</i>	<i>n. sign.</i>	<i>n. sign.</i>	<i>n. sign.</i>
	Adjusted R²	0.61	0.38	0.58	0.41	0.54	0.22	0.59	0.63
Stand. Err. [$\mu\text{g}/\text{m}^3 \cdot \text{x}$]*	8.2	12.7	1545	1676	2331	3248	4861	8245	
Ord. krig. (OK) of LRM	Nugget	26	40	1.6E+06	9.0E+05	4.5E+06	2.1E+06	1.2E+07	2.9E+07
	Sill	52	107	2.4E+06	1.9E+06	5.0E+06	3.7E+07	1.9E+07	5.0E+07
	Range [km]	120	620	710	580	710	700	240	120
LRM + OK of its residuals	RMSE [$\mu\text{g}/\text{m}^3 \cdot \text{x}$]*	7.7	10.8	1498	1439	2332	2659	4659	8062
	Relative RMSE [%]	7.2	10.3	32.0	37.3	11.3	14.6	39.5	39.3
	Bias (MPE) [$\mu\text{g}/\text{m}^3 \cdot \text{x}$]*	0.1	0.0	-5	-2	-11	5	-9	95

* Units: 93.2 percentile of daily 8-h maximums: [$\mu\text{g}/\text{m}^3$], SOMO35 and SOMO10: [$\mu\text{g}/\text{m}^3 \cdot \text{d}$], AOT40v and AOT40f: [$\mu\text{g}/\text{m}^3 \cdot \text{h}$].

Uncertainty estimated by cross-validation

The basic uncertainty analysis is provided by cross-validation. Table A3.6 shows both absolute and relative mean uncertainty, expressed by RMSE and Relative RMSE. The relative mean uncertainty of the 2021 ozone map is around 7-10 % for the 93.2 percentile of maximum daily 8-h means, around 32-37 % for SOMO35, around 11-15 % for SOMO10 and around 39 % at AOT40 indicators. The small levels of the relative uncertainty for the 93.2 percentile of maximum daily 8-h means and SOMO10 are highly influenced by the low ratio between the relevant standard error and mean calculated based on all annual station concentration data: for these two indicators the ratio is at the level of about 0.07- 0.15, while for SOMO35 and for both AOT40 indicators it is at the level of about 0.32-0.40.

Figure A3.5 shows the cross-validation scatter plots for both the rural and urban areas of the 2021 map for the health-related ozone indicators.

The R², an indicator for the interpolation correlation with the observations, shows that for the health-related ozone indicators, about 53-65 % is attributable to the interpolation in the rural areas, while in the urban areas it is about 48-57 %.

The scatter plots indicate that the higher values are underestimated and the lower values somewhat overestimated by the interpolation method; a typical smoothing effect inherent to the interpolation method with the linear regression and its residuals kriging. For example, in the case of the 93.2 percentile of daily 8-h maximums, in urban areas (Figure A3.5, upper right panel) an observed value of 150 $\mu\text{g}/\text{m}^3$ is estimated in the interpolation as 131 $\mu\text{g}/\text{m}^3$, which is 13 % lower. Or, in the case of SOMO35, in rural areas (Figure A3.5, middle left panel) an observed value of 9 000 $\mu\text{g}/\text{m}^3 \cdot \text{d}$ is estimated in the interpolation as about 7 300 $\mu\text{g}/\text{m}^3 \cdot \text{d}$, which is 19 % lower.

Figure A3.5: Correlation between cross-validated predicted (y-axis) and measurement values for ozone indicators 93.2 percentile of max. daily 8-hourly means (top), SOMO35 (middle) and SOMO10 (bottom) for 2021 for rural (left) and urban (right) areas

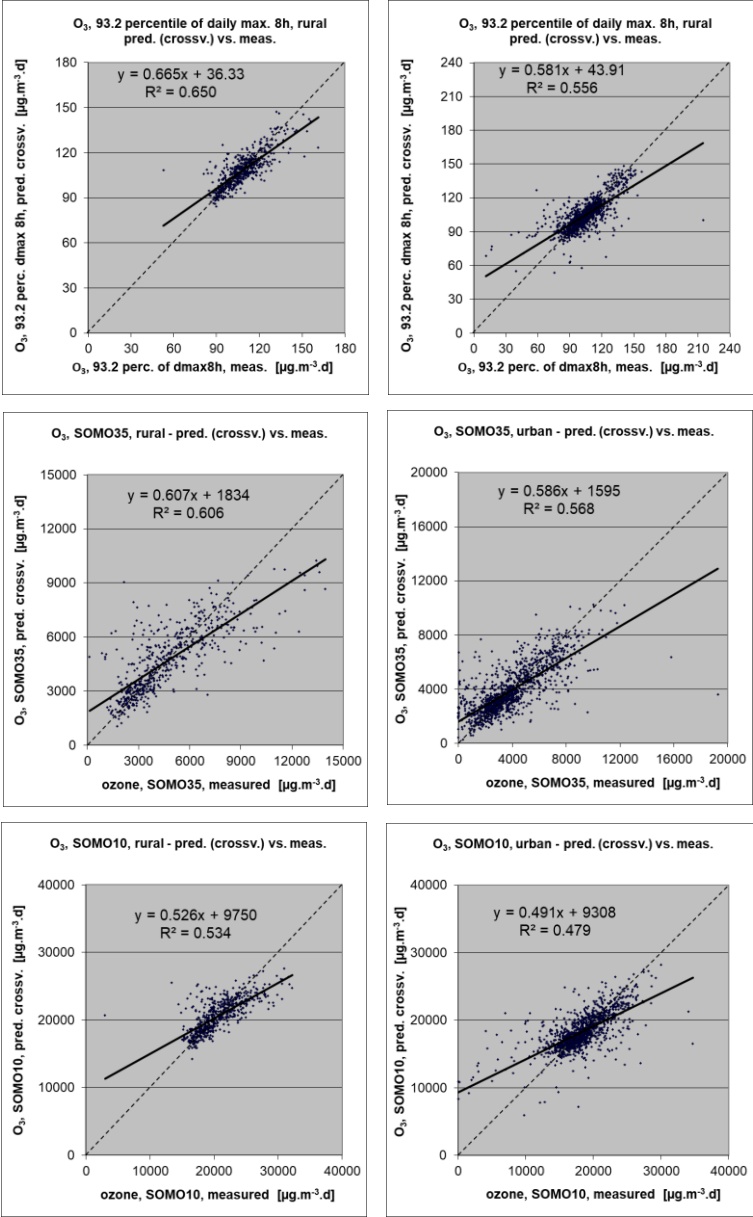
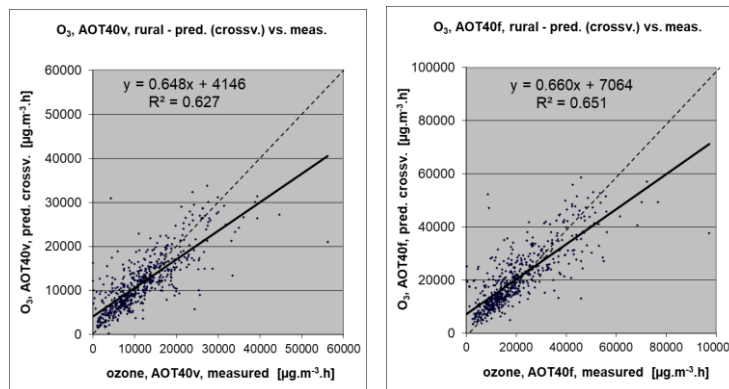


Figure A3.6 shows the cross-validation scatter plots of the AOT40 for both vegetation and forests. R² indicates that about 63 % of the variability is attributable to the interpolation in the case of AOT40 for vegetation, while for AOT40 for forests it is about 65 %.

The cross-validation scatter plots show again that in areas with higher accumulated ozone concentrations the interpolation methods tend to deliver underestimated predicted values. For example, in agricultural areas (Figure A3.6, left panel) an observed value of 25 000 µg/m³·h is estimated in the interpolation as about 20 300 µg/m³·h, i.e. an underestimation of about 19 %. In addition, an overestimation at the lower end of predicted values occurred. One could reduce this under- and overestimation by extending the number of measurement stations and by optimising the spatial distribution of those stations, specifically in areas with elevated values over years.

Figure A3.6: Correlation between cross-validated predicted (y-axis) and measurement values for ozone indicators AOT40 for vegetation (left) and AOT40 for forests (right) for 2021 for rural areas



Comparison of point measurement values with the predicted grid value

In addition to the above point observation – point prediction cross-validation, a simple comparison has been made between the point observation values and interpolated predicted grid values.

For health-related indicators, the comparison has been made primarily for the separate rural and separate urban background maps at 10 km resolution. (One can directly relate this comparison result to the cross-validation of the previous section.) Next to this, the comparison has been done also for the final combined maps at 1 km resolution.

Figure A3.7 shows the scatterplots for these comparisons, for ozone indicator 93.2 percentile of maximum daily 8-hour means only, as an illustration.

The results of the point observation – point prediction cross-validation of Figure A3.5 and those of the point observation – grid averaged prediction validation for the separate rural and the separate urban background map, and for the final combined maps are summarised in Table A3.7. By comparing the scatterplots and the statistical indicators for the separate rural and separate urban background map with the final combined maps, one can evaluate the level of representation of the rural resp. urban background areas in the final combined maps. Both the rural and the urban air quality are fairly well represented in the 1 km x1 km final combined map.

The uncertainty of the map layers at measurement locations is caused partly by the smoothing effect of interpolation and partly by the spatial averaging of the values in the 10 km x 10 km grid cells. The level of smoothing, which leads to underestimation in areas with high values, is weaker in areas where measurements exist than in areas where a measurement point is not available. For example, in the case of the 93.2 percentile of daily 8-h maximums, in urban areas an observed value of 150 µg/m³ is estimated in the interpolation as about 140 µg/m³, which is about 7 % lower. It is less than the cross-validation underestimation of 13 % at the same point location, when leaving out this one actual measurement point and the interpolation without this station is done (see the previous subsection).

Figure A3.7: Correlation between predicted grid values from rural (upper left) and urban (bottom left) 10 km resolution and final combined 1 km resolution (both right) map (y-axis) versus measurements from rural (top) or urban/suburban (bottom) background stations (x-axis) for ozone indicator 93.2 percentile of daily maximum 8-hourly means for 2021

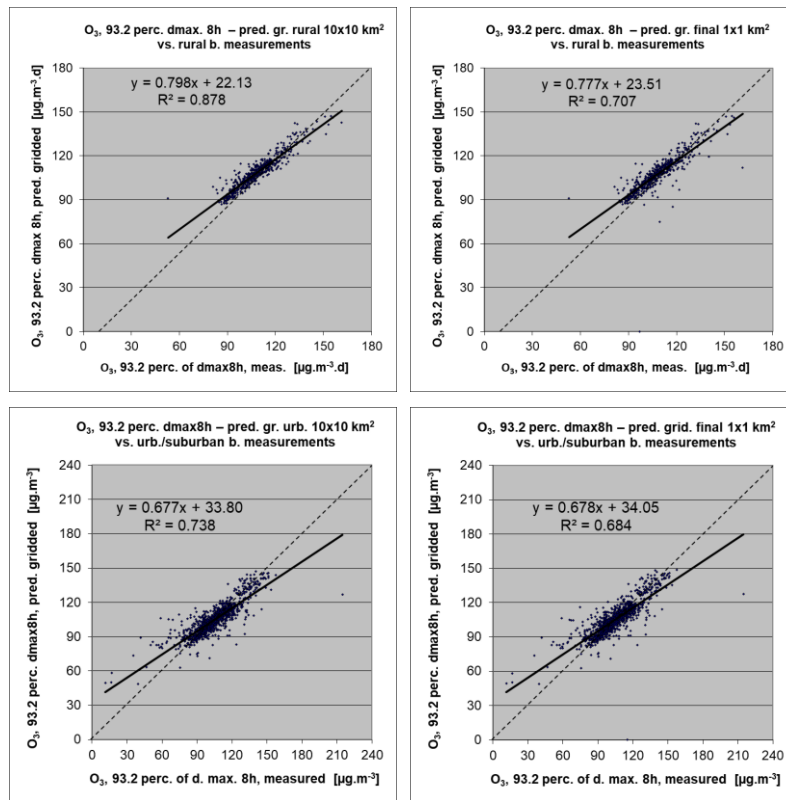


Table A3.7: Statistical indicators from the scatter plots for the predicted point values based on cross-validation and the predicted grid values from separate (rural resp. urban) 10 km resolution and final merged 1 km resolution map versus the measurement point values for rural (left) and urban (right) background stations for ozone indicators 93.2 percentile of daily max 8h means (top), SOMO35 (middle) and SOMO10 (bottom) for 2021

Ozone	rural backgr. stations				urban/suburban backgr. stations			
	RMSE	Bias	R ²	Lin. r. equation	RMSE	Bias	R ²	Lin. r. equation
93.2 percentile of daily max. 8-hour means								
cross-val. prediction, separate (r or ub) map layer	7.7	0.1	0.650	y = 0.665x + 36.33	10.8	0.0	0.556	y = 0.581x + 43.91
grid prediction, 10 km resol.separate (r or ub) map layer	4.7	0.3	0.878	y = 0.798x + 22.13	8.3	-0.1	0.738	y = 0.677x + 33.80
grid prediction, 1 km resolution final merged map	7.2	-0.6	0.707	y = 0.777x + 23.51	9.1	0.3	0.684	y = 0.678x + 34.05
SOMO35								
cross-val. prediction, separate (r or ub) map layer	1498	-5	0.606	y = 0.607x + 1834	1439	-2	0.568	y = 0.586x + 1595
grid prediction, 10 km resol.separate (r or ub) map layer	1271	13	0.720	y = 0.667x + 1570	1179	-26	0.714	y = 0.658x + 1291
grid prediction, 1 km resolution final merged map	1351	-134	0.686	y = 0.643x + 1538	1242	67	0.679	y = 0.668x + 1346
SOMO10								
cross-val. prediction, separate (r or ub) map layer	2332	-11	0.534	y = 0.526x + 9750	2659	5	0.479	y = 0.491x + 9308
grid prediction, 10 km resol.separate (r or ub) map layer	2156	10	0.605	y = 0.561x + 9036	2102	-2	0.685	y = 0.598x + 7339
grid prediction, 1 km resolution final merged map	2430	-313	0.506	y = 0.550x + 8941	2281	176	0.619	y = 0.604x + 7405

Table A3.8 presents the results of the point observation – point prediction cross-validation of Figure A3.6 and those of the point-grid validation for the rural map, for vegetation related indicators AOT40 for vegetation and AOT40 for forests. Again, one can see for both indicators a better correlation between the station measurements and the averaged interpolated predicted values of the corresponding grid cells, than at the point cross-validation predictions, of Figure A3.6.

Table A3.8: Statistical indicators from the scatter plots for predicted point values based on cross-validation and predicted grid values from rural 2 km resolution map versus measurement point values for rural background stations for ozone indicators AOT40 for vegetation (top) and forests (bottom) for 2021

Ozone	rural backgr. stations			
	RMSE	bias	R ²	linear regression equation
AOT40 for vegetation				
cross-valid. prediction, rural map	4659	-9	0.627	y = 0.648x + 4146
grid prediction, 2 km resolution rural map	2207	2	0.810	y = 0.752x + 2929
AOT40 for forests				
cross-valid. prediction, rural map	8062	95	0.651	y = 0.660x + 7064
grid prediction, 2 km resolution rural map	4929	48	0.877	y = 0.795x + 4253

Details of POD_y maps

POD₆ maps have been calculated using the ozone based on the hourly ozone rural maps, hourly meteorological data and soil hydraulic properties data, according to the methodology described in Annex 1, Section A1.3.

The hourly ozone maps needed for POD_y (i.e. POD₆ and POD₁) calculation have been calculated at the 2 km resolution, based on rural background measurements. The maps for each hour of the year 2021 have been constructed using the same methodology as for the annual maps, i.e. the multiple linear regression followed by the kriging of its residuals (see Annex 1, Section A1.1) based on the measurement data, CAMS-ENS Forecast model output, altitude and the surface solar radiation. Table A3.9 presents the summary results of the RMSE, RRMSE and bias for the whole year, based on the annual average and percentiles of these three statistics. For bias, annual sum is also shown in addition.

Table A3.9: Annual statistics average, 2nd percentile, 25th percentile, 50th percentile (median), 75th percentile, 98th percentile and sum (where relevant) for average ozone concentration, number of stations considered, and cross-validation parameters RMSE, RRMSE and Bias of hourly ozone maps, 1.1.2021-31.12.2021. Units: µg/m³ apart from N and RRMSE.

	Rural background areas						
	avg	p2	p25	p50	p75	p98	Sum
N	561	538	556	562	567	574	
avg	60.6	35.1	48.0	57.9	71.6	97.0	
RMSE	14.7	9.6	12.3	14.2	16.6	22.8	
RRMSE	26.3%	11.7%	17.7%	25.7%	33.2%	46.6%	
Bias	-0.10	-0.58	-0.21	-0.07	0.02	0.31	-876

Figure A3.8 and A3.9 presents the averages of the cross-validation indicators Bias and RMSE in the individual hours of the year 2021.

Figure A3.8: Cross-validation statistical indicator Bias of hourly ozone maps, average at rural background stations, 1.1.2021-31.12.2021

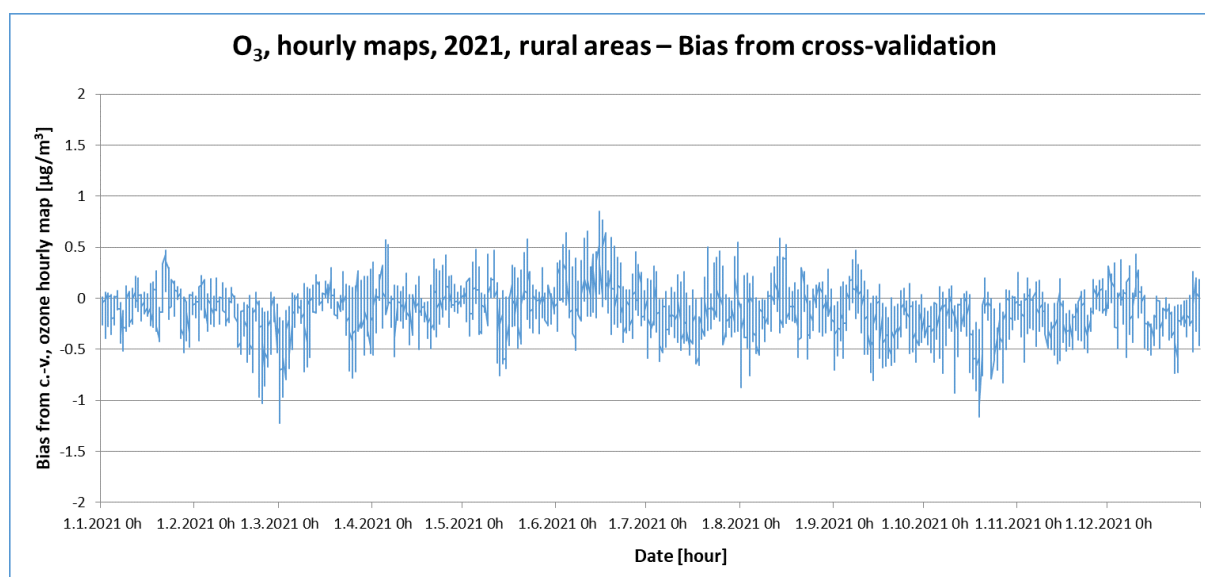
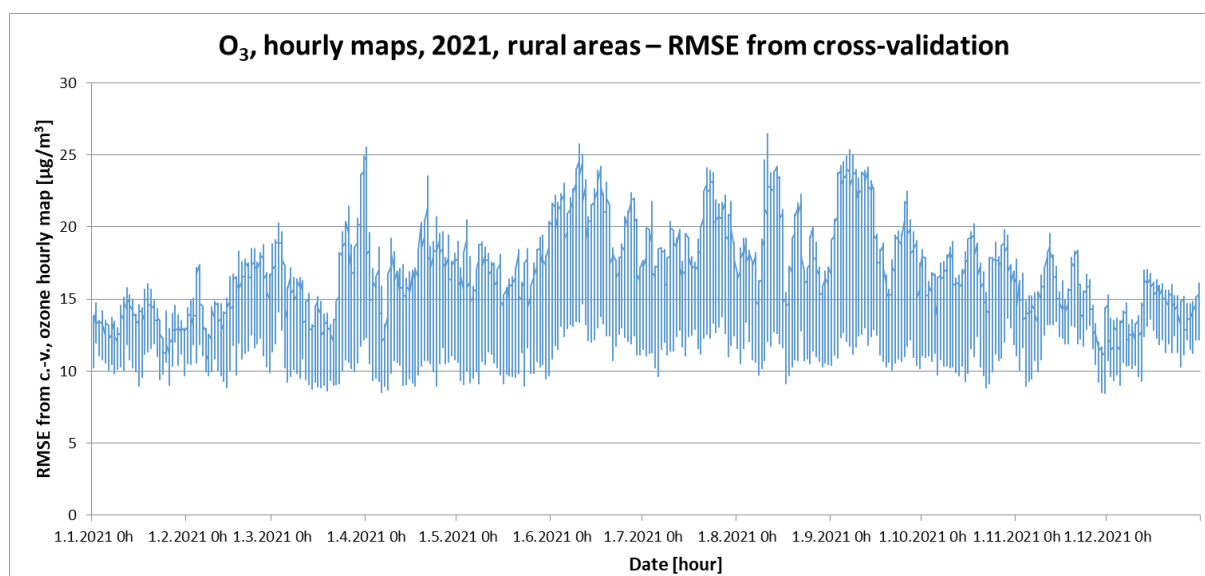


Figure A3.9: Cross-validation statistical indicator RMSE of hourly ozone maps, average at rural background stations, 1.1.2021-31.12.2021



In the POD_y calculations, the module to estimate phytotoxic ozone doses from a given atmospheric ozone exposure developed by INERIS and adapted by CHMI has been used.

During the POD_y maps calculation, different biogeographical regions were considered. Plant stomatal functioning varies per plant species and can vary by biogeographical region, reflecting different adaptations of plants to climate and soil water in these regions. Parametrization for POD_6 (i.e. for wheat, potato and tomato) is currently available for all different biogeographic regions of Europe apart from Alpine region, i.e. for Atlantic, Boreal, Continental, Pannonian, Steppic, and Mediterranean regions (CLRTAP, 2017a). In the case of wheat, the parametrization is the same for most of these regions (namely Atlantic, Boreal, Continental, Pannonian, and Steppic), while for Mediterranean regions is different. For Alpine region, the parametrization of the Continental and several other regions are used. For potato and tomato, only one parametrization exists – in the case of potato, the parametrization is set for all regions apart from the Alpine one, while for tomato for the Mediterranean

region only (see Table 1.2). In the calculations, the existing parametrisation has been applied for the entire mapping area. Parametrization for POD_1 for spruce is available for all biogeographical regions apart from the Mediterranean, Anatolian and Black Sea ones.

The values calculated in $0.1^\circ \times 0.1^\circ$ resolution were converted into the standard ETRS89-LAEA5210 projection and transferred into the EEA 2 km resolution grid.

A3.4 NO_2 and NO_x

In this section, the technical details and the uncertainty estimates for the maps of NO_2 annual average and NO_x annual average, for Maps 4.1 and 4.2, are presented.

Technical details on the mapping

In agreement with Horálek et al. (2007) and Annex 1, the NO_x measurements are supplemented by the so-called pseudo NO_x stations. The pseudo NO_x data are calculated based on the NO_2 data, using quadratic regression Eq. A1.2a. The regression coefficients were estimated based on 388 rural background stations with both NO_x and NO_2 measurements (see Section 2.1.1). The estimated coefficients of Eq. A1.2 are: $a = 0.0381$, $b = 0.846$, $c = 1.25$. Adjusted R^2 is 0.94, the standard error is $1.4 \mu\text{g}/\text{m}^3$.

Table A3.10 presents the estimated parameters of the linear regression models and of the residual kriging and includes the statistical indicators of both the regression and the kriging.

Table A3.10: Parameters and statistics of linear regression model and ordinary kriging of NO_2 annual average for 2021 in rural, urban background and urban traffic areas for the final combined map (left) and NO_x annual average for 2021 in rural areas (right)

		NO_2 Annual average			NO_x Annual average
		Rural areas	Urb. b. areas	Urb. tr. areas	Rural areas
Linear regression model (LRM, Eq. A1.3)	c (constant)	7.2	15.2	22.00	0.1
	a1 (CAMS model)	0.307	<i>non signif.</i>	<i>non signif.</i>	0.828
	a2 (altitude)	<i>non signif.</i>		<i>non signif.</i>	-0.0045
	a3 (altitude_5km_radius)	<i>non signif.</i>		<i>non signif.</i>	
	a4 (wind speed)	-1.00	-2.14	-2.28	-1.74
	a5 (solar radiation)				0.003
	a6 (satellite TROPOMI)	1.06	1.76	1.68	
	a7 (population*1000)	0.00056	0.00020		
	a8 (NAT_1km)		-0.0429		
	a9 (AGR_1km)		-0.0287		
	a10 (TRAF_1km)		0.0692		
	a11 (LDR_5km_radius)	<i>non signif.</i>	<i>non signif.</i>	0.0011	
	a12 (HDR_5km_radius)		0.0017	0.0029	
	a13 (NAT_5km_radius)	-0.00063			
	Adjusted R^2	0.66	0.44	0.35	0.55
	Standard Error [$\mu\text{g}\cdot\text{m}^{-3}$]	2.6	5.5	7.8	4.7
Ordinary kriging (OK) of LRM residuals	nugget	4	9	19	11
	sill	6	17	39	15
	range [km]	470	79	80	330
LRM + OK of its residuals	RMSE [$\mu\text{g}\cdot\text{m}^{-3}$]	2.1	3.7	6.0	3.9
	Relative RMSE [%]	32.3	23.8	23.6	46.1
	Bias (MPE) [$\mu\text{g}\cdot\text{m}^{-3}$]	0.0	0.0	0.0	42.4

Only stations with actual measurement data of the relevant pollutant (i.e. not the pseudo stations) have been used for calculating the cross-validation parameters RMSE and bias.

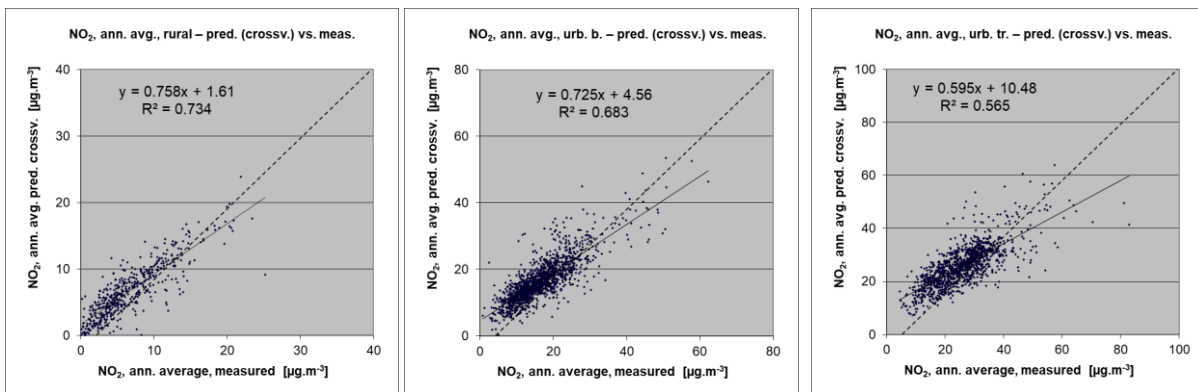
Uncertainty estimated by cross-validation

Table A3.10 shows both absolute and relative mean uncertainty, expressed by RMSE and Relative RMSE. The absolute mean uncertainty of the final combined map of NO₂ annual average expressed as RMSE is 2.1 µg/m³ for the rural areas, 3.7 µg/m³ for the urban background areas and 6.0 µg/m³ for the urban traffic areas. For the NO_x rural map it is 3.9 µg/m³.

The relative mean uncertainty of the NO₂ annual average map is 32 % for rural areas, 24 % for both urban background and urban traffic areas. The NO_x annual average rural map has a relative mean uncertainty of 46 %.

Figure A3.10 shows the point observation – point prediction cross-validation scatter plots for NO₂ annual average. The R² indicates that about 73 % of the variability is attributable to the interpolation for the rural areas, while for the urban background areas it is 68 % and for the urban traffic 57 %.

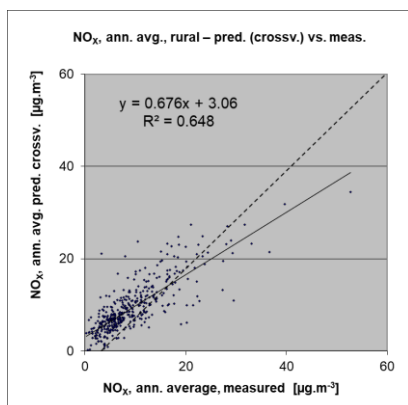
Figure A3.10: Correlation between cross-validated predicted and measurement values for NO₂ annual average 2021 for rural (left), urban background (middle) and urban traffic (right) areas



Like in the case of other pollutants, the cross-validation scatter plots show the underestimation of predictions at high concentrations at locations with no measurements. For example, in urban background areas an observed value of 40 µg/m³ is estimated in the interpolations to be about 34 µg/m³, which is an underestimated prediction of about 16 %.

Figure A3.11 shows the cross-validation scatter plot for NO_x annual average rural map. The R² indicates that about 65 % of the variability is attributable to the interpolation.

Figure A3.11: Correlation between cross-validated predicted and measurement values for NO_x annual average 2021 for rural areas



Comparison of point measurement values with the predicted grid value

Next to the above presented cross-validation, a simple comparison was made between the point observation values and interpolated predicted 1 km and 2 km grid values, respectively.

For NO₂ annual average, the comparison has been made primarily for the separate map layers at 1 km resolution. Besides, the comparison has been done also for the final combined map. Table A3.11 presents the results of this comparison, together with the results of cross-validation prediction of Figure A3.10. One can conclude that the final combined map in 1 km resolution is representative for rural and urban background areas, but not for urban traffic areas.

Table A3.11: Statistical indicators from the scatter plots for the predicted grid values from separate (rural, urban background or urban traffic) map layers and final combined map versus the measurement point values for rural (upper left), urban background (upper right) and urban traffic (bottom left) stations for NO₂ annual average 2021

NO ₂	rural backgr. stations				urban/suburban backgr. stations			
	RMSE	Bias	R ²	lin. r. equation	RMSE	Bias	R ²	lin r. equation
cross-val. prediction, separate (r or ub) map layer	2.1	0.0	0.734	y = 0.758x + 1.61	6.0	0.0	0.683	y = 0.725x + 4.56
grid prediction, 1x1 km ² separate (r or ub) map layer	1.9	-0.2	0.813	y = 0.788x + 1.25	2.5	0.1	0.857	y = 0.824x + 2.96
grid prediction, 1x1 km ² final merged map	2.2	0.4	0.743	y = 0.912x + 1.05	3.1	0.3	0.804	y = 0.847x + 2.90

NO ₂	urban/suburban traffic stations			
	RMSE	Bias	R ²	lin. r. equation
cross-valid. prediction, urban traffic map layer	6.0	0.0	0.565	y = 0.595x + 10.5
grid prediction, 1x1 km ² urban traffic map layer	4.1	0.0	0.807	y = 0.735x + 6.92
grid prediction, 1x1 km ² final merged map	9.7	-7.4	0.544	y = 0.501x + 5.44

Table A3.12 presents the cross-validation results of Figure A3.11 and those of the point observation – grid averaged prediction validation for the rural map of NO_x annual average.

Table A3.12: Statistical indicators from the scatter plots for predicted point values based on cross-validation and predicted grid values from rural 2 km resolution map versus measurement point values for rural background stations for NO_x annual average 2021

NO _x	rural background stations			
	RMSE	Bias	R ²	linear regression equation
cross-valid. prediction, rural map	3.9	0.1	0.648	y = 0.676x + 3.06
grid prediction, 2x2 km ² rural map	3.2	0.1	0.764	y = 0.733x + 2.52

A3.5 BaP

In this section, the technical details and the uncertainty estimates for Map 5.1 of BaP annual average are presented.

Technical details on the mapping

The methodology as developed and tested in Horálek et al. (2022) has been used. Table A3.13 presents the regression coefficients determined for pseudo BaP stations data estimates, based on the 356 rural and urban/suburban background that have both BaP and PM_{2.5} measurements available (see Section 2.1.1). Looking at the parameters of the regression, one can note that the adjusted R² of 0.76 is a relatively poor correlation. Based on this and in agreement with Horálek et al. (2022), the pseudo stations have only been used in areas with a significant lack of the BaP measurements. The pseudo stations have been applied for countries and areas, as follows. For the rural areas: All the mapping

area, apart from Austria, Benelux, Czechia, Germany, Poland, Slovakia, Spain, Switzerland, and Italy north of 44 degrees latitude. For the urban background areas: Iceland, Portugal, Scandinavia (including Denmark), Greece and west Balkan countries (namely, Albania, Bosnia and Herzegovina, Montenegro, Northern Macedonia, and Serbia including Kosovo).

Table A3.13: Parameters and statistics of linear regression model for generating pseudo BaP annual average data for 2021 in rural and urban background areas

		Rural and urban background areas
Nonlinear regression model (NLRM, Eq. A1.2b)	c (constant)	-5.44
	a1 (PM _{2.5} annual average)	0.136
	a2 (latitude)	0.051
	a3 (longitude)	0.054
	a4 (land cover NAT_1km)	-0.0002
	a5 (land cover NAT_5km r)	0.0000
Adjusted R²		0.76
Standard Error [ng/m³]		0.70

Table A3.14 presents the estimated parameters of the linear regression models (c, a₁, a₂,...) and of the residual kriging (nugget, sill, range) and includes the statistical indicators of both the regression and the kriging of its residuals. Almost the same supplementary data as in Horálek et al. (2022) has been used. The only change was the use of the CHIMERE model results instead of the EMEP model output (see Section A2.2). Note that the domain of the CHIMERE model output does not cover Iceland. However, the EMEP model results for 2020 show a correlation with the CHIMERE model results for 2021 (R²=0.76, after the exclusion of one outlier). Thus, an alternative BaP map using the EMEP model output for 2020 has been constructed for the whole domain and applied for the area of Iceland.

Table A3.14: Parameters and statistics of linear regression model and ordinary kriging of BaP annual average 2021 in rural, urban background and urban traffic areas for the final combined map

BaP		Annual average	
		Rural areas	Urban b. areas
Linear regression model (LRM, Eq. A1.3)	c (constant)	0.76	1.76
	a1 (log. CHIMERE model)	0.665	0.682
	a2 (altitude GMTED)	-0.00055	
	a3 (wind speed)	<i>n. sign.</i>	
	a4 (temperature)	-0.079	-0.15
	a5 (land cover NAT_1km)	-0.0054	
Adjusted R²		0.43	0.48
Standard Error [ng/m³]		0.97	1.04
Ordinary kriging (OK) of LRM residuals	nugget	0.149	0.209
	sill	0.733	1.119
	range [km]	220	730
LRM + OK of its residuals	RMSE [ng/m³]	0.67	1.25
	Relative RMSE [%]	143.8	86.9
	Bias (MPE) [ng/m³]	0.03	0.09

The adjusted R² is 0.43 for the rural areas and 0.48 for urban background areas.

Uncertainty estimated by cross-validation

Table A3.14 shows that the absolute mean uncertainty of the final combined map of BaP annual average expressed as RMSE is 0.67 ng/m³ for the rural areas and 1.25 ng/m³ for the urban background areas. The RRMSE of this map is 143.8 % for rural areas and 86.9 % for urban background areas. The cross-validation relative uncertainty RRMSE is still at the considerably higher level (especially in the rural areas) compared to the 60%, being the data quality objective for the modelling uncertainty in the European directive (EC, 2004).

Annex 4

Concentration maps including stations

Throughout the report, the concentration maps presented do not include the concentration values measured at the stations. The reason is to better visualise the health-related indicators with their distinct concentration levels at the more fragmented and smaller urban areas.

As presented in Annex 3, the kriging interpolation methodology somewhat smooths the concentration field. Therefore, it is valuable to present in this Annex 4 the indicator maps including the concentration values resulting from the measurement data at the stations. These points provide important additional visual information on the smoothing effect caused by the interpolation. For instance, maps A4.1 and A4.2 present PM₁₀ indicators annual average and 90.4 percentile of daily means and include the stations points used in the interpolation. They correspond to Maps 2.1 and 2.3 of the main report, which do not have stations. Table A4.1 provides an overview of the maps in the main report and the corresponding maps including stations point values as presented in this annex.

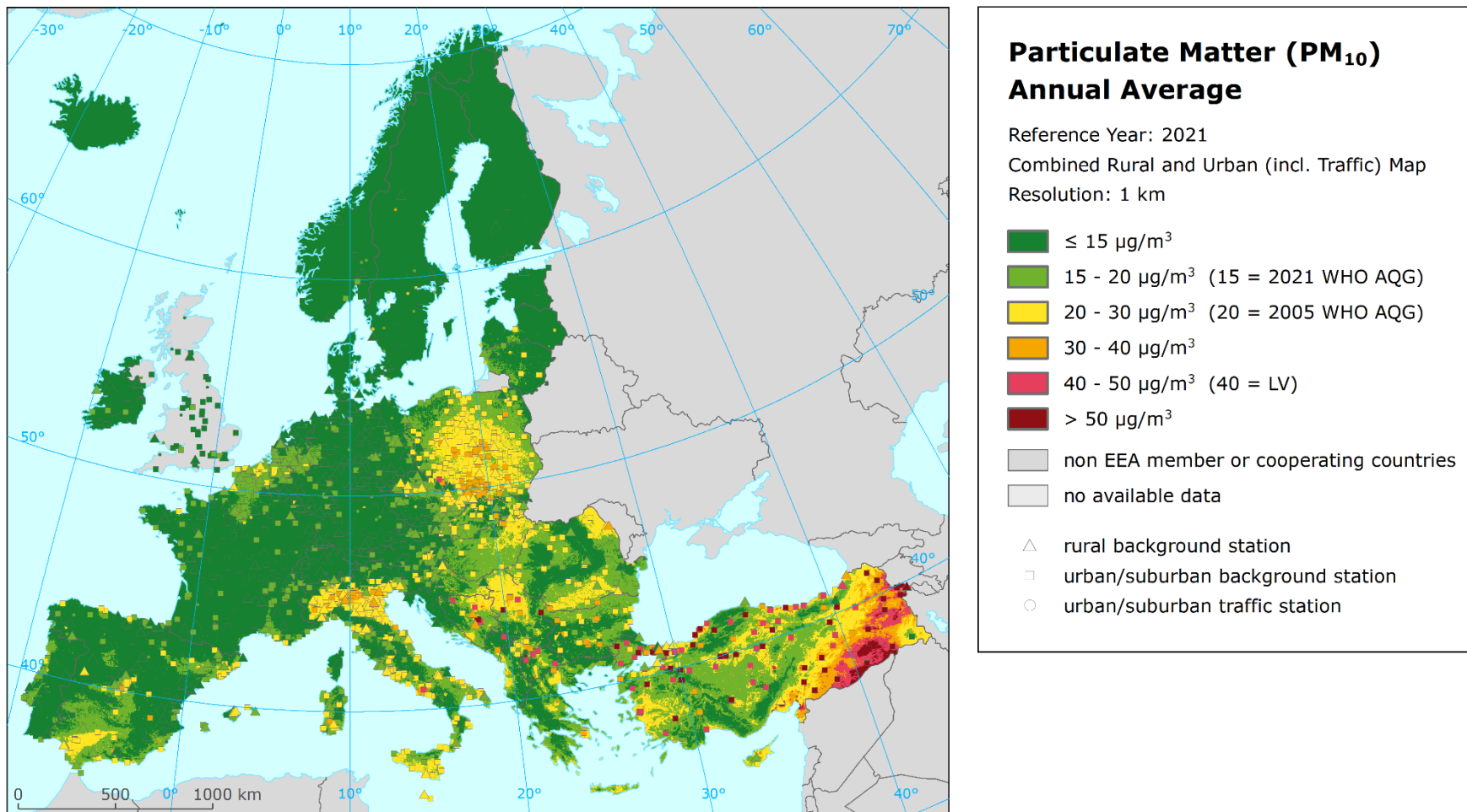
Both the rural and the urban/suburban background stations and also urban/ traffic stations for PM and NO₂ are included in the maps of the health related indicators, while the rural stations only are shown in the maps of vegetation related indicators. For PM_{2.5}, NO_x and BaP, only the stations with relevant measured data (i.e. not the pseudo stations) are presented.

Table A4.1: Overview of maps presented in this Annex 4 and their relation with the maps presented in the main report

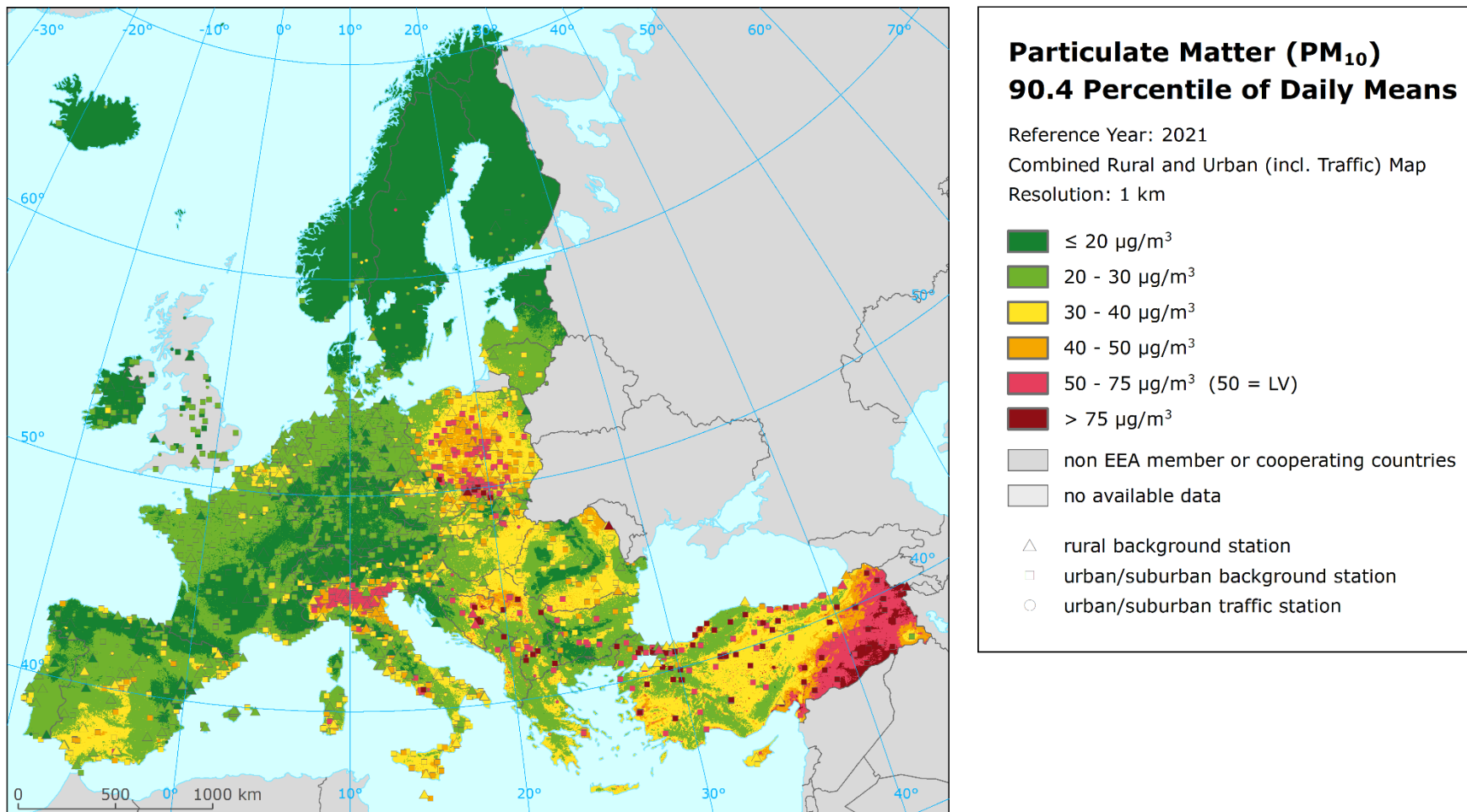
Air pollutant	Indicator	Map including stations	Map without stations
PM ₁₀	Annual average	A4.1	2.1
	90.4 percentile of daily means	A4.2	2.3
PM _{2.5}	Annual average	A4.3	2.5
Ozone	93.2 percentile of maximum daily 8-hour means	A4.4	3.1
	SOMO35	A4.5	3.3
	SOMO10	A4.6	3.4
	AOT40 for vegetation ^(a)	A4.7	3.6
	AOT40 for forests ^(a)	A4.8	3.7
NO ₂	Annual average	A4.9	4.1
NO _x	Annual average ^(a)	A4.10	4.3
BaP	Annual average	A4.11	5.1

^(a) Rural map, applicable for rural areas only.

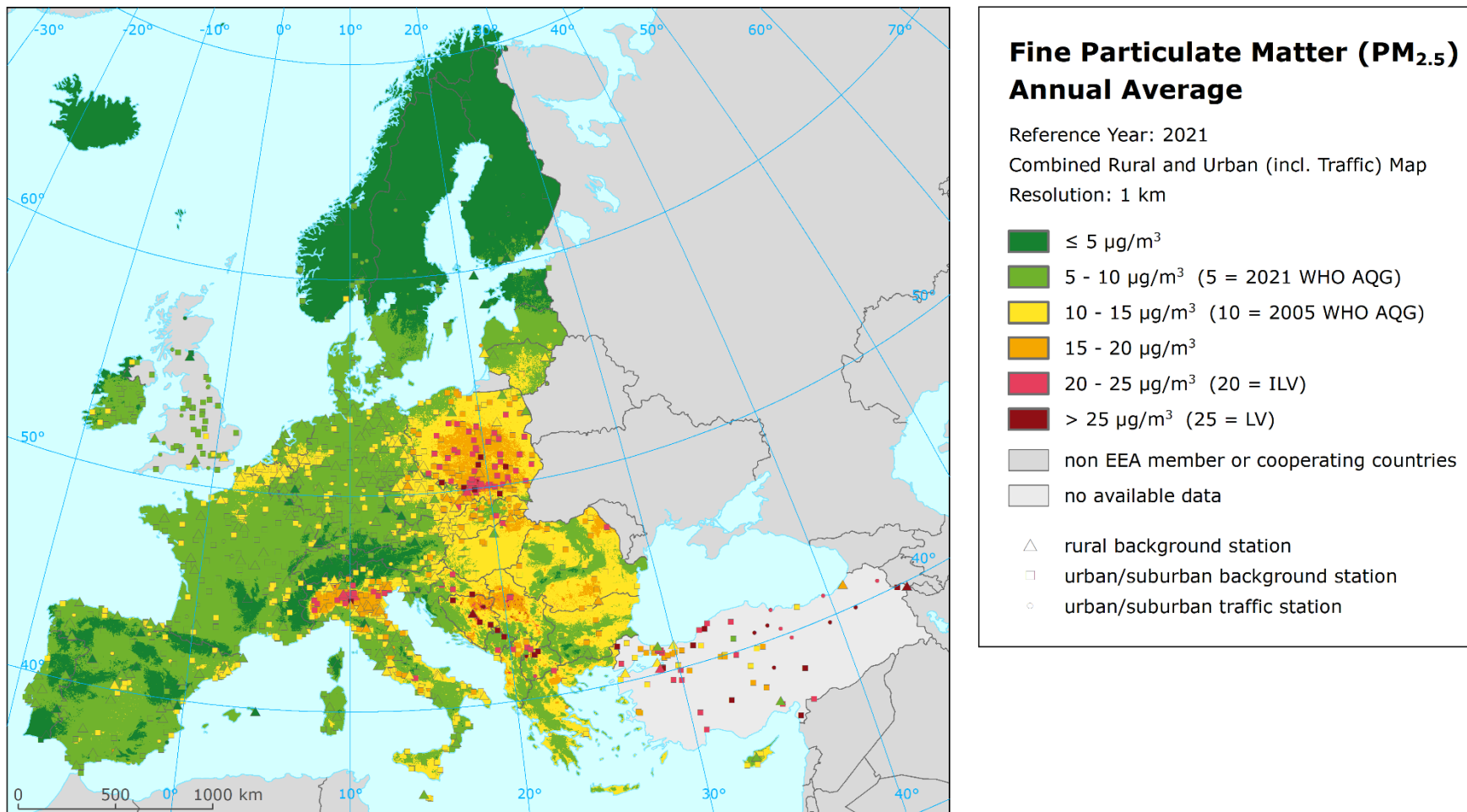
Map A4.1: Concentration map of PM₁₀ annual average including station measurement values, 2021



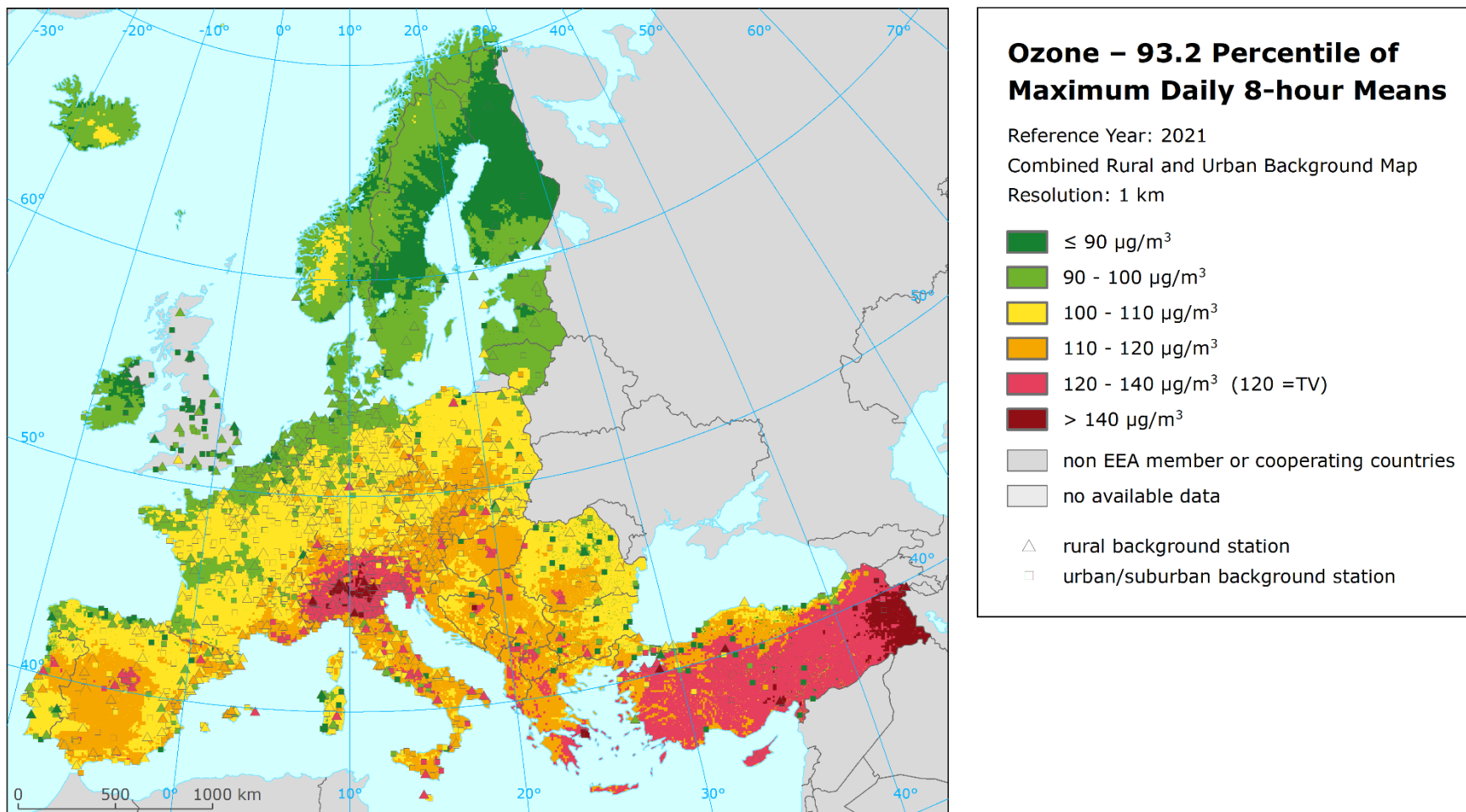
Map A4.2: Concentration map of PM₁₀ indicator 90.4 percentile of daily means including station measurement values, 2021



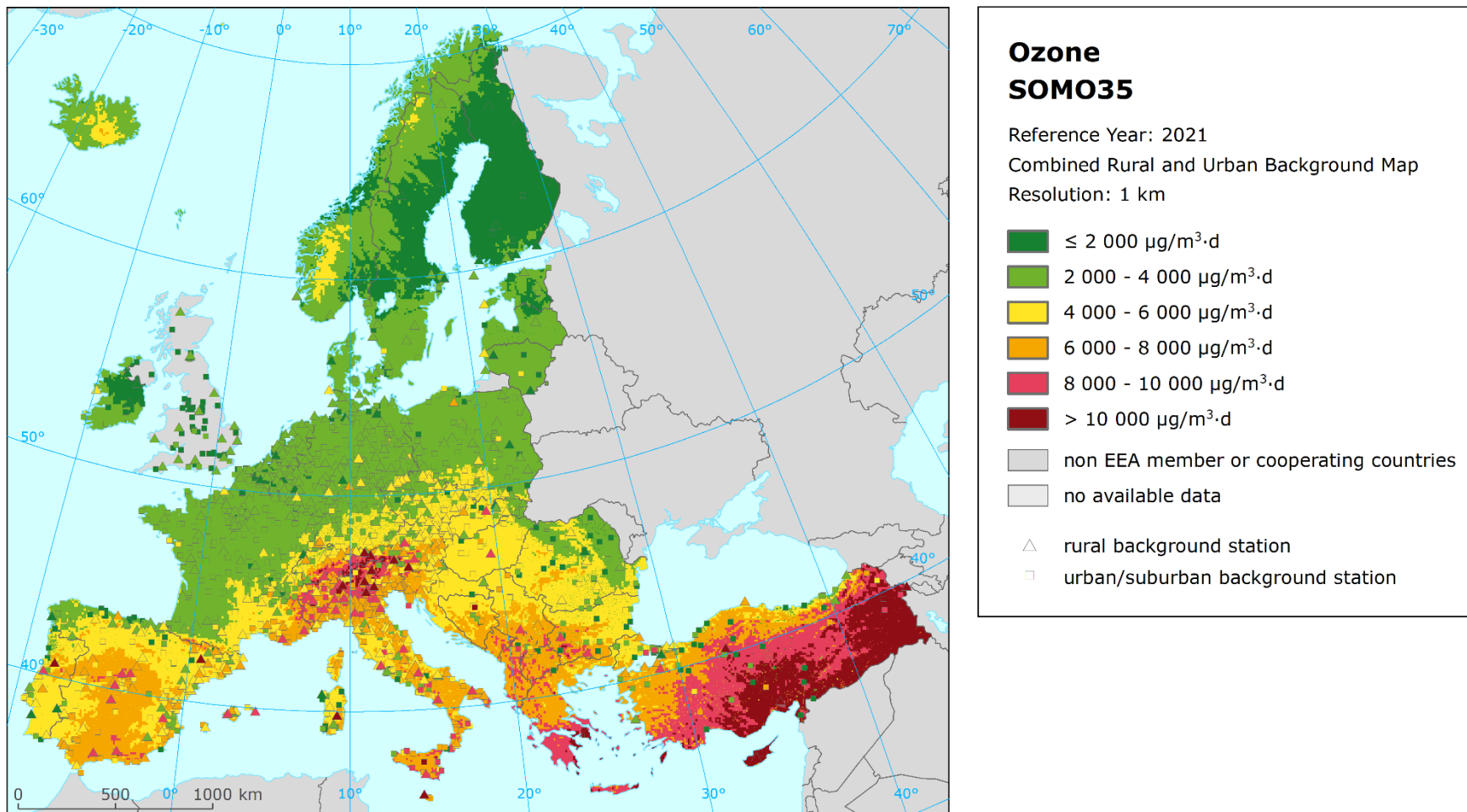
Map A4.3: Concentration map of PM_{2.5} annual average including station measurement values, 2021



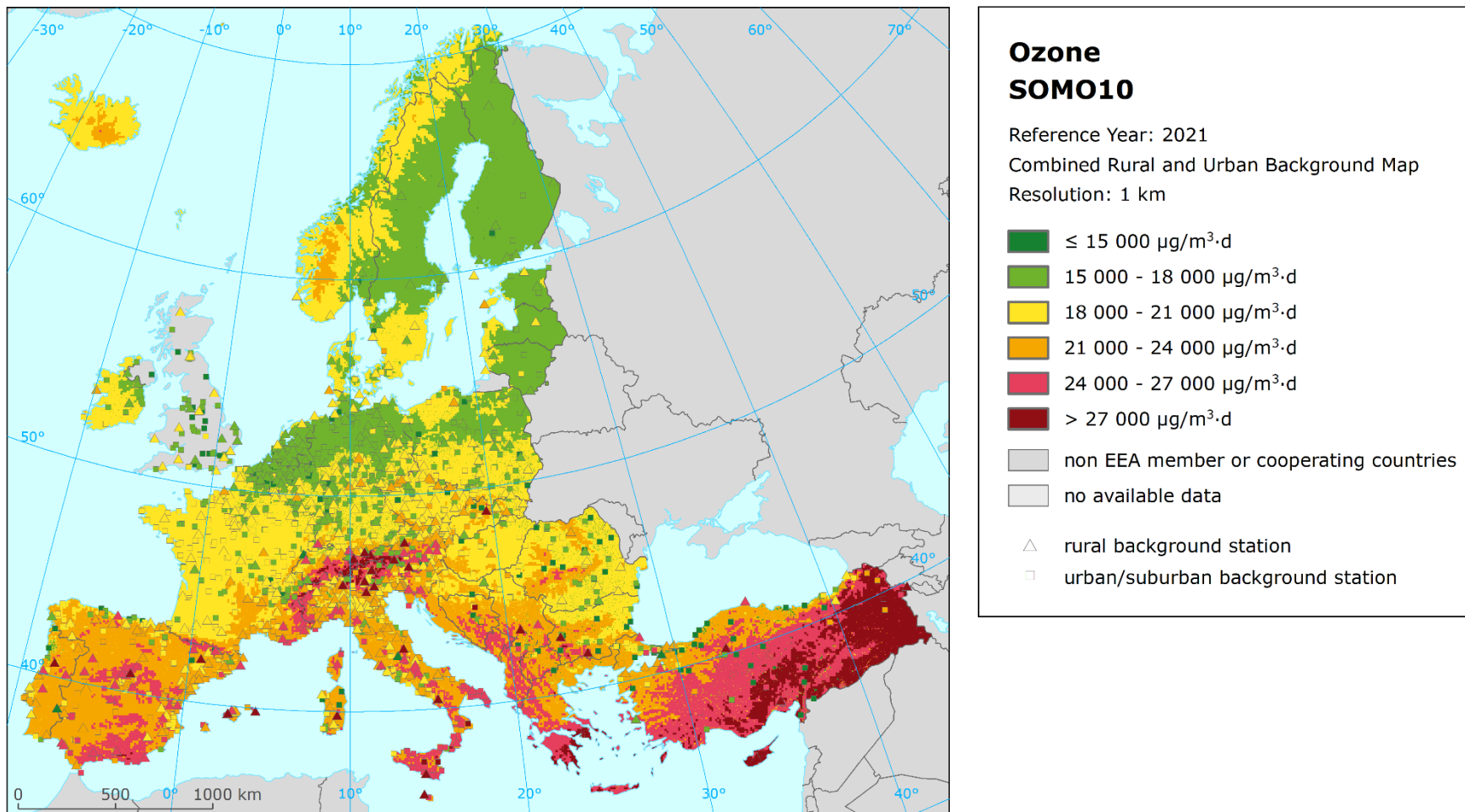
Map A4.4: Concentration map of ozone indicator 93.2 percentile of maximum daily 8-hour means including station measurement values, 2021



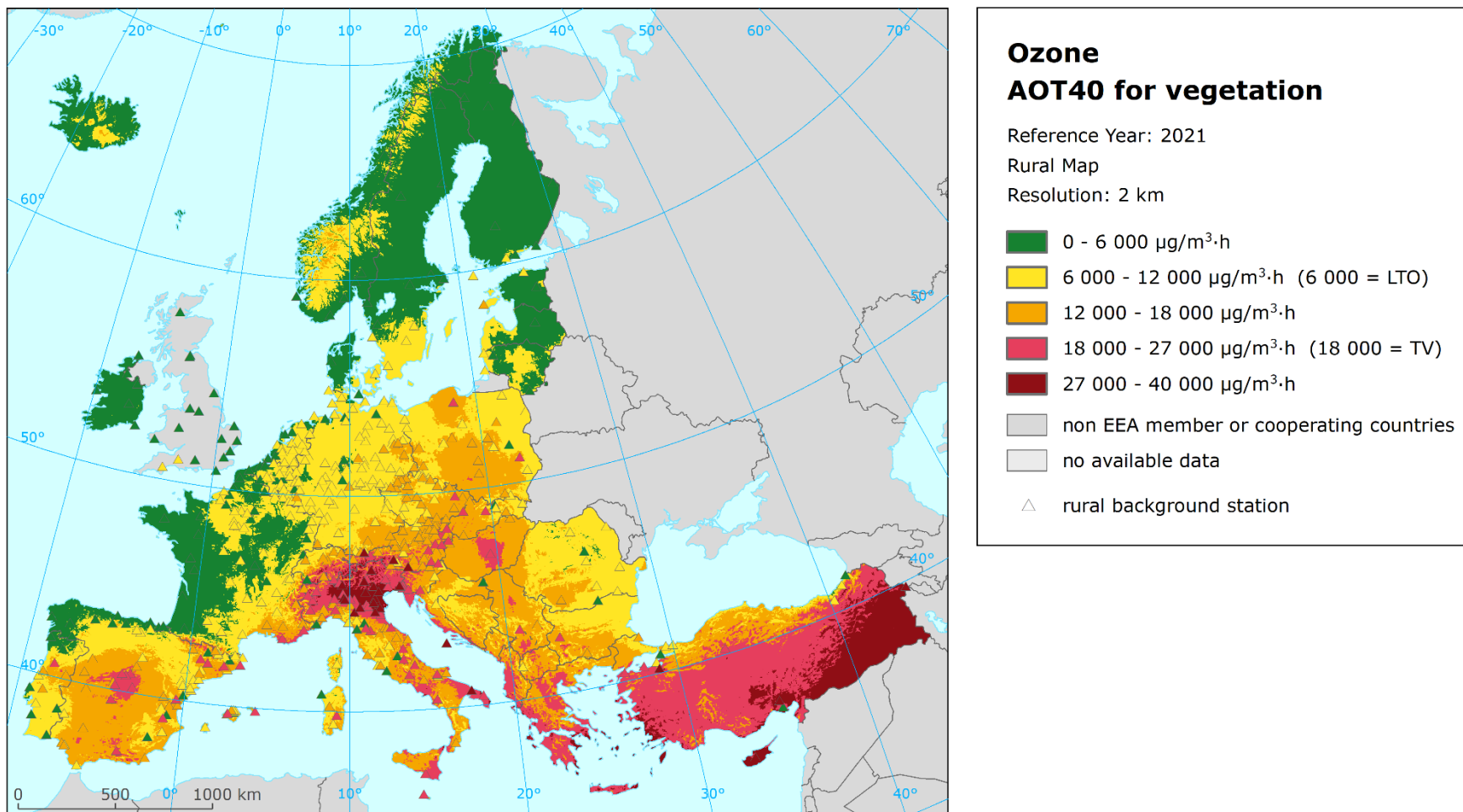
Map A4.5: Concentration map of ozone indicator SOMO35 including station measurement values, 2021



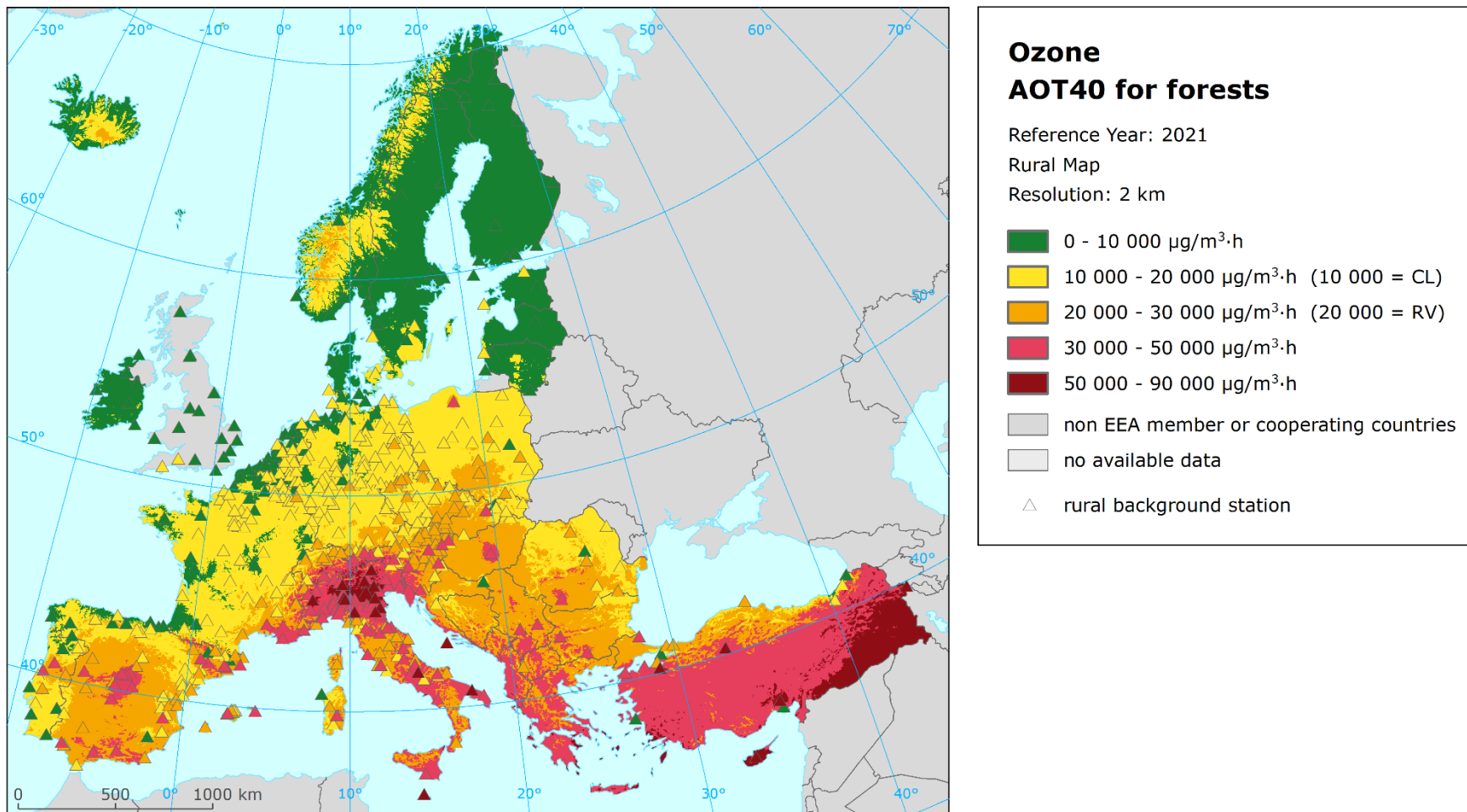
Map A4.6: Concentration map of ozone indicator SOMO10 including station measurement values, 2021



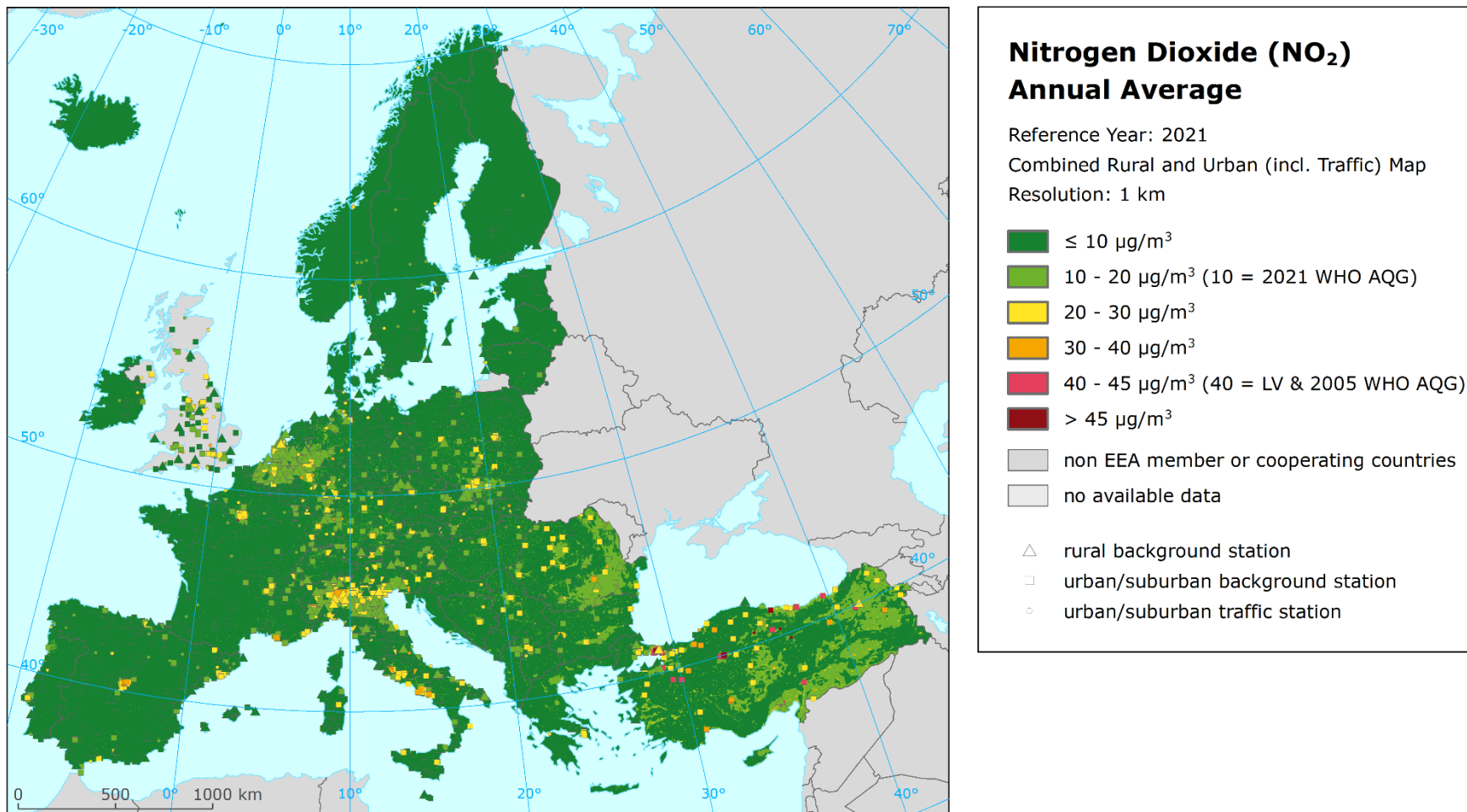
Map A4.7: Concentration map of ozone indicator AOT40 for vegetation including station measurement values, rural air quality, 2021



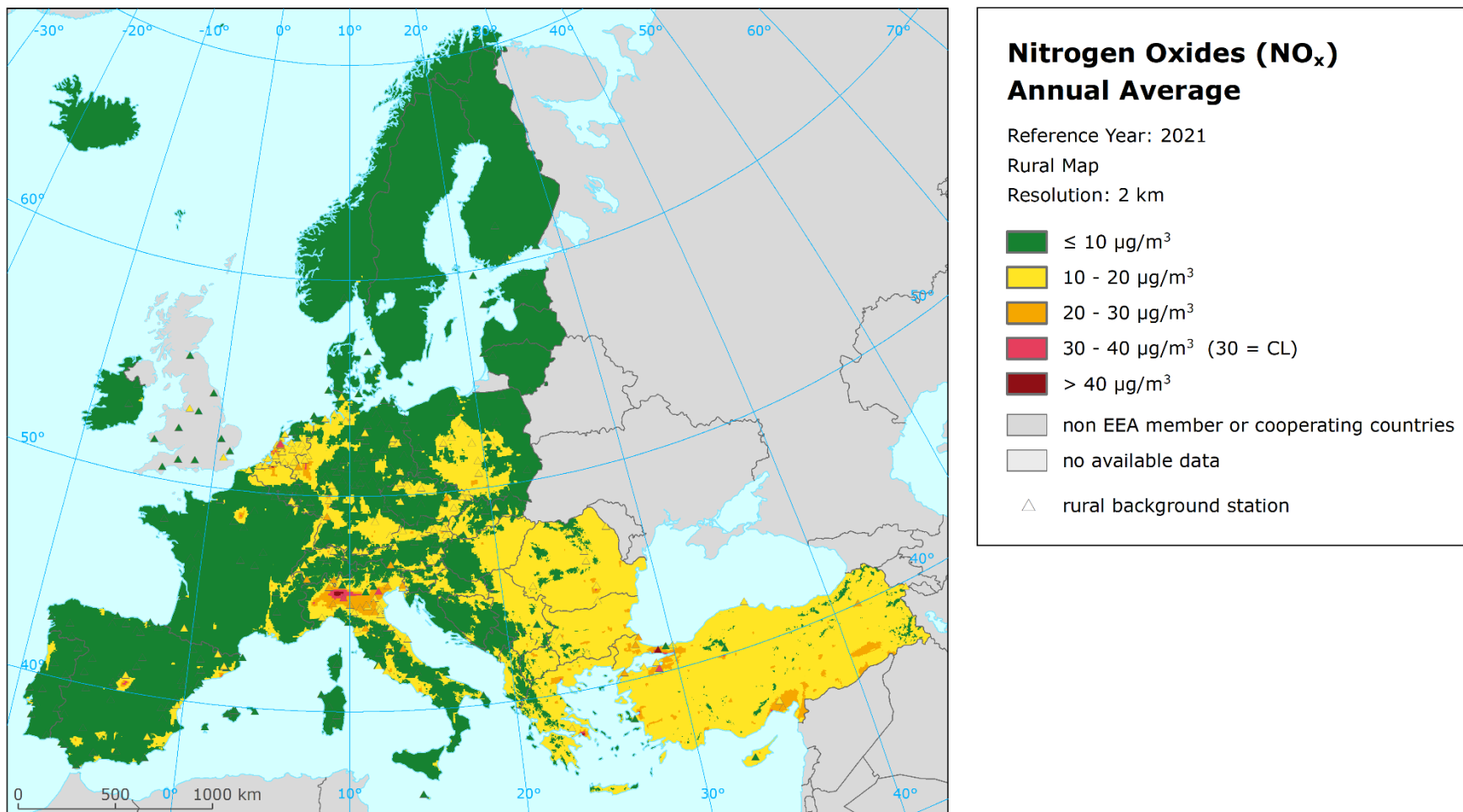
Map A4.8: Concentration map of ozone indicator AOT40 for forests including station measurement values, rural air quality, 2021



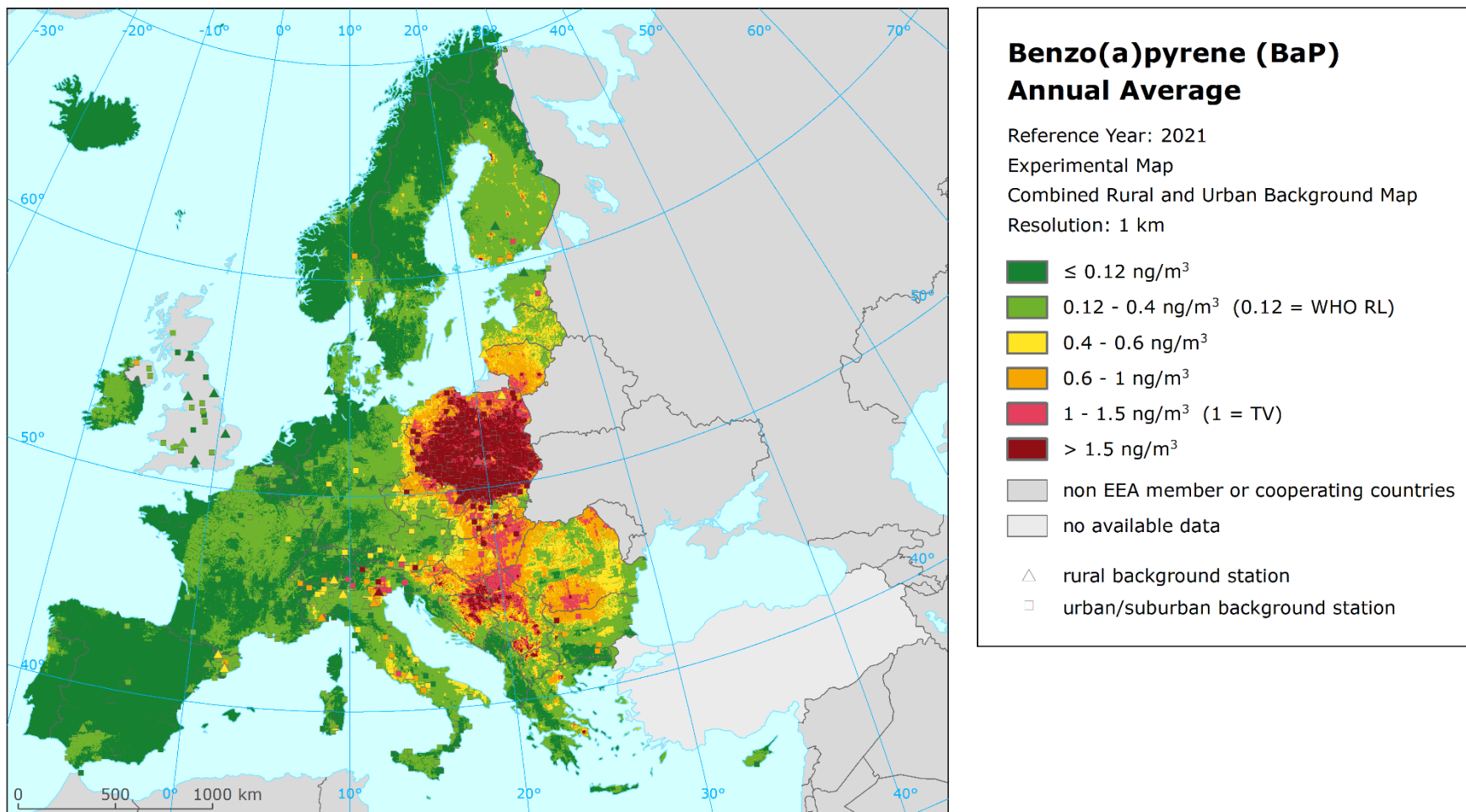
Map A4.9: Concentration map of NO₂ annual average including station measurement values, 2021



Map A4.10: Concentration map of NO_x annual average including station measurement values, rural air quality, 2021



Map A4.11: Concentration map of benzo(a)pyrene annual average including station measurement values, 2021, experimental map



European Topic Centre on
Human Health and the Environment
<https://www.eionet.europa.eu/etcs/etc-he>

The European Topic Centre on Human health and
the environment (ETC HE) is a consortium of
European institutes under contract of the European
Environment Agency.

European Environment Agency
European Topic Centre
Human health and the environment

